



CRYOGENIC RESINS FOR
GLASS-FILAMENT-WOUND COMPOSITES

by

Louis M. Soffer and Ralph Molho

prepared for

NATIONAL AERONAUTICS AND SPACE ADMINISTRATION

CONTRACT NAS 3-6287

N 6 7 - 2 5 0 7 . 6	
(ACCESSION NUMBER)	(THRU)
1	NONE
(PAGES)	(CODE)
CR-72114	18
(NASA CR OR TMX OR AD NUMBER)	(CATEGORY)

Reproduced by
NATIONAL TECHNICAL
INFORMATION SERVICE
Springfield, Va. 22151

AEROJET-GENERAL CORPORATION
VON KARMAN CENTER
AZUSA, CALIFORNIA

FINAL REPORT

CRYOGENIC RESINS FOR GLASS-FILAMENT-WOUND COMPOSITES

by

Louis M. Soffer and Ralph Molho

prepared for

NATIONAL AERONAUTICS AND SPACE ADMINISTRATION

January 1967

Contract NAS 3-6287

Technical Management
NASA Lewis Research Center
Cleveland, Ohio
Liquid Rocket Technology Branch
R. F. Lark

AEROJET-GENERAL CORPORATION
Von Karman Center
Azusa, California

FOREWORD

This report is submitted by Aerojet-General Corporation in fulfillment of the contract and covers all work done between 6 May 1965 and 31 December 1966.

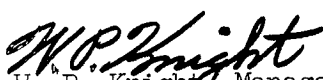
The program was performed jointly by the Applied Chemistry Department and the Composite Structures Department of the Chemical and Structural Products Division. Tasks I, II, and III were managed by L. M. Soffer. The selection, formulation, and preliminary screening of candidate resin systems were performed by O. S. Schaeffler and Dr. Soffer; Mr. Schaeffler made significant contributions to Task I and is co-author of this phase of the effort. Task IV was planned and managed by R. Molho, who was also responsible for the performance and evaluation of the entire physical/mechanical-test program.

Special acknowledgement is due to E. E. Morris for contributions in the area of test analysis. Other contributors were R. F. Borden, W. D. Bowers, N. R. Dunavant, J. Garancovsky, P. B. Guhl, H. Hollis, A. H. Hussung, R. J. Robinson, T. R. Sakakura, A. Taoyama, and W. R. Waite.


Guidance was provided throughout the program by the Project Manager, R. F. Lark, Liquid Rocket Technology Branch, Lewis Research Center, National Aeronautics and Space Administration.

Details of illustrations in
this document may be better
studied on microfiche

Approved by:


W. P. Knight, Manager
Applied Chemistry Department


S. B. Fabeck, Manager
Composite Structures Department


L. R. Rapp, Manager
Chemical and Structural Products Division

CRYOGENIC RESINS FOR GLASS-FILAMENT-WOUND COMPOSITES

by

Louis M. Soffer and Ralph Molho

ABSTRACT

A modified epoxy system, Resin 2, was developed for use in cryogenic applications of S-901 glass-filament-wound-composite structures. It was selected from 41 initial candidates in a three-phase program consisting of (1) resin formulation, (2) physical screening, and (3) physical and mechanical testing. Candidate resins were evaluated for their adaptability to conventional filament-winding techniques, cast-resin properties, and performance as glass-filament-wound-composite specimens.

The structural properties of Resin 2 as a matrix were then compared with a standard epoxy resin, 58-68R, in a series of single-cycle burst tests on metal-lined, glass-filament-wound-composite, pressure vessels. At cryogenic temperatures (-320 and -423°F), Resin 2 exhibited longitudinal-filament stresses that were 15.4 and 6.6% greater, respectively, than those obtained in vessels fabricated from 58-68R. At ambient temperature, the performance of the two systems was essentially the same.

CONTENTS

	<u>Page</u>
Glossary _____	xiii
SUMMARY _____	1
I. INTRODUCTION _____	3
A. Background _____	3
B. Program Plan _____	4
II. TASK I - IDENTIFICATION AND SELECTION OF SUPERIOR CRYOGENIC RESINS _____	6
A. Candidate Known Resin Systems _____	6
B. Candidate Modified Resin Systems _____	11
1. Background _____	11
2. Candidate Resin Systems _____	12
3. Preliminary Screening of Candidate Resin Systems _____	12
C. Physical Screening of Candidate Resin Systems _____	18
1. Background _____	18
2. Test Methods _____	18
3. Test Results _____	20
D. Selection of Candidate Resin Systems for Task II _____	29
III. TASK II - EVALUATION OF CANDIDATE CRYOGENIC RESINS _____	32
A. Test Methods _____	32
B. Test Results _____	32
1. Tensile Strength and Associated Properties _____	32
2. Notch Toughness _____	48
3. Impact Strength _____	48
4. Interlaminar Shear Strength _____	52
5. Coefficient of Linear Thermal Contraction _____	64
C. Selection of Candidate Resins for Task III _____	64
IV. TASK III - EVALUATION OF CANDIDATE CRYOGENIC RESINS AS FILAMENT-WOUND-COMPOSITE SPECIMENS _____	69
A. Test Methods _____	69
B. Test Results _____	69
1. Tensile Strength and Associated Properties _____	69
2. Thermal-Shock Resistance _____	75

CONTENTS (cont.)

	<u>Page</u>
3. Coefficient of Linear Thermal Contraction _____	75
4. Interlaminar Shear Strength _____	80
C. Selection of the Optimum Cryogenic Resin System _____	88
V. TASK IV - FABRICATION AND EVALUATION OF FILAMENT-WOUND-COMPOSITE PRESSURE VESSELS _____	92
A. Design _____	92
B. Fabrication _____	95
1. Metal Liner _____	95
2. Filament-Wound Pressure Vessel _____	99
C. Instrumentation _____	100
D. Test Results _____	103
1. Room-Temperature Tests (+75°F) _____	103
2. LN ₂ Tests (-320°F) _____	113
3. LH ₂ Tests (-423°F) _____	119
4. Evaluation of Test Data _____	123
VI. CONCLUSIONS _____	127
VII. RECOMMENDATIONS _____	129
References _____	131

Table

1 Candidate Known Epoxy Systems _____	7
2 Candidate Known Non-epoxy Systems _____	8
3 Cure Schedules and Casting Results for Table 1 Formulations _____	9
4 Glass-Transition Temperatures (T _g) by Strain Response _____	10
5 Ten Known Cryogenic Candidates _____	10
6 Modified Resin Systems _____	13
7 Materials Used in Table 6 Resin Systems _____	15
8 Thermal-Shock and T _g Data on Candidate Resin Systems _____	17
9 Candidate Systems for Task I Screening _____	19
10 Summary of Task I Screening Tests, Candidate Cryogenic Resin Systems _____	21
11 Preliminary Screening, Results of Tensile and Notch-Toughness Tests (Room Temperature) _____	22

CONTENTS (cont.)

<u>Table</u>		<u>Page</u>
12	Preliminary Screening, Results of Tensile and Notch-Toughness Tests (-423°F) _____	23
13	Viscosity Test Results _____	25
14	Comparison Factors for Candidate Cryogenic Resin Systems _____	30
15	Candidate Resin Systems for Task II Testing _____	31
16	Tensile-Test Results at +75°F (Task II) _____	33
17	Tensile-Test Results at -320°F (Task II) _____	34
18	Tensile-Test Results at -423°F (Task II) _____	35
19	Test Results for Cryogenic Resins (Tasks I and II) _____	41
20	Notch-Toughness Test Results (Task II) _____	49
21	Impact-Strength Test Results (Charpy Unnotched) _____	51
22	Interlaminar-Shear Test Results (NOL Horizontal-Shear Method) _____	53
23	Effects of MEK on Interlaminar-Shear Test Results for Resin 4A (NOL Horizontal-Shear Method) _____	62
24	Interlaminar-Shear Test Results (Short-Span-Shear Method) _____	63
25	Cast-Resin Linear-Thermal-Contraction Test Results (Task II) _____	67
26	Comparative Performance of Resin Systems in Mechanical Tests _____	68
27	Composite-Tensile-Strength Test Results (Unidirectional 1:0 Orientation) _____	70
28	Composite-Tensile-Strength Test Results (Bidirectional 1:1 Orientation) _____	71
29	Composite-Tensile-Strength Test Results (Bidirectional 1:2 Orientation) _____	72
30	Composite Thermal-Shock-Resistance Test Results (NOL Horizontal-Shear Method) _____	76
31	Composite Linear-Thermal-Contraction Test Results (Resin 2) _____	77
32	Composite Linear-Thermal-Contraction Test Results (Resin 4A) _____	78
33	Interlaminar-Shear Test Results, Resin 4A (NOL Horizontal-Shear Method) _____	82
34	Interlaminar-Shear Test Results, Resin 2 (NOL Horizontal-Shear Method) _____	87

CONTENTS (cont.)

<u>Table</u>	<u>Page</u>
35 Design Criteria, Pressure Vessels for Cryogenic-Resin Evaluation _____	93
36 Dimensional and Material Parameters, Pressure Vessels for Cryogenic-Resin Evaluation _____	94
37 Weight Analysis, Pressure Vessels for Cryogenic-Resin Evaluation _____	98
38 Fabrication Data, 8-in.-dia Pressure Vessels for Cryogenic-Resin Evaluation _____	101
39 Test Results, 8-in.-dia Pressure Vessels for Cryogenic-Resin Evaluation _____	105
40 Structural Data, 8-in.-dia Pressure Vessels for Cryogenic-Resin Evaluation _____	106
41 Cryogenic-Temperature Measurements, 8-in.-dia Pressure Vessels _____	122

Figure

1 Viscosity-Time Curves (Potential Prepreg Systems) _____	26
2 Viscosity-Time Curves (Potential In-Process or Prepreg Systems) _____	27
3 Stress-Strain Curves for Cryogenic Resin Systems at 75°F _____	37
4 Stress-Strain Curves for Cryogenic Resin Systems at -320°F _____	38
5 Stress-Strain Curves for Cryogenic Resin Systems at -423°F _____	39
6 Stress-Strain Curves for Epoxy-Polyurethane Resin System 4A at Various Temperatures _____	40
7 Effect of Temperature on Tensile Stress at Fracture, Cryogenic Resin Systems _____	44
8 Effect of Temperature on Strain at Fracture, Cryogenic Resin Systems _____	45
9 Effect of Temperature on Tensile Modulus, Cryogenic Resin Systems _____	46
10 Effect of Temperature on Toughness (Area Under Stress-Strain Curve), Cryogenic Resin Systems _____	47
11 Effect of Temperature on Notch Toughness, Cryogenic Resin Systems _____	50
12 Effect of Temperature on Interlaminar Shear Stress, S-901/Cryogenic Resin Systems (Horizontal-Shear Test Method) _____	55
13 Relationship Between Interlaminar Shear Stress and Resin Void Content, S-901/Cryogenic Resin Systems _____	56

CONTENTS (cont.)

<u>Figure</u>		<u>Page</u>
14	Photomicrograph, Resin 2 Horizontal-Shear Segment (4.70 vol% Voids)	57
15	Photomicrograph, Resin 3 Horizontal-Shear Segment (3.41 vol% Voids)	58
16	Photomicrograph, Resin 4A Horizontal-Shear Segment (9.56 vol% Voids)	59
17	Photomicrograph, Resin 6 Horizontal-Shear Segment (5.63 vol% Voids)	60
18	Photomicrograph, Resin 4A Horizontal-Shear Segment (5.66 vol% Voids)	61
19	Effect of Temperature on Interlaminar Shear Stress, S-901/ Cryogenic Resin Systems (Short-Span-Shear Test Method)	65
20	Linear Thermal Contraction, Cryogenic Resin Systems	66
21	Effect of Temperature on Filament Tensile Strength, S-901/Cryo- genic-Resin Composites with Alternate Filament Orientations	74
22	Linear Thermal Contraction, S-901/Cryogenic-Resin Composites	79
23	Effect of Resin Content and Filament Orientation on Linear Thermal Contraction, S-901/Cryogenic-Resin Composites	81
24	Effect of Temperature and Voids on Interlaminar Shear Stress, S-901/Resin 4A Composite (Horizontal-Shear Method)	83
25	Photomicrograph, Resin 4A Horizontal-Shear Segment (3.92 vol% Voids)	84
26	Photomicrograph, Resin 4A Horizontal-Shear Segment After Shear Test at -423°F (3.92 vol% Voids)	85
27	Photomicrograph, Resin 4A Horizontal-Shear Segment in Area of Shear Failure (3.92 vol% Voids)	86
28	Photomicrograph, Resin 2 Horizontal-Shear Segment (2.54 vol% Voids)	89
29	Photomicrograph, Resin 2 Horizontal-Shear Segment After Shear Test at -423°F (2.54 vol% Voids)	90
30	Welded Liner, 8-in.-dia Pressure Vessel (Engineering Drawing)	96
31	8-in.-dia Pressure Vessel (Engineering Drawing)	97
32	Instrumentation Diagram, 8-in.-dia Cryogenic Pressure Vessels	102
33	Test Assembly, 8-in.-dia Pressure Vessel (Engineering Drawing)	104
34	Typical Head Failure in Vessels Tested to Burst Point at Room Temperature	107

CONTENTS (cont.)

<u>Figure</u>	<u>Page</u>
35 Typical Explosive Reaction on Opposite Head of Vessels Tested to Burst Point at Room Temperature _____	108
36 Pressure/Longitudinal-Strain Curves for Filament-Wound, Metal-Lined, Pressure Vessels at +75°F _____	110
37 Pressure/Hoop-Strain Curves for Filament-Wound, Metal- Lined, Pressure Vessels at +75°F _____	111
38 Design and Actual Pressure-Strain Curves for Filament- Wound, Metal-Lined, Pressure Vessels at +75°F _____	112
39 Pressure/Longitudinal-Strain Curves for Filament-Wound, Metal-Lined, Pressure Vessels at -320°F _____	114
40 Pressure/Hoop-Strain Curves for Filament-Wound, Metal- Lined, Pressure Vessels at -320°F _____	115
41 Typical Pressure Vessel Assembled for Cryogenic Testing in Vacuum-Chamber Facility _____	116
42 Vessel 7 After Liquid-Nitrogen Burst Test _____	118
43 Pressure/Longitudinal-Strain Curves for Filament-Wound, Metal-Lined, Pressure Vessels at -423°F _____	120
44 Pressure/Hoop-Strain Curves for Filament-Wound, Metal- Lined, Pressure Vessels at -423°F _____	121
45 Effect of Temperature on Ultimate Filament Strength, Various Configurations of S-901/Resin 2 Specimens _____	124
46 Effect of Temperature on Longitudinal Tensile Strengths, Pressure Vessels with S-901 Glass and Alternate Resin Combinations _____	125
APPENDIX A - TEST METHODS _____	A-1
 <u>Figure</u>	
A-1 Routing Fixture, Tensile-Test Specimen (Engineering Drawing) _____	A-3
A-2 Clamp Fixture, Tensile-Test Specimen (Engineering Drawing) _____	A-4
A-3 Cryostat/Tensile-Machine Facility _____	A-5
A-4 Cryostat/Tensile-Test Machine _____	A-6
A-5 Tensile-Test Specimen _____	A-8
A-6 Tensile-Test-Fixture Setup _____	A-9
A-7 Routing Fixture, Notch-Toughness Test Specimen (Engi- neering Drawing) _____	A-11
A-8 Clamp Fixture, Notch-Toughness Test Specimen (Engineering Drawing) _____	A-12

CONTENTS (cont.)

<u>Figure</u>	<u>Page</u>
A-9 Notch-Toughness Specimen _____	A-13
A-10 Notch-Toughness Test-Fixture Setup _____	A-14
A-11 Simple-Beam (Charpy-Type) Impact Test _____	A-17
A-12 Cryogenic Tester, Interlaminar Shear (Engineering Drawing) _____	A-19
A-13 Short-Span-Shear Test-Fixture Setup _____	A-20
A-14 Horizontal-Shear Test-Fixture Setup _____	A-22
A-15 Filament-Pattern Orientations for Tensile-Strength Specimens _____	A-29
 APPENDIX B - PREVIOUS AEROJET STUDIES OF GLASS-FILAMENT/ RESIN INTERACTION _____	 B-1
<u>Table</u>	
B-1 Formulations and Physical Properties of Resin Systems Used in 4-in.-dia Vessels _____	B-2
B-2 Summary of Composite and Resin Properties _____	B-6
<u>Figure</u>	
B-1 Filament Stress vs Glass and Resin Types for 4-in.-dia Test Vessels _____	B-3
B-2 Filament Efficiency vs Ultimate Tensile Strength Times Notch Toughness, 4-in.-dia Specimens Incorporating Epoxy-Amine Resin Systems _____	B-5
B-3 Vessel Burst Pressure vs Cast-Resin Properties _____	B-7
B-4 Correlations of Cast-Resin Properties _____	B-8
B-5 Correlations of NOL-Ring Ultimate Fiber Stress _____	B-13
 APPENDIX C - PREPARATION OF BOHET _____	 C-1
APPENDIX D - SOLVENTS FOR EPOXY/POLYURETHANE SYSTEMS _____	D-1
APPENDIX E - CALCULATION OF FILAMENT AND COMPOSITE TENSILE STRESS IN COMPOSITE-TEST SPECIMENS _____	E-1
<u>Figure</u>	
E-1 Typical Physical Properties, Glass/Cryogenic-Resin Composites _____	E-3
 APPENDIX F - DESIGN ANALYSIS, 8-IN.-DIA, FILAMENT-WOUND, PRESSURE VESSELS FOR CRYOGENIC-RESIN EVALUATION _____	 F-1

CONTENTS (cont.)

<u>Figure</u>	<u>Page</u>
F-1 Calibration Curves for Continuous-Strip-Chart Recorder, Pressure Vessel 10 _____	F-11
F-2 Calibration-Test Data to Demonstrate Linearity of Strain-Gage Displacement Transducers _____	F-12
APPENDIX G - FABRICATION PROCEDURES FOR 8-IN.-DIA, CRYOGENIC- RESIN, PRESSURE VESSEL _____	G-1
Distribution List _____	H-1

GLOSSARY

ASTM	American Society for Testing Materials
BOHET	HET-acid bis(octafluoropentyl)ester
FWC	filament-wound composite
FTM	Federal Test Method
LH ₂	liquid hydrogen
LN ₂	liquid nitrogen
MEK	methyl ethyl ketone
NOL	Naval Ordnance Laboratory
S-901	high-strength glass filament (formerly S-994) (Owens-Corning Fiberglas Corporation)

CRYOGENIC RESINS FOR GLASS-FILAMENT-WOUND COMPOSITES

by Louis M. Soffer and Ralph Molho

Aerojet-General Corporation

SUMMARY

A flexibilized epoxy system designated as Resin 2 was developed for use in resin/S-901 glass-filament-wound construction for cryogenic application. The system consists of Epon 828 (a bisphenol A epoxy), dodecenyl succinic anhydride (a flexibilizing curing agent), Empol 1040 (a high-molecular-weight tricarboxy acid), and benzyldimethylamine (a cure catalyst).

Resin 2 was selected by a process of elimination in a four-task program consisting of (a) candidate-resin selection and formulation, (b) preliminary screening, (c) physical and mechanical testing of uncured resins, cast resin, and composite specimens, and (d) fabrication and testing of resin/S-901 glass-filament-wound pressure vessels.

On the basis of certain guidelines and performance criteria, 41 initial candidates were ultimately narrowed in Task I to four systems by a series of screening tests of uncured-resin and cast-resin specimens at +75 and -423°F. Further investigation of physical and mechanical characteristics in Task II narrowed these widely different candidates to two clearly superior systems - Resin 4A (a bisphenol A epoxy/polyurethane) and Resin 2 (a highly modified bisphenol A epoxy). Although Resin 4A was superior to Resin 2 in nearly every composite-specimen test performed in Task III, its pot-life and viscosity characteristics were unsatisfactory - thus making Resin 2 the optimum candidate system.

In Task IV the performance of Resin 2 was compared with that of the 58-68R resin (a standard epoxy system) in internally loaded, metal-lined, filament-wound-composite, pressure vessels. At test temperatures of +75 and -423°F, vessels fabricated from Resin 2 exhibited average longitudinal-filament stresses that were, respectively, the same as and 6.6% greater than those obtained for vessels fabricated from the standard epoxy system. At -320°F, the filament stress in the Resin 2 vessel was 15.4% greater than the stress in the standard; this result, however, was based on only one stress value for each resin system.

At -320 and -423°F, the longitudinal-filament stress attained in Resin 2 vessels was approximately 25% greater than at room temperature; at the same cryogenic temperatures, the stresses exhibited by the standard-epoxy vessels were only 7.9% and 17.4% greater, respectively, than the stresses in standard-epoxy vessels at room temperature.

On the basis of a pressure-vessel performance factor (burst pressure times vessel volume divided by vessel weight, pV/W), Resin 2 vessels exhibited structural efficiencies, relative to 58-68R vessels, that were comparable at +75°F, 16.6% higher at -320°F, and 12.7% higher at -423°F.

Specific recommendations are made for the further development of two types of Resin 4A-like epoxy/polyurethane systems on the ground that they are likely to provide resins superior to Resin 2 for filament-wound composites under cryogenic conditions.

In addition to demonstrating an improved cryogenic resin and obtaining physical and mechanical data for a number of chemically different epoxy systems at ambient and cryogenic temperatures, this program developed improved fabrication techniques, tooling, and test methods for filament-wound-composite test specimens and pressure vessels.

I. INTRODUCTION

A. BACKGROUND

The successful application of filament-wound, glass-reinforced-resin construction to the design of pressure vessels, particularly in solid-propellant rocket-motor cases, has suggested its use for the containment of cryogenic fluids. The high strength-to-density ratio, dimensional stability, structural reliability, low thermal conductivity, and ease and low cost of fabrication of these glass/resin composite structures are characteristics inherently attractive for cryogenic applications, including efficient cryogenic tankage.

Operation at high fiber stresses and strains contributes to the high performance levels exhibited by glass filament-wound-composite (FWC) structures, but also creates problems when such structures are considered for the containment of cryogenic fluids. There is a need, for example, for a homogeneous, impermeable liner material capable of withstanding repeated, equal, bidirectional strains to a level of 2.5% at cryogenic temperatures.

This required strain level, at which the glass fibers are extended to their design stress value, also points up the limitations of currently available resin systems; the latter, having been developed for use at ambient and higher temperatures, are not necessarily satisfactory under cryogenic conditions. When exposed to low temperatures, these systems are subject to internal mechanical defects (e.g., crazing and cracking) as a result of (1) increased resin brittleness, (2) increased modulus of elasticity, and (3) residual composite stress from resin thermal contraction and shrinkage during cure. These changes impair the ability of the matrix to perform its primary structural function of efficient shear-load transfer.

Although relatively few data are available on the behavior of polymeric materials and filament-wound composites at cryogenic temperatures, certain trends are evident (Refs. 1, 2, 3). There is a reduction in elongation and an increase in strength and modulus in tension, compression, and flexure. A 50% or greater increase over the room-temperature strength is not uncommon for glass-reinforced-plastic composites at cryogenic temperatures. (The measured strength of E-glass or of Aerojet's Hi-Stren monofilaments increases about 60% at cryogenic temperatures.)

Data available for structural adhesives at cryogenic temperatures indicate that unmodified epoxy resins are brittle. Modified epoxy resins formulated for increased extensibility (epoxy/phenolic, epoxy/nylon, and epoxy/polyamide) showed marked improvement in tensile-shear properties. Epoxy/nylons, in particular, gave consistently high shear strengths at cryogenic temperatures. Excellent adhesion and good low-temperature flexibility were exhibited with polyurethane adhesives. Liquid-urethane polymers have been recommended as candidates for the filament winding of cryogenic vessels on the basis of their toughness, curing properties, high shear strength, peel strength, and thermal-shock resistance.

In laminates based on 181-glass cloth, bisphenol A epoxys have outperformed phenolic, polyester, and silicone resins at both ambient and cryogenic temperatures. Because of their overall superior structural properties and suitability for composite fabrication, epoxy systems are prime candidates for the filament winding of cryogenic vessels.

A recent paper has reviewed all the available information on the behavior of reinforced plastics at cryogenic temperatures (Ref. 4). A broad spectrum of commercially available epoxies, phenolics, phenylsilanes, silicones, imidites, epoxy/nylons, polyesters, and fluorocarbons were included. The following conclusions, drawn from tests on laminates reinforced with woven E-glass cloth, were of particular interest:

1. All the laminates tested had higher tensile strength at cryogenic temperature, the effect being greater for the more flexible systems.
2. Increased flexural strength of laminates with decreased temperature was particularly pronounced for the more flexible systems.
3. The flexural strength and stiffness of a laminate decreased as the cohesive strength and modulus of the resin decreased.
4. For almost all design purposes, the laminates at cryogenic temperatures would be as good or better than at room temperatures.

The present report provides a detailed summary of all work performed during the program, the data obtained, and the resulting conclusions and recommendations. Test methods, including fabrication procedures, specimen configurations, apparatus, and calculations, are covered in appendixes. This work and complementing programs funded by the National Aeronautics and Space Administration for the development of metallic liners, improved filament coatings and surface treatments, and glass-fiber-reinforced metallic tanks (under Contracts NAS 3-4189, NAS 3-6297, and NAS 3-6292) are helping to provide the data, new materials, and improved techniques needed for the continuing development of filament-wound cryogenic tankage.

B. PROGRAM PLAN

The objective of the work under Contract NAS 3-6287 was the development of an improved cryogenic resin for S-901 glass-filament-wound structures. The minimum goal was a resin/glass system that would have increased extensibility and improved shear transfer and flexural strengths at -423°F , as compared with presently available resin/S-901 glass systems.

The original program consisted of a three-task, 14-month technical effort. Task I was concerned with the selection and physical examination of potential cryogenic resins in order to identify the most promising candidates. Forty-one initial candidates (ten "known" and 31 "modified") were ultimately narrowed to four systems. The selection was based primarily on physical-screening tests of cast-resin specimens at $+75$ and -423°F to evaluate the following characteristics: (1) notch toughness, (2) tensile strength at fracture, (3) the product of notch toughness times tensile strength at fracture, (4) elongation, (5) glass-transition temperature, (6) viscosity, and (7) pot life.

The cast-resin and composite specimen data providing a basis for the selection of two superior resin systems were obtained in Task II. The following tests were performed on the four selected resins at +75, -320, and -423°F: (1) interlaminar shear strength by short-span and horizontal-shear methods (including resin and void contents), (2) tensile strength, including tensile modulus, maximum elongation, and toughness, (3) coefficient of thermal contraction, (4) impact strength, (5) thermal-shock resistance, (6) specific gravity, (7) notch toughness, (8) viscosity and pot life of uncured resin, and (9) resin shrinkage (%) during cure. After a thorough evaluation of the data, two resins were recommended to the NASA Lewis Research Center Project Manager for approval.

Task III covered evaluations of the two selected resins as S-901 glass, FWC, test specimens. Tests of the following composite properties were conducted at +75, -320, and -423°F, except as noted:

1. Tensile strength, including tensile modulus and elongation, at three different filament orientations: (a) unidirectional, with a 1:0 longitudinal-to-transverse filament ratio, (b) bidirectional, with a 1:1 longitudinal-to-transverse filament ratio, and (c) bidirectional, with a 1:2 longitudinal-to-transverse filament ratio
2. Thermal-shock resistance (temperature cycling between +75 and -423°F, followed by a horizontal-shear-strength test at -423°F)
3. Horizontal shear strength
4. Linear thermal contraction in the longitudinal and transverse directions (between +75 and -423°F)
5. Resin content of all test specimens (at 75°F only)
6. Void content of all test specimens (at 75°F only).

After thorough data evaluation, an optimum cryogenic filament-winding resin was recommended to the Project Manager for approval.

The program was extended in June 1966 to include Task IV, an experimental evaluation of the superior cryogenic system (Resin 2) selected in Task III. Evaluation of the Resin 2/S-901 glass composite was performed by fabricating filament-wound cylindrical pressure vessels and testing under biaxial-loading conditions at +75, -320, and -423°F. For purposes of comparison, tests were also made on similar vessels fabricated with S-901 glass filaments and a standard epoxy-resin system (Shell 58-68R). In brief, two filament-wound pressure vessels using Resin 2 and two using the standard resin were tested at each of the three test temperatures. The internal pressure, temperature, and hoop and longitudinal strains were monitored continuously for all 12 vessels.

After Task IV data were obtained, the two resin systems and their relative influences on composite behavior were subjected to a comprehensive analysis.

II. TASK I - IDENTIFICATION AND SELECTION OF SUPERIOR CRYOGENIC RESINS

A. CANDIDATE KNOWN RESIN SYSTEMS

Resin formulations previously studied at cryogenic temperatures, and for which data were available, were considered as known resin systems. The first step in the selection of ten such systems was a thorough search of the literature for promising candidates (Refs. 1 through 8). Following the search, 30 leading resin suppliers were asked for recommendations in the light of program objectives and requirements. This effort led to the acquisition of 36 resins of five chemical types and an equal number of resin modifiers and curing agents. Infrared spectra were obtained for all the materials in order to assure that they would be used most effectively.

Candidate resin systems that were cast successfully are listed in Table 1 (epoxy systems) and Table 2 (non-epoxy systems). The castings were used to observe the cure behavior of the materials, to determine the gross properties of the cast specimen, and to provide samples for possible determinations of the glass-transition temperature (T_g). The pertinent cure schedules for epoxy systems and the results obtained in casting these resins are presented in Table 3.

The T_g determinations were included in the Task I physical-screening tests to provide a useful indication of inherent resin-system flexibility. Although cryogenic temperatures of -197°C (liquid nitrogen, LN_2) and -252°C (liquid hydrogen, LH_2) are considerably lower than the T_g values for known or even conceivable resins, it was desired to minimize stresses incurred at any low temperature (even if noncryogenic); thus, a system with $T_g = 0^\circ\text{C}$ might be expected to have an overall greater stress resistance at low temperatures than one with $T_g = 50^\circ\text{C}$.*

The T_g data were determined by means of the strain-response method (Ref. 10 and Appendix A). This method was chosen for its relative simplicity, speed, and accuracy, after trials of a number of methods for second-order-transition assays, including buoyancy (Ref. 11), differential thermal assay (Ref. 12), brittleness point (Ref. 13), and dilatometry. The T_g results obtained for known resin systems are shown in Table 4.

The ten resins listed in Table 5 were chosen as affording the most promise for glass-FWC structures for cryogenic use. The selection was based on the overall composite and cast-resin mechanical properties at cryogenic temperatures, as reported in the literature or by the supplier (if the material had not been evaluated by others). When it was necessary to choose between equally attractive candidates, and a choice could not otherwise be made, the system with the lower T_g was favored.

* In one program directed at obtaining an elastomer that would be useful as a seal below 140°K , many materials were examined whose T_g values were between 200 and 262°F (Ref. 9).

TABLE 1

CANDIDATE KNOWN EPOXY SYSTEMS*

	Parts													
	1	2	3	4	5	6	7	8	9	10	11	12	13	14
Resins														
Epon H-825 (1)	100	100	100											
Epon 828 (1)				50	100	100	50	100						100
Epon 1031 (1)				50			50							
Epi-Rez 510 (2)									65	100	100			
Epi-Rez 502 (2)									35					
Narmco 3170 (3)												100		
Narmco 3135 (3)													100	
Curing Agents														
Metaphenylenediamine, CL (4)	12.5													
Diaminodiphenylsulfone, DDS (5)		20												24
Nadic methyl anhydride, NMA (6)			90	90										
Dodecenyl succinic anhydride, DSA (4)					133	134	133							
Curing Agent Z (1)								20						
Epi-Cure 86 (2)									10					
Epi-Cure 891 (2)										60				
Epi-Cure 8501 (2)											75			
Narmco 7133 (3)												100		
Narmco 7111 (3)													100	
Accelerators														
BF ₃ -400 (6)		1.0												1.0
Benzyltrimethylamine, BDMA (7)			1.0	0.5	0.55	1.0	0.55							
Tetraethylenepentamine, TEPA (8)											8			

*Column headings 1, 2, 3, etc. represent formulation numbers. For resins, entries represent parts by weight; for curing agents and accelerators, entries represent parts per 100 parts of resin (phr). Sources of compounds as follows: (1) Shell Chemical Co., Plastics and Resins Division, Downey, Calif.; (2) Jones-Dabney Co., Louisville, Ky.; (3) Narmco Materials Division, Whittaker Corp., San Diego, Calif.; (4) Allied Chemical Corp., New York, N.Y.; (5) K & K Laboratories, Inc., New York, N.Y.; (6) EVRA Plastics Co., Los Angeles, Calif.; (7) Sumner Chemical Co., New York, N.Y.; and (8) Union Carbide Chemical Co., Plastics Division, New York, N.Y.

TABLE 2

CANDIDATE KNOWN NON-EPOXY SYSTEMS

<u>Resin/Catalyst System*</u>	<u>Resin:Catalyst Ratio</u>	<u>Cure Schedule, hours/°F</u>	<u>Results</u>
Polyesters			
AP-262M (1)/BP	100:1	1/150 + 1/250	Excellent cast, tough
P-43 (1)/BP	100:1	1/150 + 1/250	Excellent cast, tough
Hetron-31 (2)/BP	100:1	1/250	Slight air inclusion, tough
Polyurethanes			
Adiprene L-100 (3)/MOCA	100:11	3/250	Excellent cast, resilient
Adiprene L-420 (3)/MOCA	100:8.8	3/250	Some minute air inclu- sions, resilient
Narmco 7343/7139 (4)	100:11	3/212	Excellent cast, resilient, resembles Adiprene L-100
Silicone			
RTV-655A/RTV-655B (5)	100:10	4/150	Excellent cast, elasto- meric

*BP = benzoyl peroxide. MOCA = 4,4'-methylene-bis-(2-chloroaniline). Sources of proprietary materials as follows: (1) Rohm & Haas Co., Philadelphia, Pa.; (2) Hooker Chemical Corp., Durez Plastics Div., North Tonawanda, N.Y.; (3) E. I. du Pont de Nemours & Co., Wilmington, Del.; (4) Narmco Materials Div., Whittaker Corp., San Diego, Calif.; and (5) General Electric Co., Silicone Products Dept., Waterford, N.Y.

TABLE 3

CURE SCHEDULES AND CASTING RESULTS FOR TABLE 1 FORMULATIONS

<u>Formulation No.</u>	<u>Cure Schedule, hours/°F</u>	<u>Results</u>
1	2.5/175 + 2/300	Excellent cast, tough
2	2/260 + 2/390	Excellent cast, tough
3	3/250 + 4/300	Excellent cast, tough
4	2/150 + 4/250 + 6/300	Excellent cast, tough
5 (a)	1/150 + 3/250 + 6/300	Excellent cast, tough
5 (b)	1/150 + 4/250	Excellent cast, tough
5 (c)	1/150 + 4/300	Excellent cast, tough
5 (d)	2/150 + 4/300	Excellent cast, tough
6	2/150 + 5/300	Excellent cast, tough
7 (a)	1/150 + 3/250 + 6/300	Excellent cast, tough
7 (b)	1/150 + 4/250	Excellent cast, tough
7 (c)	1/150 + 4/300	Excellent cast, tough
7 (d)	2/150 + 4/300	Excellent cast, tough
8	2/150 + 2/300	Excellent cast, tough
9	1/220	Excellent cast, moderate toughness
10	20/77 + 2/200	Minute amount of trapped air, moderate toughness
11	20/77 + 2/200	Minute amount of trapped air, moderate toughness
12	1/200	Large amount of trapped air
13	2/150	Large amount of trapped air
14	2/260 + 2/390	Excellent cast, tough

TABLE 4

GLASS-TRANSITION TEMPERATURES (T_g) BY STRAIN RESPONSE

Resin System	Formulation		T_g , °C
	No.	Table	
Epon 828/DSA	6	1	52
Epon 828/Z	8	1	>135
AP-262M/BP	-	2	81
P-43/BP	-	2	86

TABLE 5

TEN KNOWN CRYOGENIC CANDIDATES

Formulation No.	Resin or Resin System	Chemical Type
1	Shell 58-68R	Epoxy (hybrid)
2	Epon 826 (or H-825)* /CL	Epoxy
3	Epon 828/DSA	Modified epoxy
4	Epon 828 (or 826)/DDS	Epoxy
5	P-43	Polyester
6	AP-262M**	Polyester
7	Epon 828/Z	Epoxy
8	Epi-Rez 510/Epi-Cure 8501/TEPA	Modified epoxy
9	Epi-Rez 510/Epi-Cure 891	Modified epoxy
10	Epon 828 (or 826)/hexahydrophthalic anhydride (or phthalic anhydride)/BDMA	Epoxy

* According to the manufacturer, a new pure bisphenol A epichlorohydrin.

** A new polyester with improved low-temperature properties (Rohm & Haas Co.).

Table 5 provides data for only epoxies and polyesters. Other chemical types (e.g., polyurethanes, silicones, silanes, and phenolics) were considered, but were rejected as inadequate on the basis of the data; these materials were of interest, however, for the development of "modified" resins.

B. CANDIDATE MODIFIED RESIN SYSTEMS

1. Background

Modified resin systems were considered to be new formulations based on the known systems but devised to provide improvements over them. As specified in the contract, a minimum of ten known and six modified resins were initially required for study in Task I. Of these 16 systems, five were to undergo physical screening; of these five, four were to be further evaluated in Task II. Although the five candidate resins were to be selected from both known and unknown (i.e., modified) systems, previous work at Aerojet strongly suggested that superior cryogenic resins would more likely be of the second type (Ref. 14).^{*} A major part of the identification and selection effort was therefore assigned to the formulation and evaluation of modified systems.

The following considerations provided a basis for the formulation of modified resin systems:

a. Systems having increased flexibility were desired as a solution to the embrittlement that results from the inability of a resin/composite structure, fabricated at ordinary temperatures, to take up new conformations required by the change to an extremely cold environment. Because of such factors as (1) embrittlement, (2) increased modulus of elasticity, and (3) the building up of residual stresses due to resin thermal contraction and shrinkage during cure, the resin properties were expected to control composite performance to a greater extent at cryogenic temperatures than at higher temperatures.

b. It was assumed that the relationships between cast-resin properties and composite performance (vessel burst pressure) established by Aerojet glass/resin-interaction studies (Ref. 14 and Appendix B) at ambient conditions would be generally maintained at lower temperatures.

c. The properties of high notch toughness, high elongation, and high interlaminar shear strength were taken to be of primary importance, with secondary importance assigned to high fatigue strength, high impact strength, and low shrinkage during the cure.

d. Systems with adequate pot life, sufficiently low viscosity, and feasible cure temperatures (300 to 350°F) were required.

e. The results of prior cryogenic-resin work on glass-cloth-reinforced-plastic laminates (Ref. 4), also served as guidelines, as did the known relationships between the physical properties of polymers and their

^{*}Major results of these investigations pertinent to the present effort are briefly summarized in Appendix B.

chemical and molecular structure, and the known surface chemistry of S-901* glass fibers and the glass/resin interface (Refs. 15 to 19).

2. Candidate Resin Systems

Modified resin systems studied during Task I are summarized in Table 6; the materials used and the sources of supply are identified in Table 7. All the formulations were judged to have adequate pot-life and viscosity characteristics. Usually, only one or two variations were attempted for each formulation shown.

The 31 formulations were either epoxy-, polyester-, or polyurethane-based systems that were modified in order to obtain the desired properties. Although Epon 828 (a bisphenol A epoxy) was favored, Epon 826 (which is of lower viscosity) could have been substituted for 828 in many of the formulations with equally good results. Epon 828 was modified by the addition of various materials, including other epoxies, epoxy/silicone, silicones, polyurethanes, and a number of flexibilizing curing agents and modifiers. Polyester systems were based on a resin recommended for its low-temperature properties.

Two other materials were present in the formulations as chemically unreactive additives. BOHET, or HET-acid bis(octafluoropentyl)ester, had previously provided glass monofilaments some protection against moisture in an HTS-type (A-1100/bisphenol A) finish (Ref. 16). It is believed that this protective action was due to an improved, BOHET-induced, surface coverage or a strengthened adhesive bond. The second material, silicon carbide (SiC) whiskers, was expected to increase the strength properties of the resins.** Unfortunately, a worthwhile evaluation of the merits of SiC-reinforced resin systems would have required considerable effort that was not justified by the scope of the program. Based on the very limited data obtained, it would appear that the presence of SiC was at least not harmful in the thermal-shock test (see Table 8, Formulations 8 and 9). Arguments for and against SiC whiskers as a resin-reinforcing agent were given recently by Milewski (Ref. 20) and West (Ref. 21).

3. Preliminary Screening of Candidate Resin Systems

To facilitate the eventual selection of five systems for physical screening, promising candidates were subjected to preliminary screening by means of a T_g determination and a thermal-shock-resistance test. T_g values for candidate resin systems are considered indicative of inherent resin flexibility; all else being equal, the lower the T_g the better a resin can resist the buildup of damaging thermal-contraction stresses at low temperatures (Ref. 22). Thermal-shock resistance was measured by a modification of a standard test (MIL-I-16923E, 19 July 1963). Details on both test procedures are given in Appendix A.

Thermal-shock and T_g data are given in Table 8. In general, unmodified systems, or those modified by flexibilizers such as LP-3 and Cardolite NC513, failed the thermal-shock test. Systems modified by materials such

* Formerly known as S-HTS or S-994-HTS.

** The incorporation of SiC whiskers was suggested by the NASA Project Manager.

TABLE 6

MODIFIED RESIN SYSTEMS

No.	Formulation	Cure Schedule hours/°F	Results
	(Parts by Weight) Ingredient*		
1	(50) Epon 828/(50) Epon 1031/(134) DSA/ (1.0) BDMA	2/150 + 4/250 + 6/300	Satisfactory
2	(50) Epon 828/(50) Epon 1031/(90) NMA/ (21) BOHET/(1.0) BDMA	2/150 + 4/250 + 6/300	Satisfactory
3	(100) Epon 828/(93.8) DSA/(27) NMA/(1.0) BDMA	4/300	Satisfactory
4	(100) Epon 828/(115.9) DSA/(20) Empol 1040/(1.0) BDMA	2/150 + 4/300	Satisfactory
5	(100) Epon 828/(115.9) DSA/(20) Empol 1040/(41) SiC/(1.0) BDMA	2/150 + 4/300	Some minute air inclusions
6	(100) Epon 828/(160) Empol 1040/(2.6) BDMA	2/150 + 4/300	Flexible, with some tackiness
7	(100) Epon 828/(160) Empol 1040/(46) SiC/ (2.6) BDMA	2/150 + 4/300	Bleeding out of one of compo- nents in upper half of cast specimen
8	(80) Epon 828/(20) Z-6077/(115.9) DSA/ (20) Empol 1040/(1.0) BDMA	4/300	Satisfactory
9	(80) Epon 828/(20) Empol 1040/(20) Z-6077/(17.2) Z	4/300	Specimen cloudy, ingredi- ents not com- patible
10	(100) Epon 828/(134) DSA/(26) BOHET/(1.0) BDMA	2/150 + 4/300	Satisfactory
11	(100) Epon 828/(25) Mod-Epoxy/(14) Z	2/225	Satisfactory
12	(100) Epon 828/(25) Mod-Epoxy/(22) SiC/ (14) Z	2/225	Some minute air inclusions
13	(100) Epon 828/(20) R-15 M/(75) HHPA/ (1.0) BDMA	4/300	Ingredients not compatible
14	(90) Epon 828/(10) LP-3/(18) Z	1/195 + 2/350	Satisfactory
15	(70) Epon 828/(30) LP-3/(14) Z	1/195 + 2/350	Satisfactory
16	(70) Epon 828/(30) Cardolite NC513/ (16.2) Z	1/195 + 2/350	Satisfactory

(cont.)

* Ingredients are further identified in Table 7.

TABLE 6 (cont.)

No.	Formulation	Cure Schedule hours/°F	Results
	(Parts by Weight) Ingredient		
17	(65) Epi-Rez 510/Epi-Rez 502/(10) Epi-Cure 86	1/220	Satisfactory
18	(80) Epon 828/(20) Z-6077/(50) Epi-Cure 8501/(10) TEPA	16/77 + 2/200	Satisfactory
19	(80) Epon 828/(20) Z-6077/(25) MDA	6/250 + 16/300	Satisfactory
20	(100) Adiprene L-100/(10.2) DDS	5/285	Resilient, slight tacki- ness
21	(50) Epon H-825/(50) Adiprene L-420/(22) MOCA	5/285	Satisfactory
22	(70) Epon H-825/(30) Adiprene L-420/(27.2) MOCA	5/285	Satisfactory
23	(50) Epon 828/(50) Adiprene L-100/(22.4) DDS	5/285	Satisfactory
24	(50) Epon 871/(50) Adiprene L-420/(12.2) MOCA	5/285 + 5/285	Tacky after 5 hours cure; cured specimen resilient, poor resistance to tear
25	(35) Epon 828/(15) Epon 871/(50) Adiprene L-100/(21.15) MOCA	5/285	Satisfactory
26	(35) Epon 828/(15) Epon 871/(50) Adiprene L-100/(19.65) DDS	5/285	Satisfactory
27	(35) Epon 828/(15) Epi-Rez 502/(50) Adiprene L-100/(21) DDS	5/285	Satisfactory
28	(80) AP-262M/(20) Z-6077/(1.0) BP	1/150 + 1/250	Satisfactory
29	(80) AP-262M/(20) Z-6077/(18) SiC/(110) BP	1/150 + 1/250	Satisfactory
30	(80) AP-262M/(20) RTV-655/(1.8) BP	1/150 + 1/250	Ingredients not compatible
31	(50) AP-262M/(50) Buton 100/(1.0) BP	1/150 + 1/250	Ingredients not compatible

TABLE 7

MATERIALS USED IN TABLE 6 RESIN SYSTEMS

Ingredients	Source
Adiprene L-100, L-420, polyurethane resins	E. I. du Pont de Nemours & Co., Wilmington, Del.
AP-262M, polyester resin	Rohm & Haas Co., Philadelphia, Pa.
BDMA, benzyldimethylamine	Sumner Chemical Co., New York, N.Y.
BOHET, HET-acid bis(octafluoropentyl)- ester	Aerojet-General Corporation, Azusa, Calif.
BP, benzoyl peroxide	
Buton 100, butadiene/styrene co- polymer	Enjay Laboratories, Linden, N.J.
Cardolite NC513, epoxy modifier	Minnesota Mining and Manufacturing Co., Newark, N.J.
DDS, diaminodiphenylsulfone	K & K Laboratories, Inc., New York, N.Y.
DSA, dodecenyl succinic anhydride	Allied Chemical Corp., New York, N.Y.
Epi-Rez 510, 502; Epi-Cure 8501, 86, epoxy resins and curing agents	Jones-Dabney Co., Louisville, Ky.
Epon H-825, 828, 871, 1031, epoxy resins	Shell Chemical Co., Plastics and Resins Division, Downey, Calif.
HHPA, hexahydrophthalic anhydride	Allied Chemical Corp., New York, N.Y.
LP-3, polysulfide	Thiokol Chemical Corp., Trenton, N.J.
MDA, p,p'-methylenedianiline	Dow-Corning Corp., Midland, Mich.
MOCA, 4,4'-methylene-bis(2-chloro- aniline)	E. I. du Pont de Nemours & Co., Wilmington, Del.
Mod-Epoxy, epoxy resin modifier	Monsanto Chemical Co., St. Louis, Mo.
NMA, nadic methyl anhydride	Allied Chemical Corp., New York, N.Y.
R-15M, Poly B-D liquid resins	Sinclair Petrochemicals, Inc., New York, N.Y.
RTV-655, silicone resin	General Electric Co., Waterford, N.Y.
SiC, silicon carbide fiber, single crystals	Carborundum Co., Niagara Falls, N.Y.
TEPA, tetraethylene pentamine	Union Carbide Corp., New York, N.Y.
Empol 1040	Emery Industries, Inc., Cincinnati, Ohio

(cont.)

TABLE 7 (cont.)

<u>Ingredients</u>	<u>Source</u>
Curing Agent Z	Shell Chemical Co., Plastics and Resins Division, Downey, Calif.
Z-6077, 1,3-bis(3-glycidoxypropyl)- tetramethyldisiloxane	Dow-Corning Corp., Midland, Mich.

TABLE 8

THERMAL-SHOCK AND T_g DATA ON CANDIDATE RESIN SYSTEMS

No.	Resin System	Ref: Item Nos. in Table 6	Thermal-Shock Test Results	T _g , °C
1	Epon 828/Epon 1031/NMA/BDMA	(Table 1)	-	>115
2	Epon 828/HHPA/BDMA	-	Narrowly marginal	>100
3	Adiprene L-100/MOCA	(Table 2)	-	<23
4	Adiprene L-420/MOCA	(Table 2)	-	<23
5	Epon 828/Epon 1031/DSA/BDMA	1	-	78
6	Epon 828/Epon 1031/NMA/BOHET/BDMA	2	Failed	>88
7	Epon 828/DSA/NMA/BDMA	3	Marginal	-
8	Epon 828/DSA/Empol 1040/BDMA	4	Passed*	44
9	Epon 828/DSA/Empol 1040/SiC/BDMA	5	Passed	57
10	Epon 828/Z-6077/DSA/Empol 1040/BDMA	8	Passed	13
11	Epon 828/DSA/BOHET/BDMA	10	Passed	34
12	Epon 828/Mod-Epoxy/Z	11	Passed	39
13	Epon 828/Mod-Epoxy/SiC/Z	12	Failed**	-
14	Epon 828/LP-3/Z	14,15	Failed	-
15	Epon 828/Cardolite NC513/Z	16	Failed	-
16	Epi-Rez 510/Epi-Rez 502/Epi-Cure 86	17	-	41
17	Epon 828/Z-6077/Epi-Cure 8501/TEPA	18	Passed	16
18	Epon 828/Z-6077/MDA	19	Passed	12
19	Epon H-825/Adiprene L-420/MOCA	21	Passed	-
20	Epon 828/Adiprene L-100/DDS	23	Passed	-
21	Epon 828/Epon 871/Adiprene L-100/ MOCA	25	Passed	12.5
22	Epon 828/Epon 871/Adiprene L-100/DDS	26	Passed	40
23	Epon 828/Epi-Rez 502/Adiprene L-100/ DDS	27	Passed	24
24	AP-262M/Z-6077/BP	28	Failed	14,72***

* After the completion of ten cycles between +90 and -55°C, the sample was still strongly bonded to the test tube in which it was cast. In "failed" samples, the strain was sufficient to break the bond between the glass test tube and the resin.

** Failure may have been due to air inclusion.

*** Two inflections were noted in the strain/temperature plot.

as DSA, Empol 1040, Z-6077, Adiprene L-100, and Adiprene L-420 generally passed the test. As a result, Formulations 8, 11, 17, and 21 were selected as the preferred candidates for further evaluation.

The T_g values were high (above 100°C) for unmodified (high-strength) systems. Modification by Z-6077 or an Adiprene resulted in T_g values under 40°C . Intermediate T_g values ($40^{\circ}\text{C} < T_g < 100^{\circ}\text{C}$) were obtained in systems modified by DSA and Empol 1040.

Based on the guidelines and considerations noted in Section II,B,1 and results obtained in resin casting, thermal-shock tests, and T_g determinations, five candidate cryogenic resin systems were selected for physical screening (Table 9).

Formulation 1 was chosen in order to have a representative unmodified (high-strength) system for which cryogenic data existed. Such a system served as a standard with which the modified systems were compared. The actual or full benefits that might derive from the presence of BOHET in Formulation 3 could not be known until composite specimens were tested. Formulations 2, 4, and 5 were highly modified epoxys. In Formulation 2, modification was accomplished with a long-chain anhydride and a high-molecular-weight tricarboxy acid. Formulation 4, a hybrid epoxy modified by L-100 polyurethane, was expected to have improved low-temperature properties. In Formulation 5, Epon 828 was modified by an epoxy/silicone and a long-chain polyamine. The silicone was expected to improve resin-wetting action and low-temperature properties.

C. PHYSICAL SCREENING OF CANDIDATE RESIN SYSTEMS

1. Background

The cast-resin properties influencing the performance of FWC structures at ambient temperature, and the interrelationships between these properties, had been identified in earlier studies at Aerojet (Appendix B). In essence, the resin properties were ranked in the following order of importance: (a) notch toughness, (b) tensile strength at fracture, (c) ultimate elongation, and (d) toughness (the area under the stress-strain curve). When the cross products of properties from all the resin systems were used in linear-regression analysis, the ranking of the most significant properties was (a) notch toughness times tensile strength at fracture, (b) tensile strength at fracture, (c) elongation times notch toughness, (d) toughness, and (e) tensile strength at fracture times toughness.

The physical-screening phase of Task I included determination of the foregoing mechanical properties and cross-product indices, as well as the viscosity and pot-life characteristics. Resins for further testing in Task II were selected essentially on the basis of these results.

2. Test Methods

Test methods for Task I physical screening are presented in Appendix A. The procedures used adhered generally to those described in

TABLE 9

CANDIDATE SYSTEMS FOR TASK I SCREENING

Resin No.	Formulation (Parts by Weight)	Mixing Procedure and Cure Schedule
1	(100) Epon 828/(20) DDS/(1) BF ₃ -400	Heat resin to 300°F, add DDS and mix until homogeneous. Cool to 195°F and add BF ₃ -400, with stirring. Pour into heated mold. Cure: 2 hours at 260°F, 4 hours at 350°F.
2	(100) Epon 828/(115.9) DSA/ (20) Empol 1040/(1) BDMA	(a) Mix and warm epoxy and Empol 1040 to 212°F. While stirring, add DSA and then BDMA. Cure: 2 hours at 150°F, 4 hours at 300°F. (b) Mix and warm epoxy and Empol 1040 to 212°F. Cool to room temperature and add DSA and BDMA. Cure: 2 hours at 150°F, 4 hours at 300°F.
3	(100) Epon 828/(134) DSA/ (26) BOHET*/(1) BDMA	Mix epoxy, DSA, and BOHET, and add BDMA. Cure: 2 hours at 150°F, 4 hours at 300°F.
4	(35) Epon 828/(15) Epon 871/ (50) Adiprene L-100/(21) MOCA	Heat the epoxies and L-100 to 212°F and degas for 10 min, with continuous stirring, at a 29-in.-Hg vacuum. Add molten MOCA (225°F) and degas the mix as before, with stirring, for 3 min. Cure: Pour into heated mold at 200°F. Heat 5 hours at 285°F.
5	(80) Epon 828/(20) Z-6077/ (50) Epi-Cure 8501/(10) TEPA	Mix ingredients and pour into mold. Cure: 16 hours at 77°F, 2 hours at 200°F.

*The preparation of BOHET is described in Appendix C.

American Society for Testing Materials (ASTM) Standards and Federal Test Method (FTM) Standard No. 406, with necessary modifications for testing under cryogenic conditions. Room-temperature tests were performed between 70 and 75°F.

3. Test Results

a. Tensile and Notch Toughness

The tensile and notch-toughness specimens were formed to the desired configuration from flat panels that had been cast and cured in steel molds. Void-free specimens were obtained by mixing and degassing all formulations in a vacuum environment for 1/2 hour before the resin was poured into the molds. Cracks noted in the panels of Resin 3 were eliminated by modifying the cure schedule toward a lower final temperature. After curing, the specimens were cut with a diamond saw into rectangular shapes to permit insertion into the routing fixture. The specimens were routed to a final configuration having tapered ends and were carefully sanded with No. 400A sandpaper to promote a uniform surface and thereby minimize data scatter. Resin 4, being a high-elongation system, proved the most difficult to rout because of specimen flexibility. Notches of the desired dimensions were incorporated in all specimens with a special cutting tool. Care was required in inserting the tool in specimens of Resin 1 because of its brittle nature.

The specimens were assembled in tapered-grip fixtures that matched their shape. Problems were encountered with some notch-toughness specimens during preparation for cryogenic testing, and some specimens (Resins 1 and 2) cracked while being aligned in the test fixture. Cryogenic testing was performed with LH₂ (-423°F) in the cryostat/Baldwin tensile-testing facility. The tests were performed in a remote area, and all recommended safety precautions were observed.

As shown in Table 10, the candidate resins displayed a wide range of values at room temperature. The ultimate tensile strength was 10,930 psi (10.93 ksi) for Resin 1 and 1.27 ksi for Resin 4. The values for tensile strength at fracture and for ultimate strength were identical in each case for Resins 1, 4, and 5; Resins 2 and 3 exhibited plastic tensile instability after reaching the ultimate tensile strength, with a resultant lower value for the tensile strength at fracture. This instability (strain increase without a concomitant stress increase) was particularly evident with Resin 2 (4.0% elongation at ultimate tensile strength, 26.5% elongation at fracture). Values for tensile modulus ranged from an average of 456.2 ksi for Resin 1 to 2.3 ksi for Resin 4. Elongation at ultimate tensile strength ranged from 3.6% (No. 3) and 3.7% (No. 1) to 79% (No. 4). The highest value for notch toughness at room temperature was obtained with Resin 2. Table 11 summarizes the room-temperature test results for all systems.

As might be expected, a much less pronounced range of values occurred when the resins were tested at -423°F (Table 12). The ultimate tensile strength increased for all systems; the greatest increase (1310%) and the highest strength (17.90 ksi) were exhibited by Resin 4. For each system, fracture occurred at the ultimate tensile strength. Some tensile data were rejected because examination of fractured specimens indicated that failure might

TABLE 10

SUMMARY OF TASK I SCREENING TESTS, CANDIDATE CRYOGENIC RESIN SYSTEMS

Resin System (Parts by Weight)	Tensile Strength				Tensile Modulus		Elongation, %				Notch Toughness		Glass Trans Temp °C	Initial Viscosity cp	Hours*	
	ksi		ksi		ksi		Ultimate Stress		At Fracture		psi/in.				Pot Life	Gel Time
	RT	-423°F	RT	-423°F	RT	-423°F	RT	-423°F	RT	-423°F	RT	-423°F				
Epon 826/DDS/BF ₃ -400 (100/20/1)	10.93	13.85	10.93	13.85	456.2	1297	3.7	1.2	3.7	1.2	504	659	135	138.2 (177°F)	1.25	>16.5
Epon 828/DSA/Empol 1040/BDMA (100/115.9/20/1)	4.25	13.80	2.60	13.80	220.9	917	4.0	1.5	26.5	1.5	2745	1204	44	1656 (79°F)	1.8	> 22
Epon 828/DSA/BOHET/BDMA (100/134/26/1)	6.41	12.14	5.12	12.14	322.9	1212	3.6	1.0	5.6	1.0	1463	986	34	1207 (78.5°F)	11.0	~ 15
Epon 828/Epon 871/Adiprene L-100/MOCA (35/15/50/21)	1.27	17.90	1.27	17.90	2.3	1377	79.0	1.3	79.0	1.3	279	2916	12.5	1590 (132°F)	0.1	> 24
Epon 828/Z-6077/Epi-Cure 8501/TEPA (80/20/50/10)	1.30	10.18	1.30	10.18	24.8	1225	24.0	0.8	24.0	0.8	562	1012	16	534.5 (76°F)	1.5	1.6

* Pot life is defined here as the period during which the resin viscosity remained below 2500 cp.

Gel time is defined here as the period during which viscosity readings could be recorded (before gelation).

TABLE 11

PRELIMINARY SCREENING, RESULTS OF TENSILE AND NOTCH-TOUGHNESS TESTS (ROOM TEMPERATURE)

Resin No.	Resin System (Parts by Weight)	Tensile Stress, ksi		Tensile Modulus ksi	Elongation, %		Notch Toughness psi√in.
		Ultimate	At Fracture		Ultimate Stress	At Fracture	
1	Epon 826/DDS/RF ₃ -400 (100/20/1)	12.28	12.28	467.8	4.6	4.6	541.2
		10.31	10.31	458.7	3.2	3.2	-
		10.22	10.22	442.1	3.3	3.3	467.7
		Av 10.93	10.93	456.2	3.7	3.7	504.4
2	Epon 828/DSA/Empol 1040/BDMA (100/15.9/20/1)	4.48	2.65	220.7	4.1	31.0	2810.0
		4.13	2.58	218.0	4.0	24.0	2713.3
		4.14	2.58	224.1	4.0	25.0	2713.7
		Av 4.25	2.60	220.9	4.0	26.5	2745.7
3	Epon 828/DSA/BOHET/BDMA (100/134/26/1)	2.21*	2.21*	336.7	0.65*	0.65*	1590.5
		6.52	5.09	320.8	3.6	5.8	1192.0
		6.31	5.16	311.3	3.7	5.4	1608.7
		Av 6.41	5.12	322.9	3.6	5.6	1463.4
4	Epon 828/Epon 871/ Adiprene L-100/MOCA (35/15/50/21.1)	1.22	1.22	1.6	79.0	79.0	297.2
		1.33	1.33	2.2	78.5	78.5	275.6
		1.28	1.28	3.2	79.0	79.0	266.1
		Av 1.27	1.27	2.3	79.0	79.0	279.6
5	Epon 828/Z-6077/Epi-Cure 8501/TEPA (80/20/50/10)	1.31	1.31	26.2	21.5	21.5	566.8
		1.36	1.36	21.5	26.5	26.5	550.8
		1.24	1.24	26.6	24.0	24.0	569.3
		Av 1.30	1.30	24.8	24.0	24.0	562.3

* Specimen exhibited air voids, and data rejected.

TABLE 12

PRELIMINARY SCREENING, RESULTS OF TENSILE AND NOTCH-TOUGHNESS TESTS (-423°F)

Resin No.	Resin System (Parts by Weight)	Tensile Stress, ksi		Tensile Modulus ksi	Elongation, %		Notch Toughness psi√in.
		Ultimate	At Fracture		Ultimate Stress	At Fracture	
1	Epon 826/DDS/BF ₃ -400 (100/20/1)	10.85*	10.85	1164	0.9	0.9	**
		15.17	15.17	1297	1.2	1.2	**
		12.53	12.53	--	-	-	659.1
		Av 13.85	13.85	1297	1.2	1.2	659.1
2	Epon 828/DSA/Epon 1040/BDMA (100/15.9/20/1)	12.84	12.84	958	1.3	1.3	**
		15.13	15.13	951	1.6	1.6	1227.5
		13.43	13.43	842	1.6	1.6	1180.9
		Av 13.80	13.80	917	1.5	1.5	1204.2
3	Epon 828/DSA/BOHET/BDMA (100/134/26/1)	7.06*	7.06	--	-	-	945.4
		12.56	12.56	1209	1.0	1.0	976.7
		11.72	11.72	1216	1.0	1.0	1037.1
		Av 12.14	12.14	1212	1.0	1.0	986.4
4	Epon 828/Epon 871/Adiprene L-100/MOCA (35/15/50/21.1)	11.56*	11.56	1251	0.9	0.9	2567.1
		17.90	17.90	1377	1.3	1.3	2728.3
		15.64*	15.64	--	0.7	0.7	3453.3
		Av 17.90	17.9	1377	1.3	1.3	2916.2
5	Epon 828/Z-6077/Epi-Cure 8501/TEPA (80/20/50/10)	10.15	10.15	1220	0.8	0.8	987.6
		9.00*	9.00	1270	0.7	0.7	428.3***
		10.21	10.21	1230	0.8	0.8	1036.4
		Av 10.18	10.18	1225	0.8	0.8	1012.0

* Data rejected because failure may have been due to notch effect caused by extensometer.

** Specimen fractured during setting up in cryostat/tensile-machine facility.

*** In averaging results, data rejected as extreme.

be attributable to a notch effect caused by placing the extensometer on the specimen. (It was shown in Task II, however, that the extensometer had no significant effect on the tensile-strength level obtained.) Tensile-modulus values increased for all systems, with the largest being shown by Resin 4 (from 2.3 ksi to 1377 ksi). The elongation at fracture was considerably reduced (and the inter-resin range of values constricted) at -423°F ; the highest value was 1.5% (No. 2), and the lowest 0.8% (No. 5). The notch toughness of Resin 4 increased tenfold at -423°F , whereas that of Resin 2, which had the highest value at ambient temperature ($2745 \text{ psi}\sqrt{\text{in.}}$), declined to $1204 \text{ psi}\sqrt{\text{in.}}$. At this level, however, Resin 2 was still the second best system.

b. Viscosity and Pot Life

The two processes used in the manufacture of filament-wound composites (in-process impregnation and preimpregnation) impose different viscosity and pot-life requirements on the resin systems used. A principal goal of this program was the development of a number of resins suitable for in-process impregnation (wet winding).^{*} For this purpose a desirable viscosity of resin mix is considered to be 1000 to 2500 cp (room temperature), with a maximum viscosity, before curing agent is added, of about 10,000 cp. The latter viscosity is permissible only if resin heating lowers the viscosity into the 2000 to 2500-cp range where in-process impregnation can be accomplished effectively. A promising resin system is one that has an adequate pot life at that practicable temperature (preferably but not necessarily ambient) where its viscosity is 2500 cp or less.

For in-process impregnation, an indefinite pot life would be ideal, but in practice minimum pot lives of 1 to 2 hours are satisfactory for laboratory and subscale impregnation, provided the viscosity remains in a working range. For large fabricated structures, a pot life of at least one work shift (8 hours) is desirable.

Viscosity readings in this program were obtained with a Brookfield Viscometer, Model LVT. During the determination of viscosity for pot-life evaluations, it was necessary at times to change the spindle or the rate of rotation in order to keep the torque readings on the dial. Viscosity and pot-life test results are summarized in Tables 10 and 13 and provide the basis for viscosity/time curves in Figures 1 and 2.

(1) Resin 1 (Epon 826/DDS/BF₃-400)

Because the mixing procedure for this system was completed at 195°F , initial viscosity readings were obtained near this temperature. The values were 120 and 237 cp at 182 and 165°F , respectively. The

^{*}For application as prepreg (preimpregnated roving) a resin mix must be sufficiently soluble in a suitable working solvent, such as acetone or methyl ethyl ketone (MEK). The solvent-free resin must have enough pot life or gel time so that heat may be added to remove the solvent without advancing the resin past the B-stage. Ideally, the prepreg itself should be indefinitely stable, but a practical minimum useful life is 24 hours at room temperature.

TABLE 13

VISCOSITY TEST RESULTS

Resin No.	Resin System (Parts by Weight)	Initial Viscosity cp	Initial Temp °F	Notes
1	Epon 826/DDS/BF ₃ -400 (100/20/1)	120.0	180	*
		138.2	177	*
		236.8	165	*
2	Epon 828/DSA/Empol 1040/BDMA (100/115.9/20/1)	365.0	106.5	*
		798.0	92.0	**
		792.3	90.0	*
		1656.2	79.0	***
3	Epon 828/DSA/BOHET/BDMA (100/134/26/1)	1207.5	78.5	***
		1791.2	72.5	***
		1825.0	73.5	***
4	Epon 828/Epon 871/Adiprene L-100/ MOCA (35/15/50/21.1)	1263.3	167.0	*
		1590.0	132.0	*
		2460.0	122.5	*
5	Epon 828/Z-6077/Epi-Cure 8501/ TEPA (80/20/50/10)	517.5	77	*
		534.5	76	*
		553.5	75	*

-
- * Viscosity and temperature are average of three readings at spindle speeds of 6, 12, and 30 rpm.
- ** Viscosity and temperature are average of three readings at spindle speeds of 4, 10, and 20 rpm.
- *** Viscosity and temperature are average of two readings at spindle speeds of 6 and 12 rpm.

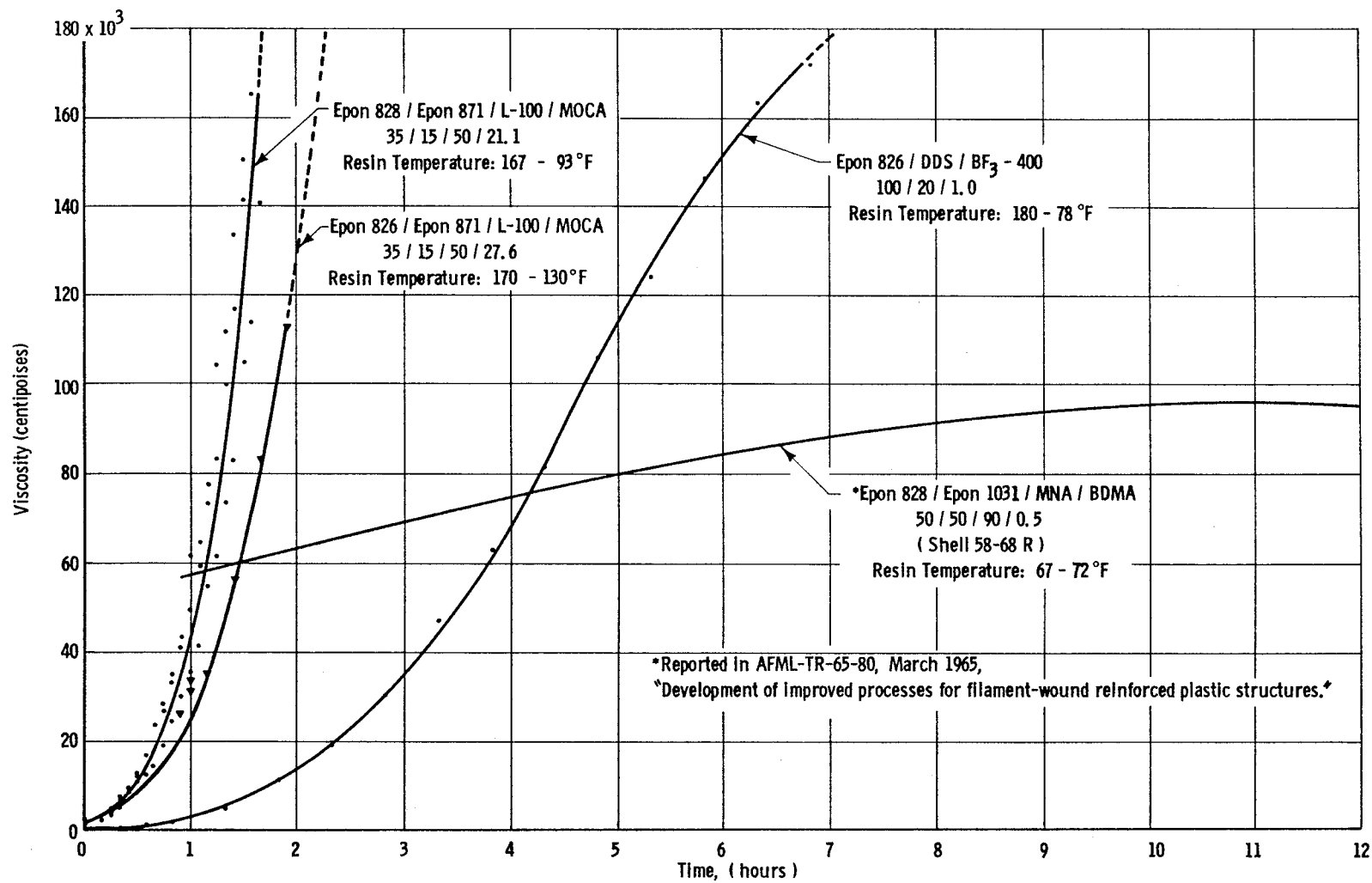


Figure 1. Viscosity-Time Curves (Potential Prepreg Systems)

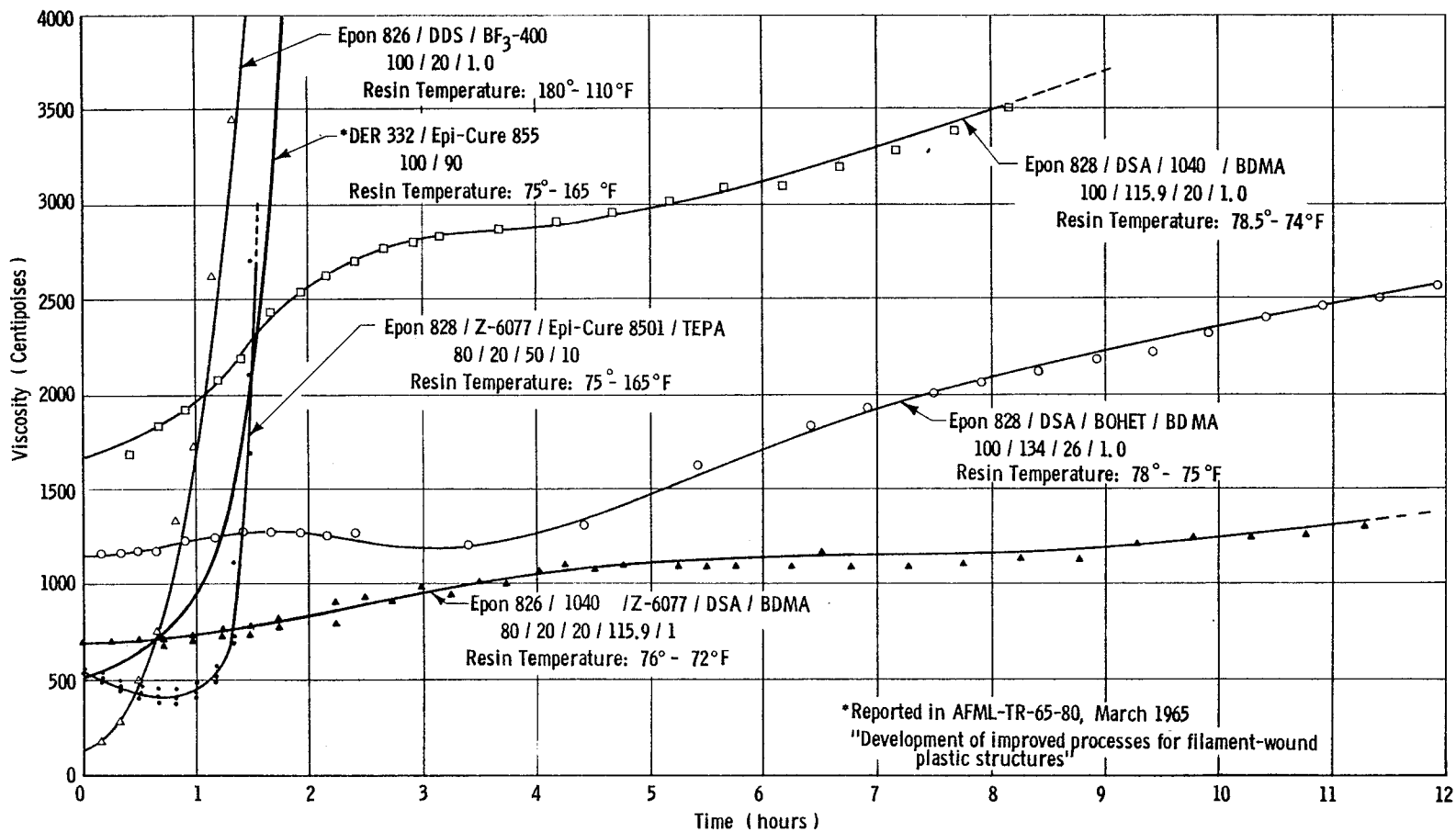


Figure 2. Viscosity-Time Curves (Potential In-Process or Prepreg Systems)

viscosity remained below 2500 cp for about 1.2 hours, the temperature gradually falling to ambient over 10 to 16 hours. The mix did not harden during this period, but the viscosity reached 204,000 and 228,000 cp.

(2) Resin 2 (Epon 828/DSA/Empol 1040/BDMA)

Viscosity and pot life were determined using two different mixing procedures (Table 9). If the epoxy and Empol 1040 were heated to 212°F, mixed, and DSA and BDMA added at this temperature, 2500 cp (80 to 84°F) was attained within 1 to 2-2/3 hours, exhibiting some variability. After 22 hours of testing, the system had a viscosity of 7420 cp and showed no signs of "setting up."

If the mixture of epoxy and Empol 1040 was cooled from 212°F to room temperature prior to the addition of DSA and BDMA, the resulting mix had values of 1656 cp (80°F) initially and 2448 cp after 1.7 hours (76°F). Over an 8-to 10-hour period, the viscosity increased gradually to 3510 cp (74°F).

(3) Resin 3 (Epon 828/DSA/BOHET/BDMA)

The ingredients were easily mixed. The mix viscosity remained below 2500 cp for approximately 11 hours. The test was terminated after 15 hours, with no sign of resin hardening; viscosity at this point was 2960 cp. The mix was still workable after 72 hours.

(4) Resin 4 (Epon 828/Epon 871/L-100/MOCA)

The initial viscosity readings were approximately 1550 cp at 133°F and 2300 cp at 122°F. The readings were generally in excess of 10,000 cp after 30 min of testing. The mix had not set up after 24 hours.

(5) Resin 5 (Epon 828/Z-6077/Epi-Cure 8501/TEPA)

The initial value of 550 cp (73°F) increased to approximately 2700 cp (151°F) within 1-1/2 hours. The pot life was estimated at 1.5 hours, with the mix hardening rapidly thereafter.

On the basis of these data, the following conclusions were drawn:

- Resin 1 was probably suitable for in-process impregnation at a mix temperature of about 120°F.
- Resin 2 was probably suitable for in-process impregnation at a slightly advanced temperature of 90°F if prepared by mix procedure (1), and at 75 to 80°F if prepared by mix procedure (2).
- Resin 3 was suitable for in-process impregnation at ambient temperature.

- Resin 4 was unsuitable for in-process impregnation. As shown in Appendix D, however, it was readily miscible with both acetone and MEK, suggesting that this formulation would be of possible interest for the preparation of prepreg.

- Although Resin 5 was exothermic, it was probable that the pot life and viscosity would be adequate for in-process impregnation if the mix were cooled, thus controlling the temperature rise. It was also possible that modification by reducing the concentration of TEPA would effectively slow the reaction.

- Although solubility in a suitable solvent was demonstrated only for Resin 4, it was considered likely that the other four systems would also be sufficiently soluble for use in prepreg formulations.

D. SELECTION OF CANDIDATE RESINS FOR TASK II

Evaluation of Task I screening results led to the selection of Resins 2, 3, 4, and 5 for further examination in Task II. As noted previously, the resins were chosen essentially on the basis of their notch toughness, tensile strength at fracture, elongation, and resultant cross-product indices; the data are shown in Table 14. It is noteworthy that although System 4 had the lowest ambient-temperature value for notch toughness times tensile strength at fracture, it had by far the highest value at -423°F . The outstanding low-temperature properties of this system are also evident from its larger value for notch toughness times elongation at fracture at -423°F , relative to the other systems.

Resin 1 was originally included as a known, "high-strength" system that might serve as a benchmark or comparison standard, against which the modified (and unknown) resins might be compared. At no time in the program was it expected that such a system would be outstanding for cryogenic application. That expectation (as well as the underlying hypotheses) was confirmed by the screening tests, which suggest that the other four systems are preferable for cryogenic use.

Although Resins 2 and 3 were clearly very promising, it was recognized that Resins 4 and 5 had serious shortcomings in addition to their attractive features. Resin 4 had outstanding low-temperature, but poor ambient properties, and its viscosity was too high for in-process impregnation. Resin 5 was exothermic after mixing, which would necessitate mix cooling during processing. Besides their desirable properties, both were considered inherently attractive because of their chemical natures - epoxy/polyurethane and epoxy/silicone, respectively. For these reasons, both formulations were modified for Task II in an attempt to moderate their weaknesses without surrendering too much of their strengths. This effort was not required by the scope of the program. Formulation 4 was changed only to the extent of a 31.4% increase in the curing agent, and was renamed Resin 4A. Formulation 5 was extensively modified and renamed Resin 6 (Table 15).

TABLE 14

COMPARISON FACTORS FOR CANDIDATE CRYOGENIC RESIN SYSTEMS

Resin No.	Resin System (Parts by Weight)	Notch Toughness Times		Tensile Strength at		Notch Toughness Times	
		Tensile, RT	Fracture, -423°F	Fracture, ksi RT	Fracture, ksi -423°F	Elongation at RT	Elongation at Fracture -423°F
1	Epon 826/DDS/BF ₃ -400 (100/20/1)	5,509	9,127	10.93	13.85	1,865	791
2	Epon 828/DSA/Empol 1040/ BDMA (100/115.9/20/1)	7,137	16,615	2.60	13.80	72,743	1,806
3	Epon 828/DSA/BOHET/BDMA (100/134/26/1)	7,490	11,970	5.12	12.14	8,193	986
4	Epon 828/Epon 871/Adiprene L-100/MOCA (35/15/50/21.1)	355	52,196	1.27	17.90	22,041	3,791
5	Epon 828/Z-6077/Epi-Cure 8501/ TEPA (80/20/50/10)	731	10,302	1.30	10.18	13,488	810

TABLE 15

CANDIDATE RESIN SYSTEMS FOR TASK II TESTING

<u>Resin No.</u>	<u>Resin System (Parts by Weight)</u>	<u>Mixing Procedure and Cure Schedule</u>
2	Epon 828/DSA/Empol 1040/BDMA (100/115.9/20/1)	Mix and warm epoxy and Empol 1040 to 212°F. Cool to room temperature and add DSA and BDMA. Cure: 2 hours at 150°F, 4 hours at 300°F.
3	Epon 828/DSA/BOHET/BDMA (100/134/26/1)	Mix epoxy, DSA, and BOHET; then add BDMA. Cure: 2 hours at 150°F, 4 hours at 300°F. Alternate cure: 8 hours at 225°F.
4A	Epon 826/Epon 871/Adiprene L-100/MOCA (35/15/50/27.6)	Heat the epoxies and L-100 to 212°F and degas them for 10 min, with continuous stirring, in a 29-in.-Hg vacuum. Melt MOCA (ground with mortar and pestle) at 225°F and add it to the mix. Degas the mix as before, with stirring, for 3 min. Cure: Pour into heated mold at 200°F, heat 5 hours at 285°F.
6	Epon 826/Empol 1040/Z-6077/DSA/BDMA (80/20/20/115.9/1)	Heat Epon 826 and Empol 1040 to 212°F and mix thoroughly at this temperature. Cool to ambient temperature and add, while stirring, Z-6077, DSA, and finally BDMA. Cure: 8 hours at 260°F.

III. TASK II - EVALUATION OF CANDIDATE CRYOGENIC RESINS

A. TEST METHODS

Following approval of the four candidate resins (Table 15) by the NASA Project Manager, characterization of the systems was undertaken in extensive testing of cast resin and filament-wound composites. The following tests were conducted at ambient temperature (approximately 75°F), -320, and -423°F, except as noted:

1. Tensile strength, including tensile modulus, elongation, and toughness
2. Notch toughness
3. Impact strength
4. Interlaminar shear strength (by short-span-shear and horizontal-shear methods, including the determination of resin and void contents)
5. Coefficient of linear thermal contraction
6. Thermal-shock resistance (temperature cycling between +75 and -423°F)
7. Specific gravity (at 75°F only)
8. Viscosity (at 75°F and higher)
9. Pot life (at 75°F and higher)
10. Resin shrinkage (%) during cure (at 75°F only).

Tensile-strength, notch-toughness, viscosity, and pot-life tests were performed as described in Appendix A, which also gives procedures for the remaining tests in Task II. In general, the methods adhered to those described in the latest ASTM Standards or in FTM Standard No. 406.

B. TEST RESULTS

1. Tensile Strength and Associated Properties

Tapered-end tensile-strength test specimens were routed from 0.125-in.-thick flat-panel castings, and were assembled in fixtures that matched their shape. Testing was performed at room temperature and in a cryostat utilizing LN₂ (-320°F) or LH₂ (-423°F). The specimens were stressed in tension, using a 0.05-in./min crosshead travel, until failure occurred.

Tables 16 through 18 present test data, including ultimate tensile strength, tensile strength at fracture, tensile modulus, elongation at ultimate stress and at fracture, and toughness. The latter, an indication of

TABLE 16

TENSILE-TEST RESULTS AT 75°F (TASK II)

Resin No.	Resin System (Parts by Weight)	Tensile Stress, ksi		Tensile Modulus ksi	Elongation, %		Toughness* lb-in./cu in.
		Ultimate	At Fracture		At Ultimate Stress	At Fracture	
2	Epon 828/DSA/Empol 1040/BDMA (100/115.9/20/1)	6.80	6.15	253.1	3.6	5.0	233.1
		6.72	6.13	308.0	3.6	4.4	
		6.60	6.17	308.0	3.7	4.0	
		6.87	5.92	-	-	-	
		6.65	5.13	-	-	-	
		Av 6.73	5.90	289.7	3.6	4.5	
3	Epon 828/DSA/BOHET/BDMA** (100/134/26/1)	6.14	6.14	353.4	2.2	2.2	157.1
		7.27	7.27	349.0	3.5	3.5	
		7.22	7.00	330.7	3.8	4.2	
		7.43	6.47	-	-	-	
		7.55	7.55	-	-	-	
		Av 7.12	6.89	344.3	3.16	3.3	
4A	Epon 826/Epon 871/L-100/MOCA (35/15/50/27.6)	1.86	1.86	-	142	142	1715.0
		2.55	2.55	16.0	149	149	
		2.49	2.49	15.8	149	149	
		2.67	2.67	9.1	152	152	
		2.47***	2.47***	11.2***	120***	120***	
		Av 2.41	2.41	13.0	142.4	142.4	
6	Epon 826/Empol 1040/Z-6077/DSA/BDMA (80/20/20/115.9/1)	5.57	5.57	278.5	3.0	3.0	109.6
		5.75	5.75	282.4	3.1	3.1	
		5.57	5.57	294.2	3.0	3.0	
		5.70	4.37	-	-	-	
		5.66	4.26	-	-	-	
		Av 5.65	5.10	285.0	3.0	3.0	

* Calculated from the area under the stress-strain curve.

** Specimens prepared using alternate cure (8 hours at 225°F).

*** Value included in averaging of results, although specimen did not fail but slipped out of grip at level shown.

TABLE 17

TENSILE-TEST RESULTS AT -320°F (TASK II)

Resin No.	Resin System (Parts by Weight)	Tensile Stress, ksi		Tensile Modulus ksi	Elongation, %		Toughness* lb-in./cu in.
		Ultimate	At Fracture		At Ultimate Stress	At Fracture	
2	Epon 828/DSA/Empol 1040/BDMA (100/115.9/20/1)	15.26	15.26	758	2.0	2.0	145.0
		**	**	**	**	**	
		14.44	14.44	745.8	2.0	2.0	
		13.75	13.75	656.8	2.0	2.0	
		15.76	15.76	-	-	-	
		Av 14.80	14.80	720.2	2.0	2.0	
3	Epon 828/DSA/BOHET/BDMA*** (100/134/26/1)	10.65	10.65	683.9	1.5	1.5	95.1
		****	****	****	****	****	
		11.79	11.79	694.9	1.7	1.7	
		****	****	727.4	****	****	
		12.33	12.33	764.5	1.6	1.6	
		Av 11.59	11.59	728.9	1.6	1.6	
4A	Epon 826/Epon 871/L-100/MOCA (35/15/50/27.6)	29.25	29.25	1004.9	3.1	3.1	446.0
		25.90	25.90	1066.8	2.8	2.8	
		27.61	27.61	1033.8	-	-	
		27.13	27.13	-	-	-	
		30.13	30.13	-	-	-	
		Av 28.00	28.00	1035.1	2.95	2.95	
6	Epon 826/Empol 1040/Z-6077/DSA/BDMA (80/20/20/115.9/1)	12.17	12.17	746.7	1.8	1.8	109.6
		12.89	12.89	-	1.4	1.4	
		11.16	11.16	753.3	1.5	1.5	
		15.28	15.28	766.6	1.9	1.9	
		-	-	771.9	-	-	
		Av 12.87	12.87	759.6	1.65	1.65	

* Calculated from the area under the stress-strain curve.

** Specimen fractured during setup in grips.

*** Specimens prepared using alternate cure (8 hours at 225°F).

**** Specimen fractured during testing in LN₂.

TABLE 18

TENSILE-TEST RESULTS AT -423°F (TASK II)

Resin No.	Resin System (Parts by Weight)	Tensile Stress, ksi		Tensile Modulus ksi	Elongation, %		Toughness* lb-in./cu in.
		Ultimate	At Fracture		At Ultimate Stress	At Fracture	
2	Epon 828/DSA/Empol 1040/BDMA (100/115.9/20/1)	14.53	14.53	978.8	1.6	1.6	137.0
		11.12	11.12	990.7	1.6	1.6	
		17.13	17.13	963.2	1.9	1.9	
		13.73	13.73	-	-	-	
		15.80	15.80	-	-	-	
		Av 14.46	14.46	977.5	1.7	1.7	
3	Epon 828/DSA/BOHET/BDMA** (100/134/26/1)	12.86	12.86	972.6	1.3	1.3	86.3
		11.65	11.65	-	-	-	
		13.08	13.08	951.7	1.4	1.4	
		10.39	10.39	-	-	-	
		13.14	13.14	-	-	-	
		Av 12.23	12.23	962.1	1.35	1.35	
4A	Epon 826/Epon 871/L-100/MOCA (35/15/50/27.6)	23.13	23.13	1835.5	2.0	2.0	226.0
		21.57	21.57	998.0	2.0	2.0	
		22.18	22.18	1145.4	2.0	2.0	
		17.15	17.15	1246.0	1.5	1.5	
		27.90	27.90	-	-	-	
		22.18	22.18	-	-	-	
6	Epon 826/Empol 1040/Z-6077/DSA/BDMA (80/20/20/115.9/1)	Av 22.35	22.35	1306.2	1.88	1.88	111.3
		13.13	13.13	827.2	1.9	1.9	
		11.14	11.14	934.2	1.5	1.5	
		12.13	12.13	942.6	1.3	1.3	
		15.75	15.75	-	-	-	
		14.10	14.10	-	-	-	
		Av 13.25	13.25	901.3	1.6	1.6	

* Calculated from the area under the stress-strain curve.

** Specimens prepared using alternate cure (8 hours at 225°F).

the work required to fracture a test specimen, was determined by plotting a stress-strain curve for each system at each of the three test temperatures and calculating the area under the curve. Figures 3 through 5 present these stress-strain curves. The pronounced influence of temperature on the stress-strain characteristics of Resin 4A is shown in Figure 6.

Data presented in Table 19* reveal that Resin 3 had the highest 75°F average strength (6.89 ksi) at fracture (3.3% strain), and that Resin 4A had the lowest average strength (2.41 ksi) but by far the greatest elongation (142.4%). Modification of the former Resin 4 system, by substituting Epon 826 for Epon 828 and increasing the quantity of the curing agent, resulted in significant increases in almost all the tensile properties.

Table 19 shows some differences between Task I and Task II values for the tensile properties of Resins 2 and 3. The differences are to be expected for Resin 3 because of the altered cure schedule used in most of Task II (lower temperature and longer durations) since cast panels had exhibited a tendency to crack during the cure. Although the change effectively eliminated cracking, it caused some of the tensile properties to vary significantly.

The differences between Task I and Task II values for Resin 2 are not understood. As might be expected, the discrepancies are larger at room temperature than at cryogenic temperatures. Fortunately, the tensile data for the four candidate resins are such that the relative ranking of Resin 2 is little affected.

The effects of cryogenic temperatures on various tensile properties are shown in Figures 7 through 10. Figure 7 shows that the tensile stress at fracture was considerably higher at cryogenic temperatures than at room temperature. Resins 3 and 6 exhibited slightly higher strengths at -423 than at -320°F, whereas Resins 2 and 4A declined in strength, the latter significantly. Even so, Resin 4A remained some 50% stronger than the next strongest system. Whereas Resins 2, 3, and 6 yielded with increased loading at room temperature, the ultimate and fractural tensile strengths were the same for all systems at cryogenic temperatures (Table 19 and Figures 4 through 7).

In order to determine if the extensometer was creating flaws in test specimens, the instrument was omitted in the testing of two of the five specimens for each resin system. No significant differences in tensile strengths were noted for the two procedures.

Figure 8 shows the "leveling effect" on strains at fracture (or elongation at fracture) experienced at cryogenic temperatures. Resin 4A, with strains of 2.95 and 1.88% at -320 and -423°F, respectively, led the other systems in this property. Although it had a lower tensile modulus at room temperature than the other systems, it displayed significantly higher values at cryogenic temperatures (Figure 9). The superior toughness of Resins 4A and 2 is shown in Figure 10.

*To facilitate data comparison, all Task I and most Task II results are summarized in Table 19.

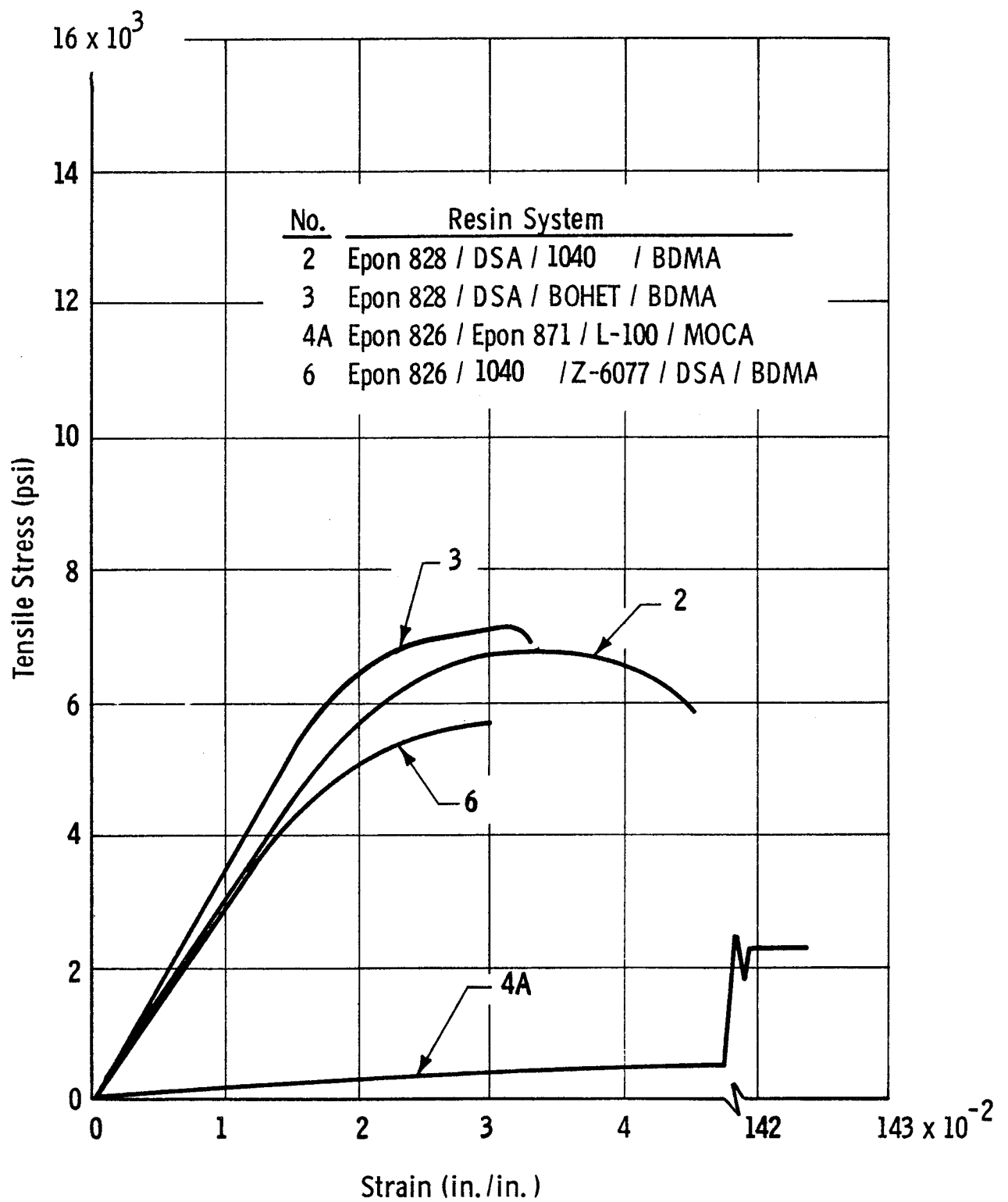


Figure 3. Stress-Strain Curves for Cryogenic Resin Systems at 75°F

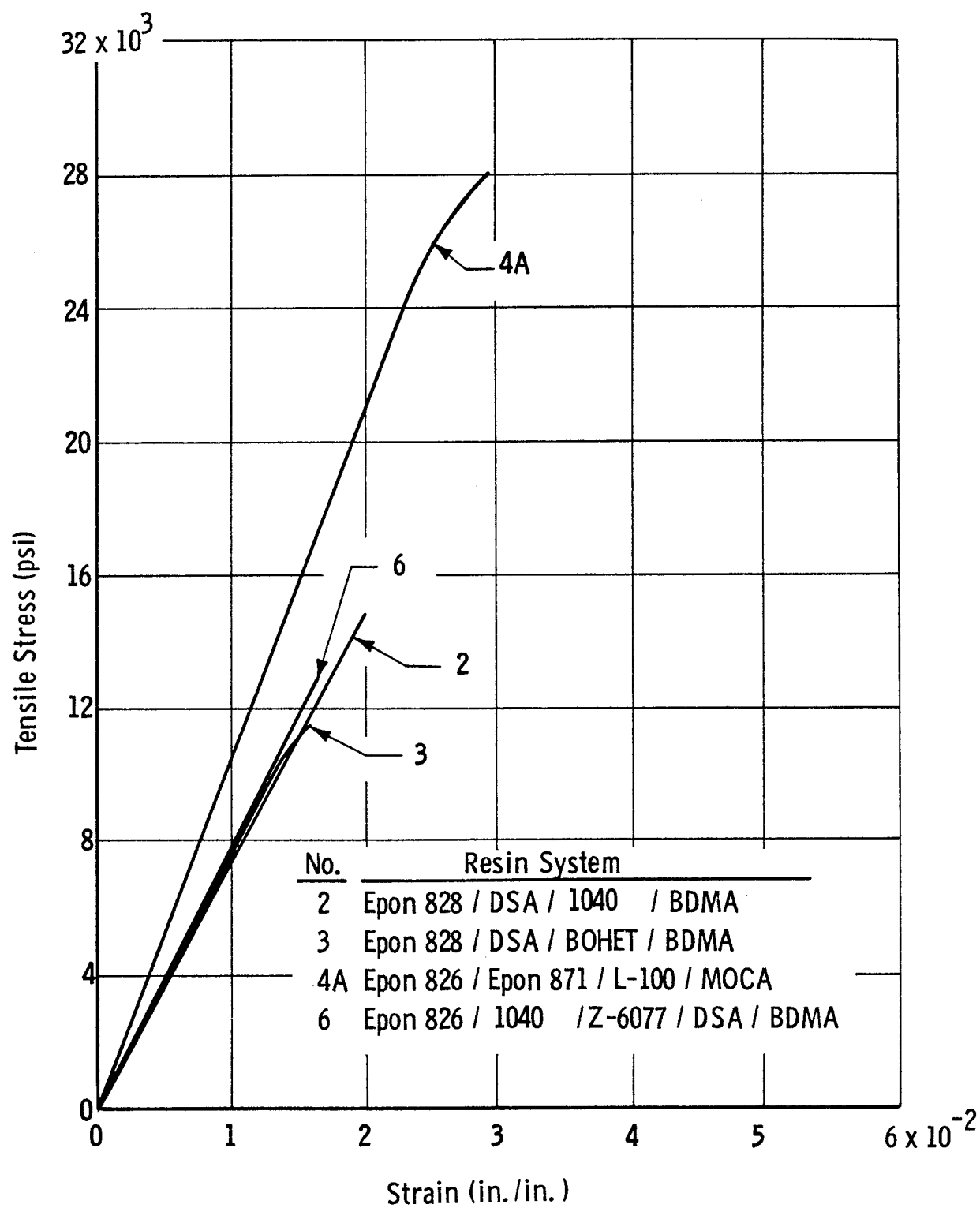


Figure 4. Stress-Strain Curves for Cryogenic Resin Systems at -320°F

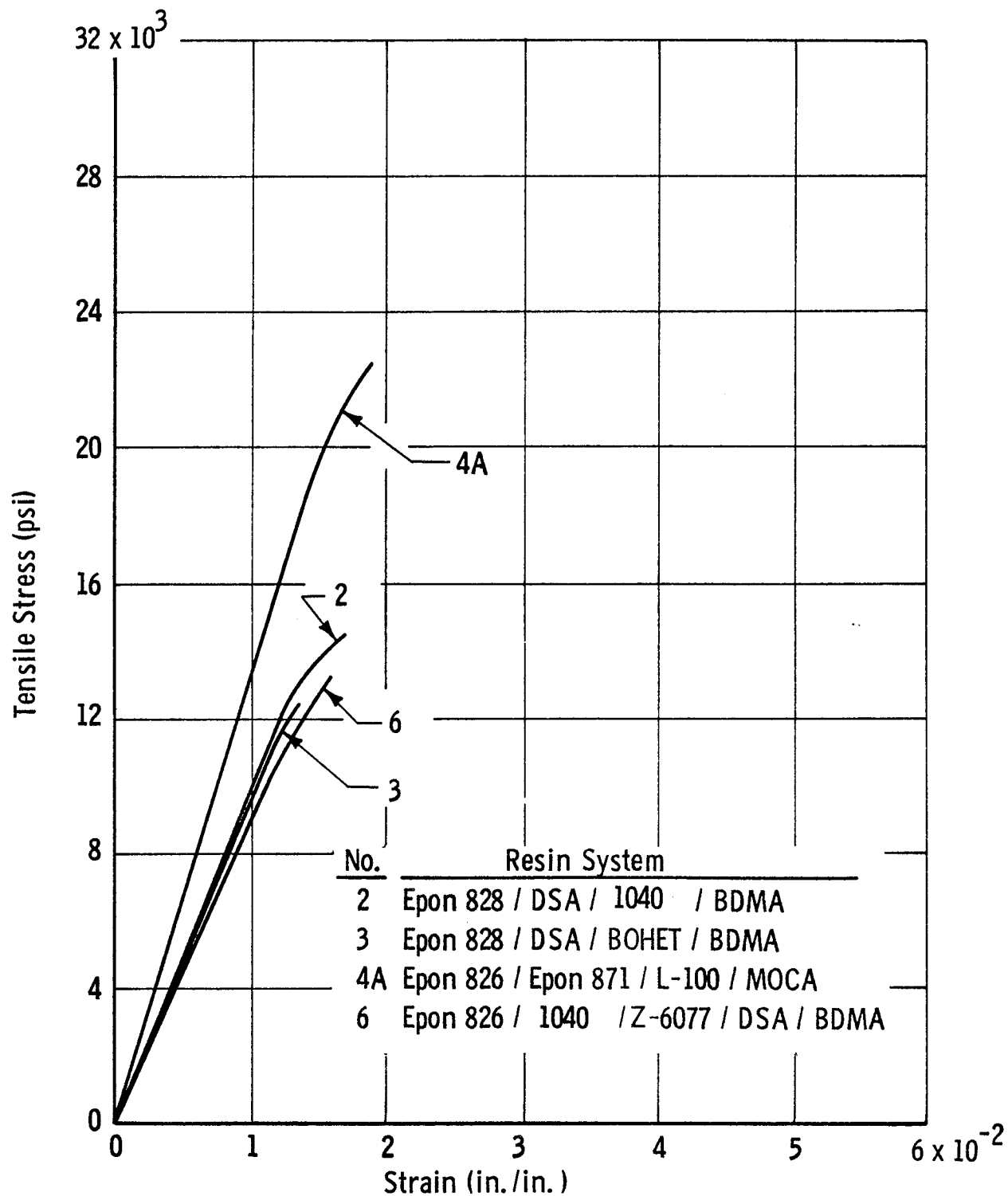


Figure 5. Stress-Strain Curves for Cryogenic Resin Systems at -423°F

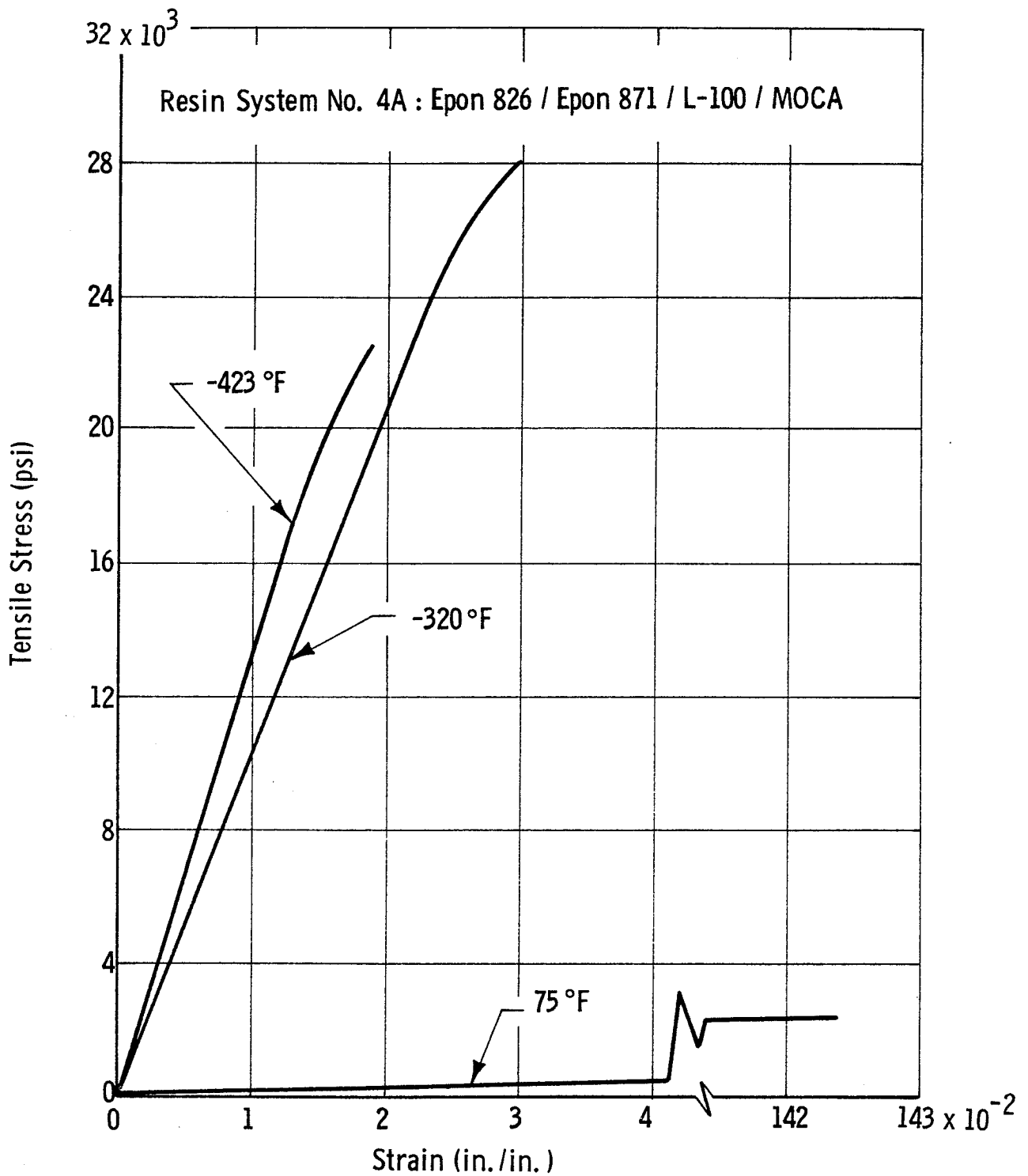


Figure 6. Stress-Strain Curves for Epoxy-Polyurethane Resin System 4A at Various Temperatures

TABLE 19

TEST RESULTS FOR CRYOGENIC RESINS (TASKS I AND II)*

Test Temp °F	Resin 2		Resin 3		Resin 4A		Resin 6
			Task I	Task II	Task I		(Task II)
	Task I	Task II	Cure A	Cure B	(Resin 4)	Task II	
Ultimate Tensile Strength, ksi							
+75	4.25	6.73	6.41	7.12	1.23	2.41	5.65
-320	-	14.80	-	11.59	-	28.00	12.87
-423	13.80	14.46	12.14	12.23	17.90	22.35	13.25
Tensile Strength at Fracture, ksi							
+75	2.60	5.90	5.12	6.89	1.23	2.41	5.10
-320	-	14.80	-	11.59	-	28.00	12.87
-423	13.80	14.46	12.14	12.23	17.90	22.35	13.25
Tensile Modulus, ksi							
+75	220.9	289.7	322.9	344.3	2.3	13.0	285.0
-320	-	683.9	-	728.9	-	1035.1	759.6
-423	917	977	1212	962	1377	1306	901
Elongation at Ultimate Stress, %							
+75	4.0	3.6	3.6	3.16	79.0	142.4	3.0
-320	-	2.0	-	1.6	-	2.95	1.65
-423	1.5	1.7	1.0	1.35	1.3	1.88	1.6
Elongation at Fracture, %							
+75	26.5	4.5	5.6	3.3	79.0	142.4	3.0
-320	-	2.0	-	1.6	-	2.95	1.65
-423	1.5	1.7	1.0	1.35	1.3	1.88	1.6
Toughness, lb-in./cu in.							
+75	-	233.1	-	157.1	-	1715.0	109.6
-320	-	145.0	-	95.1	-	446.0	106.2
-423	-	137.0	-	86.3	-	226.0	111.3

(cont.)

* Resin formulations as follows: Resin 2 = Epon 828/DSA/Empol 1040/BDMA (100/115.9/20/1), Resin 3 = Epon 828/DSA/BOHET/BDMA (100/134/26/1), Resin 4A = Epon 826/Epon 871/L-100/MOCA (35/15/50/27.6), and Resin 6 (Epon 826/Empol 1040/Z-6077/DSA/BDMA (80/20/20/115.9/1). Cure A = 2 hours at 150°F and 4 hours at 300°F. Cure B = 8 hours at 225°F.

TABLE 19 (cont.)

Test Temp °F, or Parameter	Resin 2		Resin 3		Resin 4A		Resin 6 (Task II)
	Task I	Task II	Task I	Task II	Task I	Task II	
			Cure A	Cure B	(Resin 4)		
Notch Toughness, psi√in.							
+75	2745	1441	1463	1221	279	374	2920
-320	-	1637	-	1285	-	3713	1379
-423	1204	1345	986	762	2916	2890	1328
Impact Strength (Charpy Unnotched), ft-lb/in.							
+75	-	3.23	-	3.48	-	37.70*	10.65
-320	-	2.52	-	2.27	-	12.16	3.80
-423	-	6.54	-	5.48	-	12.38	4.42
Horizontal Shear Strength, ksi							
+75	-	6.65	-	6.58	-	2.02	5.59
-320	-	14.11	-	13.03	-	10.87	15.66
-423	-	16.11	-	15.90	-	12.22	14.61
Resin wt%	-	17.86	-	17.60	-	13.11	17.47
Voids vol%	-	4.70	-	3.41	-	9.56	5.63
Specific gravity	-	1.903	-	1.954	-	1.931	1.891
Short-Span Shear Strength, ksi							
+75	-	4.32	4.04	-	-	0.54	4.35
-320	-	9.33	7.84	-	-	8.14	10.89
-423	-	8.84	8.42	-	-	7.76	9.90
Resin wt%	-	27.54	22.85	-	-	30.54	23.49
Voids vol%	-	9.42	11.91	-	-	15.44	6.31
Specific gravity	-	1.644	1.701	-	-	1.550	1.766

(cont.)

* Specimens bent but did not break; were tossed from the fixture between values of 34.6 and 41.9 ft-lb/in.

TABLE 19 (cont.)

<u>Parameter</u>	<u>Resin 2 (Task II)</u>	<u>Resin 3 (Task II) Cure A</u>	<u>Resin 4A (Task II)</u>	<u>Resin 6 (Task II)</u>
Initial viscosity, cp	1923 (78°F)	1812 (73.5°F)	1853 (144.5°F)	687 (76.5°F)
Pot life, hours*	1.8	11.0	0.1<0.2	>22
Gel time, hours**	>22	>20	>24	>22
Specific gravity	1.079	1.126	1.165	1.077
Resin shrinkage, %	7.82	5.78	5.21	8.37

* Defined here as period during which resin viscosity remained below 2500 cp.

** Defined here as period during which viscosity readings could be recorded (before gelation).

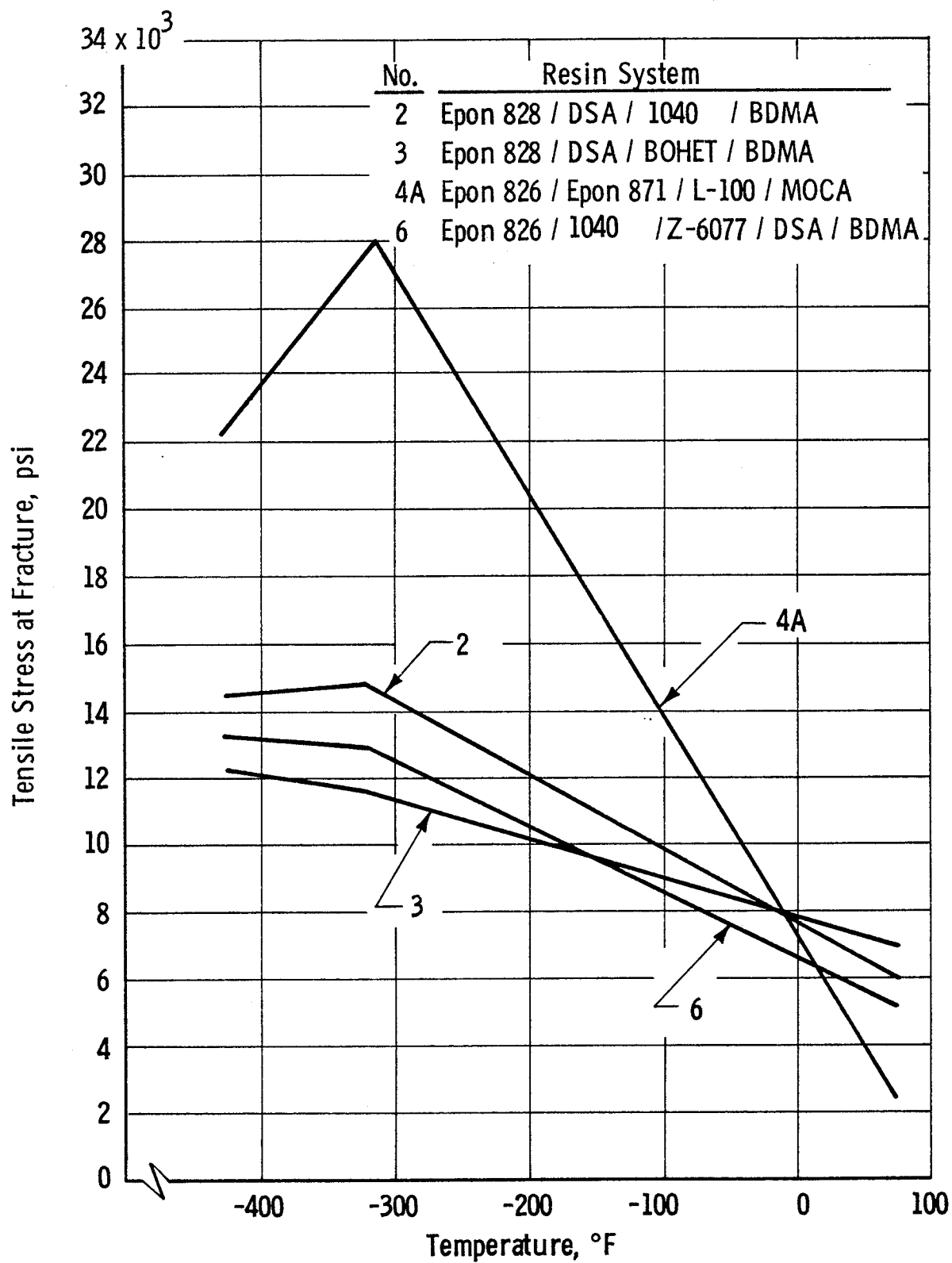


Figure 7. Effect of Temperature on Tensile Stress at Fracture
Cryogenic Resin Systems

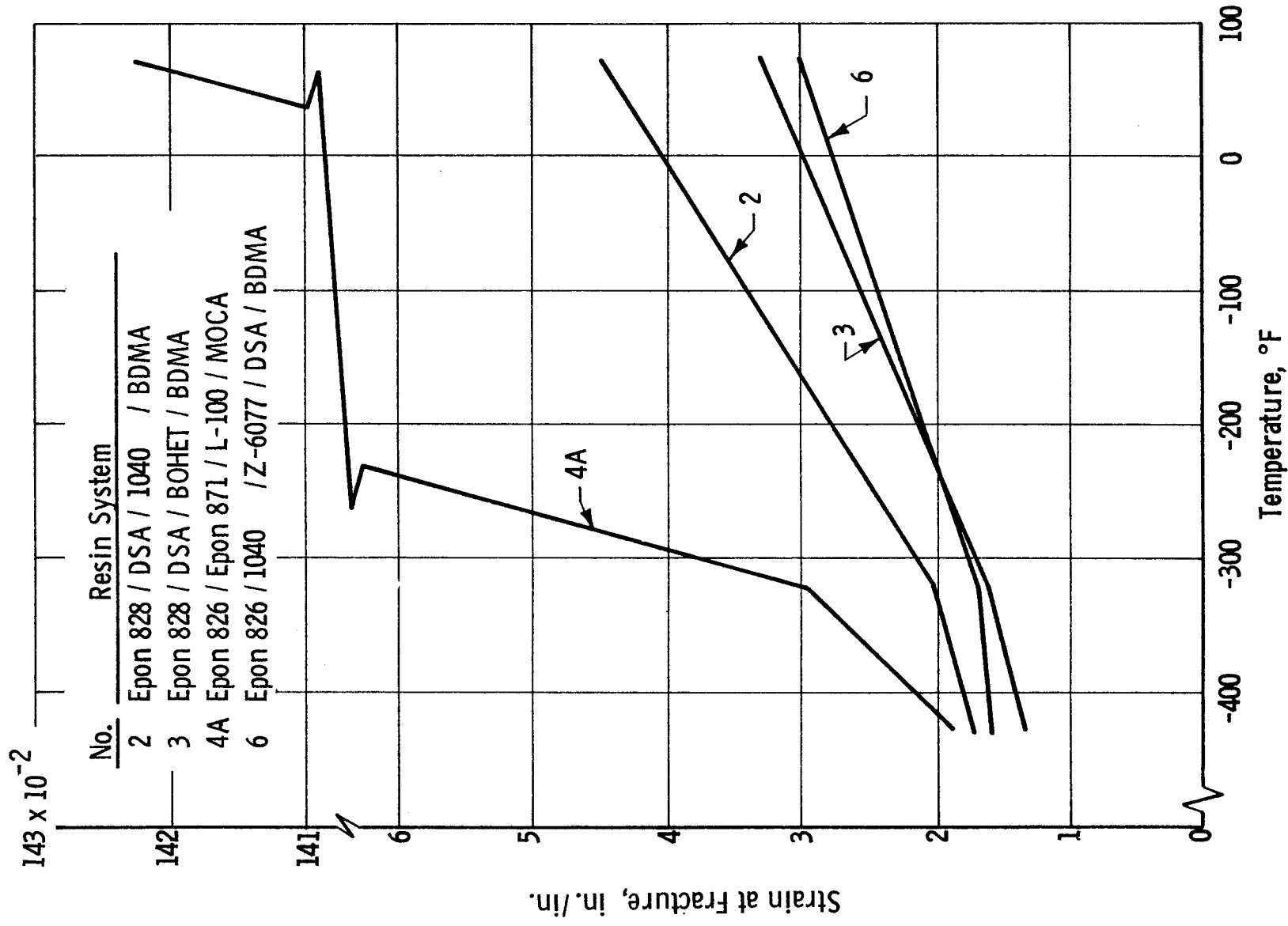


Figure 8. Effect of Temperature on Strain at Fracture
Cryogenic Resin Systems

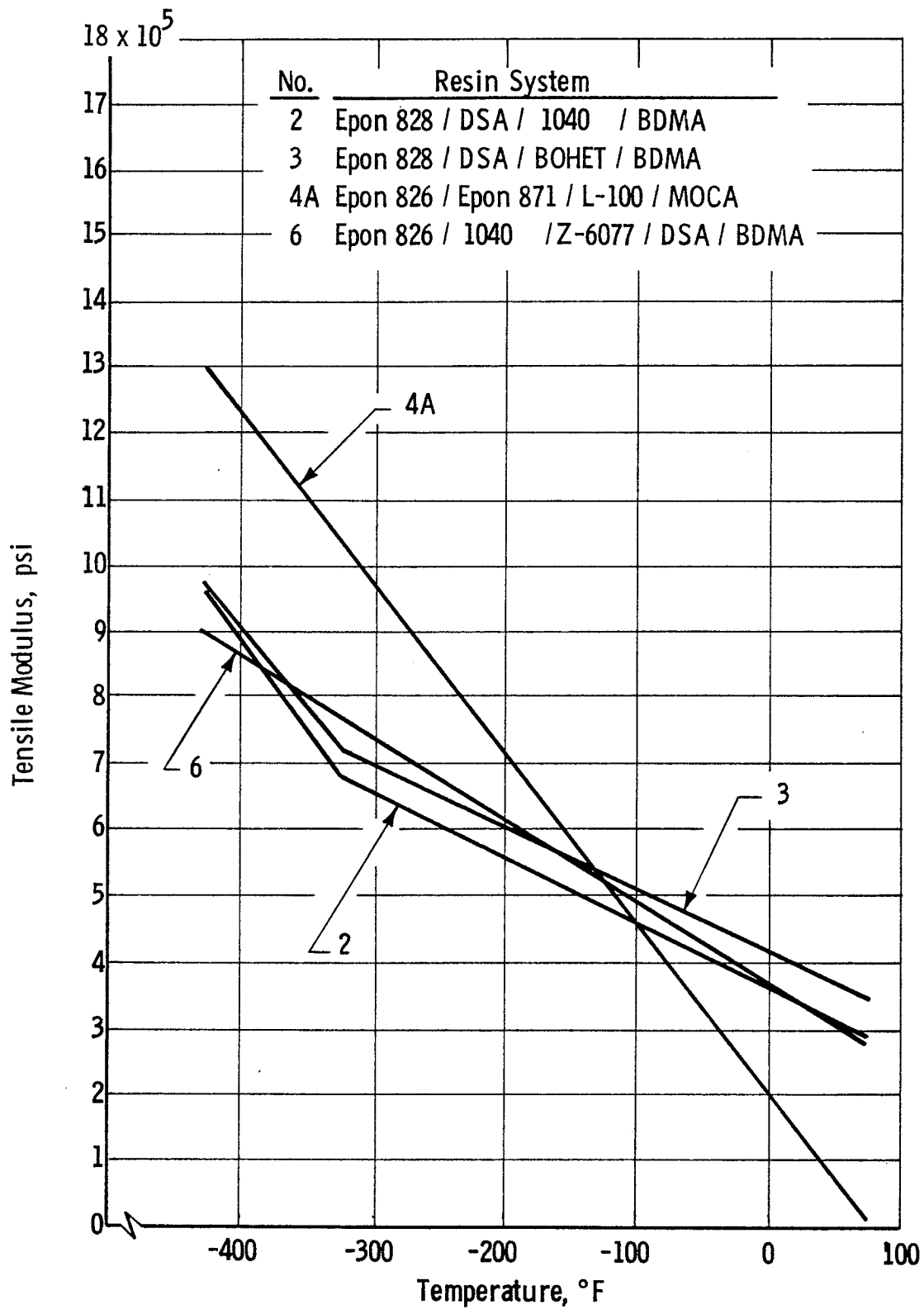


Figure 9. Effect of Temperature on Tensile Modulus
Cryogenic Resin Systems

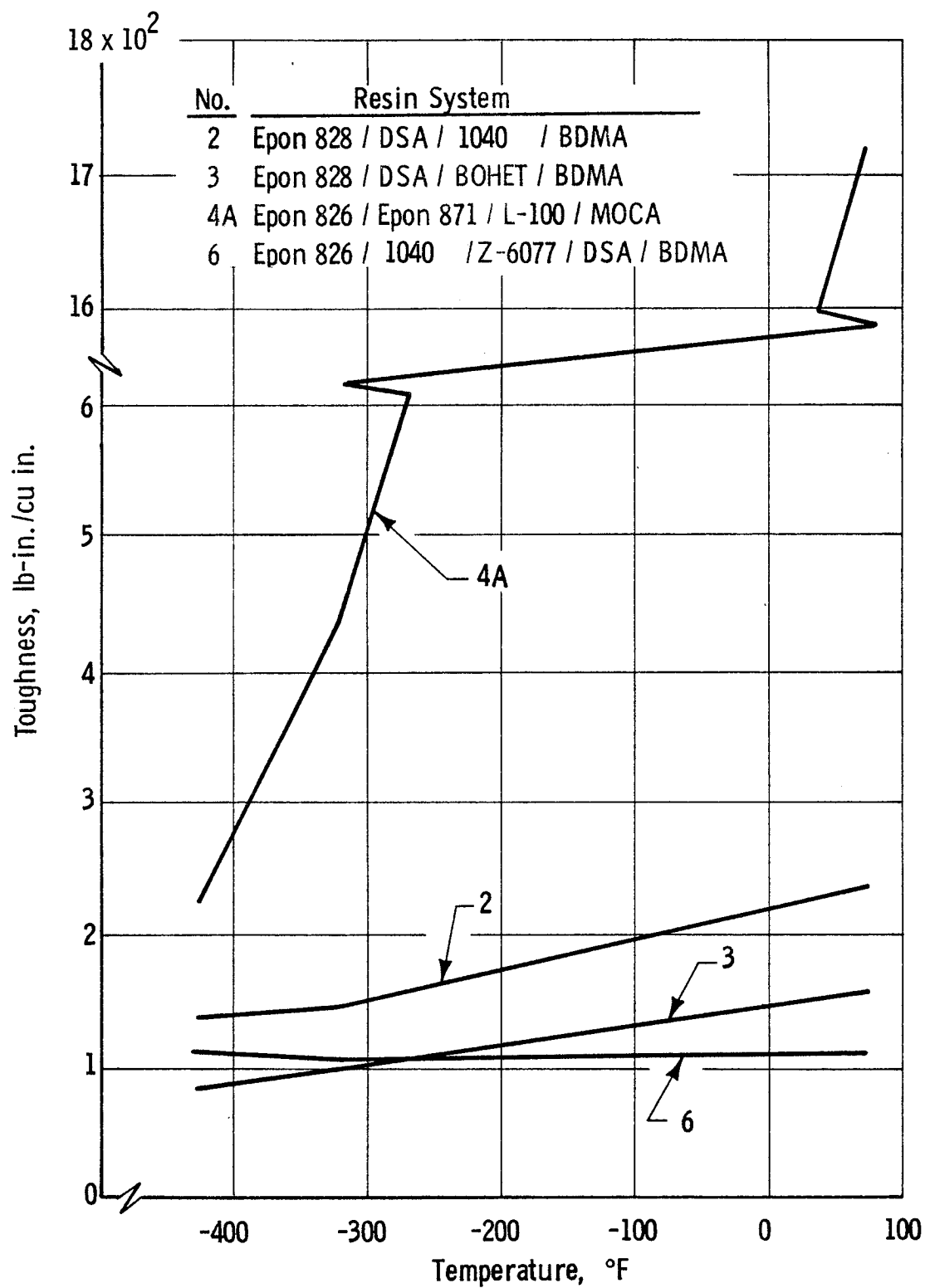


Figure 10. Effect of Temperature on Toughness (Area Under Stress-Strain Curve), Cryogenic Resin Systems

2. Notch Toughness

The notch-toughness test specimens (approximately 0.188 in. thick) were cast as flat panels and routed to a configuration having tapered ends. They were center-notched to permit measurement of the ability of the resin to sustain loads in the presence of imperfections. They were assembled in tapered-grip fixtures and tested in tension at +75, -320, and -423°F, using a 0.05-in./min crosshead travel. Details on the specimens, fixtures, test methods, and calculations are given in Appendix A, and the test results are summarized in Table 20.

Certain discrepancies appear to exist in Task I and Task II notch-toughness values in Table 19. As explained in the preceding section, they are real only for Resin 2, but even then have little actual effect when Resin 2 is compared with the other systems.

At room temperature (Figure 11), Resin 6 exhibited the greatest notch toughness, and the toughness of Resin 4A (375 psi√in.) was greater than that of its precursor (Resin 4) in Task I (279 psi√in., Table 11). Resin 4A also exhibited the highest notch toughness at both cryogenic temperatures. All resins except Resin 6 had a maximum notch toughness at -320°F, and all values were somewhat lower at -423 than at -320°F. The alternate cure schedule used with Resin 3 (8 hours at 225°F) resulted in lower values at each temperature.

Examination of the fracture surfaces of test specimens provided insight into the modes of failure. As might be expected, the rougher the fracture surface (indicative of the increased energy required for crack propagation), the higher the notch-toughness strength. In particular, this correlation was noted for Resin 4A at -423°F and for Resin 6 at +75°F; in both cases, the fracture surfaces were rough and had strain or tear lines generally oriented in the direction of crack propagation. The fracture surface of other specimens (i.e., Resins 2, 3, and 6 at -423°F) exhibited a smooth, almost glasslike texture typical of brittle materials with low energy-absorption properties. In general, the fracture surfaces of test specimens failing at a notch-toughness strength above 1400 psi√in. were distinctly rougher in texture.

3. Impact Strength

Impact strength, another index of toughness, is a measure of the amount of energy required for the rapid fracturing of a test specimen. Although the unnotched Charpy impact-strength tests performed here do not yield design data directly applicable to filament-winding conditions, they permit differences in energy absorption before fracture to be compared. Test results for 0.50 by 0.50 by 5.0-in. cast-resin specimens at +75, -320, and -423°F are presented in Table 21. Although differences between resin systems are indicated, there is considerable scatter in the data, probably because the specimens were unnotched. When a V-notch identical to that used in homogeneous-metal Charpy-impact specimens was incorporated into samples of Resin 6, the data exhibited less scatter at 75°F. (The notched and unnotched values were 0.13 and 10.65 ft-lb/in., respectively.) The use of unnotched specimens was continued, however,

TABLE 20

NOTCH-TOUGHNESS TEST RESULTS (TASK II)

Resin No.	Resin System (Parts by Weight)	Notch Toughness, $\text{psi}\sqrt{\text{in.}}$		
		+75°F	-320°F	-423°F
2	Epon 828/DSA/Empol 1040/BDMA (100/115.9/20/1)	1484.5	1639.6	1272.3
		1566.1	1742.1	1347.7
		1236.7	1541.2	1426.6
		1361.2	1585.4	1367.5
		1561.2	1678.1	1313.0
		Av 1441.9	1637.3	1345.4
3	Epon 828/DSA/BOHET/BDMA (100/134/26/1)	603.7	346.7	*
		1263.8	372.8	1399.7
		1147.1	403.1	1316.8
		915.4	500.3	1139.3*
		2178.7	443.5	688.3
		Av 1221.7**	413.3***	887.9***
4A	Epon 826/Epon 871/L-100/MOCA (35/15/50/27.6)	346.5	3954.2	3115.0
		377.0	3681.1	3093.4
		365.1	3744.1	2751.1
		399.1	3772.2	2893.7
		385.7	3417.5	2600.8
		Av 374.7	3713.8	2890.8
6	Epon 826/Empol 1040/Z-6077/DSA/BDMA (80/20/20/115.9/1)	2980.9	2035.7	1334.8
		2811.9	953.1*	1385.8
		2930.7	1586.8	1241.5
		2951.3	944.2*	1341.5
		2928.6	1379.9	1337.6
		Av 2920.7	1667.5	1328.3

* Specimen fractured when immersed in LN_2 .

** Cure schedule 2 hours at 150°F and 4 hours at 300°F.

*** Cure schedule 8 hours at 225°F.

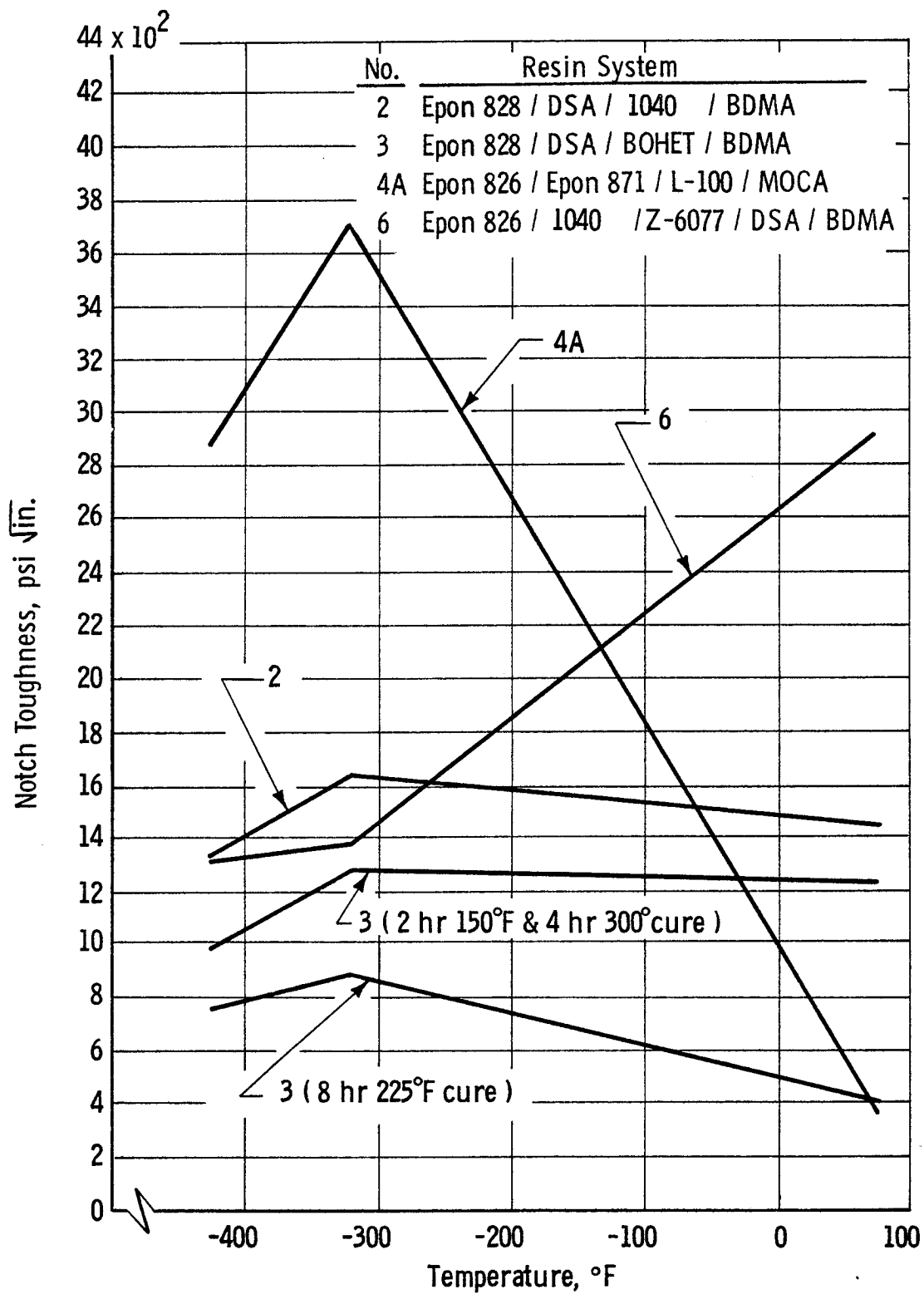


Figure 11. Effect of Temperature on Notch Toughness
Cryogenic Resin Systems

TABLE 21

IMPACT-STRENGTH TEST RESULTS (CHARPY UNNOTCHED)*

Resin No.	Resin System (Parts by Weight)	Type of Value	Impact Strength, ft-lb/in.		
			+75°F	-320°F	-423°F
2	Epon 828/DSA/Empol 1040/BDMA (100/115.9/20/1)	High	4.97	3.13**	7.99
		Low	1.27	1.65	3.68
		Av	3.23	2.52	6.54
3	Epon 828/DSA/BOHET/BDMA (100/134/26/1)	High	4.36	2.67**	8.08
		Low	3.16	1.84	3.13
		Av	3.48	2.27	5.48
4A	Epon 826/Epon 871/L-100/MOCA (35/15/50/27.6)	High	41.9***	19.59	14.80
		Low	34.6	6.52	10.36
		Av	37.7	12.16	12.38
6	Epon 826/Empol 1040/Z-6077/DSA/BDMA (80/20/20/115.9/1)	High	18.72	9.89**	6.34
		Low	5.75	1.23	2.96
		Av	10.65	3.80	4.42

* Minimum of five specimens tested for each resin system at each test temperature. -320°F data: Specimens rapidly cooled, stabilized at -320°F, and tested in aluminum-foil dish filled with LN₂. -423°F data: Specimens gradually cooled, stabilized at -423°F, and tested with 6-sec time lag (max).

** Thermal-shock cracking of specimens noted during immersion in LN₂.

*** Specimens did not fracture but were tossed from fixture.

because the unnotched results adequately differentiated between candidate-resin resistances to fracture by shock.

Of the systems that fractured at 75°F, Resin 6 had the greatest impact strength. Because of its great resilience, Resin 4A flexed sufficiently to be tossed from the fixture without fracturing.

For testing at -320°F, the specimens were cooled rapidly in LN₂ until temperature equilibrium was attained. They were then placed in aluminum-foil dishes filled with LN₂, and the test was performed while the specimens were so contained. In this way, the desired -320°F temperature was obtained, with only a negligible strength contribution from the aluminum-foil dish. During preliminary immersion in LN₂, all specimens except Resin 4A underwent thermal-shock fracture, which probably contributed to the lower impact values for Resins 2, 3, and 6 in comparison with Resin 4A.

For testing at -423°F, the specimens were cooled gradually in LH₂, were stabilized at that temperature, and (within a 6-sec period) were transferred to the machine and tested. Again, Resin 4A specimens exhibited the greatest impact strength, indicating that they required the highest energy expenditure for fracture. Because the specimens were gradually cooled to the test temperature, no thermal fracture occurred, and the average impact-strength values were higher than those at -320°F. The actual test temperature was slightly higher than -423°F, because of the time required for specimen transfer from the conditioning bath to the impact machine. On the whole, there was less scatter in the cryogenic data than occurred at 75°F.

4. Interlaminar Shear Strength

The interlaminar shear strengths of the glass/cryogenic-resin composite specimens were determined by two test methods, both employing centrally loaded, simply supported, laminate beams with geometric configurations such that failure was induced in interlaminar shear. Instead of being a singular characteristic of a material, interlaminar shear is regarded as a complex parameter dependent on several properties. Among these are resin strength, resin-to-glass adhesion, composite void content, filament orientation, and resin content. In composites subject to compressive loading, failure is believed to originate in the interlaminar resin. On the other hand, the relevance of interlaminar-shear properties to internally loaded pressure vessels has not been resolved. For either application, it is considered likely that proper fabrication and processing techniques are extremely significant in obtaining a high level of interlaminar shear strength and increased structural performance.

a. NOL Horizontal Shear

The test specimens were arc segments (0.635 in. long by 0.250 in. wide by 0.125 in. thick) cut from an NOL ring. Test data are presented in Table 22. The average values ranged from 2.02 ksi at 75°F for Resin 4A to 16.11 ksi at -423°F for Resin 2. Increases in shear strength ranged (1) from 100 to 438% in going from +75 to -320°F, and (2) from 142 to 505% in going from +75 to -423°F. Resins 2, 3, and 4A exhibited 11 to 12% increases in shear strength at -423°F over their strengths at -320°F, whereas Resin 6 declined

TABLE 22

INTERLAMINAR-SHEAR TEST RESULTS (NOL HORIZONTAL-SHEAR METHOD)*

Resin No.	Resin System (Parts by Weight)	Shear Stress, ksi		
		+75°F	-320°F	-423°F
2	Epon 828/DSA/Empol 1040/BDMA	6.41	14.31	15.93
	(100/115.9/20/1)	6.79	16.41	16.87
	Resin content 17.86 wt%	6.53	12.91	15.48
	Void content 4.70 vol%	6.91	14.61	15.28
	Composite specific gravity 1.903	6.62	14.31	16.97
	Av	6.65	14.11	16.11
3	Epon 828/DSA/BOHET/BDMA**	6.64	15.00	15.56
	(100/134/26/1)	6.40	13.01	15.28
	Resin content 17.60 wt%	6.45	16.21	18.47
	Void content 3.41 vol%	6.95	12.51	15.18
	Composite specific gravity 1.954	6.45	12.91	15.00
	Av	6.58	13.93	15.90
4A	Epon 826/Epon 871/L-100/MOCA	1.93	10.00	13.34
	(35/15/50/27.6)	2.08	9.81	13.01
	Resin content 13.11 wt%	2.08	12.61	13.02
	Void content 9.56 vol%	2.04	12.11	10.50
	Composite specific gravity 1.931	1.98	9.71	11.25
	Av	2.02	10.87	12.22
6	Epon 826/Empol 1040/Z-6077/DSA/BDMA	5.64	15.11	13.50
	(80/20/20/115.9/1)	5.72	16.31	15.00
	Resin content 17.47 wt%	5.67	15.51	14.28
	Void content 5.63 vol%	5.30	15.71	14.71
	Composite specific gravity 1.891	5.63	11.70***	15.54
	Av	5.59	15.66	14.61

* Values shown for resin content (wt%), void content (vol%), and composite specific gravity are averages of three tests for each resin system. Specimens were segments from the same NOL ring used in fabricating horizontal-shear specimens.

** Specimens prepared using alternate cure cycle (8 hours at 225°F).

*** Data rejected because specimen slipped in fixture during test.

about 6.7%. As was expected, Resin 4A showed the greatest increase in shear strength when cooled to cryogenic temperatures, although its strength was exceeded by each of the other resins.

These results, indicating the effect of temperature on interlaminar shear stress, are graphically illustrated in Figure 12. The results obtained with Resin 4A are regarded as a minimum expectation because of the relatively high void content of these specimens and (possibly) because of their low resin content. Resin- and void-content results, obtained with composite segments from the same NOL ring used in fabricating the horizontal-shear specimens, are also shown in Table 22. The indirect correlation between shear stress and void content at ambient temperature has been noted by many investigators. As is evident from Figure 13, a similar correlation appears to exist (at least to a first approximation) at ambient temperature and possibly at -423°F for resins of significantly diverse chemical types.

Photomicrographs were taken of cross sections of arc-segments cut from each NOL ring used to fabricate the horizontal-shear specimens (Figures 14 through 18). They support the relative void-content data in Table 22, particularly the high void content of Resin 4A. The latter was probably caused by residual MEK solvent, which was added to improve the resin-mix workability and for possible extension of pot life. When NOL rings were fabricated with a Resin 4A mix containing less MEK, there was a large increase in shear strength at all temperatures and a decrease in void content (Table 23).^{*} The differences in void content, and particularly the larger voids in the 9.56%-void specimen, are clearly visible in Figures 16 and 18.

b. Short-Span Shear

Test specimens (1.0 by 3 by 0.125 in.) were cut from laid-up flat panels as described in Appendix A. Test data are given in Table 24. Although general performance trends are clear, the results were influenced considerably by the fabrication technique, which unfortunately did not afford sufficiently rigid control over void content and resin content - two factors affecting shear-strength properties.

As in the horizontal-shear tests, Resin 4A composites exhibited the lowest shear stress at 75°F . Stress increases were obtained for all specimens at -320°F , with Resin 6 yielding the highest value (10.89 ksi). Except for Resin 3, the shear stresses of all were lower at -423 than at -320°F . Resin 6 exhibited the highest shear strengths among the four systems at all test temperatures, possibly owing (to some extent) to its lower void content. The low shear strengths of the Resin 4A specimens at 75°F may be attributed to great flexibility at this temperature, which hinders the efficient transfer of shear loads. The rigidity of Resin 4A specimens increased at the lower temperatures, as did the shear strength. It should be noted, however, that the unduly high void contents of the Resin 2, 3, and 4A specimens undoubtedly lowered the shear strengths obtained at all test temperatures. In

^{*} Additional data obtained in the absence of MEK was entirely consistent with these trends (see Section IV,B,4, following).

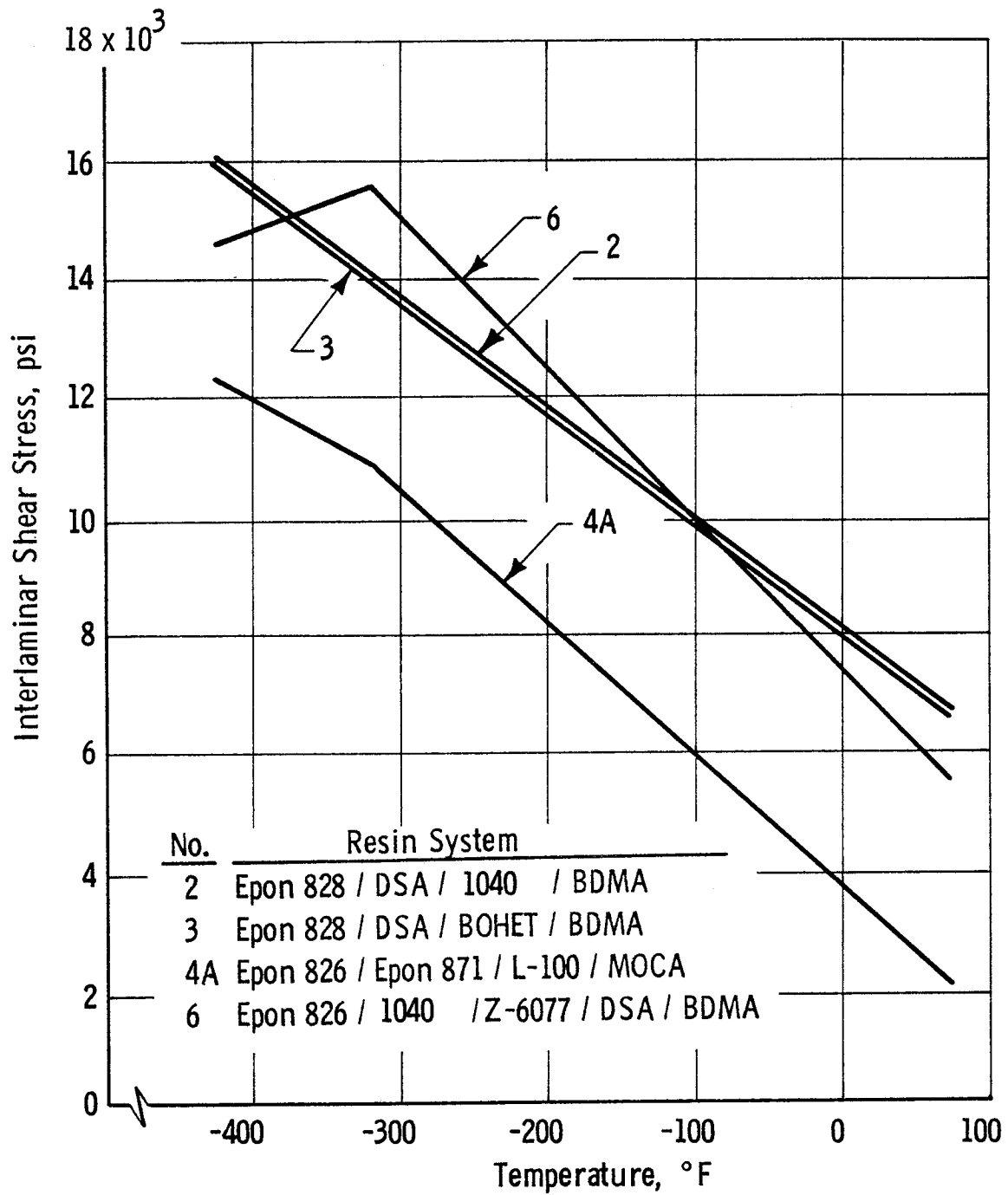


Figure 12. Effect of Temperature on Interlaminar Shear Stress
S-901/Cryogenic Resin Systems
(Horizontal-Shear Test Method)

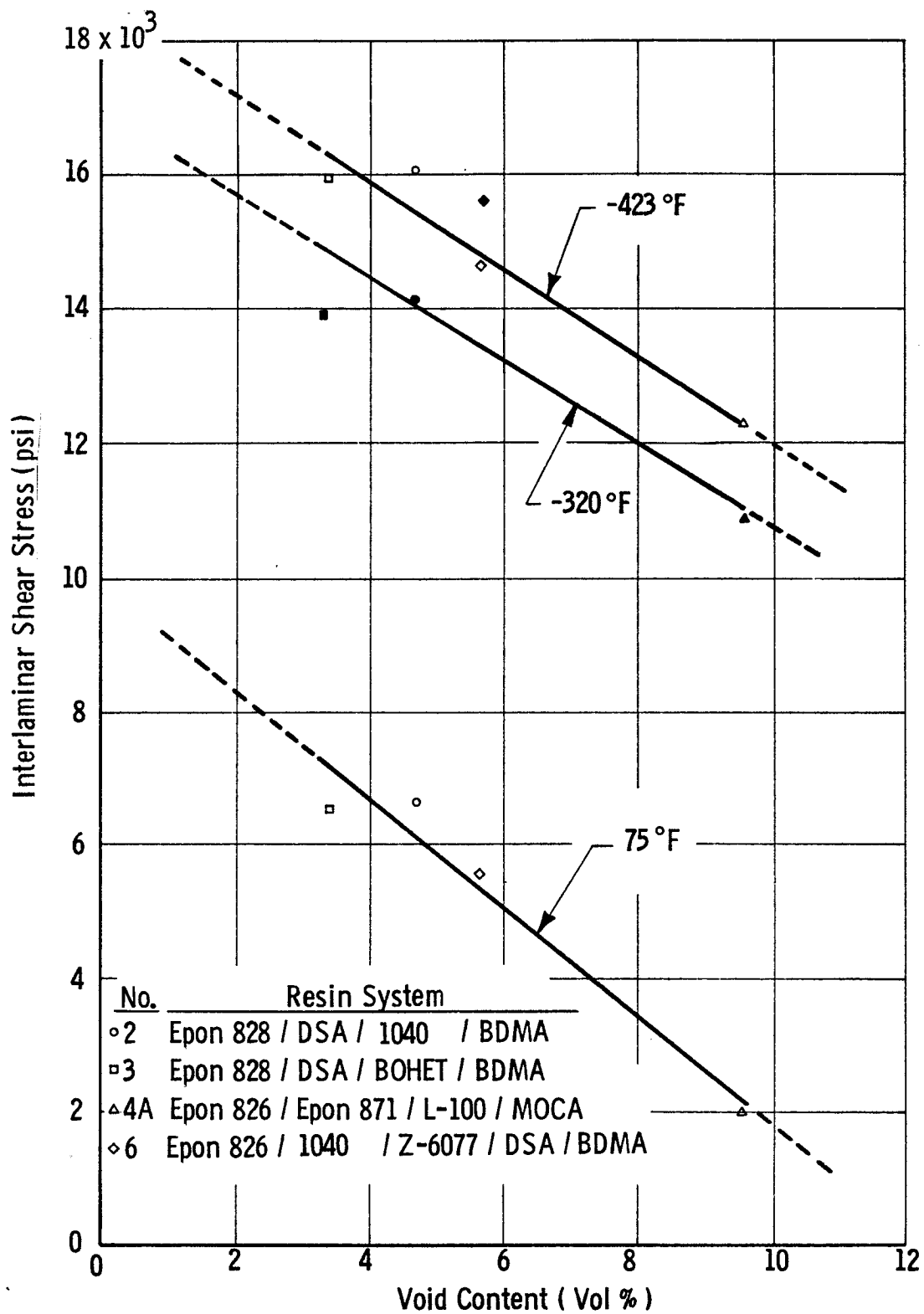


Figure 13. Relationship Between Interlaminar Shear Stress and Resin Void Content, S-901/Cryogenic Resin Systems

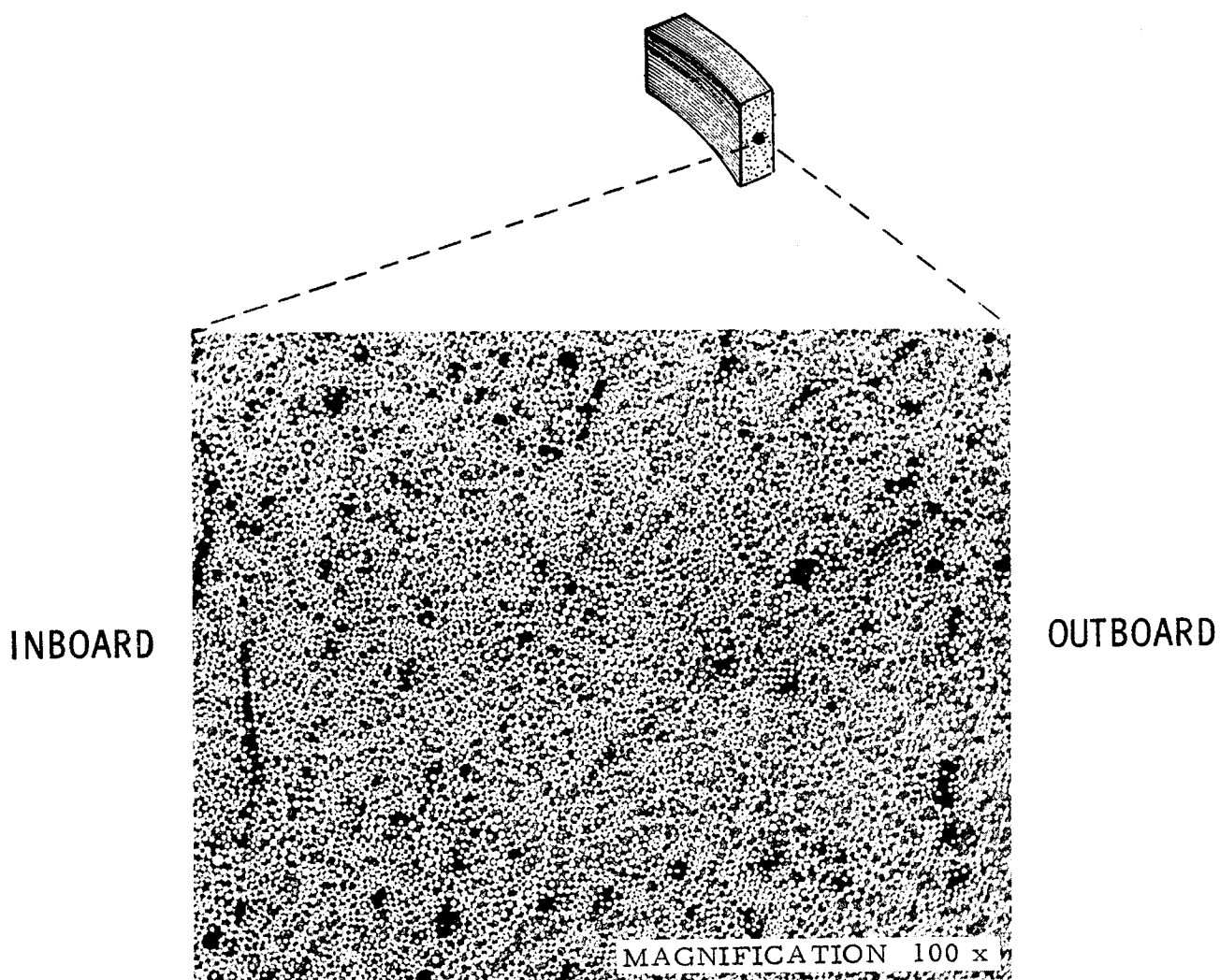


Figure 14. Resin 2 Horizontal-Shear Segment
(4.70 vol% Voids)

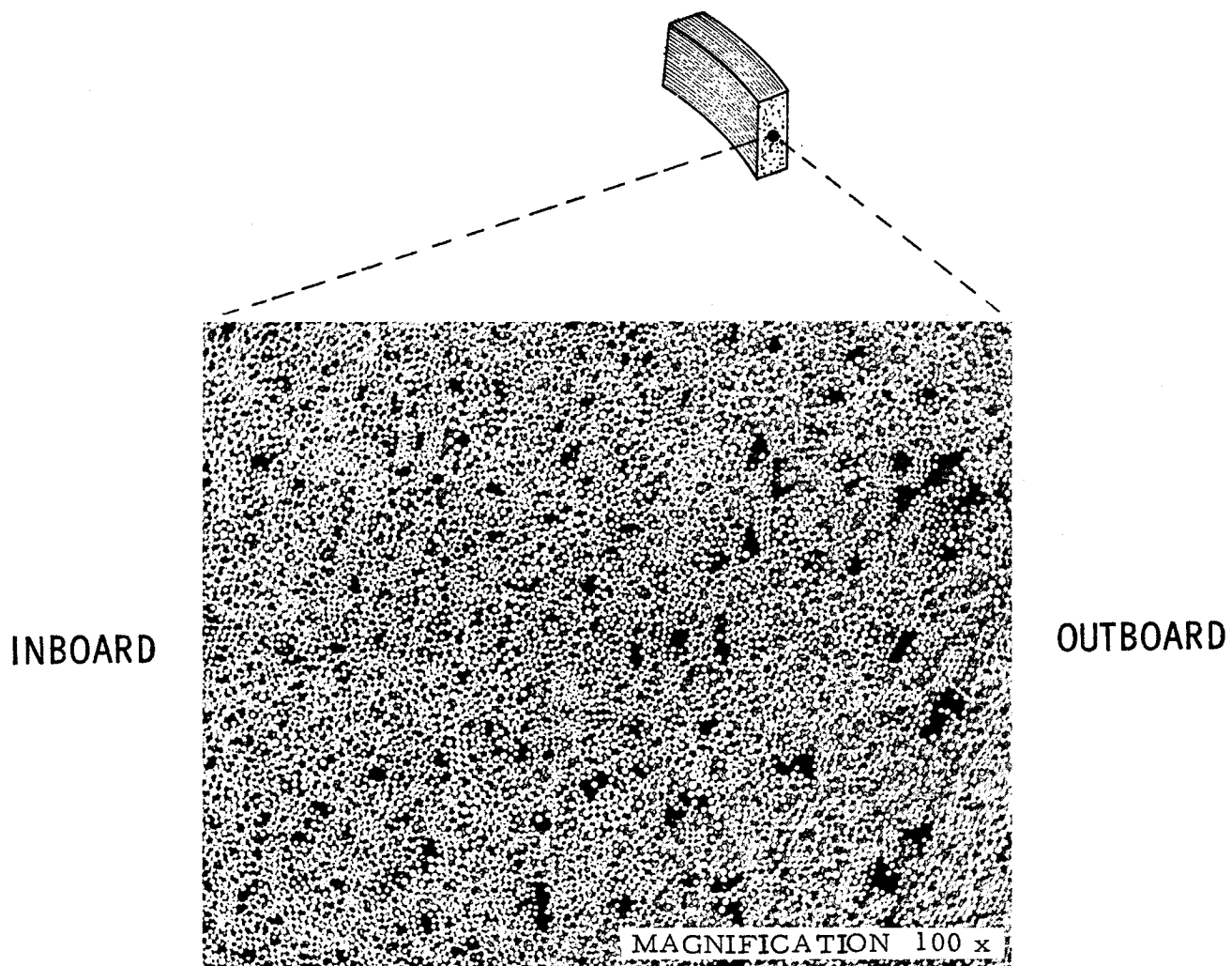


Figure 15. Resin 3 Horizontal-Shear Segment
(3.41 vol% Voids)

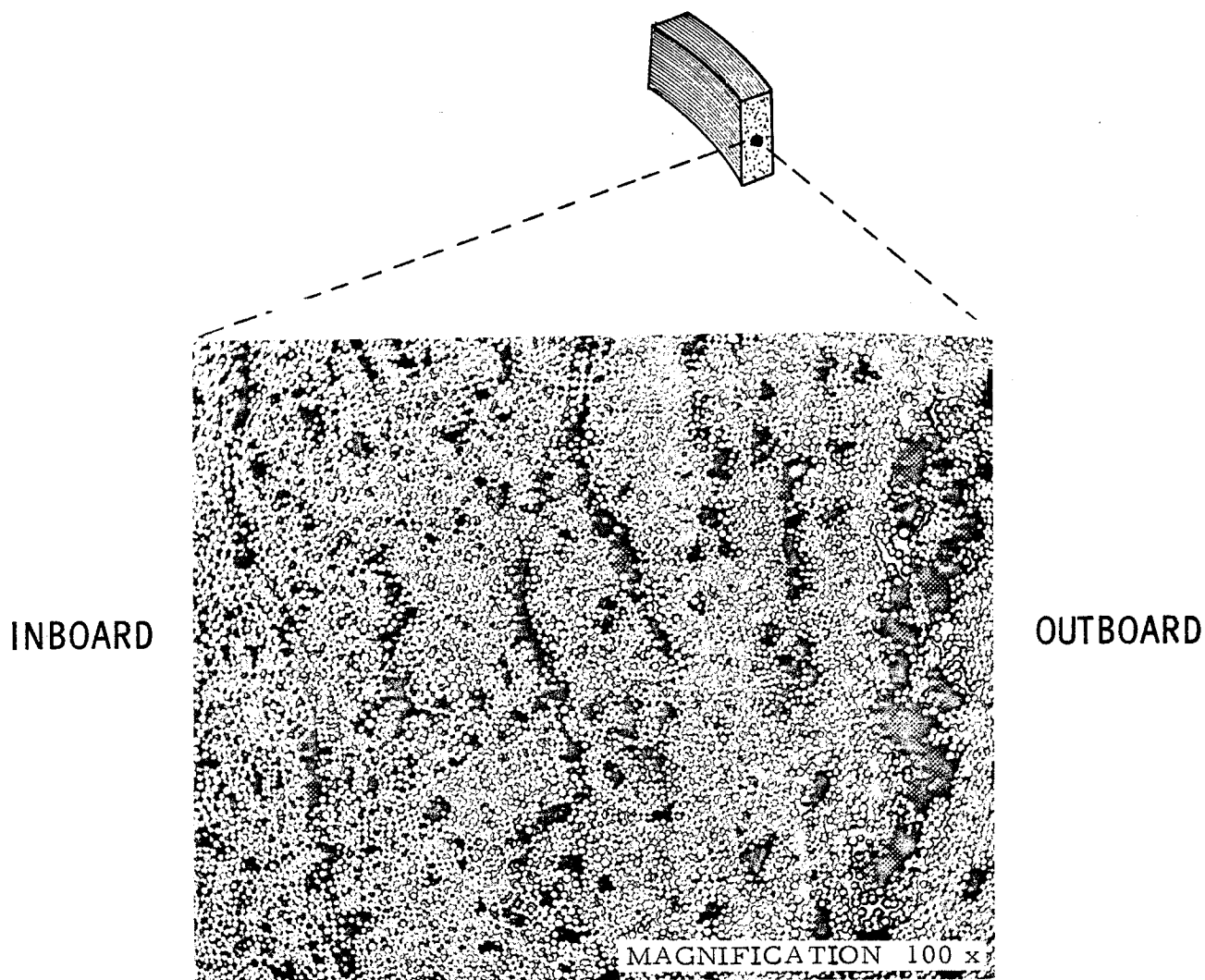


Figure 16. Resin 4A Horizontal-Shear Segment
(9.56 vol% Voids)

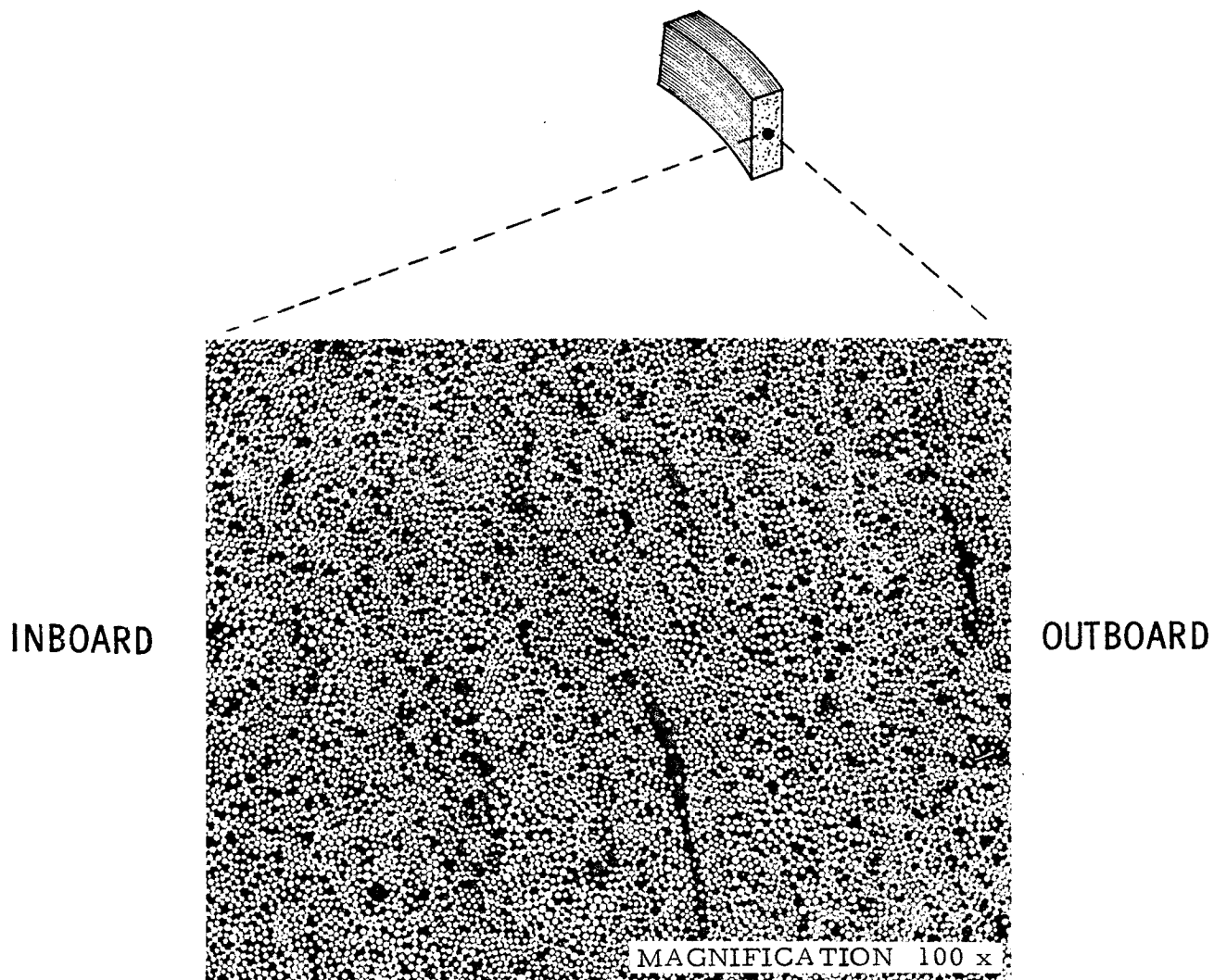


Figure 17. Resin 6 Horizontal-Shear Segment
(5.63 vol% Voids)

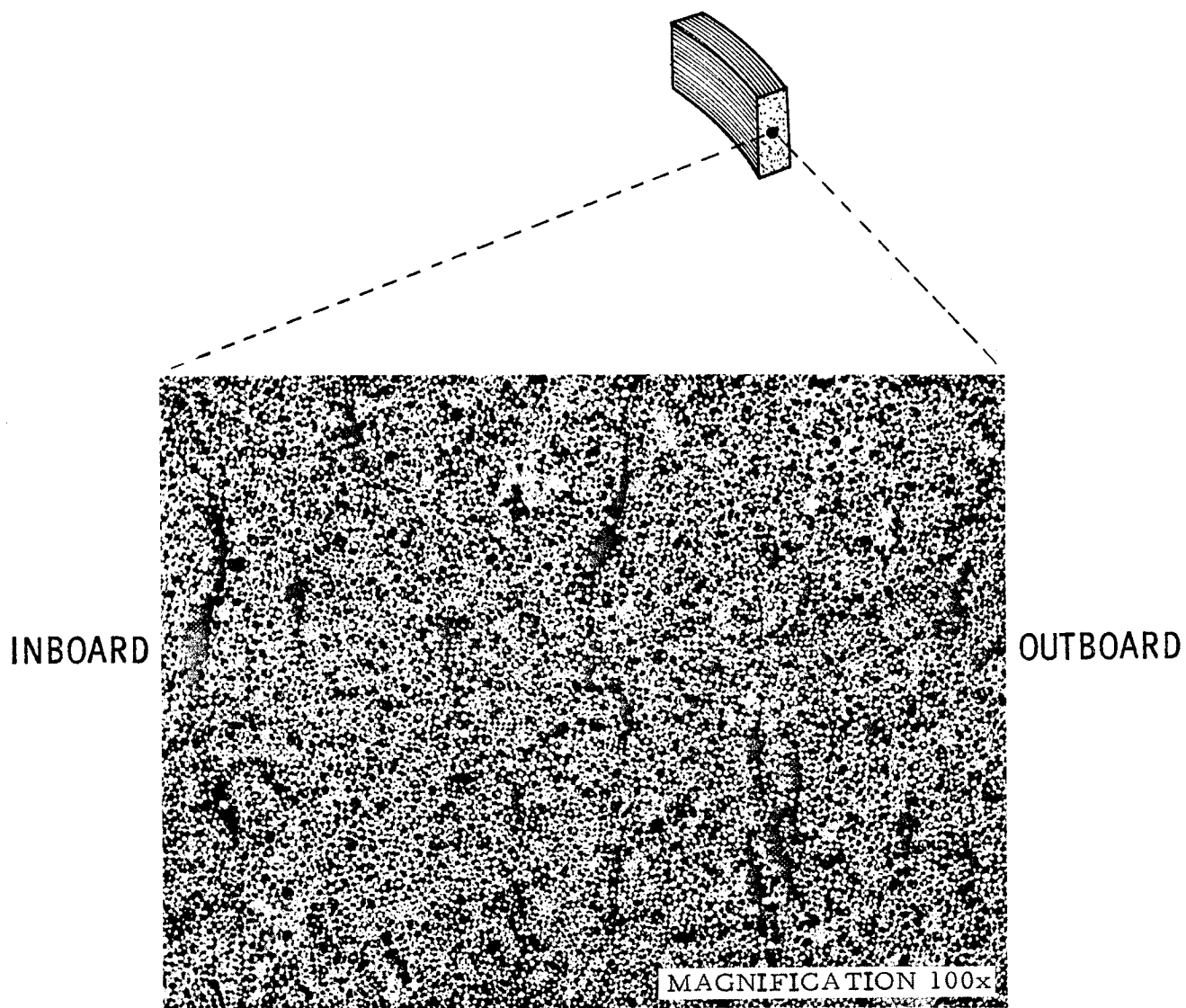


Figure 18. Resin 4A Horizontal-Shear Segment
(5.66 vol% Voids)

TABLE 23

EFFECTS OF MEK ON INTERLAMINAR-SHEAR TEST RESULTS FOR RESIN 4A*
(NOL HORIZONTAL-SHEAR METHOD)

MEK/L-100 Ratio	Resin Content wt%	Void Content vol%	Composite Specific Gravity	Shear Stress, ksi		
				+75°F	-320°F	-423°F
1 ml/1g	13.11	9.56	1.931	1.93	10.00	13.34
				2.08	9.81	13.01
				2.08	12.61	13.02
				2.04	12.11	10.50
				1.98	9.71	11.25
				Av 2.02	10.87	12.22
1 ml/4g	10.64	5.66	2.069	3.06	12.55	15.77
				3.12	12.44	12.15
				3.14	15.93	12.03
				3.09	17.41	16.29
				3.04	18.09	14.74
				Av 3.09	15.28	14.20

*Epon 826/Epon 871/L-100/MOCA (35/15/50/27.6 parts by weight).

TABLE 24

INTERLAMINAR-SHEAR TEST RESULTS (SHORT-SPAN-SHEAR METHOD)

Resin No.	Resin System (Parts by Weight)	Resin Content wt%*	Void Content vol%*	Composite Specific Gravity	Shear Stress, ksi		
					+75°F	-320°F	-423°F
2	Epon 828/DSA/Empol 1040/BDMA (100/115.9/20/1)	27.54	9.42	1.644	4.25	9.32	9.29
					4.40	8.45	8.57
					4.58	9.10	9.37
					4.16	9.48	8.46
					4.24	10.31	8.49
					Av 4.32	9.33	8.84
3	Epon 828/DSA/BOHET/BDMA (100/134/26/1)	22.85	11.91	1.701	4.03	7.31	7.77
					4.17	7.94	8.54
					4.11	8.46	8.18
					4.05	7.97	8.29
					3.82	7.51	8.30
					Av 4.04	7.84	8.42
4A	Epon 826/Epon 871/L-100/MOCA (35/15/50/27.6)	30.54	15.44	1.550	0.53	8.46	7.25
					0.52	8.31	7.16
					0.54	8.39	8.54
					0.57	7.67	7.61
					0.53	7.86	7.79
					Av 0.54	8.14	7.76
6	Epon 826/Empol 1040/Z-6077/DSA/BDMA (80/20/20/115.9/1)	23.49	6.31	1.766	4.57	11.80	9.49
					4.53	10.37	10.16
					4.26	11.41	10.47
					4.21	10.94	9.64
					4.18	9.93	9.76
					Av 4.35	10.89	9.90

* Averages of three tests for each resin system.

addition, the resin contents of the Resin 2 and 4A specimens were probably too high to yield optimum shear strengths. The effect of temperature on the short-span-shear test results is depicted in Figure 19.

5. Coefficient of Linear Thermal Contraction

Test results are plotted in Figure 20 and summarized in Table 25. The average coefficient of linear thermal contraction calculated for each resin system between -400 and +60°F ranged from 32.11×10^{-6} to 34.93×10^{-6} in./in./°F. Resins 2 and 4A had the lowest coefficients. Direct comparisons with other systems cannot be made because thermal-contraction data for other resins at cryogenic temperatures are not available. In the 150 to 250°F range, however, the 58-68R epoxy system* has a linear-thermal-contraction coefficient of 45×10^{-6} in./in./°F.

C. SELECTION OF CANDIDATE RESINS FOR TASK III

Candidate-resin performances in Task II mechanical tests are summarized in Table 26. The resins were assigned rating numbers from 1 to 4; the more favorable the performance in the specific test, the higher the number. Ratings were also assigned to the criteria indices previously established in Aerojet glass/resin-interaction studies as having a direct correlation with composite performance (vessel burst pressure).

Table 26 shows that Resins 4A and 2 generally outperformed the other two systems, either on the basis of criteria indices or of individual mechanical properties.** From the standpoint of physical properties (pot life and viscosity) Resin 2 was completely acceptable, but there were grave doubts regarding the suitability of Resin 4A for either in-process or prepreg operations. On the other hand, most of the other properties of Resin 4A were very satisfactory. In addition to those noted in Table 26, Resin 4A was the only system that did not undergo thermal cracking at cryogenic temperatures in thermal-shock and impact tests. It also had the greatest resistance to crack propagation in the notched tensile tests.

After careful evaluation of the Task II physical/mechanical-test results and the above considerations on processability, Resins 2 and 4A were chosen for Task III study.

* Epon 828(50)/Epon 1031(50)/MNA(90)/BDMA(0.5).

** Linear-thermal-contraction results did not lend themselves to inclusion in Table 26. It is clear from Figure 20, however, that Resin 2 excelled over the entire temperature range and that Resin 4A was second best from -250°F downward.

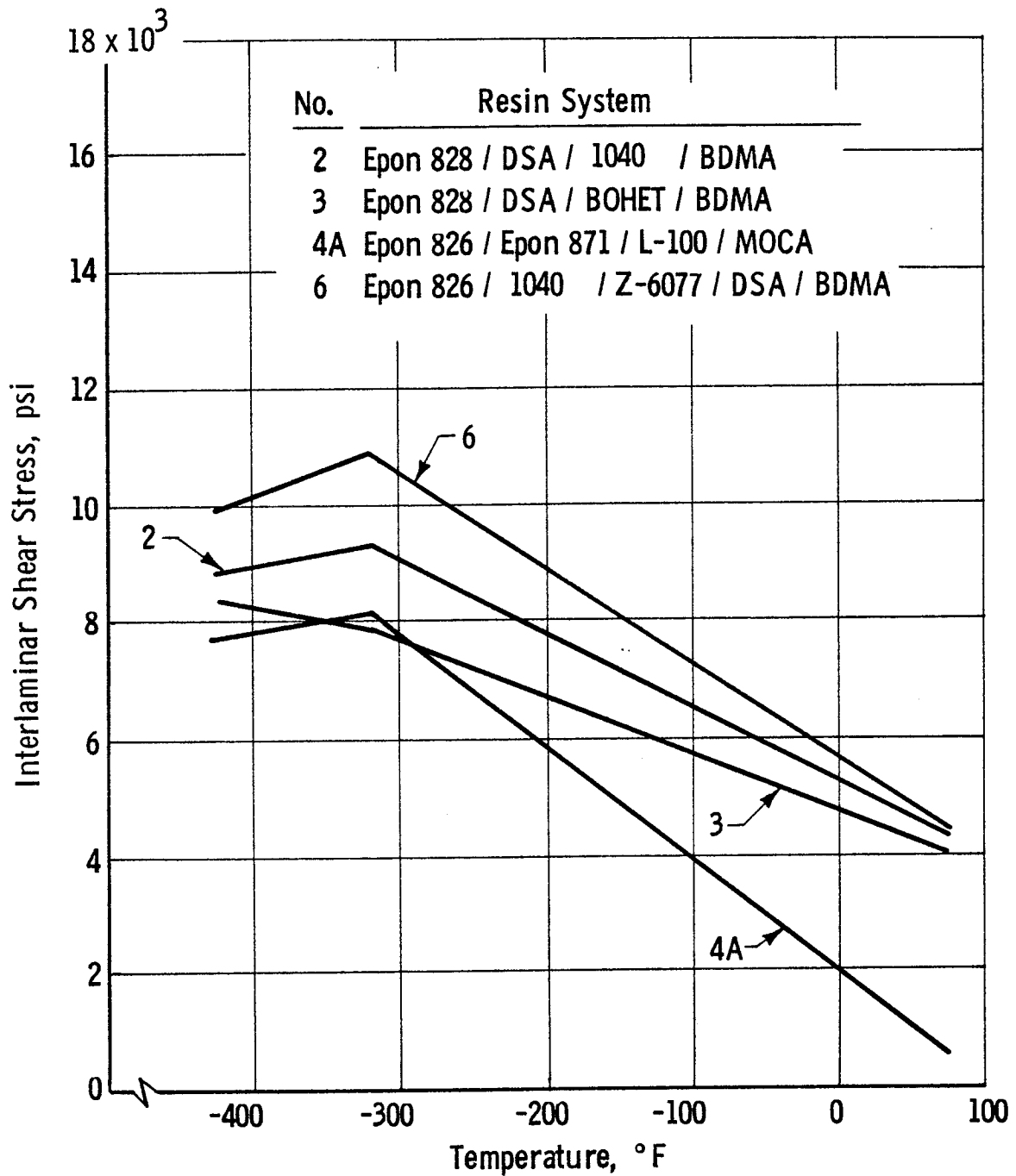


Figure 19. Effect of Temperature on Interlaminar Shear Stress
S-901/Cryogenic Resin Systems
(Short-Span-Shear Test Method)

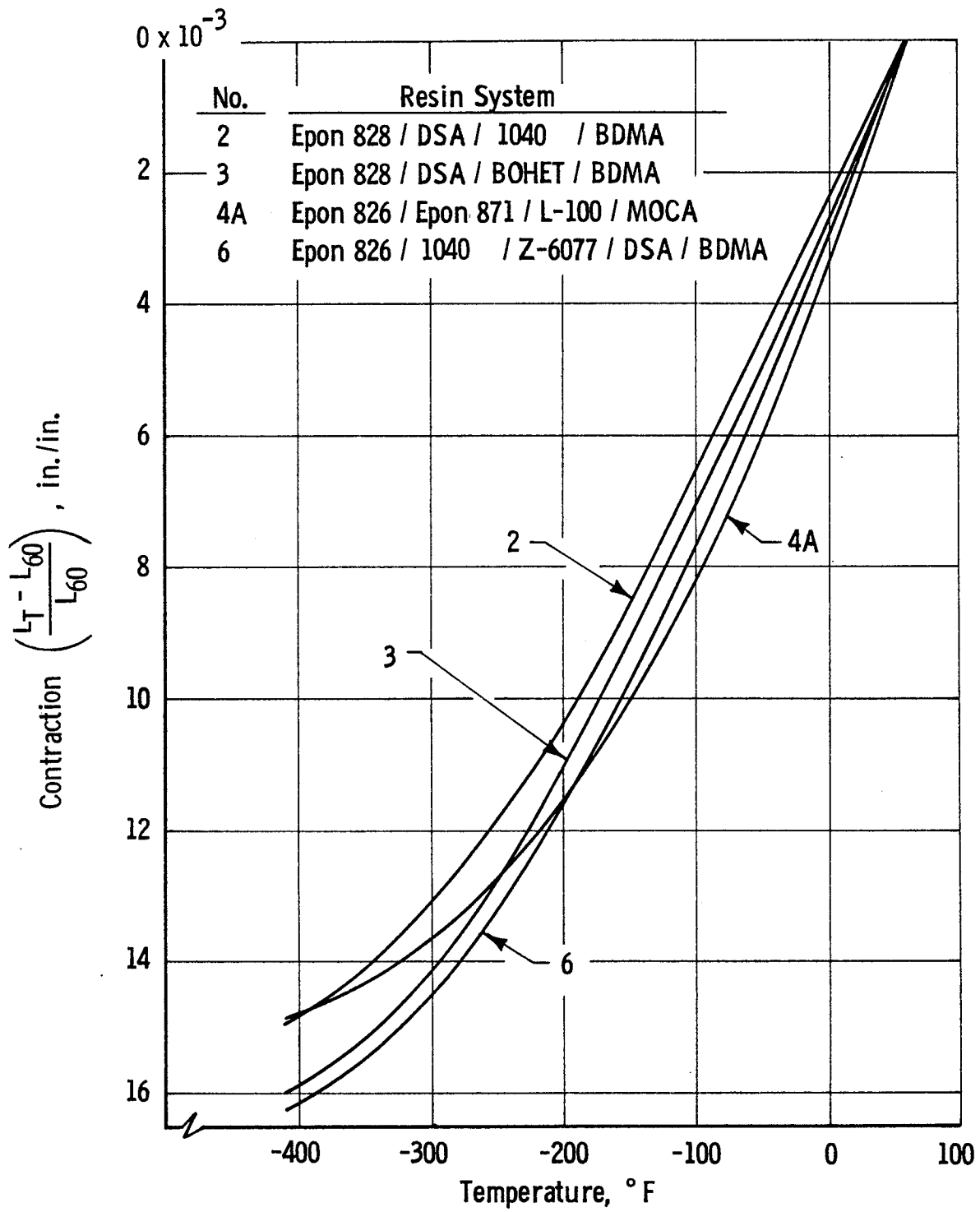


Figure 20. Linear Thermal Contraction, Cryogenic Resin Systems

TABLE 25

CAST-RESIN LINEAR-THERMAL-CONTRACTION TEST RESULTS (TASK II)*

Temperature °F	$\Delta L/L, 10^{-3} \text{ in./in.}$			
	Resin 2	Resin 3	Resin 4A	Resin 6
+60	0	0	0	0
0	2.507	2.801	3.637	3.031
-50	4.664	4.999	6.161	5.423
-100	6.853	7.145	8.237	7.741
-150	8.701	9.157	10.014	9.873
-200	10.416	10.992	11.538	11.712
-250	11.868	12.845	12.713	13.349
-300	13.156	14.172	13.635	14.592
-350	13.966	15.088	14.083	15.465
-400	14.769	15.904	14.814	16.069
-407	14.944	-	-	-
-410	-	15.948	14.839	-
-417	-	-	-	16.238

* Reported values represent averages of three runs. Calculated average coefficient of linear thermal contraction between +60 and -400°F as follows:

Resin 2 - $32.11 \times 10^{-6} \text{ in./in./°F}$
 Resin 3 - $34.46 \times 10^{-6} \text{ in./in./°F}$
 Resin 4A - $32.20 \times 10^{-6} \text{ in./in./°F}$
 Resin 6 - $34.93 \times 10^{-6} \text{ in./in./°F}$.

TABLE 26

COMPARATIVE PERFORMANCE OF RESIN SYSTEMS IN MECHANICAL TESTS*

Property	Resin 2			Resin 3			Resin 4A			Resin 6		
	+75°F	-320°F	-423°F	+75°F	-320°F	-423°F	+75°F	-320°F	-423°F	+75°F	-320°F	-423°F
Tensile strength at fracture	3	3	3	4	1	1	1	4	4	2	2	2
Tensile modulus	2	1	2	4	2	3	1	4	4	3	3	1
Elongation at fracture	3	3	3	2	1	1	4	4	4	1	2	2
Toughness	3	3	3	2	1	1	4	4	4	1	2	2
Notch toughness	3	3	2	2	1	1	1	4	4	4	2	3
Impact strength	1	2	3	2	1	2	4	4	4	3	3	1
Horizontal shear strength	4	3	4	3	2	3	1	1	1	2	4	2
Short-span shear strength	3	3	3	2	1	2	1	2	1	4	4	4
Criteria indices												
Notch toughness x tensile strength	3	3	2	2	1	1	1	4	4	4	2	3
Tensile strength at fracture	3	3	3	4	1	1	1	4	4	2	2	2
Notch toughness x elongation	2	3	3	1	1	1	4	4	4	3	2	2

* Rated as 1, 2, 3, or 4, in the direction of higher performance.

IV. TASK III - EVALUATION OF CANDIDATE CRYOGENIC RESINS AS FILAMENT-WOUND-COMPOSITE SPECIMENS

A. TEST METHODS

Task III covered the evaluation of Resins 2 and 4A as S-901 glass-FWC specimens. The following composite properties were determined at +75, -320, and -423°F: (1) "dog-bone" tensile strength, including elongation and tensile modulus, (2) thermal-shock resistance, (3) coefficient of thermal contraction, and (4) interlaminar shear strength (NOL horizontal-shear method). In addition, the resin contents of all specimens were obtained. Test methods and specimen-fabrication procedures are described in Appendix A. As in Tasks I and II, all test methods were patterned after those described in the latest ASTM Standards or in FTM Standard No. 406.

B. TEST RESULTS

1. Tensile Strength and Associated Properties

Composite tensile specimens for use in testing were fabricated from Resins 2 and 4A in three different filament orientations. They were made of glass panels wound by in-process impregnation on an 18-in.-dia steel mandrel. Each wound layer of glass was cut across the fibers into three equal sections, was properly oriented, and was laid flat on a metal sheet. The assembly, vacuum-bagged and oven-cured in accordance with the resin requirements, produced a flat panel approximately 18 in. square. Three filament-orientation patterns were investigated: unidirectional 1:0, bidirectional 1:1, and bidirectional 1:2. Twelve layers were used for each orientation pattern as depicted in Appendix A, and cross plies of 181-glass cloth were employed as reinforcement between every third layer in the grip sections of the unidirectional specimens in order to prevent failure there. The flat panels were cut and routed to a tapered-end-specimen configuration.

Tests were performed at approximately +75°F and in a cryostat utilizing LN₂ at -320°F or LH₂ at -423°F. An extensometer with a 2.0-in. gage length was used to record a continuous load-vs-deflection curve for each test specimen. Deflection monitoring by the extensometer had to be discontinued prior to failure because the total elongation of the specimen exceeded the travel limits of the extensometer. The maximum elongation (at failure) could not be determined by measuring the post-failure distance between inked reference marks because the composite specimens fractured in such a way that the marks were not legible. Elongation-at-failure values were therefore extrapolated from graphs by extending the load-deflection curve to the load at failure.

Test results are presented in Tables 27, 28, and 29 for the various filament orientations. Premature failure caused by the shearing of bolts or specimen slippage in the clamped grips (the latter particularly with unidirectionally oriented specimens) necessitated rerouting of the gage width of some test specimens from approximately 0.400 in. to 0.250 in., and in some cases to 0.125 in. This approach assured tensile failure in the gage area, and the filament-strength values were not significantly different from those obtained with the wider specimens.

TABLE 27

COMPOSITE-TENSILE-STRENGTH TEST RESULTS (UNIDIRECTIONAL 1:0 ORIENTATION)

Resin No.	Temp °F	Resin wt%	Voids vol%	Ult Load lb	Specimen Width in.	Ultimate Tensile Strength, ksi		Tensile Modulus ksi	Maximum Elongation %*
						Filament	Composite		
2	+75	21.0	7.03	**	0.197	-	-	-	-
	↓			2260	0.110	354.2	-	8.7	2.3
	↓			2625	0.121	374.0	-	8.2	2.6
	↓			2380	0.111	369.6	-	8.6	2.3
	↓			**	0.122	-	-	-	-
	+75					Av 365.9	228.2	8.5	2.4
	↓			**	0.241	-	-	-	-
	-320			**	0.245	-	-	-	-
	↓			2970	0.123	416.3	-	8.9	2.7
	↓			3325	0.125	458.6	-	8.1	1.8
	↓			3195	0.116	474.8	-	10.3	2.8
	-320					Av 449.9	280.6	9.1	2.4
	↓			5080	0.233	375.9	-	***	***
	-423			5320	0.251	365.4	-	14.5	1.4
	↓			2820	0.122	398.5	-	10.3	2.2
4A	↓	43.6	16.7	5040	0.243	357.6	-	****	***
	↓			**	0.248	-	-	-	-
	-423					Av 374.3	233.5	12.4	1.8
	↓			**	0.249	-	-	-	-
	+75			1990	0.127	270.1	-	3.8	2.0
	↓			2025	0.125	279.3	-	3.8	2.1
	↓			1975	0.130	261.9	-	3.5	2.1
	↓			1820	0.125	251.0	-	3.8	1.9
	+75					Av 265.6	101.5	3.8	2.0
	↓			4500	0.130	596.8	-	5.4	3.1
	-320			****	0.248	-	-	-	-
	↓			4550	0.123	637.7	-	9.7	2.0
	↓			4370	0.124	607.6	-	10.7	1.5
	↓			4200	0.128	565.7	-	8.2	1.1
	-320					Av 601.9	229.9	8.5	1.9
4A	↓	43.6	16.7	7950	0.252	543.9	-	3.7	4.0
	↓			3510	0.123	492.0	-	6.2	2.9
	↓			6850	0.253	466.8	-	6.2	3.7
	↓			7090	0.243	503.0	-	6.2	2.4
	↓			6820	0.253	464.7	-	7.1	2.7
	-423					Av 494.0	188.7	5.9	3.1
	↓								

* Extrapolated values.

** Specimen slipped in jaws of fixture during test.

*** Inconsistent load-elongation curve.

**** Bolt failure in test fixture.

TABLE 28

COMPOSITE-TENSILE-STRENGTH TEST RESULTS (BIDIRECTIONAL 1:1 ORIENTATION)

Resin No.	Temp Of	Resin wt%	Voids vol%	Ult Load lb	Specimen Width in.	Ultimate Tensile Strength, ksi		Tensile Modulus ksi	Maximum Elongation %*
						Filament	Composite		
2	+75	16.7	1.09	2400	0.249	332.2		4.1	2.6
				2375	0.242	338.4		4.3	2.6
				2610	0.248	362.8		4.1	2.9
				2525	0.244	356.8		4.2	2.8
				2570	0.238	372.2		4.1	3.0
	+75				Av	352.4	121.1	4.2	2.8
	-320			3950	0.241	565.1		4.4	4.2
				3675	0.242	523.6		3.9	4.4
				4065	0.252	556.2		4.1	4.4
				3175	0.244	448.6		3.8	3.7
2				3750	0.240	538.6		3.6	4.6
	-320				Av	526.4	181.0	4.0	4.3
	-423			5200	0.402	446.0		4.0	4.5
				5490	0.402	470.8		4.3	3.7
				5620	0.413	469.2		5.2	2.7
				5680	0.409	478.8		4.1	3.7
				5550	0.409	467.9		5.1	3.0
	-423	16.7	1.09		Av	466.6	160.4	4.5	3.5
	+75	17.3	5.10	1920	0.250	264.8		3.7	2.1
				1900	0.255	256.8		3.7	2.1
4A				1875	0.252	256.4		3.8	2.0
				1700	0.245	239.2		3.6	2.0
				1830	0.251	251.4		3.7	2.1
	+75				Av	253.7	88.2	3.7	2.1
	-320			4280	0.250	590.2		4.2	4.4
				4505	0.250	621.2		4.9	3.8
				4125	0.249	571.2		4.0	4.4
				3770	0.248	524.0		4.1	3.9
				4500	0.251	618.2		4.0	4.6
	-320				Av	584.9	203.2	4.2	4.2
4A	-423			6140	0.404	524.0		**	**
				6400	0.404	546.2		4.4	3.2
				5600	0.402	480.2		4.2	3.5
				3680	0.251	505.4		4.1	4.1
	-423	17.3	5.10	***	-	-		-	-
	-423				Av	513.9	178.6	4.2	3.6

* Extrapolated values.

** Inconsistent load-elongation curve.

*** Specimen broke during assembly in test fixture.

TABLE 29

COMPOSITE-TENSILE-STRENGTH TEST RESULTS (BIDIRECTIONAL 1:2 ORIENTATION)

Resin No.	Temp °F	Resin wt%	Voids vol%	Ult Load lb	Specimen Width in.	Ultimate Tensile Strength, ksi		Tensile Modulus ksi	Maximum Elongation %*
						Filament	Composite		
2	+75	19.2	1.70	2000	0.244	423.9		2.8	3.3
				1980	0.247	417.6		2.6	3.4
				1945	0.246	408.9		2.7	3.2
				1950	0.256	393.9		2.5	3.2
				1830	0.246	384.6		2.7	3.1
	↓								
	+75					Av 405.7	87.9	2.7	3.2
	-320			2125	0.244	450.3		-	-
				3375	0.252	692.7		2.6	5.4
				3100	0.264	607.2		2.4	5.3
				3125	0.245	658.5		2.8	4.7
	↓			3025	0.271	577.2		2.7	4.6
	-320					Av 597.2	129.4	2.6	4.7
	-423			4340	0.407	551.5		**	**
4A	↓			4180	0.401	539.1		2.9	3.3
				4520	0.403	580.1		3.2	3.8
	↓			3920	0.408	496.9		3.8	2.9
				4750	0.402	611.1		2.6	4.9
	-423					Av 555.7	120.4	3.1	3.8
	+75			700	0.250	144.8		2.2	1.2
				940	0.254	191.4		2.4	1.7
				1325	0.250	274.1		2.5	2.2
				705	0.253	144.1		2.3	1.3
	↓			1240	0.252	254.5		2.4	2.2
	+75					Av 201.8	44.9	2.4	1.7
	-320			1405	0.247	***		-	-
				2950	0.249	612.6		2.6	5.0
				2970	0.242	635.7		2.8	4.8
				3305	0.298	689.1		2.7	5.1
	↓			2940	0.248	612.9		2.5	4.9
	-320					Av 637.5	141.7	2.6	4.9
	-423			1860	0.400	****		-	-
				3300	0.412	****		-	-
	↓			4750	0.414	608.1		2.8	4.4
				2800	0.396	****		-	-
	-423			4580	0.407	582.0		2.4	4.4
4A	-423	19.2	5.27			Av 595.0	132.3	2.6	4.4

* Extrapolated values.

** Inconsistent load-elongation curve.

*** Statistical outlier.

**** Specimen delaminated and broke in shoulder section.

Filament strengths were not determined from the composite stresses (which are a function of the load at failure, the original cross-sectional area, and the resin content), but were calculated on the basis of the actual number of fibers wound and oriented in the direction of loading. The methods used for, and examples of, filament-tensile-strength calculations are given in Appendix E. Values for the three orientations employed are plotted in Figure 21 as a function of temperature and are summarized below.

<u>Resin No.</u>	<u>Temperature °F</u>	<u>Strength, ksi, at Designated Filament Orientation</u>		
		<u>1:0</u>	<u>1:1</u>	<u>1:2</u>
2	+75	365.9	352.4	405.7
	-320	449.9	526.4	597.2
	-423	374.3	466.6	555.7
4A	+75	265.6	253.7	201.8
	-320	601.9	584.9	637.5
	-423	494.0	513.9	595.0

This tabulation and Figure 21 reveal that Resin 4A performed better than Resin 2 at cryogenic temperatures for each orientation. In all cases, the strengths were lowest at +75°F, were highest at -320°F, and decreased somewhat at -423°F (from the value at -320°F). The sole exceptions to the general consistency are the unidirectional values for Resin 4A, particularly at -320°F; they are considered spuriously high, although no satisfactory explanation has been found. It is of interest to note in Table 27 that the high values for Resin 4A at cryogenic temperatures were achieved despite an excessive resin content (43.6%) and excessive voids (16.7%), resulting from an unsuccessful attempt to improve composite fabrication by modifying the procedures used.

For both resins at cryogenic temperatures, fiber strengths for the 1:2 bidirectional orientation were higher than for the 1:1 orientation; in turn, the latter were higher than for the unidirectional specimens, except in the case of the anomalous behavior of the unidirectional Resin 4A specimens. Higher strengths exhibited by specimens having more cross fibers suggest that the interspersing of cross plies was beneficial to the uniaxially loaded specimens, possibly because (a) they provided a more intimate bond between layers of load-carrying filaments, which in turn contributed to a more uniform load distribution, or (b) they permitted load transfer around initial fiber fractures.

This general consistency in data and trends was apparent for both resin systems even though the specimens were simple, laid-up, flat glass/resin laminates subject to processing variables attributable to different laboratory technicians. Although the use of laid-up tensile specimens and uniaxial testing is recognized as a compromise in the evaluation of glass/resin

47

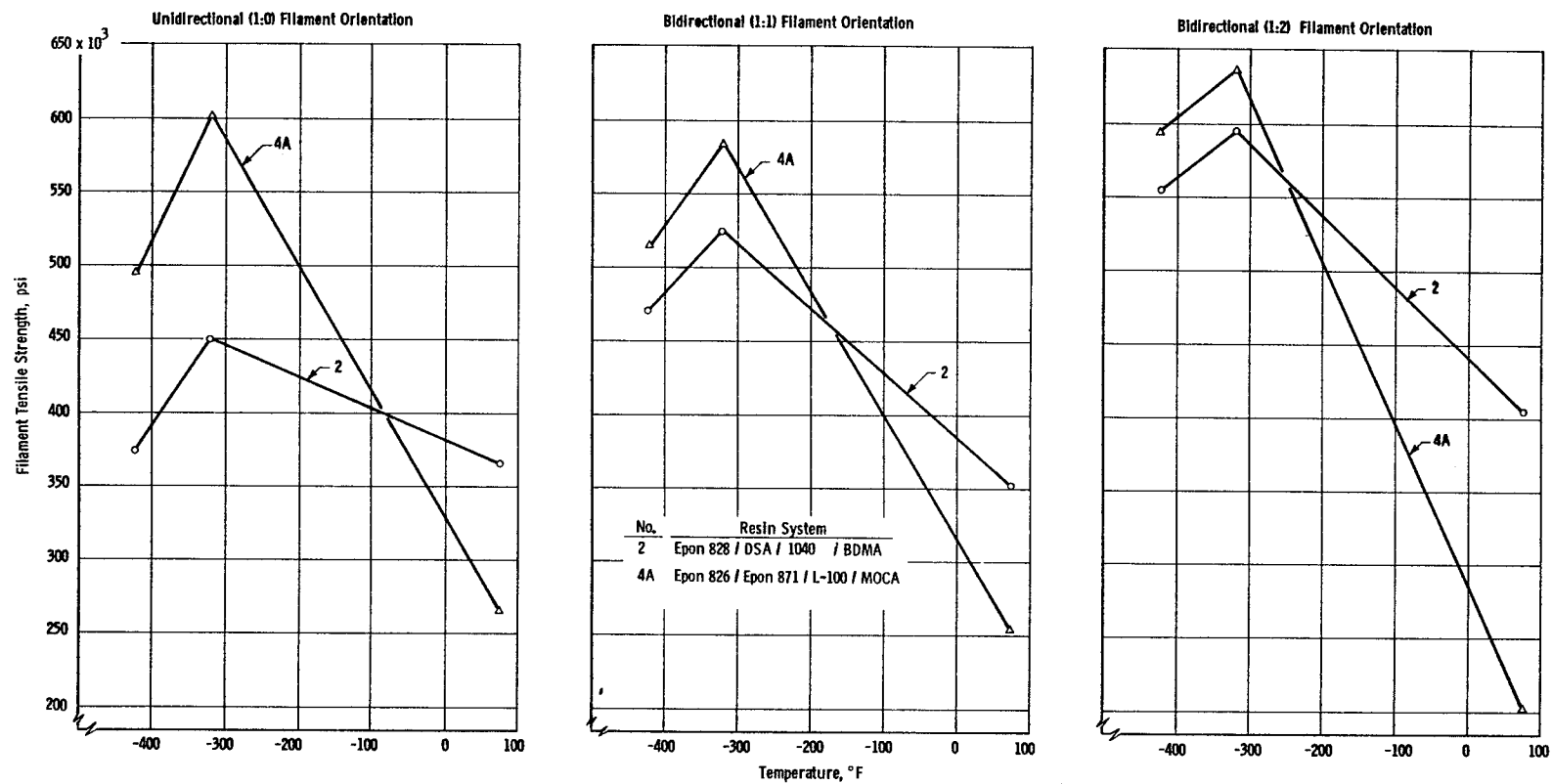


Figure 21. Effect of Temperature on Filament Tensile Strength
S-901/Cryogenic-Resin Composites with Alternate Filament Orientations

composites, the observed data consistency provides a convincing demonstration of the value of this technique, which is also relatively inexpensive when a large statistical sampling is desirable.

Tensile-modulus and elongation-at-fracture data (Tables 27, 28, and 29) reveal that the intra-resin and inter-resin results obtained for the bidirectional orientations were also consistent. On the whole, the unidirectional data were less consistent than the bidirectional with respect to these properties, perhaps because of the limited data available for Resin 2 and the excessively high resin and void contents of System 4A specimens. The increase in composite tensile modulus was less pronounced at cryogenic temperatures than for the cast resins (see Figure 9 and Table 19); in fact, slight decreases were noted for Resin 2 composites at -320°F for both bidirectional orientations. Similarly in contrast to the trend noted for the cast resins (Table 19), elongation-at-fracture values were higher at cryogenic temperatures than at $+75^{\circ}\text{F}$ for both bidirectional orientations. In general, the intra-resin elongation values were highest for the 1:2 orientation and lowest for the unidirectional orientation. There was little difference in elongations for bidirectional orientations at a specific cryogenic temperature.

Although tests such as these on uniaxially loaded specimens provide valuable tensile data readily and relatively inexpensively, it is still essential to test a biaxially loaded pressure vessel if realistic strength values for such vessels are desired. Pressure-vessel tests were performed in Task IV and are described in Section V.

2. Thermal-Shock Resistance

Composite NOL-ring segments required for the determination of thermal-shock resistance were fabricated from the same NOL rings that provided the horizontal-shear specimens, and were cut to the same finished dimensions. After being subjected to temperature cycling between -423°F and ambient, the specimens were tested in interlaminar shear at -423°F (method given in Appendix A). As shown in Table 30, the Resin 2 specimen was highly thermal-shock-resistant, giving little or no evidence of cycling-induced damage. The Resin 4A specimen, on the other hand, exhibited a decline in shear stress from 17.94 ksi to 15.39 ksi, or 12.5%. At that level, the shear stresses of the two systems were approximately the same.

3. Coefficient of Linear Thermal Contraction

Linear-thermal-contraction tests were performed on rectangular composites having filaments either parallel or normal to the specimen length. These specimens (three for each orientation and resin system) were cut from flat panels wound on a 6 by 8-in. flat mandrel and cured under vacuum-bag conditions. The tests employed a fused-quartz dilatometer technique. Dimensional changes were dynamically recorded at 10° intervals between -400 and $+70^{\circ}\text{F}$. The test results are given in Tables 31 and 32; average values are plotted in Figure 22.

Significant variations between specimens were obtained with both Resin 2 and 4A composites, in contrast to the highly consistent thermal-

TABLE 30

COMPOSITE THERMAL-SHOCK-RESISTANCE TEST RESULTS
(NOL HORIZONTAL-SHEAR METHOD)

<u>Resin No.</u>	<u>Resin System (Parts by Weight)</u>	<u>Shear Stress at -423⁰F, ksi</u>	
		<u>Cycled Specimens</u>	<u>Noncycled* Specimens</u>
2	Epon 828/DSA/Empol 1040/BDMA (100/115.9/20/1)	15.00	-
		16.99	-
		13.83	-
		12.89	-
		17.22	-
		Av 15.19	15.39
4A	Epon 826/Epon 871/L-100/MOCA (35/15/50/27.6)	14.87	-
		14.83	-
		15.13	-
		16.61	-
		17.41	-
		Av 15.70	17.94

* Noncycled specimens (see Tables 33 and 34) cut from the same NOL ring as the cycled specimens.

TABLE 31

COMPOSITE LINEAR-THERMAL-CONTRACTION TEST RESULTS (RESIN 2)*

Temp °F	$\Delta L/L, 10^{-3}$ in./in.							
	Parallel (Longitudinal)				Normal (Transverse)			
	Specimen 1	Specimen 2	Specimen 3	Average	Specimen 1	Specimen 2	Specimen 3	Average
+70	0	0	0	0	0	0	0	0
+50	0.086	0.087	0.113	0.095	0.162	0.162	0.319	0.212
0	0.111	0.136	0.138	0.128	0.636	0.636	0.010	0.761
-50	0.173	0.198	0.227	0.199	1.073	1.114	1.696	1.305
-100	0.210	0.284	0.265	0.254	1.585	1.634	2.407	1.875
-150	0.284	0.383	0.340	0.336	2.059	2.133	2.931	2.374
-200	0.371	0.420	0.353	0.381	2.421	2.569	3.443	2.811
-250	0.445	0.445	0.378	0.423	2.770	2.969	3.917	3.219
-300	0.457	0.457	0.391	0.435	3.057	3.305	4.279	3.547
-350	0.470	0.470	0.403	0.448	3.170	3.490	4.466	3.709
-400	0.519	0.495	0.429	0.481	3.419	3.817	4.790	4.009
Resin, wt%	19.1	18.5	13.8	17.1	12.9	14.7	15.4	14.4
Voids, vol%	9.0	8.85	2.73	6.9	2.84	4.3	4.26	3.8

* Epon 828/DSA/Empol 1040/BDMA (100/115.9/20/1 parts by weight).

TABLE 32

COMPOSITE LINEAR-THERMAL-CONTRACTION TEST RESULTS (RESIN 4A)*

Temp °F	$\Delta L/L, 10^{-3}$ in./in.							
	Parallel (Longitudinal)				Normal (Transverse)			
	Specimen 1	Specimen 2	Specimen 3	Average	Specimen 1	Specimen 2	Specimen 3	Average
+70	0	0	0	0	0	0	0	0
+50	0.113	0.112	0.112	0.112	0.534	0.742	0.783	0.686
0	0.213	0.212	0.212	0.212	1.975	2.429	2.549	2.318
-50	0.352	0.324	0.324	0.333	3.007	3.700	3.805	3.504
-100	0.490	0.462	0.462	0.471	3.963	4.745	4.863	4.524
-150	0.641	0.587	0.586	0.605	4.833	5.652	5.883	5.456
-200	0.780	0.674	0.724	0.726	5.541	6.445	6.741	6.242
-250	0.881	0.749	0.824	0.818	6.113	7.099	7.412	6.875
-300	0.969	0.812	0.936	0.905	6.523	7.590	7.873	7.329
-350	1.032	0.849	0.974	0.951	6.734	7.754	8.134	7.541
-400	1.132	0.924	1.048	1.035	7.032	7.854	8.507	7.798
Resin, wt%	33.9	39.7	39.6	37.7	26.7	31.7	32.8	30.4
Voids, vol%	8.10	7.66	6.80	7.5	6.30	8.53	7.16	7.3

* Epon 826/Epon 871/L-100/MOCA (35/15/50/27.6 parts by weight).

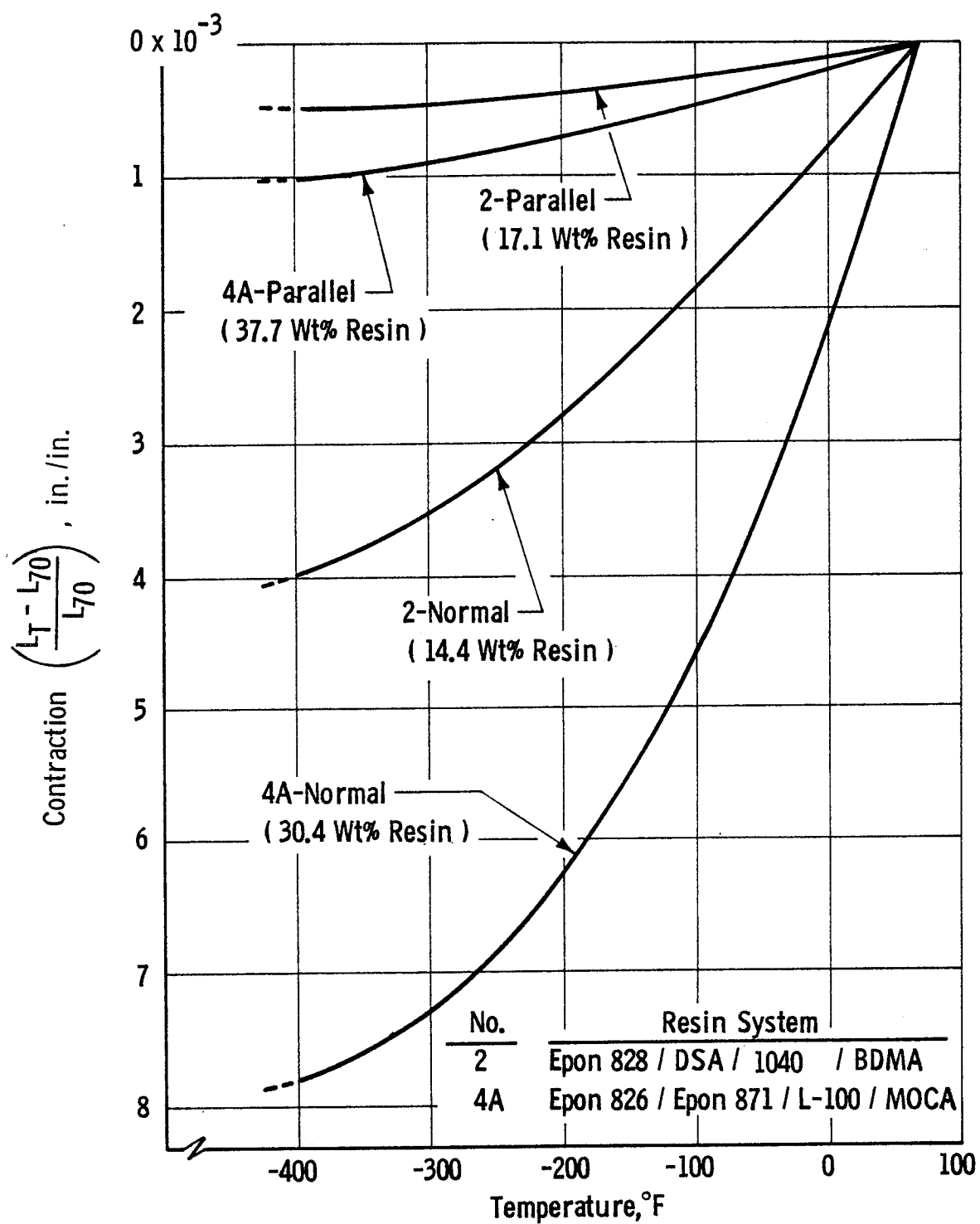


Figure 22. Linear Thermal Contraction, S-901/Cryogenic-Resin Composites

contraction data obtained with analogous cast-resin specimens in Task II. Comparison of resin contents with contraction behavior reveals a direct correlation for both the longitudinal and transverse Resin 2 specimens, as well as for the transverse Resin 4A specimens. The 4A longitudinal-contraction data, however, exhibit no single consistent pattern throughout.

With regard to differences between resins, Tables 31 and 32 show that the total average thermal contractions of the Resin 4A specimens were about twice those of Resin 2. Because the resins exhibited highly similar thermal-contraction characteristics (Figure 20), it is reasonable to attribute the greater Resin 4A contraction to higher resin contents, rather than to any innate difference between the two resins. In addition, the data fail to suggest a simple relationship between a normal range of voids and thermal-contraction behavior.

The relationship between total thermal contraction and resin content is plotted for each orientation and resin in Figure 23. Least-square lines are drawn through the data points. The plots indicate (at least for these particular resin systems) that (a) filament orientation is an overriding factor in the thermal-contraction behavior of composites, (b) in parallel filament orientation, the glass filament determines the composite thermal-contraction characteristics, and (c) in normal filament orientation, the resin matrix and the resin content are dominant factors.

4. Interlaminar Shear Strength

Composite NOL-ring segments for the determination of horizontal shear strength and thermal-shock resistance were fabricated and tested as described in Appendix A.

Table 33 compares horizontal-shear-test results for Resin 4A composites with Task II results. At a resin content comparable to the previous values, the voids in the Task III specimen dropped from 5.66 to 3.92% and the average shear strengths increased 66.3, 7.3, and 26.4% at +75, -320, and -423°F, respectively. The decrease in voids, which is attributed to the omission of solvent in the mix, was accompanied by the highest average shear-strength values at cryogenic temperatures obtained in the program (Table 33 and Figure 24).

Figure 25 shows a typical Task III Resin 4A specimen photographically. As compared with 4A specimens from Task II (Figures 16 and 18), Figure 25 reveals an increased filament-packing density. Also apparent, in all three figures, is the higher incidence of voids in the outboard sections, probably due to inner-filament compaction caused by the winding tension. Figures 26* and 27 show the Resin 4A failure area at magnifications of 100X and 500X, respectively.

Table 34 compares horizontal-shear-test results for Resin 2 with analogous values obtained in Task II. It shows that reduced void content

*The relatively large white areas in this figure were caused by water droplets.

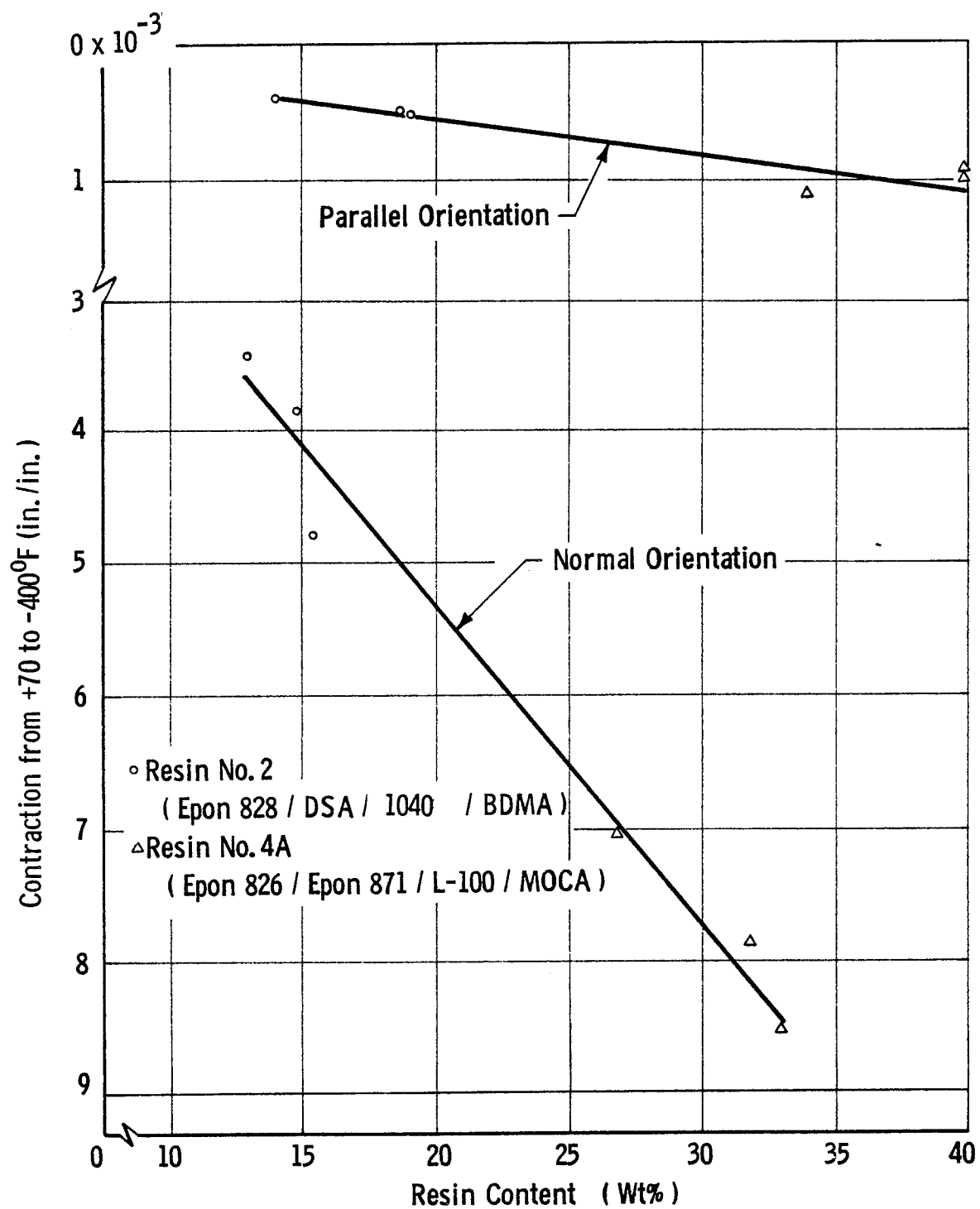


Figure 23. Effect of Resin Content and Filament Orientation on Linear Thermal Contraction, S-901/Cryogenic-Resin Composites

TABIE 33

INTERLAMINAR-SHEAR TEST RESULTS, RESIN 4A*
(NOL HORIZONTAL-SHEAR METHOD)

<u>Task</u>	<u>MEK/L-100 Ratio</u>	<u>Resin Content wt%</u>	<u>Void Content vol%</u>	<u>Composite Specific Gravity</u>	<u>Shear Stress, ksi</u>		
					<u>+75°F</u>	<u>-320°F</u>	<u>-423°F</u>
II	1 ml/lg	13.11	9.56	1.931	1.93	10.00	13.34
					2.08	9.81	13.01
					2.08	12.61	13.02
					2.04	12.11	10.50
					1.98	9.71	11.25
				Av	2.02	10.87	12.22
II	1 ml/4g	10.64	5.66	2.069	3.06	12.55	15.77
					3.12	12.44	12.15
					3.14	15.93	12.03
					3.09	17.41	16.29
					3.04	18.09	14.74
				Av	3.09	15.28	14.20
III	0 ml/lg	13.31	3.92	2.053	5.17	17.11	15.67
					5.09	15.13	17.41
					5.14	12.85	19.82
					5.01	16.82	17.14
					5.27	20.06	19.65
				Av	5.14	16.40	17.94

*Epon 826/Epon 871/L-100/MOCA (35/15/50/27.6 parts by weight).

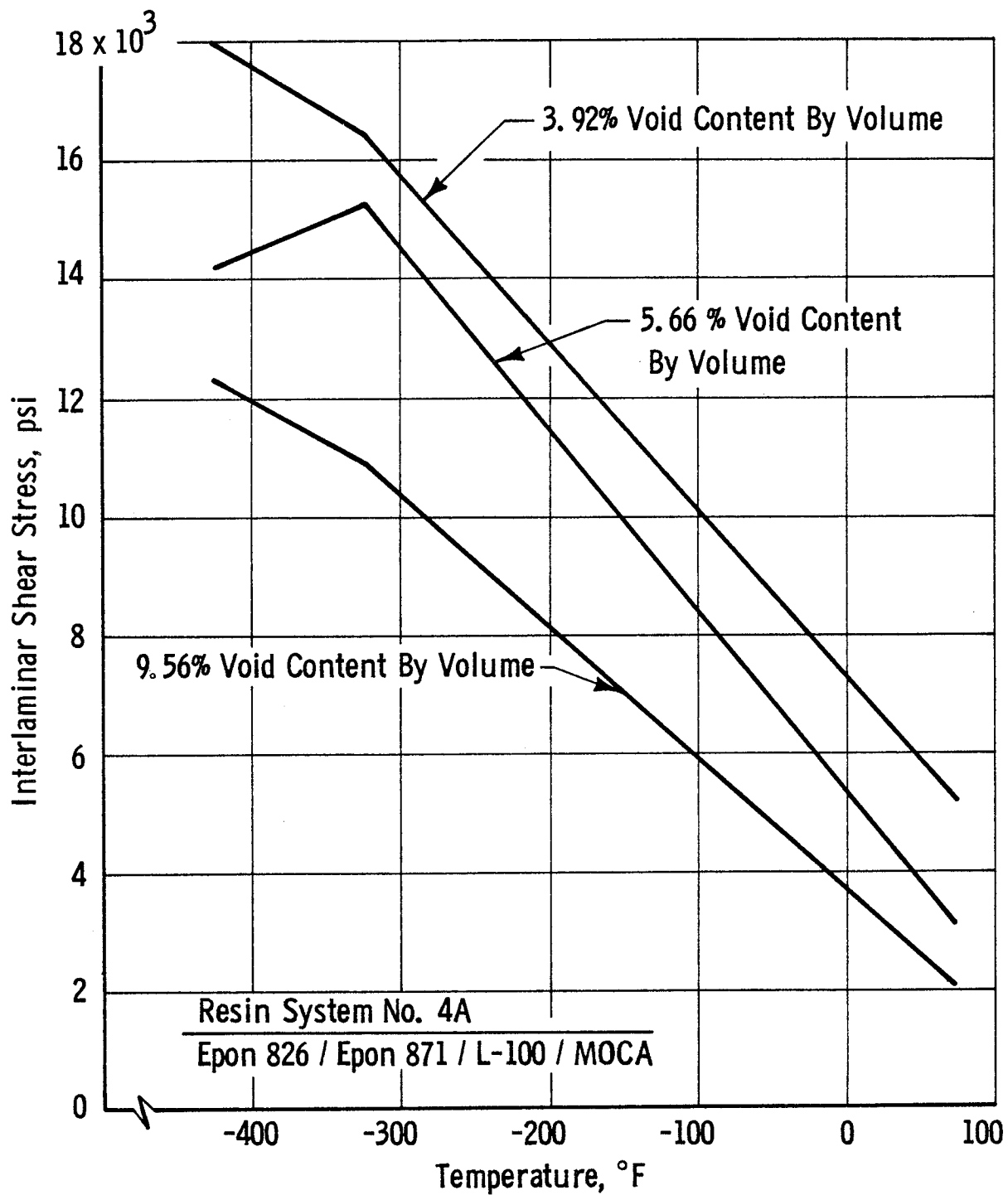


Figure 24. Effect of Temperature and Voids on Interlaminar Shear Stress, S-901/Resin 4A Composite (Horizontal-Shear Method)

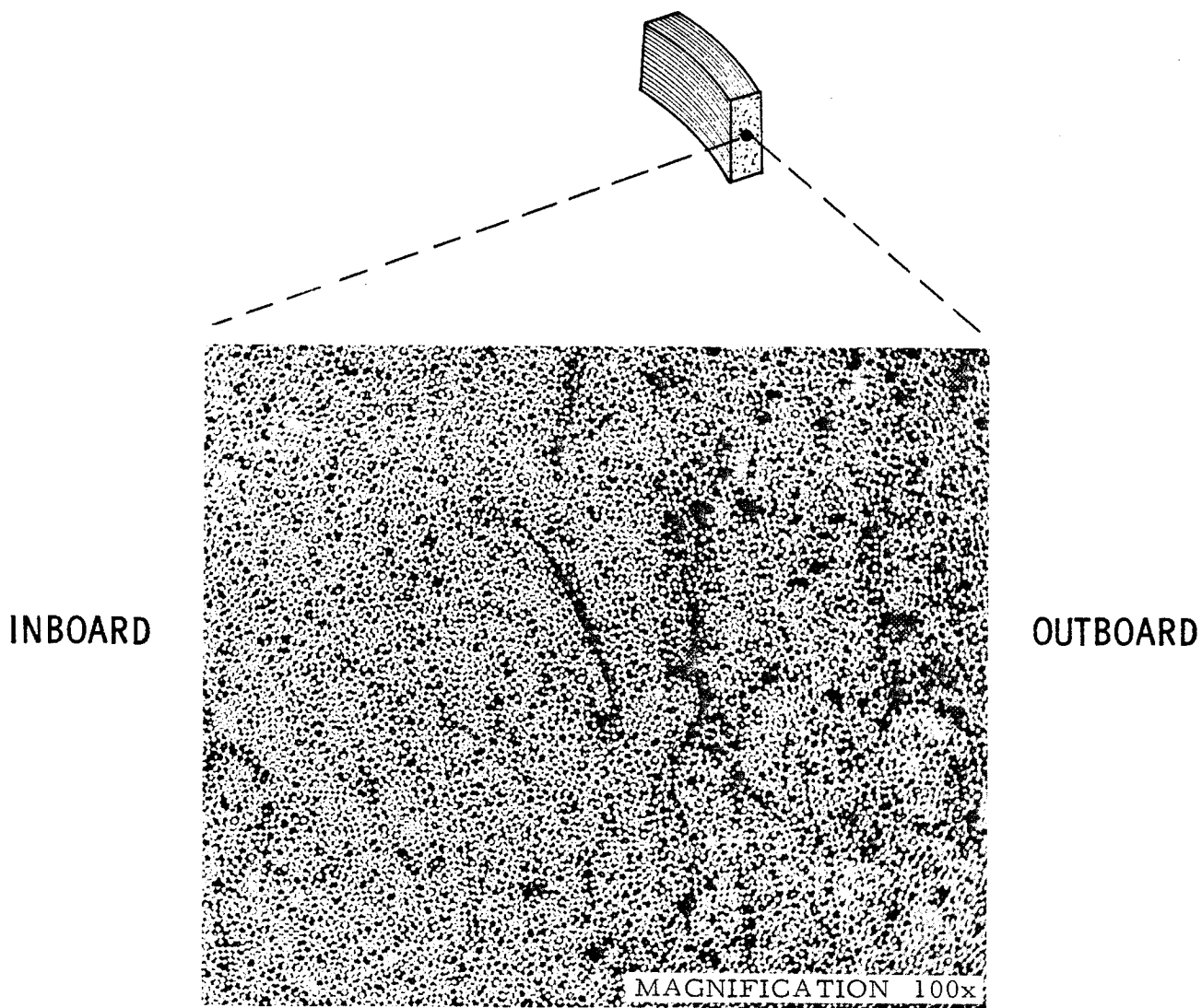


Figure 25. Resin 4A Horizontal-Shear Segment
(3.92 vol% Voids)

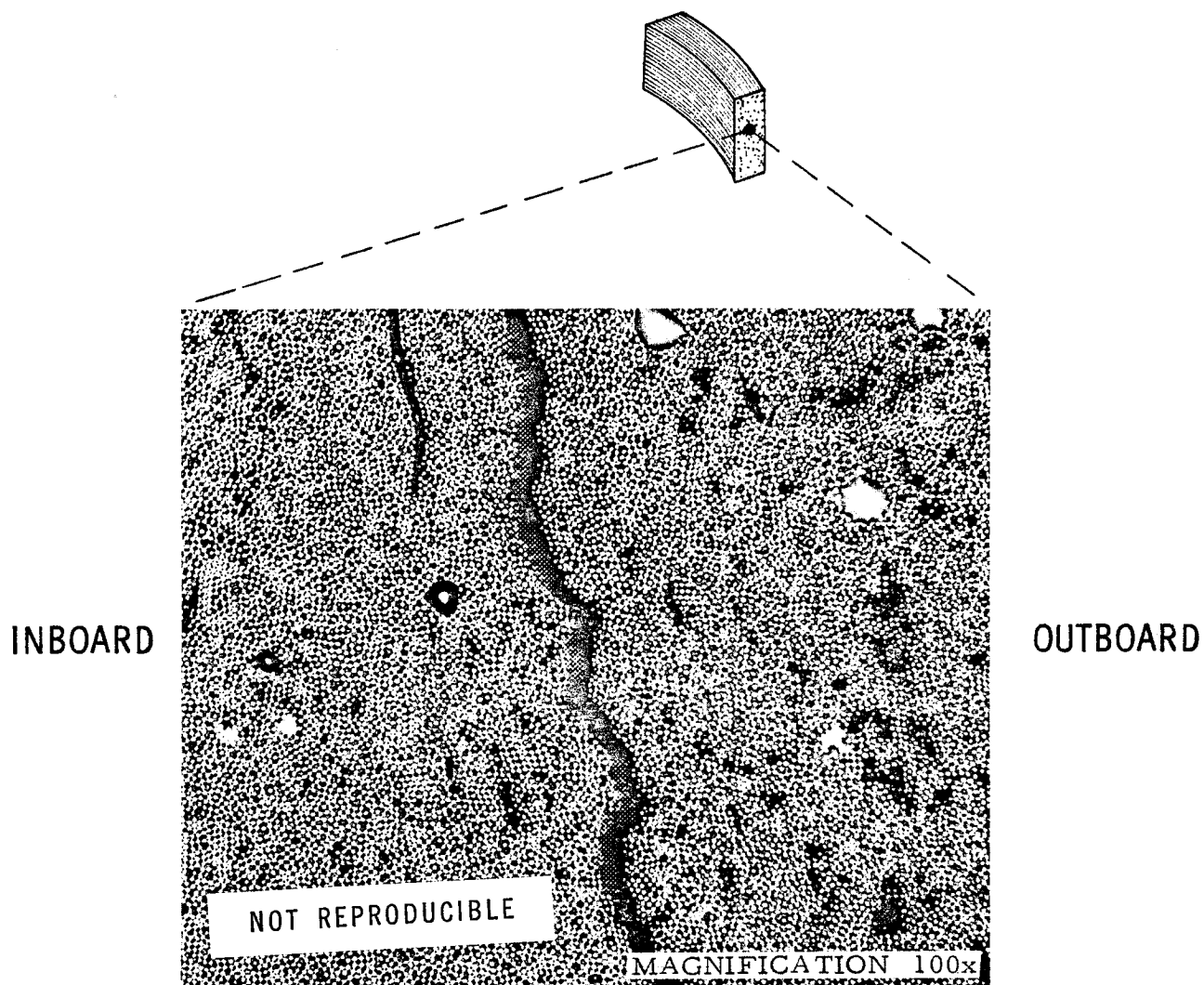


Figure 26. Resin 4A Horizontal-Shear Segment
After Shear Test at -423°F
(3.92 vol% Voids)

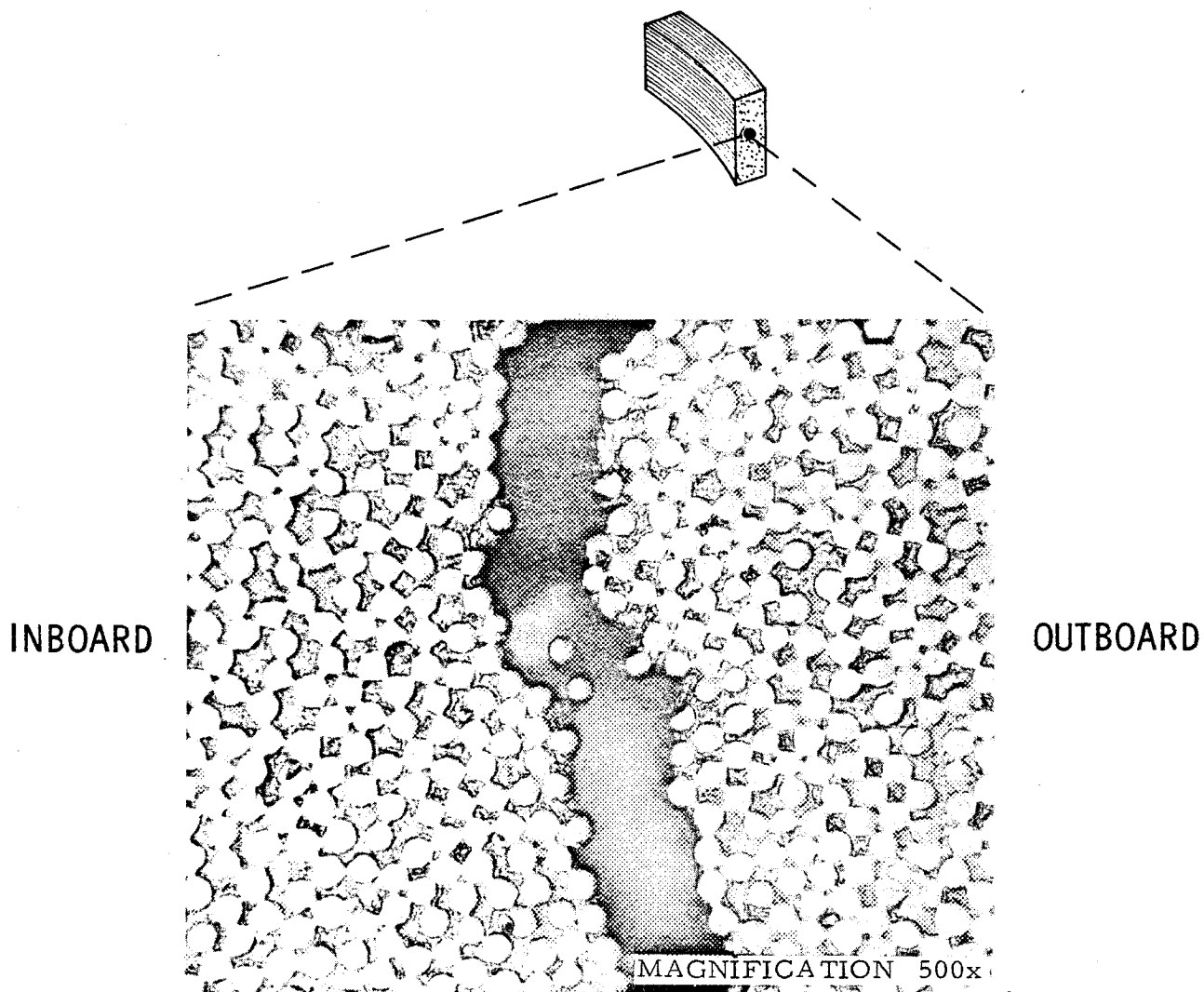


Figure 27. Resin 4A Horizontal-Shear Segment
in Area of Shear Failure (3.92 vol% Voids)

TABLE 34

INTERLAMINAR-SHEAR TEST RESULTS, RESIN 2*
(NOL HORIZONTAL-SHEAR METHOD)

<u>Task</u>	<u>Resin Content wt%</u>	<u>Void Content vol%</u>	<u>Composite Specific Gravity</u>	<u>Shear Stress, ksi</u>		
				<u>+75°F</u>	<u>-320°F</u>	<u>-423°F</u>
II	17.86	4.70	1.903	6.41	14.31	15.93
				6.79	16.41	16.87
				6.53	12.91	15.48
				6.91	14.61	15.28
				6.62	14.31	16.97
				Av 6.65	14.11	16.11
III	11.44	2.54	2.086	5.92	13.71	14.50
				5.85	13.76	16.75
				6.36	15.85	15.48
				6.23	15.04	15.58
				6.50	12.45	14.64
				Av 6.17	14.16	15.39

* Epon 828/DSA/Empol 1040/BDMA (100/115.9/20/1 parts by weight).

was not accompanied by an increase in average shear stress, the latter values being either essentially unchanged from or slightly lower than those obtained in Task II. The data suggest that resin content, which was considerably different in the two specimens, may contribute to horizontal shear strength.

Figure 28 reveals a fairly uniform distribution of filaments and an absence of sizable concentrations of voids in the Resin 2 specimen. In the fractured specimen (Figure 29*), a secondary shear failure can be seen to the right of the main shear plane.

Finally, the Task III interlaminar-shear data show that, at comparable resin contents, (a) both resins provided composites of satisfactorily low void content, and (b) the Resin 2 shear strength was higher at 75°F, but Resin 4A values were higher at cryogenic temperatures.

C. SELECTION OF OPTIMUM CRYOGENIC RESIN SYSTEM

The four candidate resins chosen in Task I of this program were narrowed to the following systems in Task II: (1) Resin 2 (Epon 828/DSA/Empol 1040/BDMA), a bisphenol A epoxy system modified for low-temperature flexibility by means of a long-chain anhydride and a high-molecular-weight tri-carboxy acid, and (2) Resin 4A (Epon 826/Epon 871/L-100/MOCA), an epoxy/polyurethane system modified by a higher-molecular-weight aliphatic epoxy.

Resin 4A was superior to Resin 2 at cryogenic temperatures in Task II on the basis of criteria indices as well as all individual mechanical-property tests except for horizontal and short-span shear. Additional horizontal-shear tests in Task III demonstrated that earlier low values for 4A composites probably resulted from high void content, which in turn probably resulted from residual solvent. Thus, for 4A composites of low void content, the resulting shear strengths were at least comparable to those of Resin 2 (Tables 33 and 34).

The processing and testing of composite samples in Task III demonstrated that both resin systems were fully compatible with S-901 glass fibers. Resin 2 showed no deterioration in horizontal shear strength under thermal shock (-423°F); in similar temperature cycling, the shear stress of Resin 4A declined 12.5%, but was still as high as that of Resin 2. Linear-thermal-contraction data on composite specimens led to the conclusion that the two systems were probably very similar in this regard, given composites of similar resin content. At cryogenic temperatures, the tensile strengths of filaments in Resin 4A composites were significantly superior to those of Resin 2.

A preference for Resin 4A could easily be justified on the basis of mechanical-property comparisons, particularly if room-temperature properties were considered of secondary importance in cryogenic applications. However, the weakness of Resin 4A lay in its physical properties (pot life and viscosity) and its workability and processing characteristics. In the preparation of flat-panel laminates, pot-life and viscosity deficiencies were successfully overcome,

* Ibid.

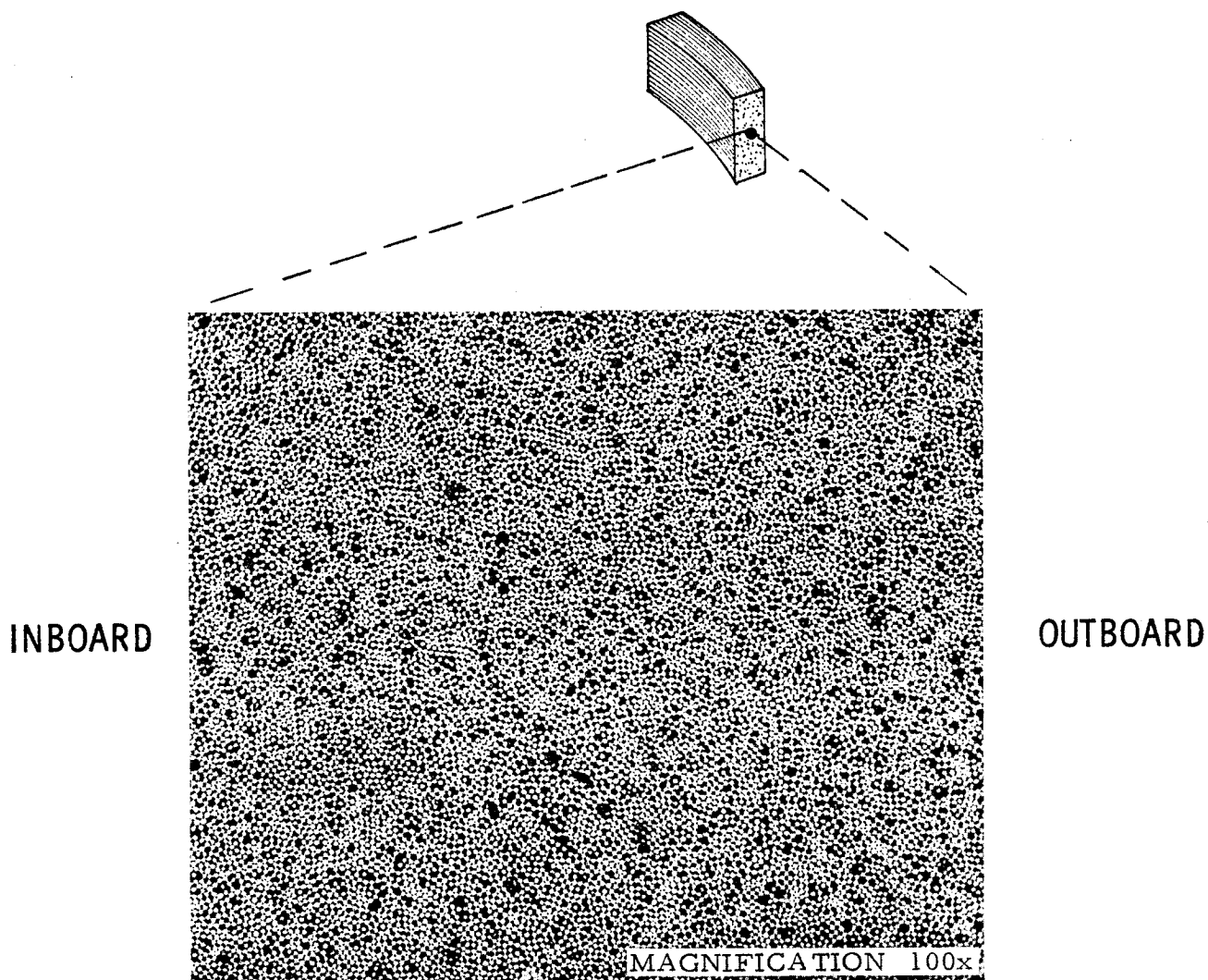


Figure 28. Resin 2 Horizontal-Shear Segment
(2.54 vol% Voids)

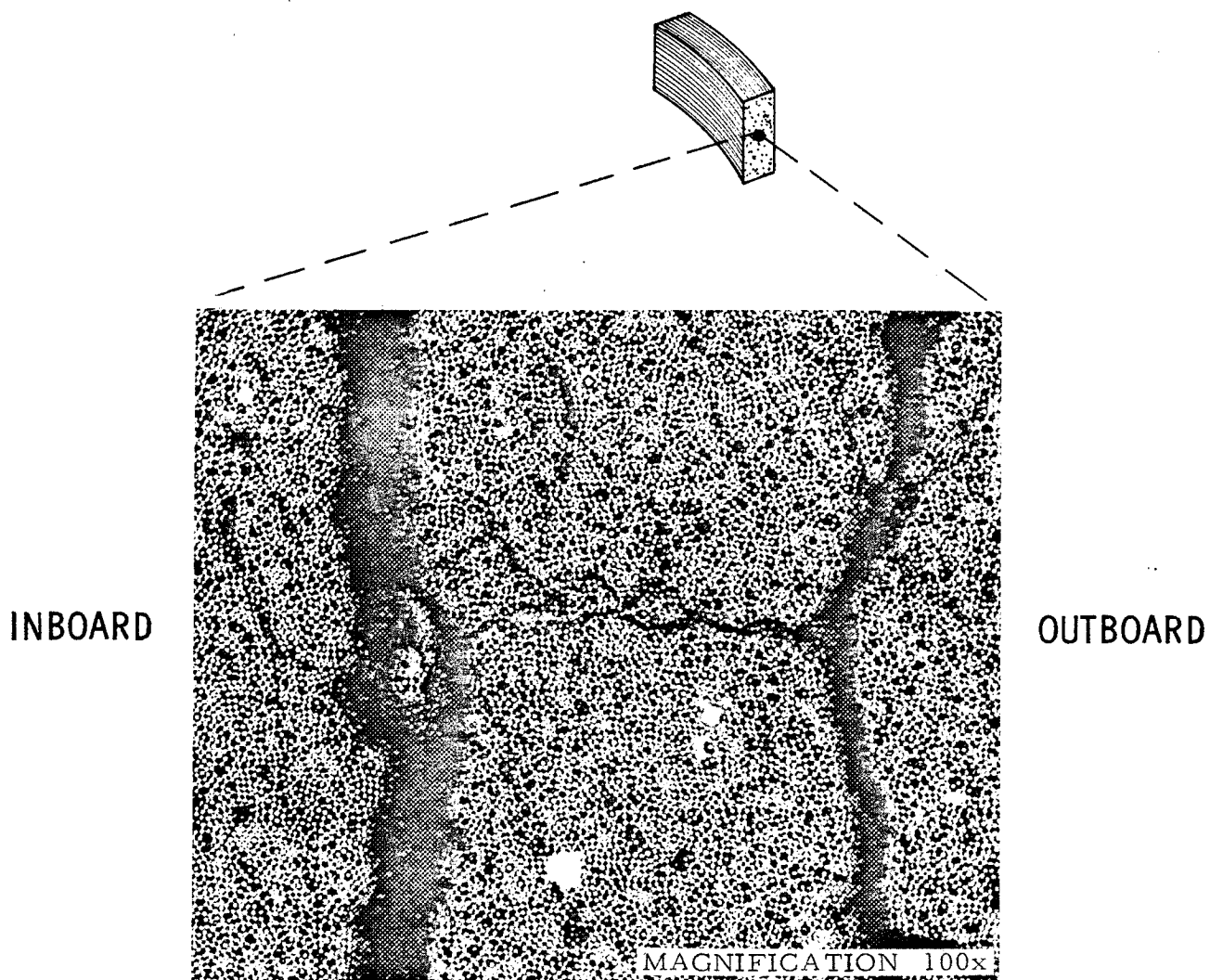


Figure 29. Resin 2 Horizontal-Shear Segment
After Shear Test at -423°F (2.54 vol% Voids)

and satisfactory resin and void contents were obtained, by a special mixing technique (at a small cost in extra labor). Doubt remained, however, that these methods would be adequate or practicable for cylindrical vessels, or for larger structures in general, using the filament-winding techniques now employed. It is believed that problems might be encountered in achieving adequate resin flow and resin bleedout that in turn could lead to excessively heavy structures with high resin and void contents.

The use of a solvent with Resin 4A might ameliorate the pot-life/viscosity deficiencies, but this approach would complicate the processing. In any event, the development of such a procedure and the demonstration of its practicality were beyond the scope of this program.

Resin 2, on the other hand, had attractive mechanical properties at cryogenic and room temperatures. Its pot life, viscosity, workability, and processing characteristics were highly satisfactory. No special precautions were required in its formulation. Its use did not require excessive effort for the cleaning of winding-machinery guide wheels and tooling, as was the case with Resin 4A. Another attractive aspect of Resin 2 is suggested by the horizontal-shear-test results for composites fabricated from this resin and a glass-fiber/finish combination other than S-901. With Aerojet Hi-Stren glass fiber and an experimental finish containing A-1100, Aerojet has reported excellent horizontal shear strengths at ambient and cryogenic temperatures.* On the other hand, the analogous results obtained with Resin 4A were poor. It is thus possible that Resin 2 is "less specialized" and more adaptable to other glass/finish combinations than is 4A. Finally, its adaptation to prepreg should not be difficult.

These considerations led to the selection of System 2 as the optimum cryogenic resin for further evaluation in Task IV.

* NASA Contract NAS 3-6297, Monthly Letter Report, 10 May 1966.

V. TASK IV - FABRICATION AND EVALUATION OF FILAMENT-WOUND-
COMPOSITE PRESSURE VESSELS

The performance of Resin 2 in S-901 glass-FWC pressure vessels under bi-axial-loading conditions was evaluated in Task IV. Tests at +75, -320, and -423°F defined the performance levels and provided structural-property data required for comparison of Resin 2 with the standard resin system, Shell 58-68R.

Six vessels were fabricated with Resin 2 and six with 58-68R (Epon 1031/Epon 828/MNA/BDMA). The latter system has been widely used in various filament-wound pressure-vessel structures, including the Polaris A-3 rocket-motor case. It is well characterized and thus is suitable for use as a comparison standard.

A single roll of S-901 glass roving was used to wet-wind all 12 vessels. Pressure-vessel design, fabrication, and test results are discussed below.

A. DESIGN

The test vessel was an 8-in.-dia by 13-in.-long, closed-end cylinder. It was designed to achieve a 2.5% strain with a longitudinal-to-circumferential strain ratio of 1 at as low an internal pressure as possible with current winding processes. This type of vessel, fabricated from longitudinally and circumferentially oriented filaments wound over a 0.006-in.-thick Type 304 stainless steel foil liner, was selected on the basis of experience acquired in previous development efforts (Ref. 23).

A filament-wound, cylindrical, pressure vessel requires at least two longitudinal layers (produced by one rotation of the liner during the winding) and a specified number of complementing circumferential layers in the cylindrical section. It has been determined experimentally that a cured single layer of S-901 glass roving will produce an average composite thickness of approximately 0.0075, 0.0055, and 0.0035 in. for 20-end, 12-end, and single-end material, respectively.* Calculations showed that the 20-end-roving structure would produce a higher chamber burst pressure (approximately 2800 psig) than is normally associated with cryogenic tankage. A vessel wound with the minimum number of layers of single-end roving, although exhibiting the lower burst pressure applicable to cryogenic tankage, nevertheless requires additional fabrication time and increases winding complexity, in comparison with the use of multiple-end roving. The 12-end material was therefore selected as a logical compromise.

Dimensional coordinates of the pressure-vessel heads and other vessel characteristics were defined with the aid of a computer program that analyzed and designed the vessels. Input variables were based on design criteria presented in Table 35. Other dimensional and material parameters are presented in Table 36. The computer program, developed by Aerojet under Contract NAS 3-6292, analyzes the filament shell by means of a netting analysis, which assumes that stresses are constant along the path of the filament and that the structural contribution of the resin matrix is negligible. The filament-wound shell and

*An end is the smallest commercially available bundle of glass filaments, and consists of 204 monofilaments in a single continuous strand.

TABLE 35

DESIGN CRITERIA
PRESSURE VESSELS FOR CRYOGENIC-RESIN EVALUATION

Diameter, in.	7.766
Length, in.	12.250
Polar-boss diameter, in.	2.900
Metal-liner thickness, in.	0.006
Longitudinal-filament-wound-composite thickness, in.	0.011
Design burst pressures, psi*	
At +75°F	1338
At -320°F	2087
At -423°F	1922

Properties	Type 304 Stainless Steel, Annealed	Glass-Filament-Wound Composite
Density, lb/in. ³	0.289	0.075
Coefficient of thermal expansion, in./in./°F at +75 to -423°F	6.760×10^{-6}	2.010×10^{-6}
Tensile-yield strength, psi	38,000	-
Derivative of yield strength with respect to temperature, psi/°F	-116.0	-
Elastic modulus, psi	29.4×10^6	12.4×10^6
Derivative of elastic modulus with respect to temperature, psi/°F	-8030	-2410
Plastic modulus, psi	800,000	-
Derivative of plastic modulus with respect to temperature, psi/°F	-0.1	-
Poisson's ratio	0.295	-
Derivative of Poisson's ratio with respect to temperature, 1/°F	0.0	-
Volume fraction of filament in composite	-	0.673
Filament, design allowable stress, psi**		
At +75°F	-	330,000
At -320°F	-	495,000
At -423°F	-	445,000

* Determined from analysis of other design criteria.

** Hoop and longitudinal filaments.

TABLE 36

DIMENSIONAL AND MATERIAL PARAMETERS
PRESSURE VESSELS FOR CRYOGENIC-RESIN EVALUATION

Cryogenic-resin specimens, Aerojet drawing number	178156-5
Standard-resin specimens, Aerojet drawing number	178156-7
Internal volume, cu in.	510.0
Outside diameter, in.	7.832
Inside diameter of metal heads, in.	7.766
Inside diameter of metal cylinder, in.	7.754
Metal-liner thickness, in.	0.006
Total composite cylinder-wall thickness, in.	0.033
Hoop-wound composite	0.022
Longitudinal-wound composite	0.011
Boss-to-boss length, in.	13.16
Cylinder length (tangent to tangent), in.	7.08
Forward-boss outside diameter, in.	2.90
Aft-boss outside diameter, in.	2.90
Liner and boss material	Type 304 stainless steel (annealed)
Glass filaments	S-901
Roving type	12-end
Resin matrix	
Cryogenic-resin specimens	Epon 828/DSA/Empol 1040/BDMA (100/ 115.9/20/1)
Standard-resin specimens	Epon 1031/Epon 828/ MNA/BDMA (50/50/90/ 0.5)
Liner-to-composite adhesive	Epon 828/DSA/Empol 1040/BDMA (100/ 115.9/20/1)

metal shell were combined in the analysis by equating strains in the longitudinal and hoop directions and by adjusting the radii of curvature of the shells to match the combined material strengths at the design pressure. The computer program also defined the filament and metal-shell stresses and strains at zero pressure and at the design pressure, the required hoop-wrap thickness for the cylindrical portion of the vessel, the filament-path length, and the weight and volume of the components and complete vessel. The test vessel was designed to fail in the heads because earlier Aerojet studies of glass/resin interaction demonstrated that the resin has more influence on the structural integrity of the heads than on the cylindrical section.

Because the computer program contains optional input variables, the design vessel-burst pressures at the test temperatures (1338 psi at +75°F, 2087 psi at -320°F, and 1922 psi at -423°F) were established on the basis of (1) a longitudinal-composite thickness of 0.011 in. for the 12-end, S-901 glass-roving structure, and (2) single-cycle design-allowable strengths for S-901 glass filaments amounting to 330.0 ksi at +75°F, 495.0 ksi at -320°F, and 445.0 ksi at -423°F. These strengths were selected after a review of composite-property data indicated that the strength of glass laminates increases approximately 50% at -320°F and 35% at -423°F over the strengths at +75°F.

The designs prepared for the metal-foil liner and the filament-wound pressure vessel are shown in Figures 30 and 31. A vessel-weight analysis is presented in Table 37.

Appendix F summarizes the pressure-vessel design analysis and presents winding-pattern calculations for the longitudinal and circumferential filaments, as well as a structural analysis of critical metal components and high-stress areas.

B. FABRICATION

1. Metal Liner

The head sections of the welded-metal-foil liners were fabricated by hydroforming. The 0.006-in.-thick metal foil (Type 304 stainless steel, annealed) was cut to the required size, placed between thin mild-steel plates, and positioned on the work table. A pressure dome was lowered onto the steel plates, and hydraulic pressure was applied.

A male punch was moved upward, forcing the steel plates against a rubber diaphragm backed by hydraulic fluid under controlled high pressure. As the punch moved upward, proper control of the pressure in the dome (or forming cavity) caused the diaphragm to form the metal to the exact configuration of the punch. The punch was then lowered, the dome was lifted, and the part was removed. Negligible part thin-out occurred, because this was a forming rather than a drawing operation. After each hydroforming operation, the mild-steel plates were discarded. Each formed metal-foil head section was stress-relieved and trimmed to the required dimensions. A center opening was cut to accommodate the boss.

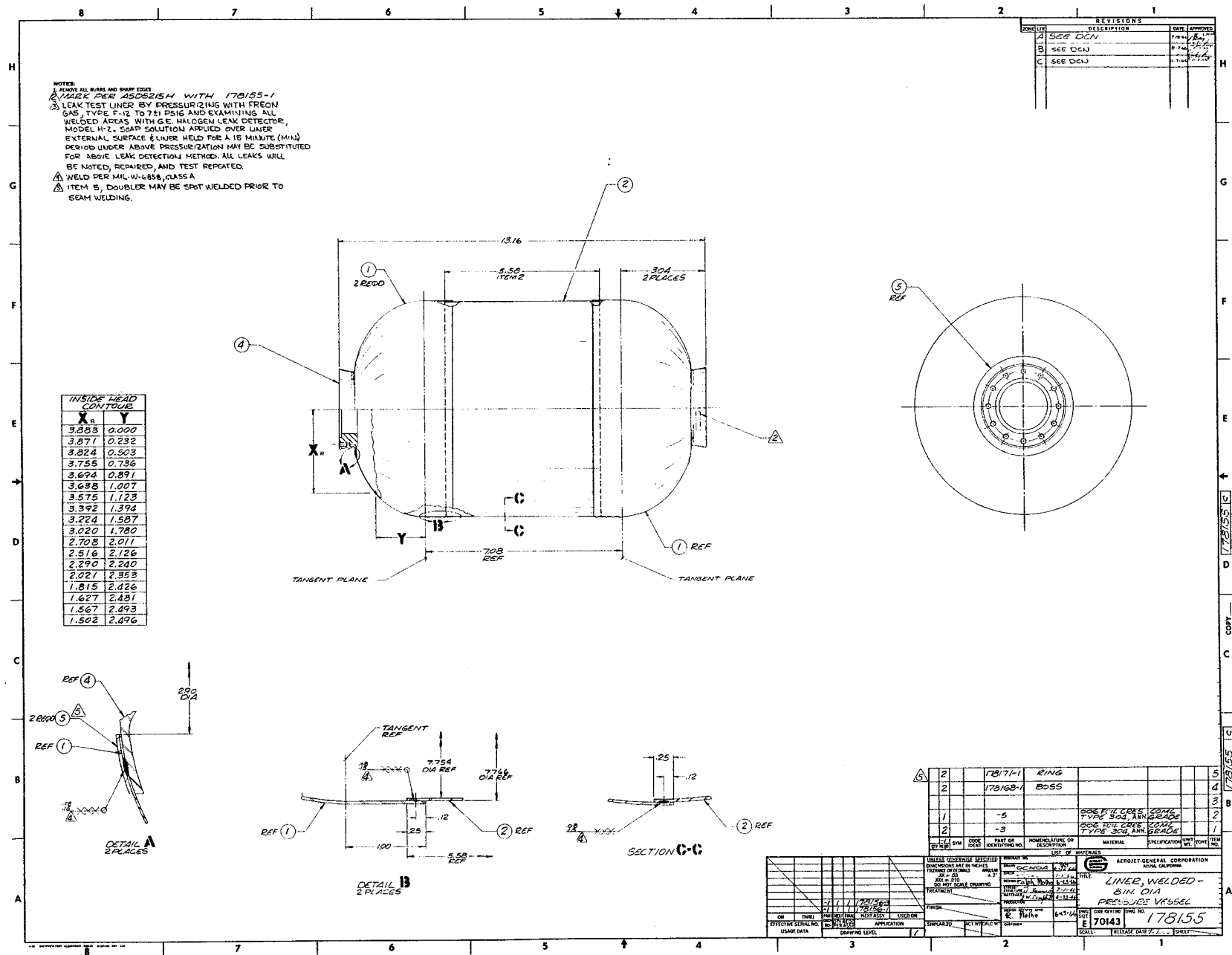


Figure 30. Welded Liner, 8-in.-dia Pressure Vessel

TABLE 37

WEIGHT ANALYSIS
PRESSURE VESSELS FOR CRYOGENIC-RESIN EVALUATION

Cryogenic-resin specimens, Aerojet drawing number		178156-5
Standard-resin specimens, Aerojet drawing number		178156-7
Internal volume, cu in.		510.0
Outside diameter, in.		7.832
Estimated weight, lb		2.69
Composite structure		0.64
Forward head	0.10	
Aft head	0.10	
Cylinder section	0.44	
Metal hardware		2.05
Metal liner	0.56	
Forward head	0.13	
Aft head	0.13	
Cylinder section	0.30	
Bosses (2)	1.46	
Doublers (2)	0.03	

The cylindrical section of the liner was fabricated from 0.006-in.-thick foil that was cut to the required size, roll-formed to the desired diameter, and joined by a single seam weld down the length. The bosses were machined from stainless steel plate (Type 304, annealed).

Resistance-roll-seam welding was used to join each boss fitting to the center opening of the head, to join the cylindrical section to each head section, and to join the cylindrical section with a longitudinal seam. The weld thus produced consists of a series of overlapping spot welds made progressively along a lapped joint with roller-type electrodes. A doubler ring was used in the boss-to-head-section joint to position the weld nugget that joined the relatively thick boss flange to the thin liner. The doubler ring, cut and formed to fit the head contour in the area where it was used, was tack-welded to position the components prior to final roll-seam welding.

Each welded-metal liner was subjected to a total of three separate pressure tests before filament winding was initiated. The first test was performed as an initial check on weld soundness and the absence of leakage across or through joints under pressure loading. In this test the tank was pressurized with Freon gas (Type F-12) to 7 \pm 1 psig, and all welded areas were examined with a General Electric halogen leak detector, Model H-2 (sensitivity, 60 ppm/division).

Two additional, more sensitive, pressure tests were then performed. The first subjected the liner to a pressure load of 20 psig with nitrogen gas for 2 min to establish liner integrity under a differential pressure of 5 psig. In the second, the liner was placed in an enclosed aluminum tank, and a vacuum was created inside and outside the liner. Helium gas was used to pressurize the liner to 5 psig while the area between the liner and aluminum tank was monitored with a Veeco leak detector, Model MS-9AB (helium-mass-spectrometer technique) for traces of helium leakage. The equipment is capable of detecting one part of helium in 10^7 parts of air. The maximum acceptable leakage rate for the liners was set at 10×10^{-5} standard cu cm/sec. All metal-foil liners successfully passed each of the three tests.

2. Filament-Wound Pressure Vessel

A detailed fabrication procedure for the FWC structure was written to facilitate planning, data collection, and all phases of filament winding (see Appendix G). The leak-tested metal-foil liners were first internally coated with Kerr DMM plaster to provide a firm mandrel support for filament winding. After the cast plaster was adequately cured to remove moisture, the exterior of the metal liner was chemically cleaned to remove contaminants and to provide a suitable bonding surface. The liners were then overwrapped with resin-impregnated glass filaments. The composite structure was heated for the prescribed resin-cure schedule; after cooling to ambient temperature, the plaster mandrel was removed with a warm, dilute, acetic-acid solution. The vessel was then prepared for testing, at the specified temperature, in accordance with the NASA-approved test procedure.

Two problems were encountered, one during mandrel fabrication and the other during filament winding. It became evident in mandrel fabrication

that the original procedure required modification to control roundness in the thin metal-foil liner structure. When the plaster was cast into the liner and rotated until a hardened coating formed, flat areas were produced in the cylindrical section of the liner. To solve this problem, the liner was pressurized at 5 to 10 psig with air and rotated as the initial plaster coating in the liner was hardening. This procedure produced a liner/thin-plaster-mandrel assembly with the correct contour and sufficient rigidity to permit subsequent plaster castings without detrimental out-of-roundness effects.

During longitudinal-filament winding of the first vessel, the relatively large boss diameters (combined with the vessel length, in-plane wrapping pattern, and wet-winding process) caused filament slippage. This slippage was particularly noticeable in the knuckle areas of the head after the winding progressed to the point where the in-process-impregnated filaments were crossing over previous windings (i.e., after about one-half of a mandrel revolution). To minimize slippage, a layer of Type 104 glass cloth (0.001 in. thick) was placed over the knuckle area, and winding was repeated at a lower speed. A single 1-in.-wide layer of the glass cloth was also used between the weld joints and the FWC structure to minimize damage that might be produced in the glass fibers by the overlapped, seam-welded, liner edges during vessel pressurization. Fabrication data and comments on each vessel were recorded and are presented in Table 38.

C. INSTRUMENTATION

Tests were conducted in conformance with a NASA-approved test plan. This procedure defined in detail all elements of the test facility and the methods to be used for vessel instrumentation and pressurization. The facility and vessels were prepared to accommodate instruments to monitor test-specimen temperature, longitudinal and circumferential strain, and internal pressure throughout the pressurization cycle. Figure 32 shows the test-vessel instrumentation.

Temperature was monitored with copper-constantan thermocouples in the -320°F tests. Because the thermocouple accuracy was questionable below -320°F , platinum resistance-thermometers were used for the -423°F tests. Two temperature measurements were made on the exterior of the vessels (90° apart circumferentially) near the center of the cylindrical section. In addition, the temperatures of the cryogenic test fluids inside and outside the vessel were measured and recorded.

Measurements of strain in the vessels were obtained with Aerojet-developed "bow-tie" extensometers. This extensometer consists of a piece of beryllium-copper sheet metal in a configuration that provides two cantilever beams fitted with bonded strain gages. Metal-foil strip, approximately 0.25 in. wide, was used to link the ends of the cantilever beams to the ends of the gage. Both the extensometer and the foil strip were positioned against the test-vessel surface. For longitudinal-strain measurements, the foil was extended around the circumference and to the ends of the cylindrical section. Each extensometer was calibrated before testing.* Any increase or decrease in vessel girth or cylinder length produced a proportional change in strain-gage bridge output.

* See paragraph 9, Appendix F.

TABLE 38

8-IN.-DIA PRESSURE VESSELS FOR CRYOGENIC-RESIN EVALUATION
FABRICATION DATA

Vessel (Liner) No.	Resin System	Weight, lb		Vessel		Turns		Comments
		Liner	Vessel	Length in.	Dia in.	Longi- tudinal	Hoop	
1	58-68R*	2.051	2.727	13.110	7.846	370	451	--
2	2	2.053	2.743	13.124	7.860	371	448	Slight buckle from initial longitudinal turn
3	-	2.057	-	-	-	-	-	Extensive wrinkles in head, liner not used
4	2	2.057	2.718	13.085	7.863	367	448	Slight buckle from initial longitudinal turn
5	2	2.068	2.732	13.085	7.859	367	425	Same as above
6	58-68R	2.037	2.787	13.095	7.873	370	447	Same as above
7	58-68R	2.055	2.716	13.076	7.860	368	452	Telescoping of hoop fibers
8	58-68R	2.059	2.752	13.070	7.860	377	449	Slight buckle from initial longitudinal turn
9	58-68R	2.055	2.633	13.095	7.871	370	454	Same as above
10	2	2.057	2.734	13.085	7.853	370	446	Same as above
11	2	2.046	2.705	13.085	7.850	368	421	--
12	58-68R	2.046	2.789	13.087	7.870	370	447	Buckled during third hoop layer (after 236 hoop turns), wraps removed (insufficient plaster, 0.1 in.)
13	2	2.064	2.723	13.118	7.847	367	416	Slight buckle from initial longitudinal turn

* Shell Resin 58-68R = Epon 828/Epon 1031/MNA/BDMA (50/50/90/0.5 parts by weight).

Symbol	Measurement
P_s	Supply Pressure
P_c	Specimen Pressure
T_s	Supply Temperature
T_o	Specimen Temperature
SG_1	Specimen Deflection, Hoop
$SG_{2, 3}$	Specimen Deflections, Longitudinal
$TSG_{1, 2, 3}$	Deflection Beam Temperatures
$TC_{1, 2}$	Specimen (Skin) Temperatures

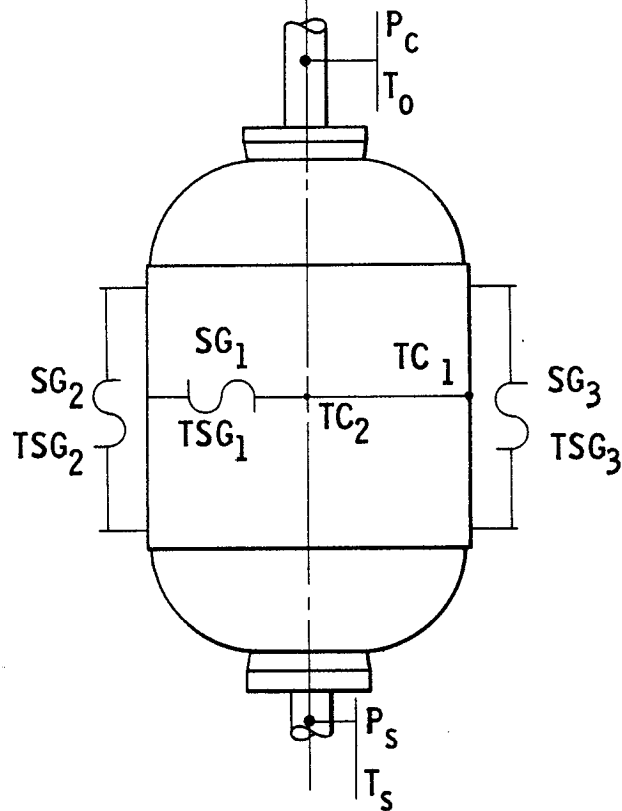


Figure 32. Instrumentation, 8-in.-dia Cryogenic Pressure Vessels

Hoop strain was measured at the center of the cylindrical section, and longitudinal strain was measured along the cylinder at two locations 180° apart. The average of these two measurements was the axial (longitudinal) strain.

A vacuum chamber was used in the cryogenic-temperature tests. Vessels were tested at a pressure of 10^{-3} mm Hg to assure attainment of the required LN₂ and LH₂ temperatures at the test-vessel walls.

The accuracy of the strain gages on the extensometers depends on the gage factor, which is extremely sensitive to cryogenic-temperature variations. To provide the required extensometer accuracy, the concept of controlled-temperature strain transduction was employed: Heaters were provided to maintain the gages at temperatures within the strain-gage compensation range and a sensor was added to record the vessel-surface temperature in the vicinity of the extensometer. This sensor was used to verify that the heat input did not generate excessive temperature discontinuity in the region of the transducer. Thermal insulation was also used under the heated extensometers to reduce heat transfer to the test vessel and to reduce or eliminate the need for power application during pressurization when strain readings were taken.

D. TEST RESULTS

Tests were performed on 12, metal-lined, filament-wound, pressure vessels. The only fabrication-parameter variation was the resin used for the matrix (either Resin 2 or the standard epoxy, 58-68R). A system was provided to fill and test two vessels fabricated from each resin system for single-cycle burst strength using water (+75°F), LN₂ (-320°F), or LH₂ (-423°F). Pressure was applied at a rate that produced approximately 1% strain/min in the test vessels. The pressure-vessel test assembly is shown in Figure 33.

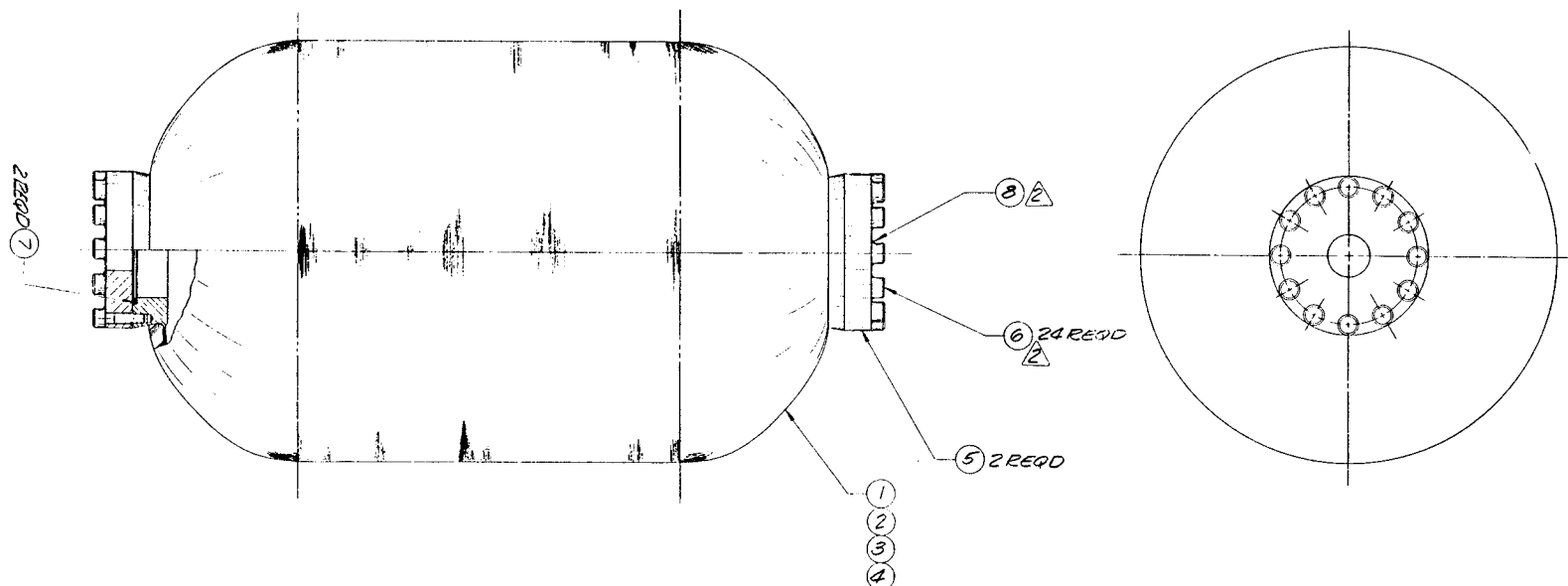
1. Room-Temperature Tests (75°F)

Four vessels (two with each resin system) were subjected to single-cycle burst tests by increasing the internal pressure at an average rate of 500 psig/min until failure occurred. Test data, including the vessel weight, internal volume, burst pressure, and type of failure, are summarized in Table 39. Structural data, including the pressure-vessel performance factor, filament and composite stresses, and longitudinal and hoop strains, are presented in Table 40.

In all four vessels, failure originated in the head area around one boss (see Figure 34). This "flower-type" burst occurred at high filament-stress levels in the area where the detrimental effects of filament crossovers, buildup, and bridging were particularly dominant. The metal boss in the failed head was blown free of the metal liner, and the opposite head section collapsed inward during the sudden explosive reaction (see Figure 35). The hoop filaments remained intact, indicating a degree of design redundancy.

Although the appearance of the burst vessels suggested that simultaneous failures of the filament-wound composite and the liner had occurred, it is believed that the filaments failed first, after which the metal boss in the same area was blown out. This interpretation is supported by

NOTES:
 1. REMOVE ALL BURRS AND SHARP EDGES
 2. APPLY 1150 P. 2 PUTTY IN AREAS SHOWN
 AFTER TIGHTENING THEM TO 48
 IN. LBS TORQUE.



QTY	SYN	CODE	PART OR IDENTIFYING NO.	NOMENCLATURE OR DESCRIPTION	MATERIAL	SPECIFICATION	UNIT WT.	ZONE	ITEM NO.
2	A	A	2099	TORQUE PUTTY					8
2	2	2	2099	SEAL					7
2	2	2	177413-1	BOLT					6
2	2	2	177413-1	PLUG					5
1			178156-7	PRESSURE VESSEL					4
1			178156-5	PRESSURE VESSEL					3
1			178156-3	PRESSURE VESSEL					2
1			178156-1	PRESSURE VESSEL					1

ON		THRU	PART NO.	EXT. ASSY	NEXT ASSY	USED ON
EFFECTIVE SERIAL NO.		APPLICATION				
USAGE DATA		DRAWING LEVEL				

UNLESS OTHERWISE SPECIFIED DIMENSIONS ARE IN INCHES TOLERANCE ON DECIMALS ANGULAR ± .05 DO NOT SCALE DRAWING		CONTRACT NO. DRAWN CHECK DATE 7-14-66	
TREATMENT FINISH		DESIGN R. Molho 7-14-66	
MATERIAL 178156-1		STRENGTH 8/15/66	
SIMILAR TO		ACT. WT. CALC. WT.	
CUSTOMER		DESIGN ACTIVITY APPR. R. Molho 7-14-66	

AEROJET-GENERAL CORPORATION AZUSA, CALIFORNIA	
TITLE TEST ASSEMBLY 8 IN. DIA PRESSURE VESSEL	
DWG NO. 70143	DWG NO. 178169
SCALE	RELEASE DATE 8/19/66 SHEET

Figure 33. Test Assembly, 8-in.-dia Pressure Vessel

TABLE 39

TEST RESULTS, 8-IN.-DIA PRESSURE VESSELS FOR CRYOGENIC-RESIN EVALUATION

Vessel (Liner) No.	Test Temp °F	Resin System	Weight, lb		Internal Volume cu in.	Resin wt%*	Burst Press. psig	Type and Location of Failure
			Liner	Vessel				
4	+75	2	2.057	2.718	509.8	16.8	1490	Longitudinal filaments in head around boss
5	↓	2	2.068	2.732	509.8	18.6	1450	Same
8		58-68R	2.059	2.752	510.1	18.4	1450	Same
9		58-68R	2.055	2.633	508.3	26.6	1535	Same
2	-320	2	2.053	2.743	509.5	17.8	1119	Pinhole liner leaks in both heads and cylinder near welded areas
10	↓	2	2.057	2.734	509.5	17.5	1914	Longitudinal filaments in head around boss
1		58-68R	2.051	2.727	510.1	25.4	1581	Pinhole liner leaks in one head
7		58-68R	2.055	2.716	509.3	19.9	1650	Hoop filaments near one tangent plane
11	-423	2	2.046	2.705	511.3	17.2	1929	Longitudinal filaments in head around boss
13	↓	2	2.064	2.723	511.3	16.2	1989	Same
6		58-68R	2.037	2.787	509.5	25.6	1767	Same
12		58-68R	2.046	2.789	509.9	22.3	1932	Same

* Based on three samples from each vessel.

TABLE 40

STRUCTURAL DATA, 8-IN.-DIA PRESSURE VESSELS FOR CRYOGENIC-RESIN EVALUATION

Vessel (Liner) No.	Test Temp °F	Resin System	Perf Factor pV/W* 10 ⁶ in.	Stress, ksi				Ultimate Strain	
				Longitudinal		Hoop		%	
				Fil	Comp	Fil	Comp	Long.	Hoop
4	+75	2	0.61	366.4	251.0	338.9	232.1	3.16	3.02
5	↓	2	0.59	356.6	233.6	347.6	227.7	2.62	2.65
8	↓	58-68R	0.58	347.2	234.2	329.1	222.1	2.62	2.24
9	+75	58-68R	0.66	374.2	212.3	344.4	195.5	3.01	2.66
2	-320	2	-	-	-	-	-	1.68	2.23**
10	↓	2	0.77	449.1	301.8	430.6	289.4*	3.56	3.26
1	↓	58-68R	-	-	-	-	-	1.93	2.59
7	-320	58-68R	0.66	389.2	255.0	366.3	240.0	2.72	2.96
11	-423	2	0.79	444.2	302.0	452.6	307.8	2.72	3.11
13	↓	2	0.81	459.2	318.5	472.4	327.5	3.99	3.65
6	↓	58-68R	0.68	404.7	234.5	387.3	224.5	3.13	3.11
12	-423	58-68R	0.74	442.5	275.5	427.0	266.0	3.39	***

* Weight (W) used in determining performance factor (pV/W) excludes weight of structurally redundant metal bosses (1.46 lb); p = burst pressure, psi, and V = internal volume, cu in.

** Strain at 86% of burst pressure. Strain gage failed at 960 psig prior to reaching maximum pressure of 1119 psig.

*** Strain gage malfunctioned after vessel pressurization had begun.



10-087-118

Figure 34. Typical Head Failure in Vessels Tested to Burst Point at Room Temperature

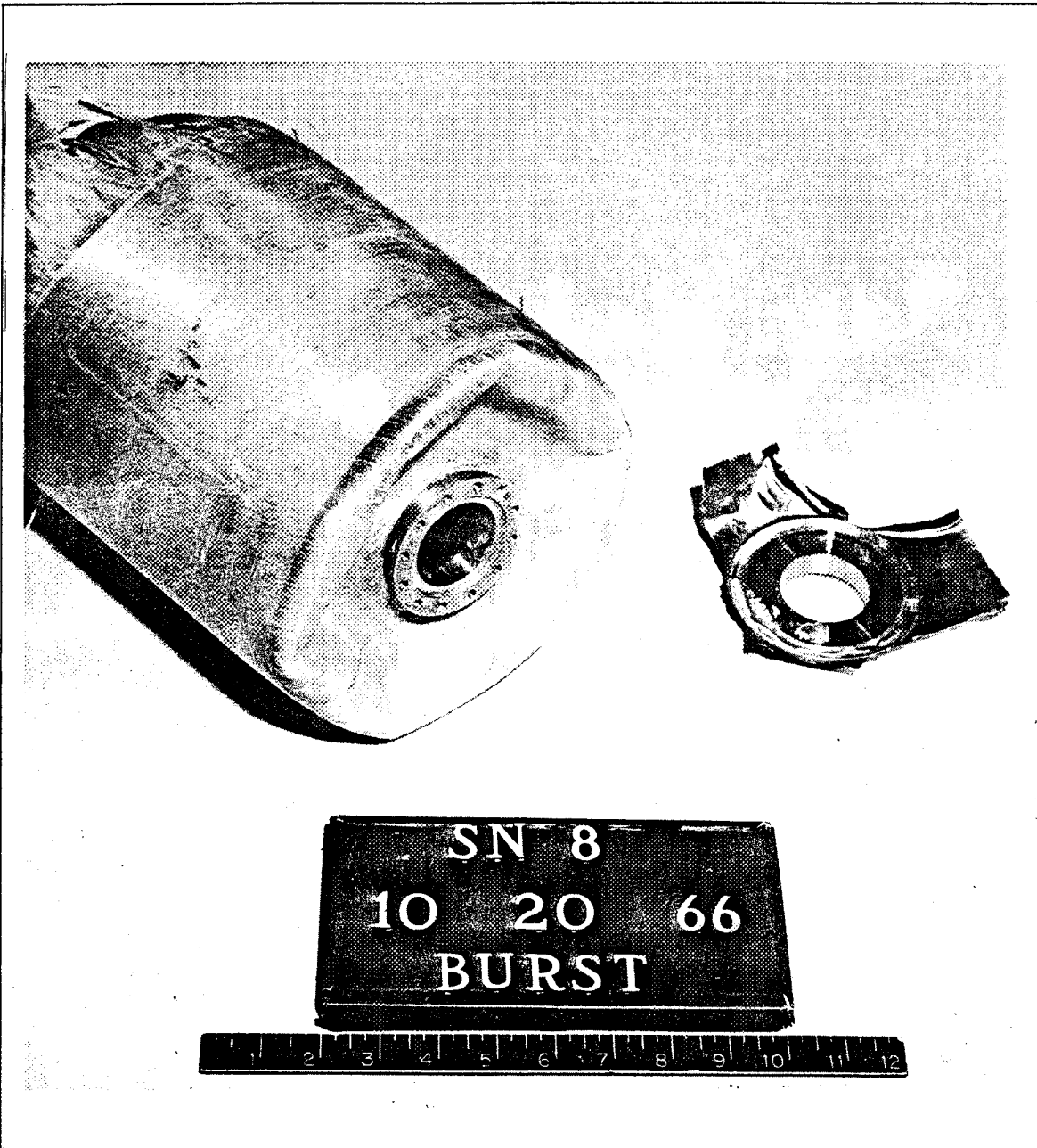


Figure 35. Typical Explosive Reaction on Opposite Head of Vessels Tested to Burst Point at Room Temperature

results from -320°F tests in which pinhole leaks in the liners of Vessels 1 and 2 were responsible for the pressure loss, the FWC structure of these vessels remaining virtually intact after testing.

All burst pressures were fairly close - 1490 and 1450 psig for the Resin 2 vessels and 1450 and 1535 psig for the 58-68R vessels. Relative performance may be compared more significantly by noting that the average ultimate longitudinal-filament stress was 361.5 ksi for the Resin 2 vessels and 360.8 ksi for 58-68R. The single-cycle-strength results thus failed to indicate a significant difference between the two systems. The average longitudinal-stress level (361.2 ksi) was 9.4% above the minimum allowable ultimate filament stress (330.0 ksi) used for design purposes. Filament-stress-level calculations are described in paragraph 8 of Appendix F.

The vessels may also be compared on the basis of the pressure-vessel performance factor, which is defined as the product of burst pressure and internal volume divided by vessel weight (pV/W).^{*} As shown in Table 39, the performance factors were 0.61 and 0.59 x 10⁶ in. for the Resin 2 vessels and 0.58 and 0.66 x 10⁶ in. for 58-68R. This similarity in vessel efficiency supported the conclusion that there was no significant difference in the room-temperature performance of the two resin systems.

Table 39 gives resin contents based on three samples from each vessel. The average contents were 17.7 wt% for Resin 2 and 22.5 wt% for 58-68R. The lower (and wet-winding-suitable) viscosity of Resin 2, and the ease with which excess resin could be removed during the initial curing phase, were responsible for the lower average resin content and the smaller range in content found in Resin 2 vessels. The viscosity of 58-68R, on the other hand, progressively increased during winding, even though the resin dip tank was warmed; this increased viscosity probably caused the higher and more variable resin contents of the 58-68R vessels.

Composite strengths, calculated from filament strengths and resin contents, are shown in Table 40. Vessel 4 exhibited the highest stresses attained in the cylindrical section for the longitudinal- and hoop-wound composites (251.0 and 232.1 ksi, respectively). The hoop-composite stresses at failure were 5 to 10% lower than the longitudinal because of redundant design used to force the failure in the longitudinal fibers..

Longitudinal and hoop strains are shown in Figures 36 and 37 as a function of internal pressure. The maximum longitudinal strains, exhibited by Vessels 4 and 9, were 3.16 and 3.01%; the maximum hoop strains, found in the same vessels, were 3.02 and 2.66%.

As shown in Figures 36 and 37, the initial vessel pressurization to approximately 200 psig produced small strains compared with those produced by the same pressure increment at higher total pressures. This condition is particularly apparent for the pressure/longitudinal-strain curves and was predicted by the design analysis. In Figure 38, the predicted pressure-strain relationship is compared with data obtained from the testing of Vessel 4. As

^{*} In this calculation the weight of the metal bosses is not included because of their structural redundancy in the design.

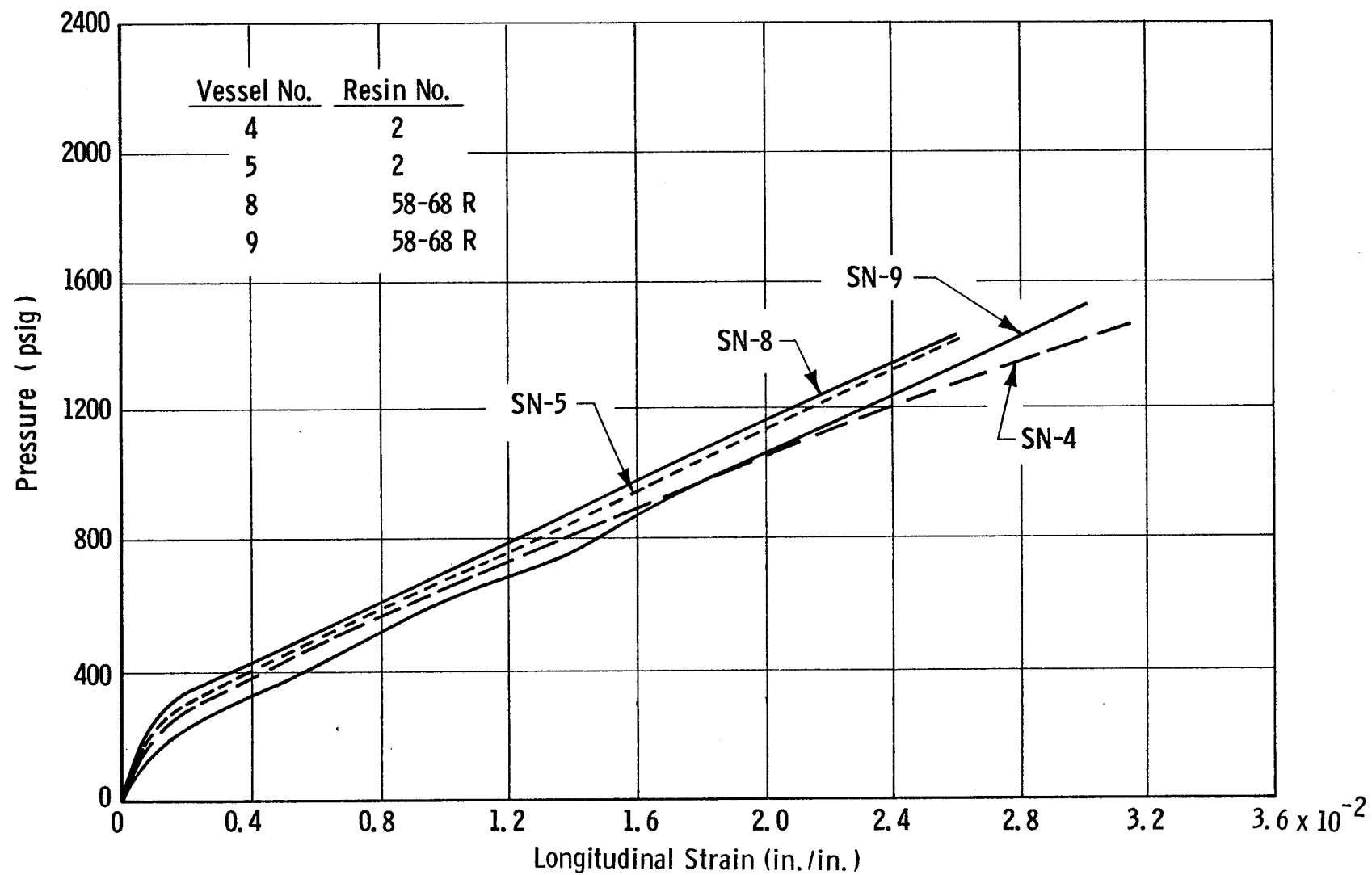


Figure 36. Pressure/Longitudinal-Strain Curves for Filament-Wound Metal-Lined Pressure Vessels at +75°F

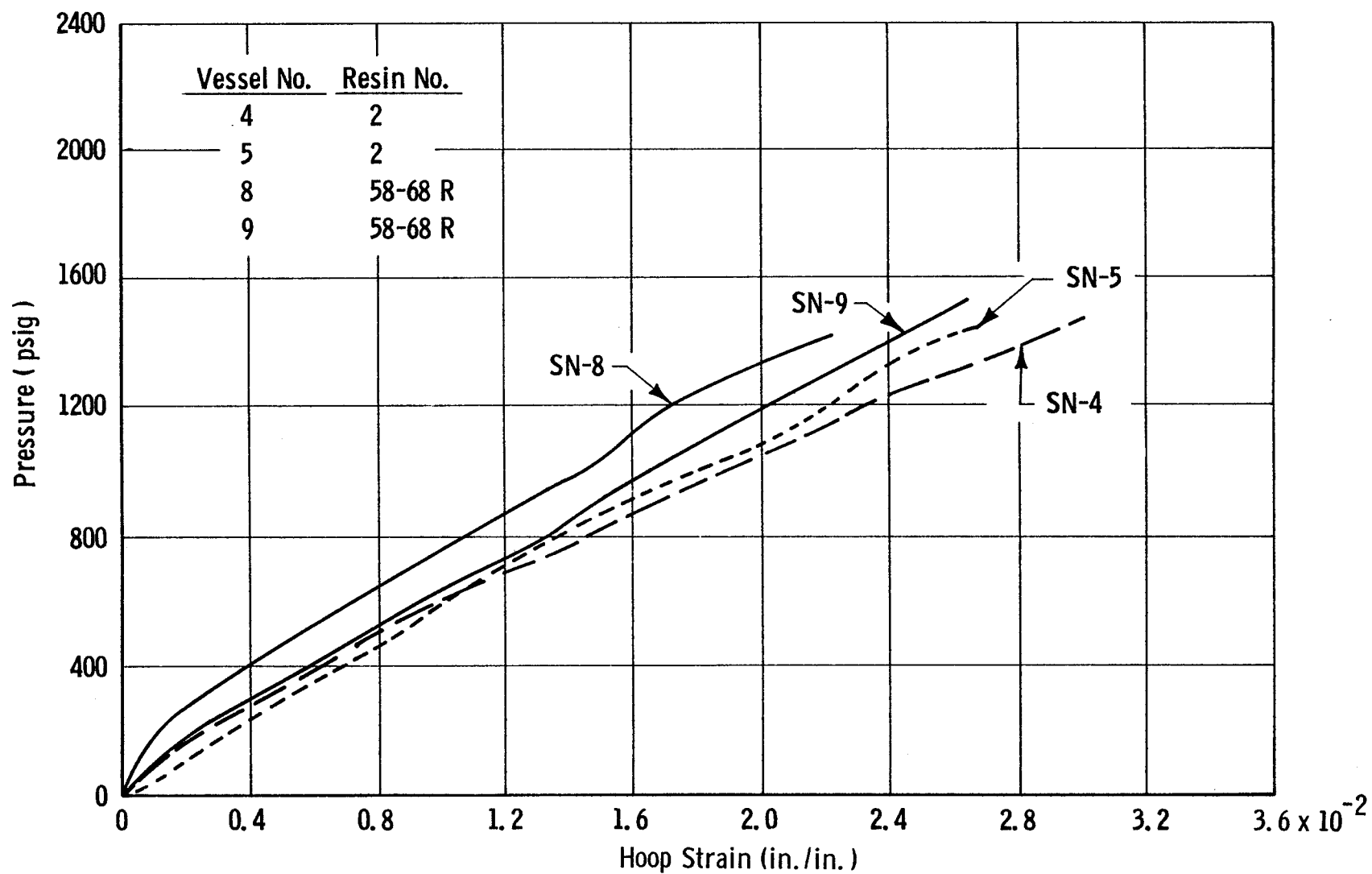


Figure 37. Pressure/Hoop-Strain Curves for Filament-Wound Metal-Lined Pressure Vessels at +75°F

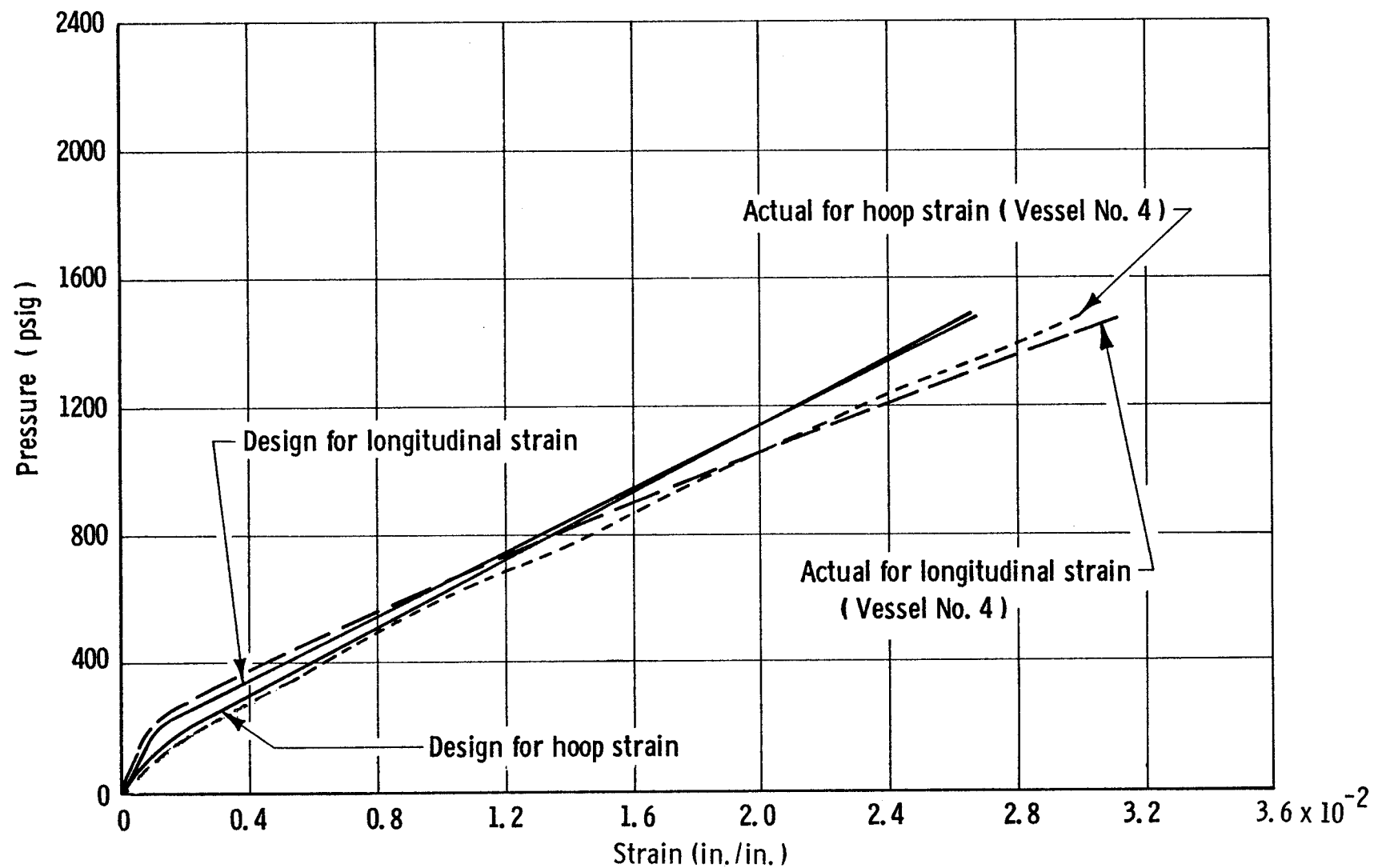


Figure 38. Design and Actual Pressure-Strain Curves for Filament-Wound Metal-Lined Pressure Vessels at +75°F

pressure was increased from zero to approximately 200 psig, the cylinder strains produced in the hoop and longitudinal directions were small because of the load-carrying capability of the metal-foil liner. At roughly 200 psig for the longitudinal direction and 100 psig for the hoop direction, the yield point of the liner was exceeded; at higher pressures, the liner deformed plastically and the increasing pressure load was carried almost entirely by the lower-modulus filament-wound composite, resulting in a greater strain-to-pressure ratio.

Data obtained in previous programs (Appendix B) indicated that resin crazing is initiated at approximately 10% of the maximum pressure attained. Therefore, in addition to the load-carrying capability of the liner, the initial (precrazing) strength and toughness of the matrix may also contribute to the smaller strain produced at the start of pressurization.

2. LN₂ Tests (-320°F)

Four pressure vessels (two with each resin system) were subjected to single-cycle burst tests at -320°F by increasing the internal pressure at an average rate of 700 psig/min until failure occurred. The test data, including vessel weight, internal volume, burst pressure, and type of failure, are presented in Table 39. The structural data, including pressure-vessel performance factor, filament and composite stresses, and longitudinal and hoop strains, are summarized in Table 40. Longitudinal and hoop strains are plotted as a function of internal pressure in Figures 39 and 40.

Figure 41 shows a typical pressure vessel assembled for cryogenic testing with bow-tie extensometers in position. The vessels were mounted in a vacuum chamber provided with taps for deflection-measurement instrument leads, thermocouples, and pressurization lines. The specimens were tested at 10^{-3} mm Hg in order to minimize heat input and assure attainment of the required cryogenic temperature. All equipment was operated remotely from a building that housed controls and instrumentation. The test vessels were filled with glass marbles to minimize the quantity of cryogen expended during a burst. The coolant flowed through the system and vessel assembly from a liquid-cryogen-transfer trailer until a liquid condition was obtained. The pressurizing gas was then liquefied and was supplied to the specimen through a heat exchanger.

The liquid-cryogen heat exchanger was acquired during this program and installed to provide economical cryogenic testing. It utilized high-pressure gaseous nitrogen for the LN₂ tests (or gaseous hydrogen for the LH₂ tests) supplied from an existing 20-cu ft storage tank. The gas was passed through a series of coils surrounded by the low-pressure cryogen from the trailer. Operating on an extremely large supply reservoir, the heat exchanger was able to achieve and maintain a low cryogenic temperature in the test specimen and to assure a constant supply of cryogen during the test.

Of the vessels tested at -320°F, Nos. 1 and 2 failed prematurely when pinhole leaks developed in the liner. An immediate pressure drop occurred when they attained their ultimate pressures; post-test examination revealed, however, that failure was not accompanied by glass-filament damage. Test-facility safety provisions were such that an increase in vacuum chamber

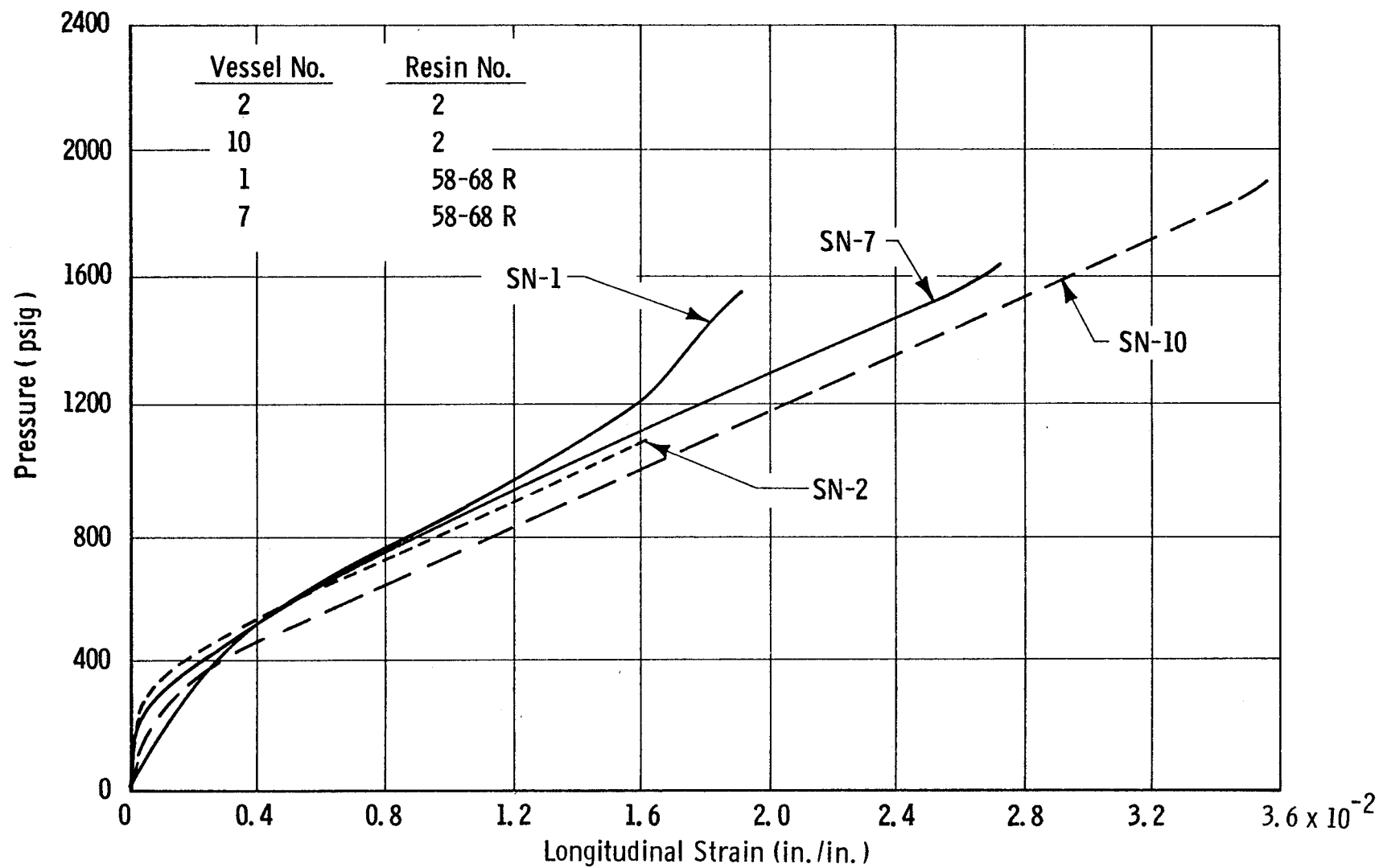


Figure 39. Pressure/Longitudinal-Strain Curves for Filament-Wound Metal-Lined Pressure Vessels at -320°F

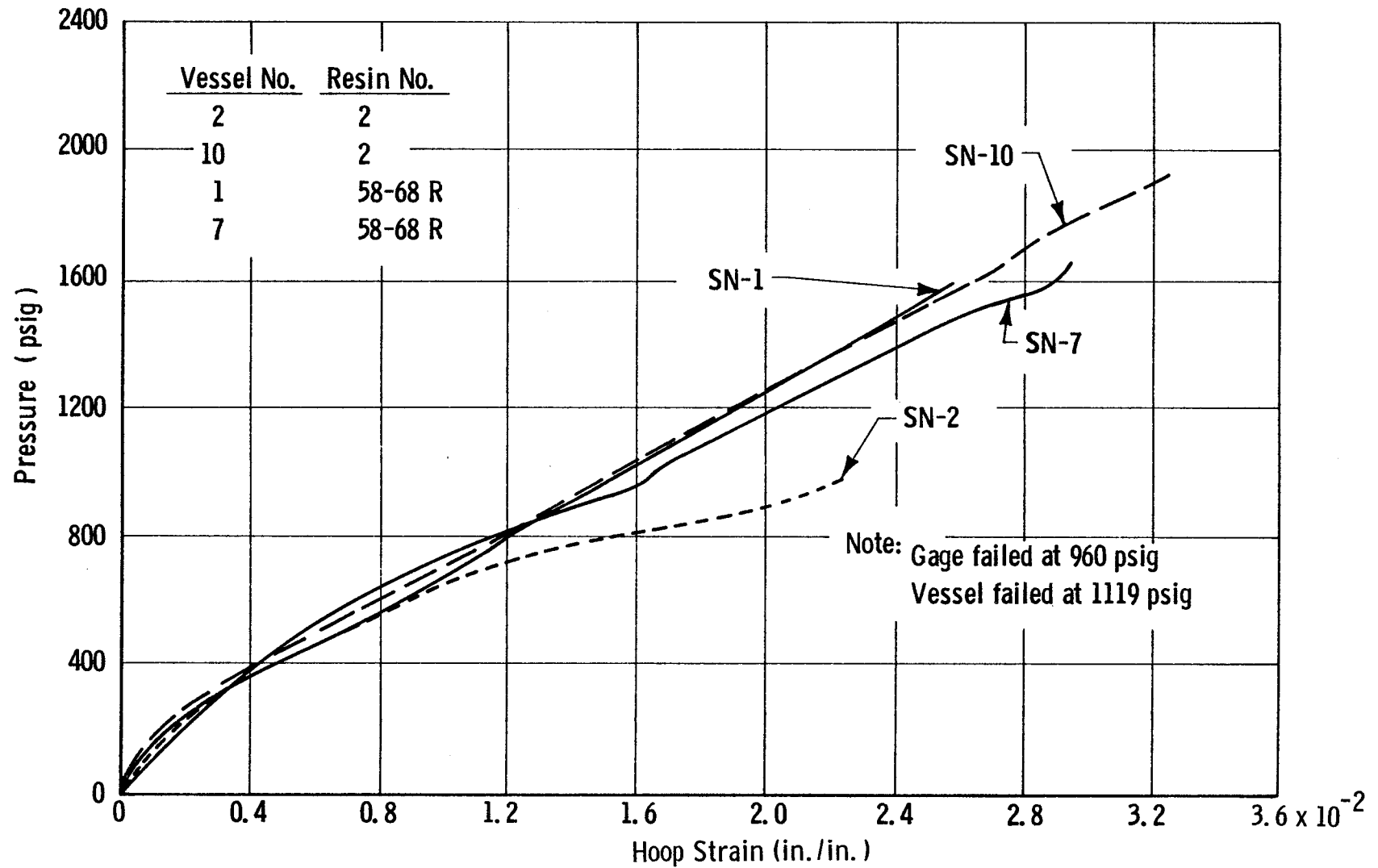


Figure 40. Pressure/Hoop-Strain Curves for Filament-Wound Metal-Lined Pressure Vessels at -320°F

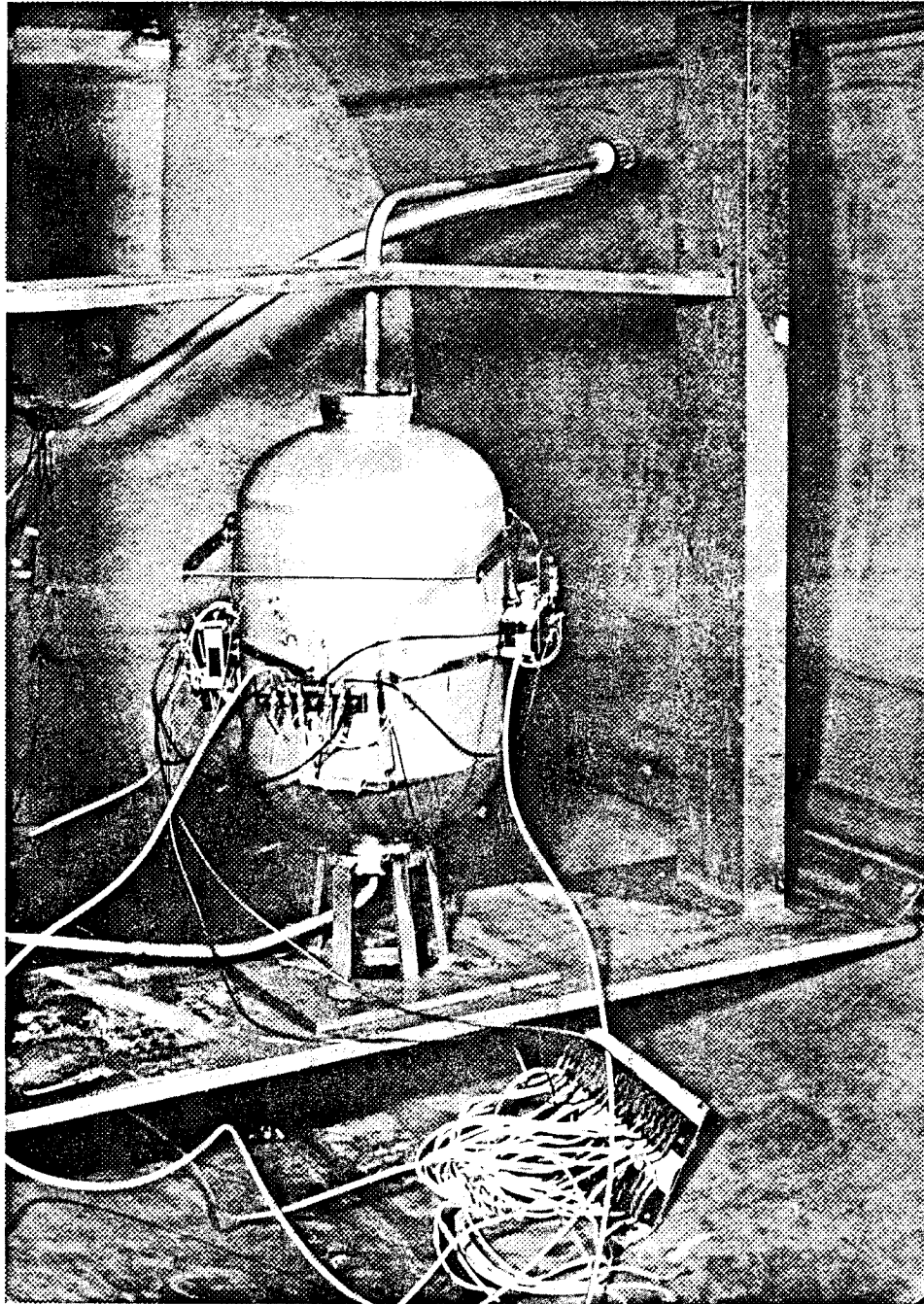


Figure 41. Typical Pressure Vessel Assembled for Cryogenic Testing in Vacuum Chamber Facility

pressure to 5 psia (due to leakage or pressurization-line malfunction) would energize an automatic system that vented the specimen and vacuum chamber and closed the specimen pressure valve. The partial decay of chamber vacuum warned the test operator of vessel leakage and prompted him to increase the pressurization rate to overcome the leak. Unfortunately, the vacuum decay came too suddenly with these two vessels to permit a sufficient increase in pressurization rate to achieve a burst. Examination of the interior of Vessel 2 disclosed several pinholes in both heads adjacent to the boss-to-head seam welds and one pinhole in the cylinder near the longitudinal-seam-weld section; similarly, two pinholes were found in one head of Vessel 1, approximately 180° apart and equidistant between the boss and the tangent plane. The causes of the leaks could not be identified in post-test examination and a review of fabrication records.

The other two vessels (Nos. 7 and 10) failed in the composite, one in the hoop filaments and the other in the longitudinal filaments of the head. The excessive bulge in the head and the cylindrical section nearest the burst area of Vessel 7 indicates that the hoop filaments failed first, after which the longitudinal fibers supported the internal pressure temporarily by distorting to meet the loads until they reached their maximum capabilities, and then also failed (see Figure 42). As noted in Table 38, "telescoping" (tapering of the hoop windings) had occurred near the tangent-plane area of each head in this vessel. This effect (produced when excess resin was removed during the early curing stage, at which time filaments in this area tended to slide over the contoured head) probably contributed to the premature failure of this vessel.

The Vessel 10 test results are considered highly satisfactory in that the actual burst pressure of 1914 psi approached the predicted design value of 2087 psi. The highest longitudinal-filament stress (449.1 ksi), as well as the maximum longitudinal and hoop strains (3.56 and 3.26%, respectively), were obtained with this vessel. The longitudinal-filament stress was 91% of the predicted level of 495.0 ksi* and 24.4% above the average of the actual room-temperature longitudinal-filament stresses (361.0 ksi).

As in the room-temperature tests, (1) the strains occurring during initial vessel pressurization were small compared with those developed at higher pressures, due to the load-carrying capability of the liner, and (2) the resin contents (see Table 39) of the System 2 vessels were consistent and at a satisfactory level (17.8 and 17.5 wt%), whereas those of the 58-68R vessels were higher and more variable (25.4 and 19.9 wt%).

Post-test examination of the liner interiors revealed buckling in various areas; the higher the burst pressure attained, the more severe the liner buckling. The cause of the poor structural bond between the liner and composite is unknown; however, lack of an adhesive bond would have had little effect, if any, on the burst pressures attained in single-cycle pressurization.

* 150% of the room-temperature design-allowable strength of 330.0 ksi.

NOT REPRODUCIBLE

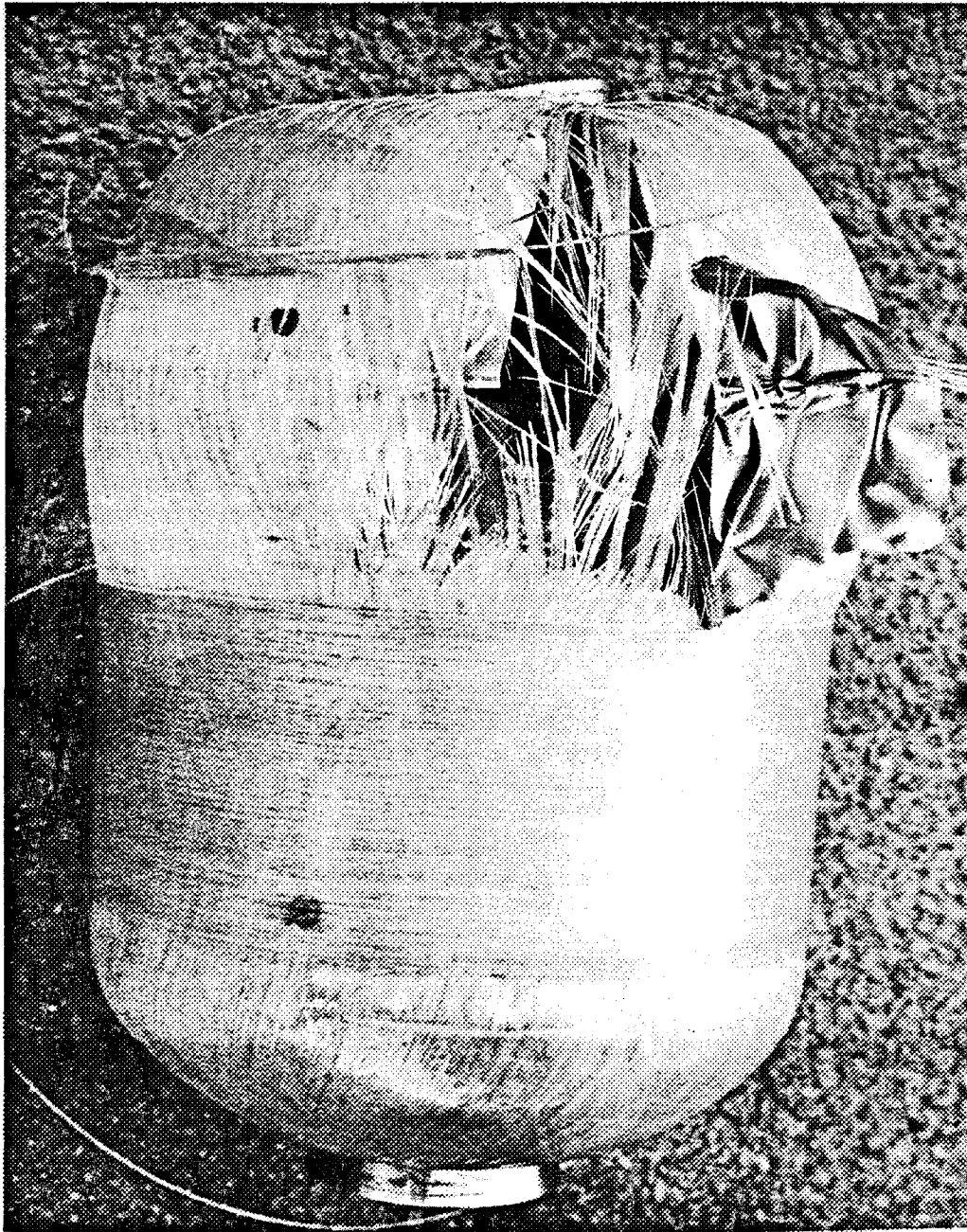


Figure 42. Vessel 7 After Liquid-Nitrogen Burst Test

3. LH₂ Tests (-423°F)

Four pressure vessels (two with each resin system) were subjected to single-cycle burst tests at -423°F by increasing the internal pressure at an average rate of 700 psig/min until failure occurred. The test data, including vessel weight, internal volume, burst pressure, and type of failure, are presented in Table 39. The structural data, including pressure-vessel performance factor, ultimate filament and composite stresses, and ultimate longitudinal and hoop strains, are summarized in Table 40. Longitudinal and hoop strains are plotted as a function of internal pressure in Figures 43 and 44.

In each of the four vessels failure originated in the longitudinal filaments around the boss area of one head. The mode of failure was the same as for all the room-temperature vessels (see Figure 34) and for Vessel 10, which was tested at -320°F. A flower-type burst resulted when the filaments attained their maximum load-carrying capabilities. The metal boss in the burst head section was separated from the metal liner, and the opposite head collapsed inward. Hoop filaments did not fail but were damaged in the sudden explosive reaction.

The adhesive bond between the stainless steel liner and the filament-wound composite did not prevent the liner from buckling when the vessel depressurized. Post-test examination of the interiors revealed that liner wrinkling was more severe in these vessels than in those tested at room temperature, probably because of the higher pressures and strains reached at the burst.

Vessel 13 (Resin 2), with an ultimate longitudinal-filament stress of 459.2 ksi, a hoop-filament stress of 472.4 ksi, maximum longitudinal and hoop strains of 3.99 and 3.65%, and a performance factor of 0.81×10^6 in., exhibited the highest structural performance of any vessel tested at cryogenic temperatures. The average longitudinal-filament stress for the Resin 2 vessels was 24.9% greater than the average stress in Resin 2 vessels at room temperature, and 6.6% greater than the average stress attained in 58-68R vessels at -423°F.

As shown in Figures 43 and 44, the strains produced during initial vessel pressurization were small in comparison with those produced later by an equivalent pressure increment. As noted previously, this behavior was predicted by the design analysis and was due to the load-carrying capability of the high-modulus metal-foil liner. After the yield point of the liner was exceeded, the liner deformed plastically and the increasing loads were supported by the low-modulus composite structure. This change in the pressure-to-strain ratio occurred at relatively higher pressures because of the higher yield point and higher tensile modulus of the liner at cryogenic temperatures.

During the tests, temperatures were continuously recorded at the points shown in Figure 32. They are presented in Table 41 for the start and end of each cryogenic test. Whereas the initial skin temperatures (TC₁ and TC₂) in the LH₂ tests were fairly close to -423°F, the analogous temperatures in the LN₂ tests were considerably higher than -320°F. To some extent such temperature differentials are to be expected. When they occur at the start of

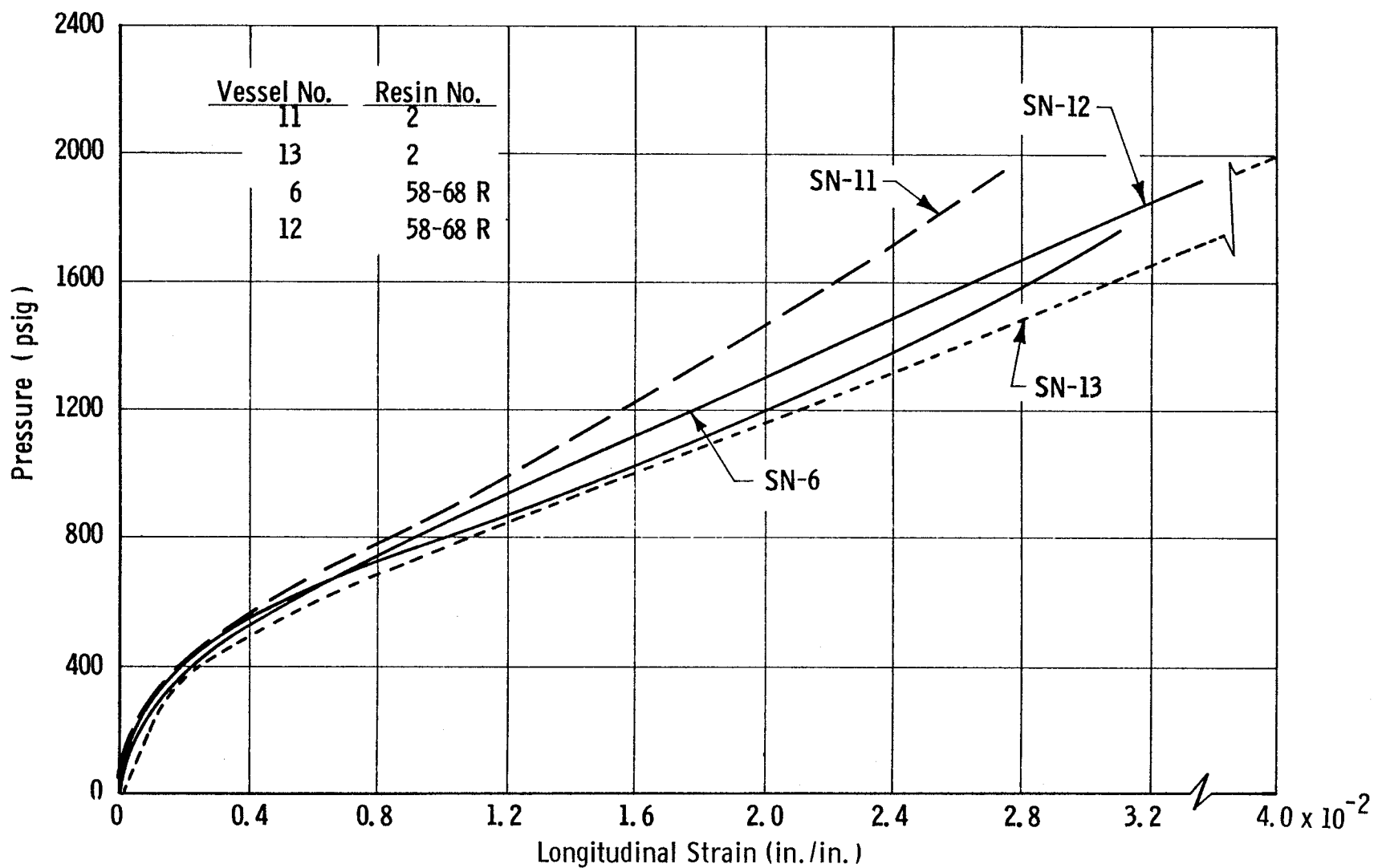


Figure 43. Pressure/Longitudinal-Strain Curves for Filament-Wound Metal-Lined Pressure Vessels at -423°F

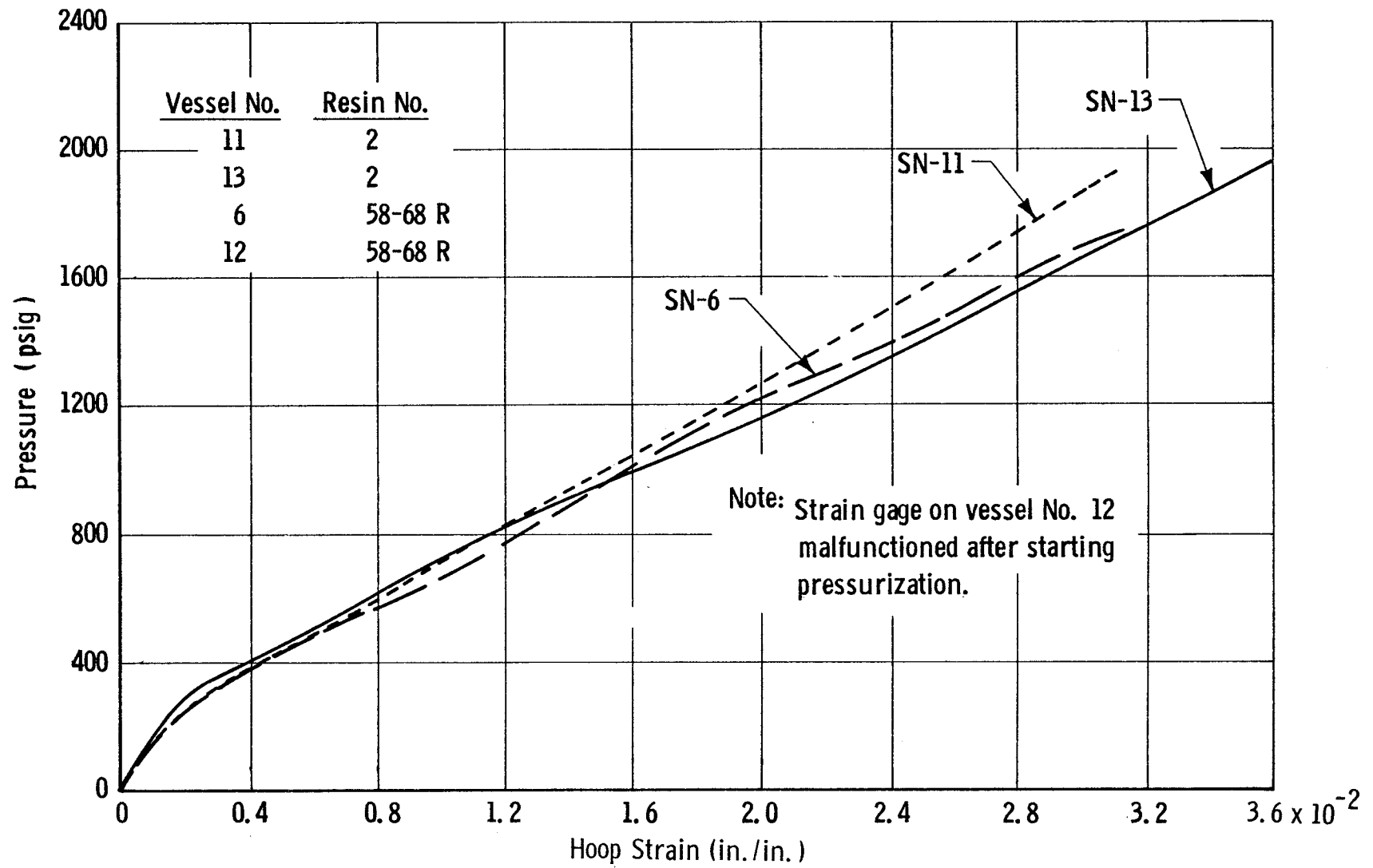


Figure 44. Pressure/Hoop-Strain Curves for Filament-Wound Metal-Lined Pressure Vessels at -423°F

TABLE 41

CRYOGENIC-TEMPERATURE MEASUREMENTS
8-IN.-DIA CRYOGENIC PRESSURE VESSELS

Vessel No.	Value	Temperature, °F*			
		<u>T_s</u>	<u>T_o</u>	<u>TC₁</u>	<u>TC₂</u>
1	Initial	-320	-320	-242	-261
	Final	-309	-297	-242	-256
2	Initial	-320	-320	-263	-251
	Final	-310	-297	-258	-266
7	Initial	-320	-320	-254	-259
	Final	-301	-308	-273	-275
10	Initial	-320	-320	-243	-262
	Final	-306	-305	-246	-263
6	Initial	-415	-417	-395	-376
	Final	-410	-316	-358	-315
11	Initial	-418	-417	-398	-383
	Final	-413	-	-316	-337
12	Initial	-418	-417	-403	-403
	Final	-415	-325	-360	-365
13	Initial	-419	-418	-398	-400
	Final	-413	-340	-308	-331

* T_s = cryogen supply temp, T_o = vessel temp, TC₁ and TC₂ = vessel (skin) temps (see Figure 32).

pressurization, they may be due to (a) radiative heat transfer from the chamber wall to the pressure-vessel wall, (b) a poor bond between the sensor connection and the outer wall of the vessel, or (c) a lack of temperature equilibrium across the vessel wall. Temperature differentials at or near the burst may have the same causes, or these additional ones: (a) During pressurization to burst, the vacuum pumps were turned off at about 700 psi, and a decay in test-chamber vacuum as pressure was further increased caused a temperature increase at the outer wall of the vessel through convective heat transfer, or (b) during pressurization, the vessels were warmed by the work done on both the cryogen and the vessel (conductive heat transfer), in addition to warming from external radiative and convective heat transfer.

Although it is not possible to estimate the respective contributions of these various factors, it is believed that equilibrium temperatures were not obtained in the LN₂ tests. Some support for this view is that the LH₂ tests, which included soak periods of 45 min to 1 hour, did not exhibit significant temperature differentials across the vessel walls.

4. Evaluation of Test Data

Figure 45 compares the Resin 2 vessel data with the uniaxial test-specimen results obtained in Task III and plotted in Figure 21. The vessel-stress values and the unidirectional (1:0) test-specimen strengths were nearly identical at +75 and -320°F. At -423°F, the pressure-vessel filament strength was essentially the same as at -320°F, but the uniaxial-test-specimen strength fell off considerably.*

Figure 46 summarizes pressure-vessel performance over the +75 to -423°F range. It compares ultimate longitudinal-filament strengths and ultimate composite strengths for Resin 2 and 58-68R vessels. At 75°F, the resins were equivalent in filament strength. At -320 and -423°F, the longitudinal-filament strengths of the Resin 2 vessels were 16.3 and 6.6% greater, respectively, than those of the 58-68R vessels. Longitudinal composite strengths for Resin 2 were superior at all temperatures because of the higher filament-stress levels developed and the consistent attainment of composite resin content within desirable limits.** These strength results indicate that, for glass-FWC

*The vessel-filament-strength value at -320°F is based on a single vessel test; the +75 and -423°F filament strengths are average values for two vessel tests each.

**Composite resin contents for the more viscous 58-68R resin could not be maintained at the optimum level and were higher than desirable. All the tests in this program, including those on pressure vessels in Task IV, were performed with specimens fabricated by in-process winding and not from prepreg. It is entirely possible that 58-68R vessels (and other test specimens) prepared from prepreg would have had lower and more desirable resin contents, with a resultant improvement in their composite-performance levels, including the pV/W factor. This, of course would not have significantly altered the relative values for filament stress exhibited by the resins. It is because of the influence of resin content on composite strength that filament-stress levels (being almost independent of resin content) are the preferred index of vessel performance.

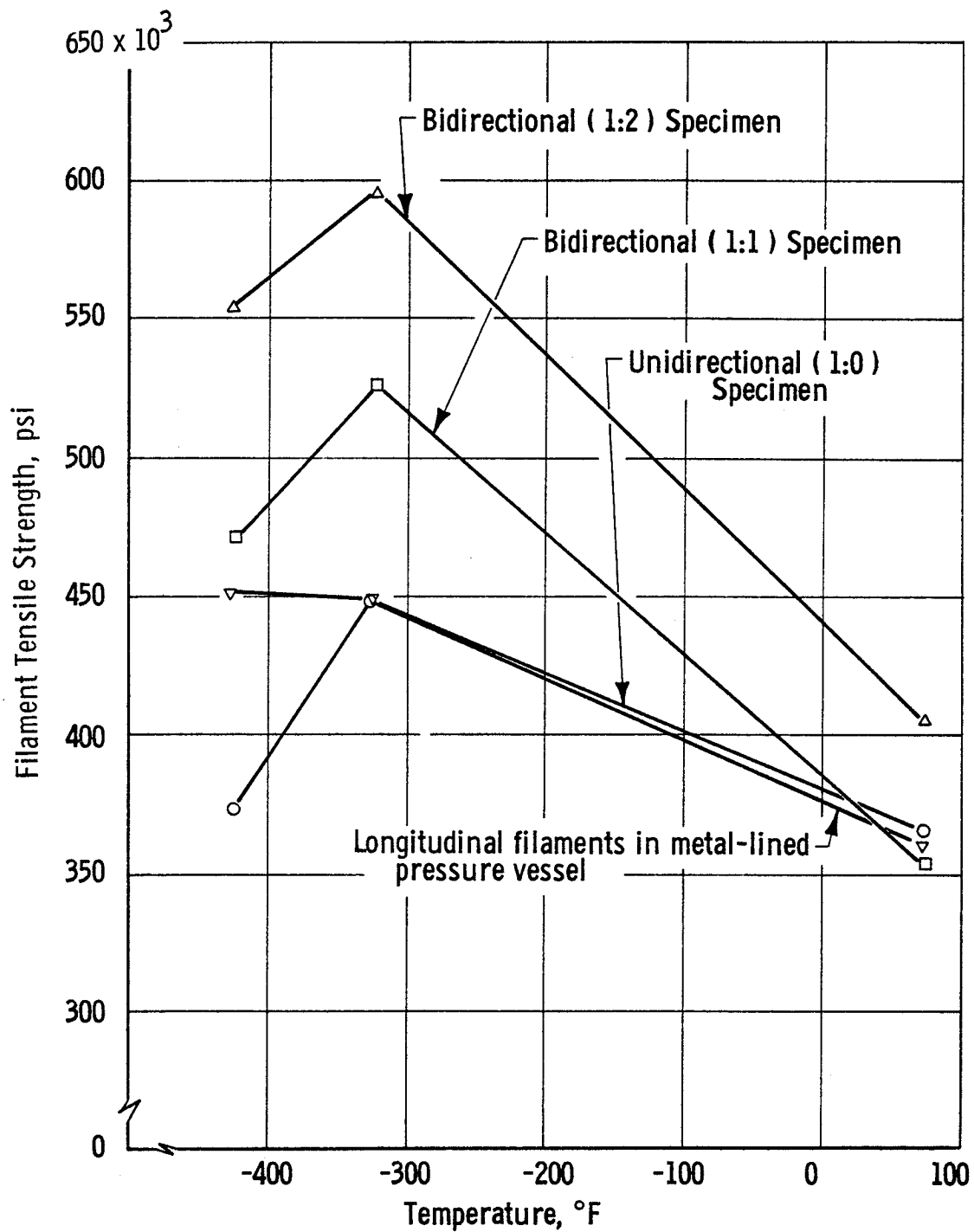


Figure 45. Effect of Temperature on Ultimate Filament Strength Various Configurations of S-901/Resin 2 Specimens

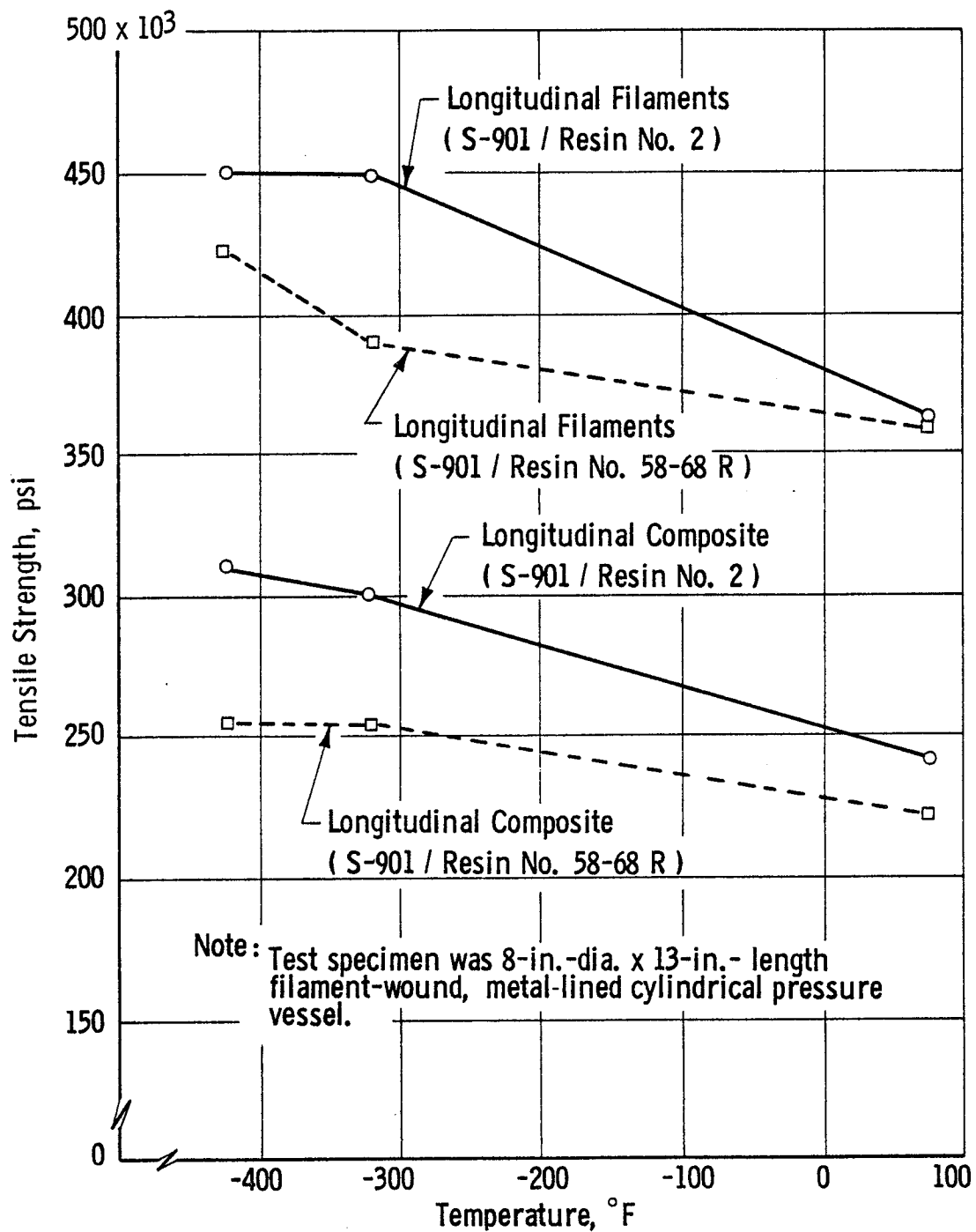


Figure 46. Effect of Temperature on Longitudinal Tensile Strengths Pressure Vessels with S-901 Glass and Alternate Resin Combinations

pressure vessels, Resin 2 is comparable to 58-68R at room temperature and superior to it at cryogenic temperatures.

Based on the pV/W factor, the structural efficiencies of Resin 2 vessels, relative to 58-68R vessels, were comparable at +75°F, 16.6% higher at -320°F, and 12.7% higher at -423°F.

With one understandable exception (Vessel 2, Table 40), all the ultimate strain levels for the longitudinal and hoop directions of Resin 2 vessels were in excess of 2.5% at all test temperatures. The highest longitudinal and hoop strains were, respectively, 3.16 and 3.02% at +75°F, 3.56 and 3.26% at -320°F, and 3.99 and 3.65% at -423°F.

It is noteworthy that a hoop-filament stress of 472.4 ksi was attained in Vessel 13 (tested at -423°F) before the longitudinal filaments failed at a stress of 459.2 ksi. As previously discussed, the pressure vessel was not fabricated to a balanced design, but was designed to fail in the heads to better differentiate between the systems under evaluation. Although the number of hoop filaments applied in vessel fabrication was inadvertently less than specified by design (Table 38), vessel failure still originated in the head, and the hoop filaments sustained a very high stress without failing. These results indicate, therefore, that a balanced-design vessel can provide hoop-filament stresses in excess of 472.4 ksi at -423°F.

An indication that some fabrication defects in the metal liner of a pressure vessel can have relatively little effect on single-cycle burst-strength was provided by Vessel 12. During the winding of the third hoop layer, the cylindrical section of the liner collapsed because the plaster-mandrel thickness was insufficient to support the winding loads. The wraps and plaster were removed, and most of the buckles were then eliminated by hand-working and internal pressurization. A thicker coating of plaster was cast in the liner and the winding operation was repeated. The relatively high burst pressure and longitudinal- and hoop-filament stress levels obtained when this vessel was tested indicate that the initial buckled-liner condition was not detrimental to vessel performance in this test.

A longitudinally oriented wrinkle was noted in the cylindrical section of several metal liners after the plaster mandrel was removed. It is attributed to the winding of the final turn of the longitudinal wrap over the initial turn to assure complete coverage with longitudinal fibers; subsequent winding of hoop fibers would increase the pressure in this area, causing the wrinkle. None of the vessel failures were attributed to this condition; in fact, Vessel 13, which had this type of wrinkle, was successfully tested at the highest stress and burst-pressure levels of any of the vessels.

VI. CONCLUSIONS

A. The principal objective of this program - the development of an improved cryogenic resin for S-901 glass-filament-wound structures - was accomplished.

B. In-process winding of metal-lined, glass-FWC, pressure vessels with Resin 2 was easily performed. The resin provided higher structural performance levels than did the standard epoxy resin, 58-68R.

At test temperatures of +75 and -423°F, pressure vessels fabricated from Resin 2 exhibited average longitudinal-filament stresses that were, respectively, equal to and 6.6% greater than those obtained in vessels fabricated from the standard epoxy system. At -320°F, the filament stress in the Resin 2 vessel was 15.4% greater than the stress in the standard; this result, however, was based on only one stress value for each resin system.*

On the basis of a pressure-vessel performance factor that includes the weight of the metal liner, Resin 2 vessels exhibited structural efficiencies, relative to 58-68R vessels, that were comparable at +75°F, 16.6% higher at -320°F, and 12.7% higher at -423°F.

C. The demonstration that System 2 is an improved cryogenic resin suggests (1) that the major assumptions and guidelines upon which the formulation of candidate resins was based were essentially sound, and (2) that further development of epoxy/polyurethanes similar to Resin 4A is warranted.

Resin 4A was clearly superior to Resin 2 at cryogenic temperatures in almost all of the mechanical properties tested. The filament tensile strengths of its composites were significantly higher than those of Resin 2. Only because of its poor physical properties (short pot life and high viscosity) was it rejected in favor of Resin 2.

Knowing that Resin 4A was significantly superior mechanically to Resin 2, and having established that Resin 2 was superior to the standard epoxy, it is reasonable to believe that an acceptable version of System 4A would be a still better cryogenic system. The realization of such a system requires merely an improvement in physical properties at little or no expense to mechanical properties.

On the basis of existing data it is possible to estimate the extent by which an improved Resin 4A system would excel over Resin 2. Thus, unidirectional (1:0) filament stresses in "dog-bone" tensile specimens of Resin 4A

* Additional data on the performance of Resin 2 FWC pressure vessels at cryogenic temperatures will be obtained in the near future under Contract NAS 3-6297. Although a different glass-filament/finish system will be involved, the results may complement the present data on the structural performance of Resin 2 at -320°F.

were approximately 18% higher at both -320 and -423°F than the same specimens prepared from Resin 2.* Noting the remarkable (but perhaps fortuitous) relationship between unidirectional (1:0) filament stress and pressure-vessel filament stress demonstrated by Resin 2, a similar 18% superiority for an improved 4A system over Resin 2 may be predicted. This margin is sufficiently large and sufficiently credible to justify further resin development work on epoxy/polyurethane systems.

*Based on data in Table 29, Resin 4A filament stresses were actually 34% higher at -320°F and 32% higher at -423°F, and not 18% as stated here. The larger figures were scaled down to 18%, because (as explained in Section IV, B,1) the unidirectional (1:0) filament strengths were considered spuriously high. The lower tensile values upon which the 18% estimate was based were obtained by extrapolation from the bidirectional (1:2) and bidirectional (1:1) data (Figure 21 and Table 29).

VII. RECOMMENDATIONS

A. On the basis of its general superiority as demonstrated in this program, it is recommended that Resin 2 be used in glass-FWC structures for current cryogenic applications.

B. The characteristics of Resin 2 as a prepreg system and as an adhesive should be investigated, particularly for use at cryogenic temperatures.

C. The development of a practicable epoxy/polyurethane laminating system should be continued. Desirable systems would possess the excellent mechanical properties of Resin 4A, but with improved pot life and viscosity characteristics.

As presently conceived, there are two possible approaches to this goal. The first has already been implemented through the resin-formulation stage. It substitutes a newly available aliphatic diisocyanate for Adiprene L-100, a new curing agent for MOCA, and various epoxy resins in place of Epon 826 and Epon 871. Preliminary results obtained on six of these systems reveal pot lives of 1 to 3 hours at 130°F and 5 to 6 hours at 150°F, as compared with a 15-min pot life at 150°F for Resin 4A. Tests of composite specimens prepared from several of these formulations are being conducted under Contract NAS 3-6297.

A second approach to improved systems of the Resin 4A type would be to attempt the preparation of a polyurethane diisocyanate prepolymer analogous to Adiprene L-100, using the above-mentioned aliphatic diisocyanate and a polyether glycol. Replacement of Adiprene L-100 with this prepolymer would provide a system chemically and structurally more like the original formulation than those of the first approach, and therefore more likely to have mechanical properties similar to those of System 4A.

D. To ensure that temperature equilibrium has been attained, the procedure for cryogenic testing of FWC pressure vessels should include an adequate soak period after the vessel is filled with cryogen and before the onset of pressurization. In addition, the test-chamber vacuum pumps should be operated to the highest possible pressure.

E. Additional studies of metal-lined, filament-wound, pressure vessels are needed to establish design, processing, and performance data at cryogenic temperatures. Areas of investigation should include

1. Methods and materials to provide a reliable adhesive bond between the metal liner and composite-wall structure, one that will eliminate metal-liner wrinkling or buckling and will withstand cyclic loads at cryogenic temperatures

2. Cyclic-pressurization testing to establish room- and cryogenic-temperature fatigue data and to determine metal-liner tolerance to cyclic testing without severe buckling from the compressive loads of the composite shell

3. Evaluations of pressure vessels fabricated from higher-modulus filaments to produce lower strains in the metal liner and improve the cyclic-fatigue characteristics

4. Investigation of the effects of winding the temperature sensor within the composite to improve the measurement of cryogenic temperatures and the attachment of the probe to the specimen.

Enough test vessels should be used in these studies so that a high degree of confidence can be assigned to the data obtained on structural properties and performance levels.

F. The 8-in.-dia, metal-lined, filament-wound, test vessel developed in this program should be used for future evaluations of FWC strengths at cryogenic temperatures. In the present program, 75% of the vessels failed in the longitudinal filaments as prescribed by the design. Refinements in liner inspection and processing procedures would probably result in 100% longitudinal-filament failures.

REFERENCES

1. R. C. Kausen, "High and Low Temperature Adhesives - Where Do We Stand?", Seventh National SAMPE Symposium, Adhesives and Elastomers for Environmental Extremes, Los Angeles, 20-22 May 1964, pp. 1-25 to 1-51.
2. L. M. Roseland, "Evaluation of Structural Adhesives for Potential Cryogenic Usage," ibid., pp. 7-1 to 7-17.
3. Cryogenic Materials Data Handbook, Air Force Materials Laboratory ML-TDR-64-280, PB 171809, revised August 1964.
4. J. Hertz, "The Effect of Cryogenic Temperatures on the Mechanical Properties of Reinforced Plastic Laminates," SPE Journal, 21, 181 (1965).
5. Proceedings, 20th Anniversary Technical Conference, SPI Reinforced Plastics Division, Chicago, 2-4 February 1965 (all papers dealing with the properties of reinforced plastics were examined).
6. M. P. Hanson, H. T. Richards, and R. O. Hickel, Preliminary Investigation of Filament-Wound Glass-Reinforced Plastics and Liners for Cryogenic Pressure Vessels, NASA TN D-2741, Lewis Research Center, Cleveland, March 1965.
7. J. M. Toth, Jr. and J. R. Barber, "Structural Properties of Glass Fiber Filament-Wound Cryogenic Pressure Vessels," NASA Technical Memorandum, Preprint J-3, August 1964.
8. D. W. Chamberlain, B. R. Lloyd, and R. L. Tennent, Determination of the Performance of Plastic Laminates at Cryogenic Temperatures, ASD-TDR-62-794, Part II, March 1964.
9. D. H. Weitzel, R. F. Robbins, P. R. Ludtke, and Y. Ohori, Elastomeric Seals and Materials at Cryogenic Temperatures, ASD-TDR-62-31, Part II, May 1963, p. 46.
10. A. Eisenberg and E. Rovira, "A New Method for the Rapid Determination of Glass Transition Temperatures," J. Polymer Sci., Part B, 2, 269-277 (1964).
11. K. W. Bills, Jr., "Thermal Volume-Expansion Coefficient and Glass Transition Temperature of Binders and Solid Propellants by the Buoyancy Method," Mechanical Properties Laboratory, Aerojet-General Corporation (Sacramento) Method 4720-14, 3 December 1964.
12. J. J. Keavney and E. C. Eberlin, "The Determination of Glass Transition Temperatures by Differential Thermal Analysis," J. Appl. Polymer Sci., 3, 47-53 (1960).
13. ASTM Standards, "Brittleness Temperature of Plastics and Elastomers by Impact," D746-64T, Part 27, p. 260 (1965).

REFERENCES (cont.)

14. F. J. Darms and P. G. Conrad, "Glass/Resin Interaction," Symposium on Chemistry of Matrices Used in Filament Winding, American Chemical Society, Chicago, September 1964.
15. L. M. Soffer, Final Report, Polaris Reliability Program, Increment VII, IWA No. 2-15467, Characterization Studies of HTS-Finish Including Polarized Light, 31 July 1963; Increment VIII, IWA No. 27367, Laboratory Test Methods Development, 23 December 1963.
16. L. M. Soffer, Superior Glass Finishes, IR&D Program Final Report, W.O. 8703-22, 29 December 1964.
17. W. D. Bascom, Some Surface Chemical Aspects of Glass/Resin Composites, Part 1 - Wetting Behavior of Epoxy Resins on Glass Filaments, NRL Report 6140, August 1964.
18. W. D. Bascom, Some Surface Chemical Aspects of Glass/Resin Composites, Part 2 - The Origin and Removal of Microvoids in Filament-Wound Composites, NRL Report 6268, May 1965.
19. W. A. Zisman, "Surface Chemistry of Glass Fiber-Reinforced Plastics," Symposium on Glass/Resin Interface, Society of Plastics Industry, Inc., 19th Annual Exhibit and Conference, Chicago, 6 February 1964.
20. J. V. Milewski, "Whisker-Reinforced Plastics," Machine Design, 37, 216 (1965).
21. P. West, "Whisker Composites; Where do They Stand Today?", Materials in Design Engineering, 61, 112 (1965).
22. H. Dannenberg, "Determination of Stresses in Cured Epoxy Resins," SPE Journal, 21, 669 (1965).
23. R. W. Buxton, R. N. Hanson, and D. Fernandez, Design Improvements in Liners for Glass-Fiber Filament-Wound Tanks to Contain Cryogenic Fluids, NASA CR 54-854 (Aerojet-General Report 3141 under Contract NAS 3-4189), January 1966.

APPENDIX A

TEST METHODS

The program goals required the determination of certain physical and mechanical properties of cast resin and of FWC specimens at ambient and cryogenic temperatures. Test methods for a number of mechanical and thermal properties of plastics at ambient and higher temperatures are described in ASTM and FTM standards, but new procedures were required for all tests at cryogenic temperatures and for some of the desired properties at ambient temperatures. Specimen fabrication and testing procedures were therefore developed for both resin and composite materials; whenever feasible, they were patterned after related procedures in ASTM Standards or FTM Standard No. 406. They are described below.

I. TASK I - IDENTIFICATION AND SELECTION OF SUPERIOR CRYOGENIC RESINS

A. PRELIMINARY PHYSICAL SCREENING TESTS

1. Determination of Cast-Resin T_g

A strain-response technique was used to determine the T_g of a cured resin sample. A strain sensor (gage) was applied to the sample, and the strains produced in the material by changing temperature were recorded in units of microstrain on a strain indicator.

a. Apparatus - Beaker (50 ml), hacksaw, 600A grit paper, strain gage (Type FAB-5012), plastics conditioner and neutralizer (W. T. Beam Co., Detroit, Mich.), epoxy adhesives, C-clamp, strain indicator (Model 120, Baldwin-Lima-Hamilton Co.), air-circulating curing oven, copper-constantan thermocouple, freezer, refrigerator.

b. Specimen Preparation - The resin system (30 to 40 g) was cured in a 50-ml beaker previously coated with mold-release agent. The cured cylindrical specimen (approximately 1.5 in. in diameter and 1 in. high) was cut in half with a hacksaw, parallel to the faces of the cylinder. The resulting surfaces were lapped smooth with wet or dry 600A grit paper. The surfaces were coated with a plastics conditioner, were swabbed clean, and were finished with a neutralizer. The strain gage was bonded between the two finished surfaces, using a minimum amount of epoxy adhesive. A C-clamp was applied to prevent slippage, and the adhesive was cured at 200°F for 1 hour. After the cure, lead wires were spot-welded to the gage.

c. Procedure - Because the response of the specimens had to be obtained over a wide temperature range, a copper-constantan thermocouple with a 0°C cold junction was used. The thermocouple was potted in an Adiprene L-100/MOCA formulation to simulate the temperature at the gage/resin interface of the test specimen. Strain measurements were made for most samples at -20°C (freezer), and +5°C (refrigerator), and at 10° intervals in the range from

21 to 128°C (oven). In making the measurements, four or five samples were placed in a glass jar and the refrigerator or oven doors were closed on the leads. Approximately 1.5 hours was required at each temperature station before equilibrium was attained.

d. Calculation - Units of microstrain were plotted as a function of temperature. The T_g is taken as the inflection point in the curve.

e. Comment - The adhesive used to bind the gage to the sample also had a T_g , and it was necessary to minimize the amount used in order to avoid possible error. Above 140°C, there was a tendency toward strain-gage delamination unless a high-temperature epoxy adhesive was used.

2. Thermal-Shock Resistance of Cast Resin

This test was a modification of MIL-I-16923E, Insulating Compound, Electrical, Embedding, which calls for the cycling of a specimen containing a steel-rod embedment between +90 and -55°C. It was devised as an economical means of assisting in the preliminary screening of candidate systems.

a. Apparatus - Test tubes (10 by 75 mm), glass rod (6 by 75 mm), air-circulating oven, silicone oil bath (-55°C).

b. Specimen Preparation - Two specimens of each formulation were prepared by casting the resin in test tubes and embedding the glass rod in the resin to approximately 10 mm from the bottom of the tube. The height of resin was about 55 mm.

c. Procedure - The cured specimens were cycled ten times by holding them alternately at +90°C for 30 min (oven) and -55°C for 10 min (silicone oil bath). A resin failure was recorded when either of the two samples tested was visibly damaged by crazing or cracking. The results were considered marginal if the resin pulled away from the glass wall, or if changes occurred that were not definitely attributable to the cycling itself. The resin was considered promising if it remained fully encapsulated by the test tube, thereby indicating that the degree of thermal contraction between the glass surface and the resin was not sufficient to significantly damage the glass-to-resin bond.

B. PHYSICAL SCREENING TESTS

1. Tensile Strength at Fracture, Elongation at Fracture, Modulus of Elasticity, and Toughness of Cast Resin

Stress-strain measurements were used to determine the tensile strength at fracture, elongation at fracture, modulus of elasticity, and toughness of a cured resin.

a. Apparatus - Holding fixture, routing fixture (Figure A-1), clamp fixture (Figure A-2), No. 600 sandpaper, tensile-test machine, cryostat facility (Figures A-3 and A-4), extensometer.

NOTES:

1. REMOVE ALL BURRS AND SHARP EDGES
2. SCRIBE LINE APPROX. .010 DEEP
3. HEAT TREAT TO 160,000 PSI MIN. TENSILE STRENGTH
4. MACHINED SURF CCS 15 UNLESS OTHERWISE SPECIFIED.
5. MATCH MACHINE -3/-5 PARTS
6. MARK MATCHED SET PER ASSIZESW WITH 177730-1
7. PARTS TO BE KEPT AS A MATCHED SET
8. DIMENSION AT CENTER
TO BE ±.00% OF MINIMUM MACHINED DIM.
OVER AREA INDICATED.
9. THIS SET TO BE USED TO FABRICATE
TENSILE TEST SPECIMENS.

REVISEMENTS			
FORM/LIN	DESCRIPTION	DATE	APPROVED

				LIST OF MATERIALS			
QTY REQD	SYM IDENT	PART OR IDENTIFYING NO	NOMENCLATURE OR DESCRIPTION	MATERIAL	SPECIFICATION	UNIT WT.	ZONE
-5			.312 THK PLATE	4130 ALLOY STEEL	QQ-S-685		
-3			.312 THK PLATE	4130 ALLOY STEEL	QQ-S-685		
-1			.				

				TITLE			
ON	THRU	FABRICATION	TESTING	DESIGN	CONSTRUCTION	CHECKING	TITLE
							ROUTING FIXTURE, TENSILE TEST SPECIMEN

EFFECTIVE SERIAL NO.	USAGE DATA	DRAWING LEVEL	APPLICATION	ACT W/CALC W/T

CHG SIZE	CHG REGR NO.	CHG NO.
D	70143	177730

RELEASE DATE 7-2-63 SHEET 1

Figure A-1. Routing Fixture, Tensile-Test Specimen

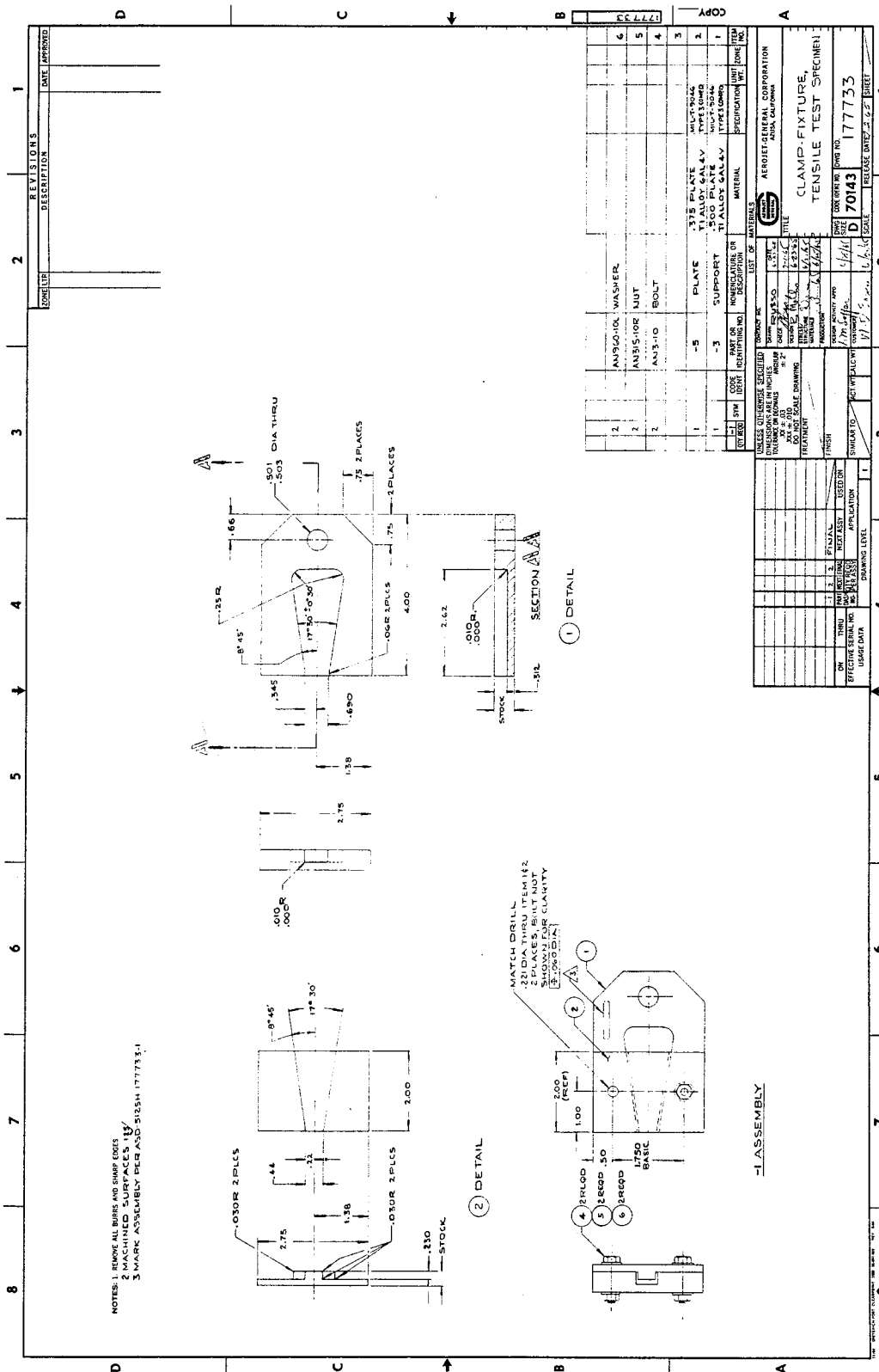


Figure A-2. Clamp Fixture, Tensile-Test Specimen

NOT REPRODUCIBLE

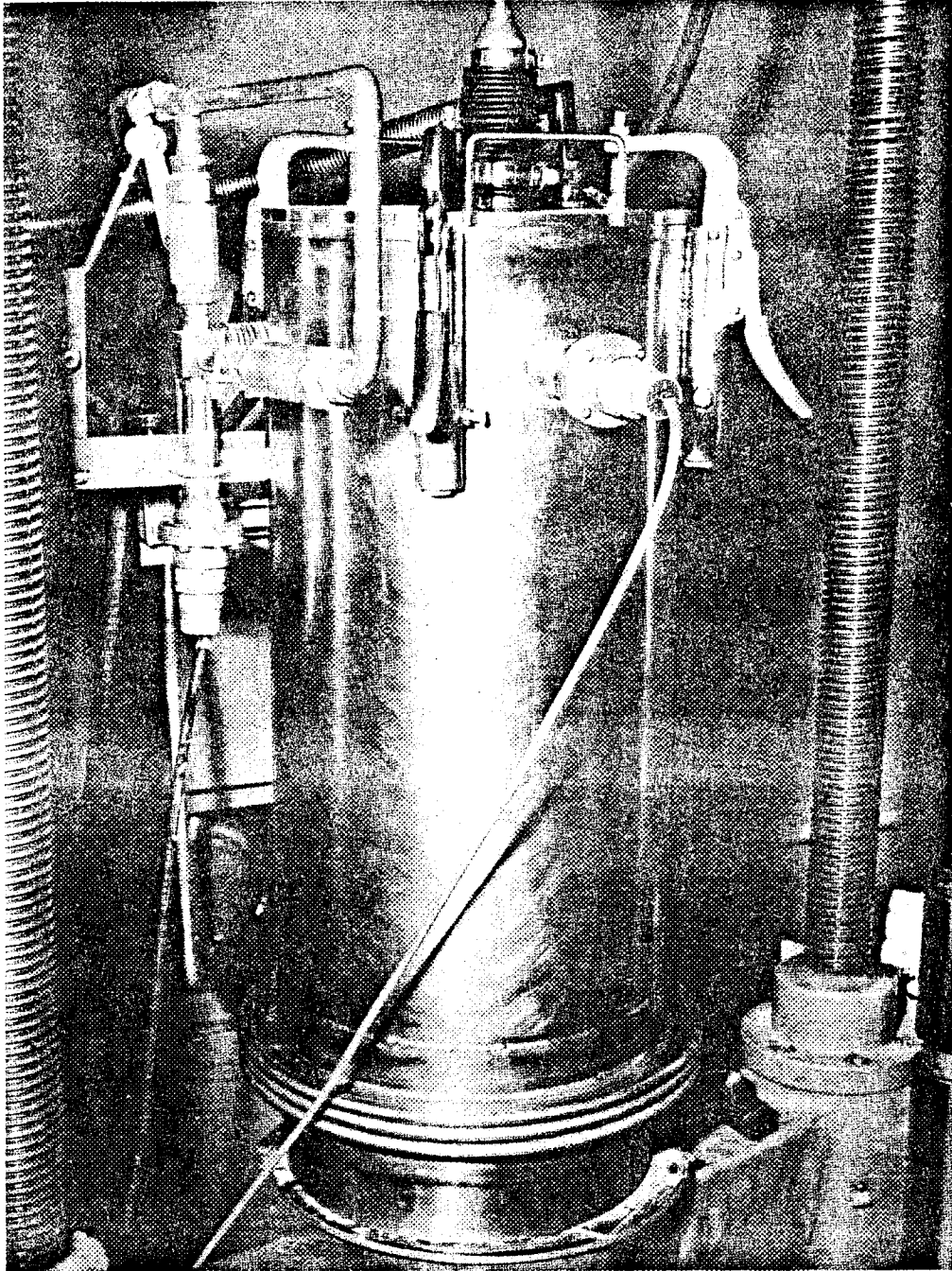


Figure A-3. Cryostat/Tensile-Machine Facility

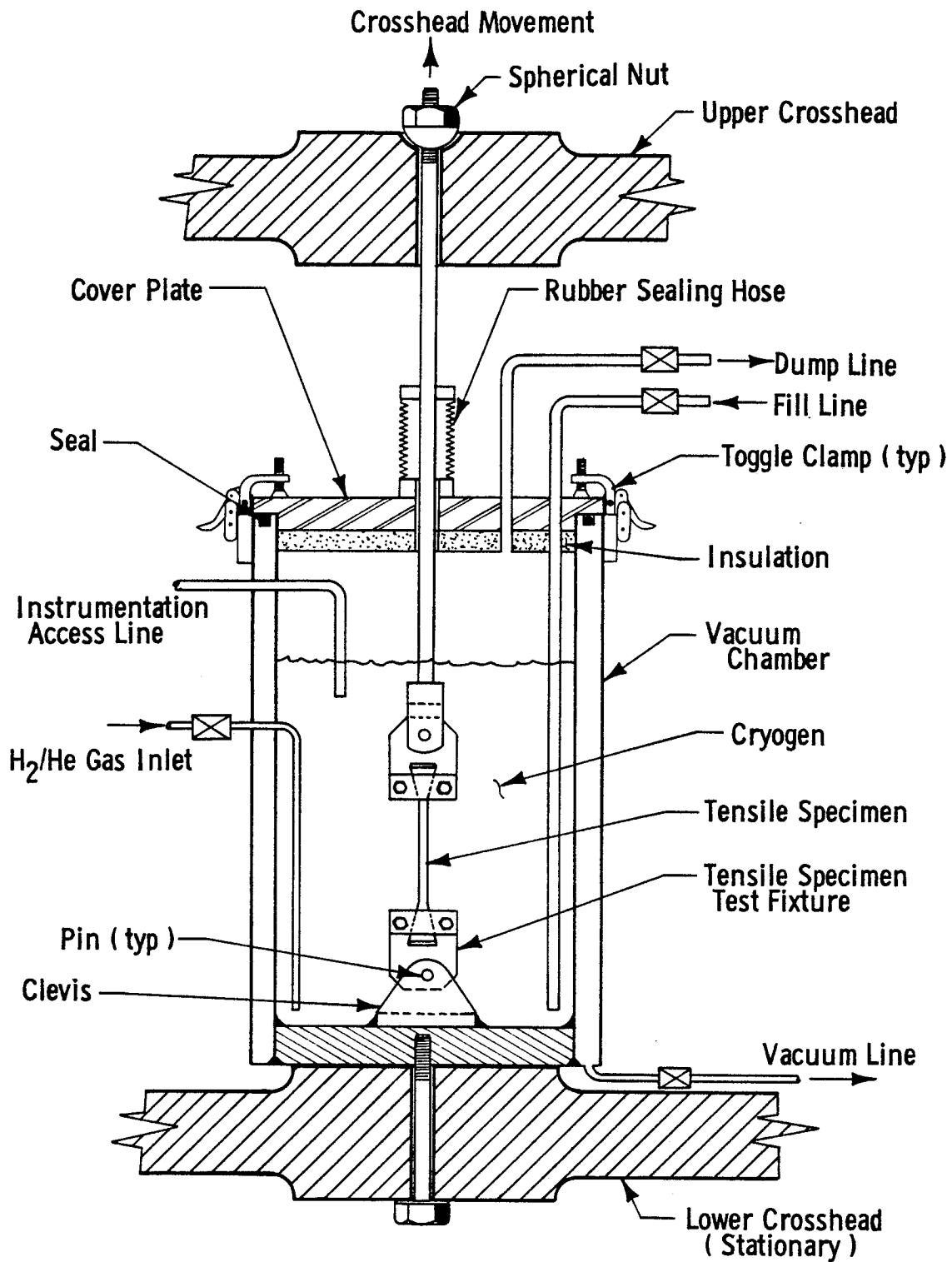


Figure A-4. Cryostat/Tensile-Test Machine

b. Specimen Preparation - Each system was mixed according to its individual requirements (see Table 9 of the main text). The mixture was degassed (approximately 23 in. Hg) for 30 min, and then bottom-drained into a 0.125-in.-thick flat-panel molding fixture preheated to the applicable initial cure temperature. The mold and contents were heated according to the individual cure schedules, and were then cooled. The panels were removed and routed to the configuration shown in Figure A-5. The specimen was carefully sanded with No. 600 sandpaper to promote a uniform surface, thereby reducing data scatter.

c. Procedure - The test specimen was placed in the clamp fixture as shown in Figure A-6. It was stressed in tension until failure occurred, using a 0.05-in./min crosshead travel rate. A 2-in. extensometer was used in conjunction with a tensile machine and recorder to provide a load-vs-strain diagram. To determine the elongation at fracture, two reference marks were inked on the specimen and were accurately measured to the nearest 0.05 in. After specimen rupture, the broken portions were fitted together and the distance between the reference marks was measured.

d. Calculations - Methods used to calculate tensile strength, elongation, elastic modulus, and toughness are described below.

The tensile strength at fracture for the test specimens was determined from

$$S_F = \frac{P_F}{A}$$

where

S_F = tensile strength at fracture, psi

P_F = load at fracture, lb

A = original cross section, sq in.

The maximum tensile strength, if different from that at fracture, was calculated by substituting the maximum load for the load at fracture.

For test-specimen elongation at fracture,

$$e_F = \frac{L_1 - L}{L} (100)$$

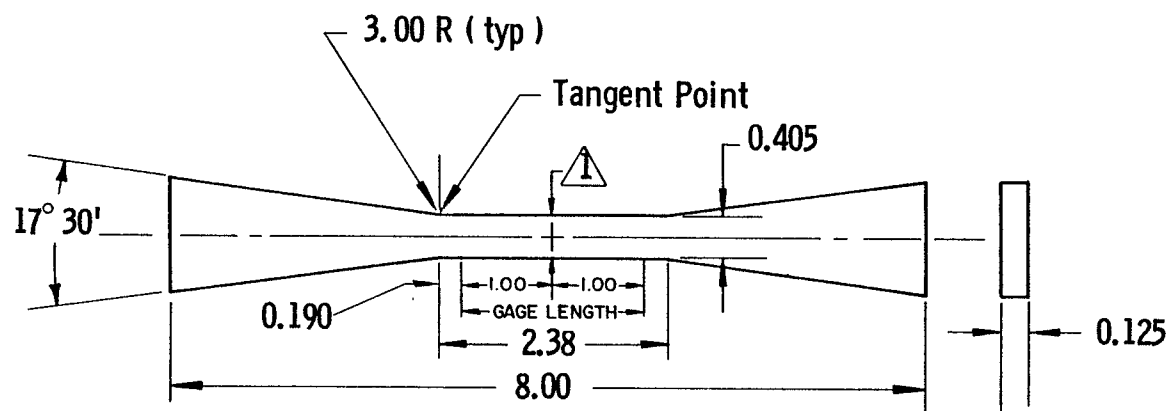
where

e_F = elongation at fracture, %

L = distance between reference marks prior to testing, in.

L_1 = distance between reference marks after testing, in.

The modulus of elasticity for the test specimens was determined by extending the straight-line portion of the load-strain curve to any convenient point on the curve and noting the corresponding load at that



Note: $\triangle 1$ Width at center shall be $\begin{matrix} + 0.000 \\ - 0.004 \end{matrix}$ compared with minimum dimension of reduced section

Figure A-5. Tensile-Test Specimen

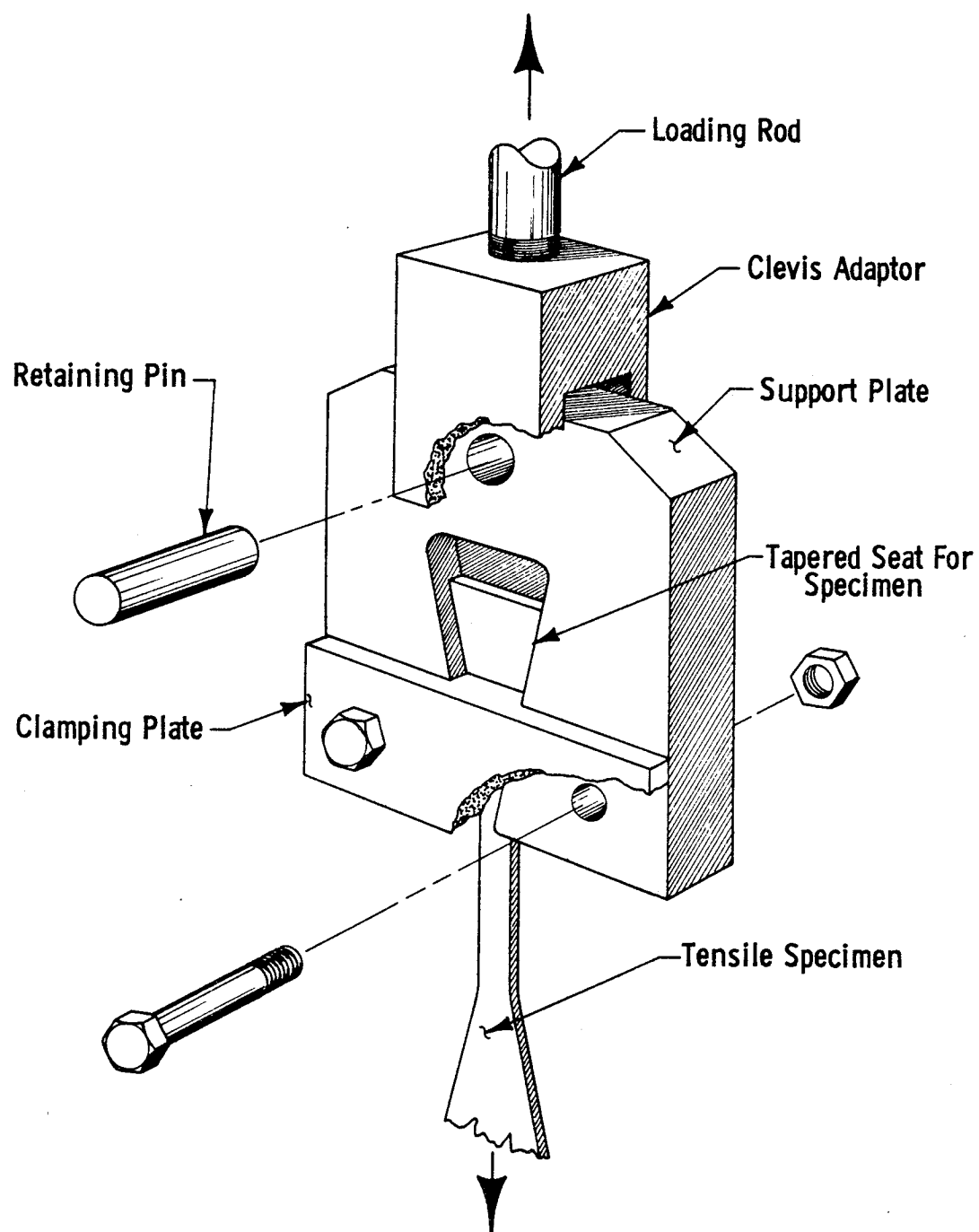


Figure A-6. Tensile-Test-Fixture Setup

point. A line for this point was dropped perpendicular to the base line. The distance from the intersection of the base line to the point where the load-strain curve crossed the base line was measured in inches and denoted as chart distance (C.D.). The modulus of elasticity was calculated from

$$E = \frac{L}{A} \bigg/ \frac{C.D.}{(mag)(gage\ length)}$$

where

L = load, lb

A = minimum cross section, sq in.

mag = magnification of extensometer

Toughness, a measure of the ability of material to absorb energy without failure, was expressed as the total energy per unit volume required to fracture the material. The toughness of resin systems was indicated by the area under the stress-strain curve, and was determined by measuring this area on resin load vs strain diagrams.

2. Notch Toughness of Cast Resin

Notched tensile specimens were stressed until failure occurred. Notch toughness is a measure of the ability of a material to sustain high stresses without failure in the presence of local stress discontinuities such as cracks, notches, and imperfections. As modified for use in resins, the property demonstrates the capacity of the system to sustain loads despite imperfections in the matrix.

a. Apparatus - Molding fixture, routing fixture (Figure A-7), clamp fixture (Figure A-8), drill, center-notch tool, tensile-test machine, cryostat facility.

b. Specimen Preparation - Each system was mixed according to its individual requirements (see Table 9 of the main text). The mixture was degassed (approximately 23 in. Hg) for 30 min, and was then bottom-drained into a 0.188-in.-thick flat-panel molding fixture preheated to the applicable initial cure temperature. After heating according to the individual cure schedules, each mold was cooled. The panels were removed and routed to the configuration shown in Figure A-9. The center notch was machined in the casting by drilling an 0.18-in.-dia hole in the center of the specimen, inserting the center-notch tool through the hole, and cutting the notch as shown in Figure A-9.

c. Procedure - The test specimen was placed in the clamp fixture as shown in Figure A-10 and was stressed in tension until failure occurred, using a 0.05-in./min crosshead travel rate.

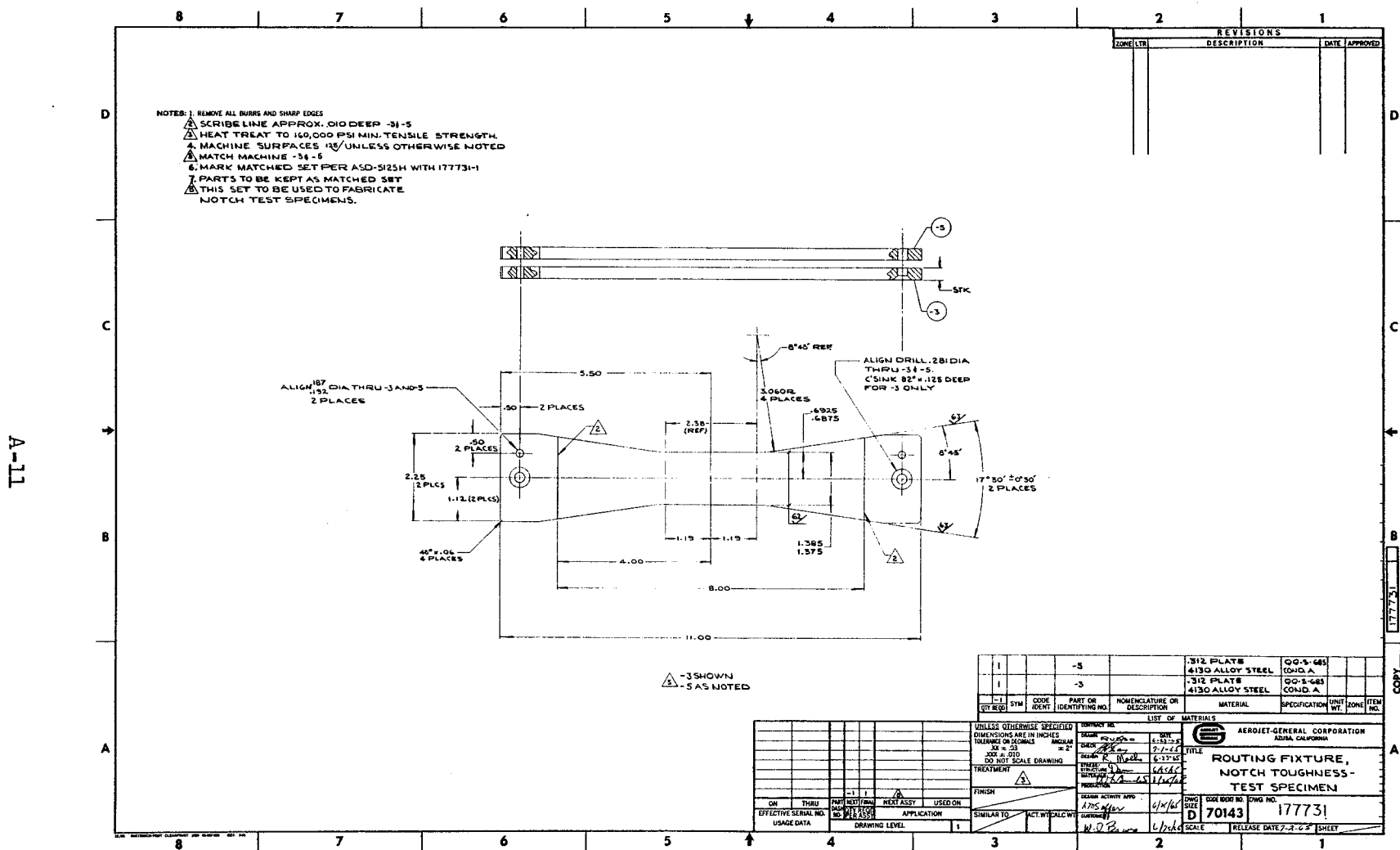


Figure A-7. Routing Fixture, Notch-Toughness Test Specimen

Figure A-8. Clamp Fixture, Notch-Toughness Test Specimen

Figure A-9. Notch-Toughness Specimen

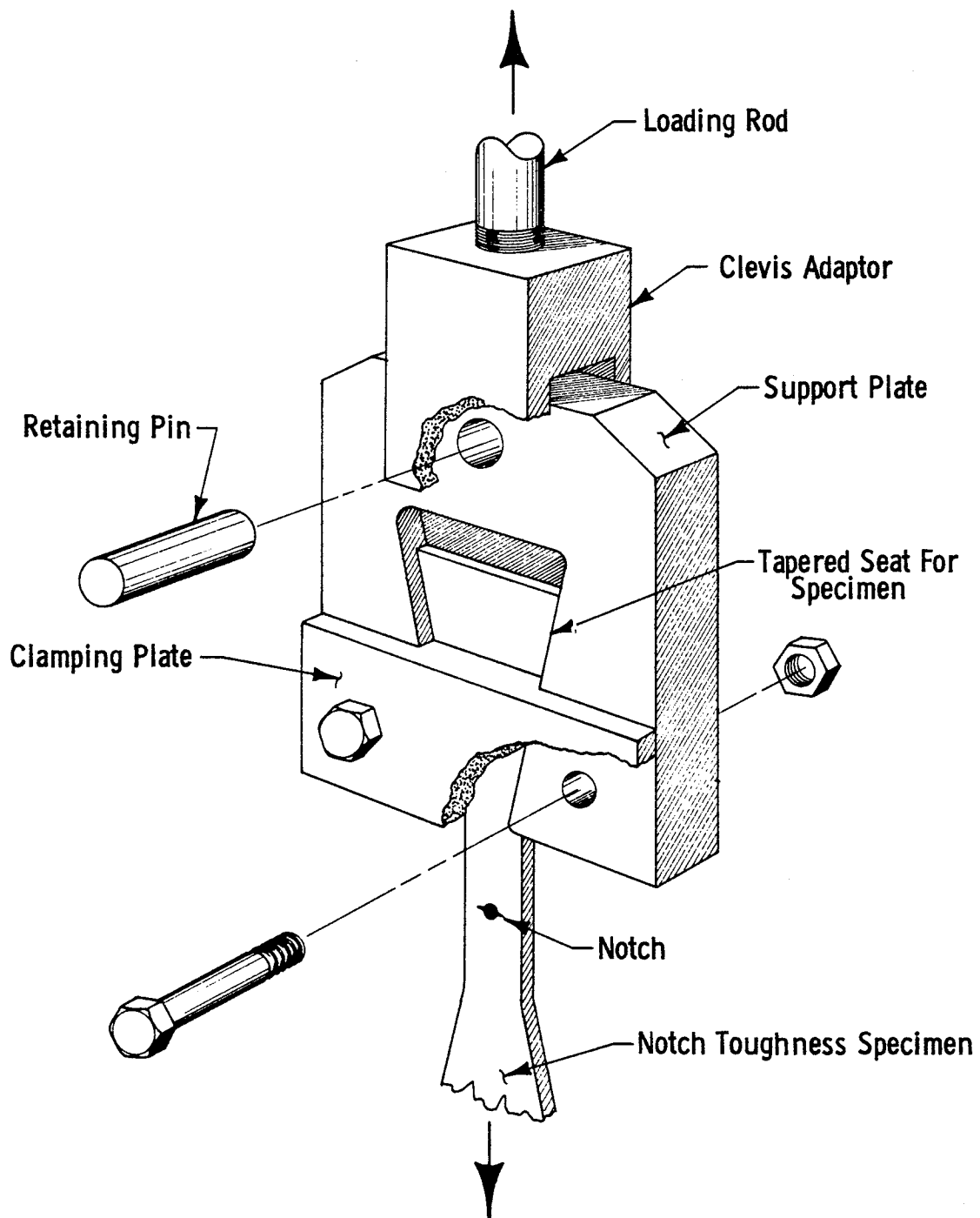


Figure A-10. Notch-Toughness Test-Fixture Setup

d. Calculation

The notch toughness of the resin specimen was determined from

$$K = \sigma \sqrt{W \left[\tan \left(\frac{90 a}{W} \right) \right]}$$

where

K = notch toughness, psi $\sqrt{\text{in.}}$

σ = tensile load divided by cross-sectional area, psi

W = specimen width, in.

a = half of the total crack width, in.

3. Viscosity of Uncured Resin

The viscosity of the uncured resin was determined with the aid of a Brookfield Viscometer.

a. Apparatus - Brookfield Viscometer (Model LVT), beaker, thermometer.

b. Specimen Preparation - The test specimen was a sample (300 to 400 ml) of catalyzed resin system in a beaker.

c. Procedure - The Viscometer spindle was positioned in the jar so that the sample surface was at the center of the shaft indentation and the spindle was in the center of the beaker. Viscometer rotation was started, and readings were taken (after 10 revolutions at each speed) at 6, 12, and 30 rpm. Measurements on the 100 scale of the dial were preferred because of their greater accuracy. The temperature after each set of readings was recorded.

d. Calculation - Resin-specimen viscosity was determined by noting the dial factor on the Brookfield Model LVT viscosity chart, which relates the specific spindle being used and the spindle speed. The viscosity (poises) was calculated from

$$\text{Viscosity} = D_{100} F_D$$

where

D_{100} = dial reading on 100 scale

F_D = dial factor from Brookfield chart

4. Pot Life of Uncured Resin

Resin pot life is defined here as the period during which the resin viscosity remained below 2500 centipoises (cp).

a. Apparatus - Brookfield Viscometer (Model LVT), beaker, thermometer, watch.

b. Specimen Preparation - The test specimen was a sample (300 to 400 ml) of catalyzed resin system in a beaker.

c. Procedure - The resin viscosity was determined as a function of time as described above (Section I,B,3).

d. Calculation - The pot life was obtained from a plot of resin viscosity vs time.

II. TASK II - EVALUATION OF CANDIDATE CRYOGENIC RESINS*

A. IMPACT RESISTANCE OF CAST RESIN

This procedure was used to determine the relative susceptibility of a cast resin material to shock fracture under standard room-temperature conditions or after exposure to a cryogenic environment. This susceptibility is indicated by the energy expended by a standard pendulum-type (Charpy) impact machine in breaking a standard specimen in one blow.

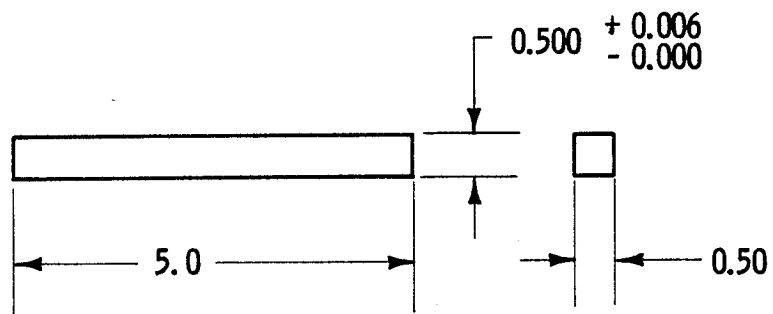
1. Apparatus - Simple-beam (Charpy-type) impact machine, impact-specimen mold.

2. Specimen Preparation - Cast panels were prepared from Resins 2 and 3 at the same time tensile and notch-toughness panels were made; the same mixing and curing procedures were used (see Section I,B,1, foregoing). Panels of Resins 4A and 6 were similarly prepared, using the mix procedures and cure schedules shown in Table 15 of the main text. Test specimens were cut and sanded to the dimensions shown in Figure A-11.

3. Procedure - The specimen was conditioned at the test temperature until temperature equilibrium was attained. It was then transferred from the conditioning bath to the impact machine and tested. The maximum elapsed time between the removal of specimens from the bath and testing was 6 sec. The specimen was supported against the steel blocks of the impact machine so that the blow was struck at the center of the specimen.

4. Calculation - The amount of energy expended in breaking each specimen, expressed in ft-lb/in. of width of the specimen face hit by the hammer, was calculated.

* Methods for the determination of tensile strength and associated properties, notch toughness, viscosity, and pot life are described in Section I,B, foregoing.



Test Specimen

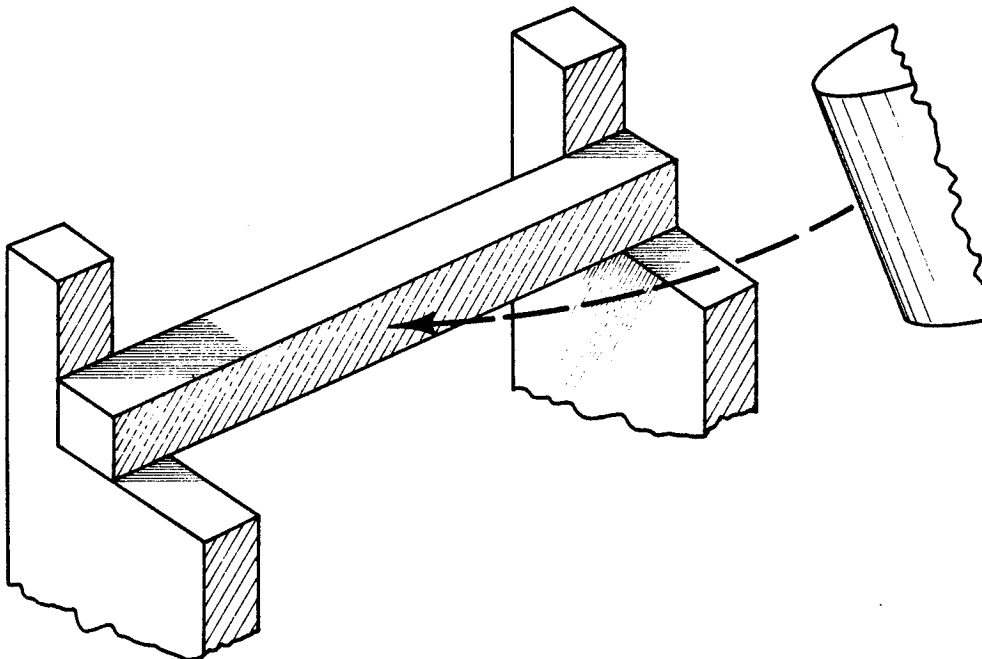


Figure A-11. Simple-Beam (Charpy-Type) Impact Test

B. INTERLAMINAR SHEAR STRENGTH OF GLASS/RESIN COMPOSITES
(SHORT-SPAN SHEAR METHOD)

The interlaminar shear strengths of unidirectional glass-FWC specimens were determined by the short-span-shear method at +75, -320, and -423⁰F.

1. Apparatus - Filament-winding machine, tension-measuring device, drum-winding fixture, air-circulating curing oven, test fixture (Figure A-12), tensile-test machine, cryostat facility, brush.

2. Specimen Preparation - Resins 2, 3, and 6 were prepared according to the procedures given in Table 15 of the main text. Using the drum-winding fixture, roving was passed through a dip tank containing the resin system and was then wound directly on the mandrel (under roving tension of 7 +2 lb) as unidirectional side-by-side filaments. Three windings were prepared, each 24 by 56 in.

Because of its viscosity Resin 4A was not suitable for "wet winding." Immediately after mixing (see Table 15 of the main text), it was diluted with MEK (0.16 ml of MEK per gram of resin mix). This solution was brushed onto a cellophane release wrap that enveloped the mandrel. Roving was wound over the wet cellophane. Resin-poor areas were touched up with the brush after winding. Three windings were prepared, each 24 by 56 in.*

The subsequent procedure was the same for all four systems. The windings were cut into six equal lengths perpendicular to the roving wind. They were laid up so as to make an 18-ply unidirectional flat-panel laminate. The laminate was sandwiched between four plies of Dacron bleeder cloth and a layer of 181-glass cloth to facilitate release. The sandwich was placed on a steel plate that had been wrapped with Teflon-coated glass cloth. This assembly was then vacuum-bagged and cured under a vacuum according to the resin-system requirements. After curing, the laminate was removed and cut into short-span-shear specimens 2.00 in. long by 1.00 in. wide by 0.125 in. thick. Specimen width and thickness were measured to the nearest 0.001 in. Any necessary polishing was done only in the longitudinal direction.

3. Procedure - The specimen was mounted in the test fixture in the calibrated testing machine, and was carefully aligned between the loading nose and supports (Figure A-13). The crosshead travel rate was 0.05 in./min, and the specimen was stressed until failure occurred.

4. Calculation - The short-span interlaminar shear strength was determined from

$$S = \frac{3 p}{4 b d}$$

* It is now believed that the MEK-diluted Resin 4A mix would have provided comparable or even better results if it had been applied to the roving from a dip tank, although this was not actually attempted.

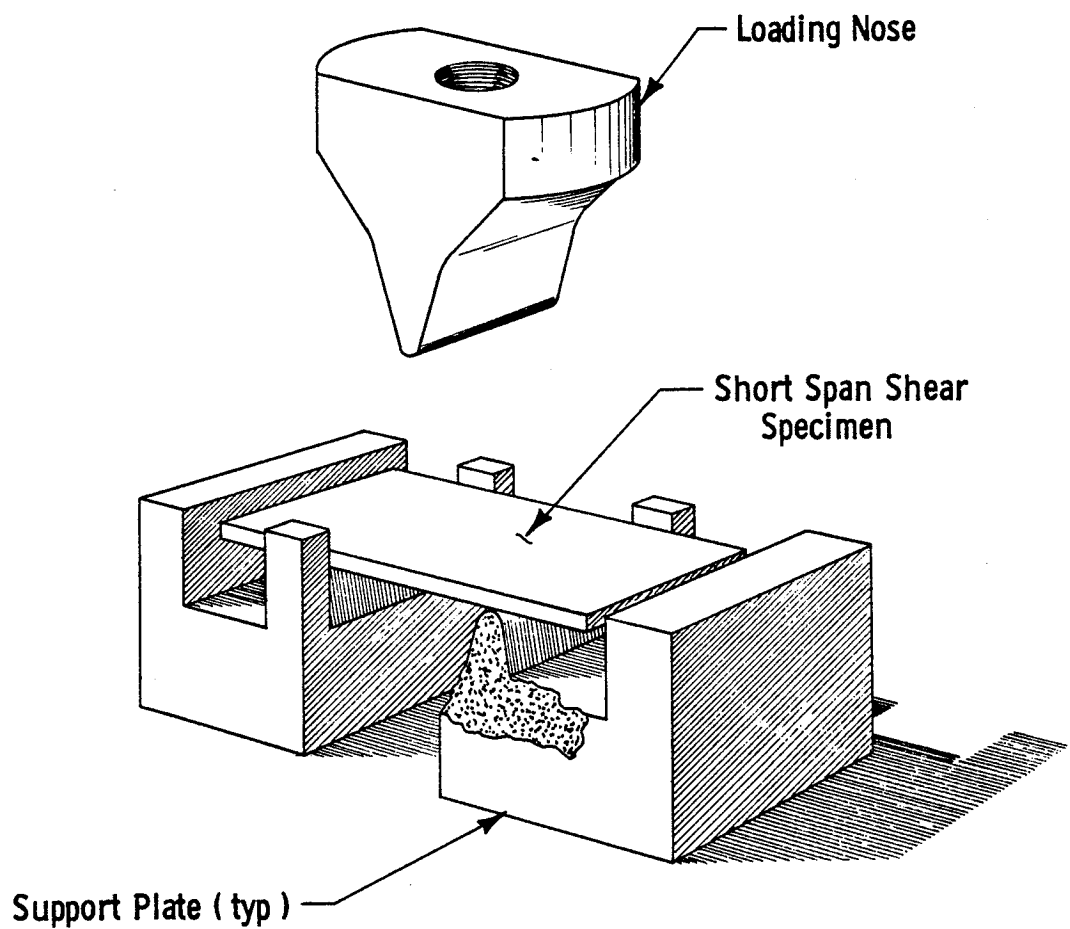
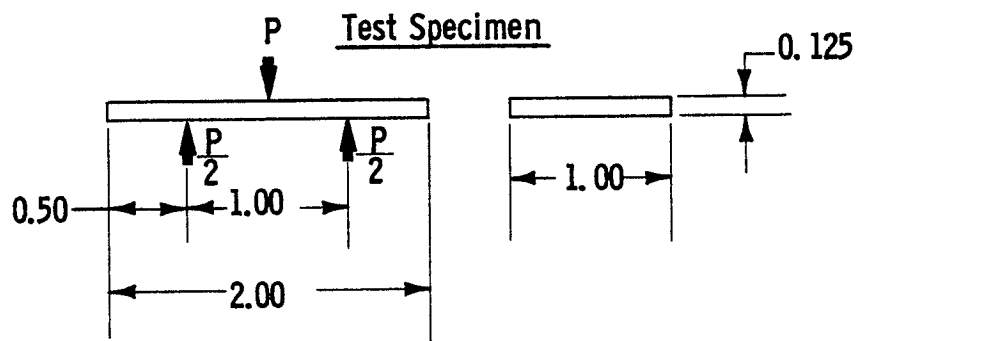


Figure A-13. Short-Span-Shear Test-Fixture Setup

where

S = interlaminar shear strength, psi

p = maximum load at failure, lb

b = specimen width, in.

d = specimen thickness, in.

C. INTERLAMINAR SHEAR STRENGTH OF GLASS/RESIN COMPOSITES
(HORIZONTAL-SHEAR METHOD)

The interlaminar shear strengths of unidirectional glass-FWC specimens were determined by the horizontal-shear method at +75, -320, and -423°F.

1. Apparatus - NOL-ring winding machine, tension-measuring device, NOL-ring winding mandrel, air-circulating curing oven, test fixture (Figure A-12), tensile-test machine, cryostat facility.

2. Specimen Preparation - Resins 2, 3, and 6 were prepared according to the procedure given in Table 15 of the main text. Using the NOL-ring winding machine, the roving was passed through a dip tank containing the resin and was then wound directly on the mandrel (70 turns) under a tension of 15 \pm 2 lb. The mandrel was heated (150 to 175°F).

A diluted mix of Resin 4A was prepared as follows: Pulverized MOCA (55.2 g) was dissolved in 100 ml of analytical-grade MEK (15 min). Adiprene L-100 (100 g), Epon 826 (70 g), and Epon 871 (30 g) were successively added to the solution, with stirring. The solution was placed in the dip tank, and winding was performed as with the other systems.

After cures according to individual requirements, the rings were removed from the winding fixture and were routed to a thickness of approximately 0.125 in. Excess resin was removed from the rings with No. 280 sandpaper. The required arc segments (15) were cut from each ring, with the width and thickness being measured to the nearest 0.001 in. The finished specimen was 0.250 in. wide, 0.635 in. long, and 0.125 in. thick. These dimensions conformed to those recently approved in the tentative method for testing under ASTM Standard D2344-65 T.

3. Procedure - The specimen was aligned between the loading nose and supports, and was center-loaded on the convex side (Figure A-14). The crosshead travel rate was 0.05 in./min, and the specimen was stressed until failure occurred.

4. Calculation - The interlaminar shear strength (horizontal shear) was calculated from

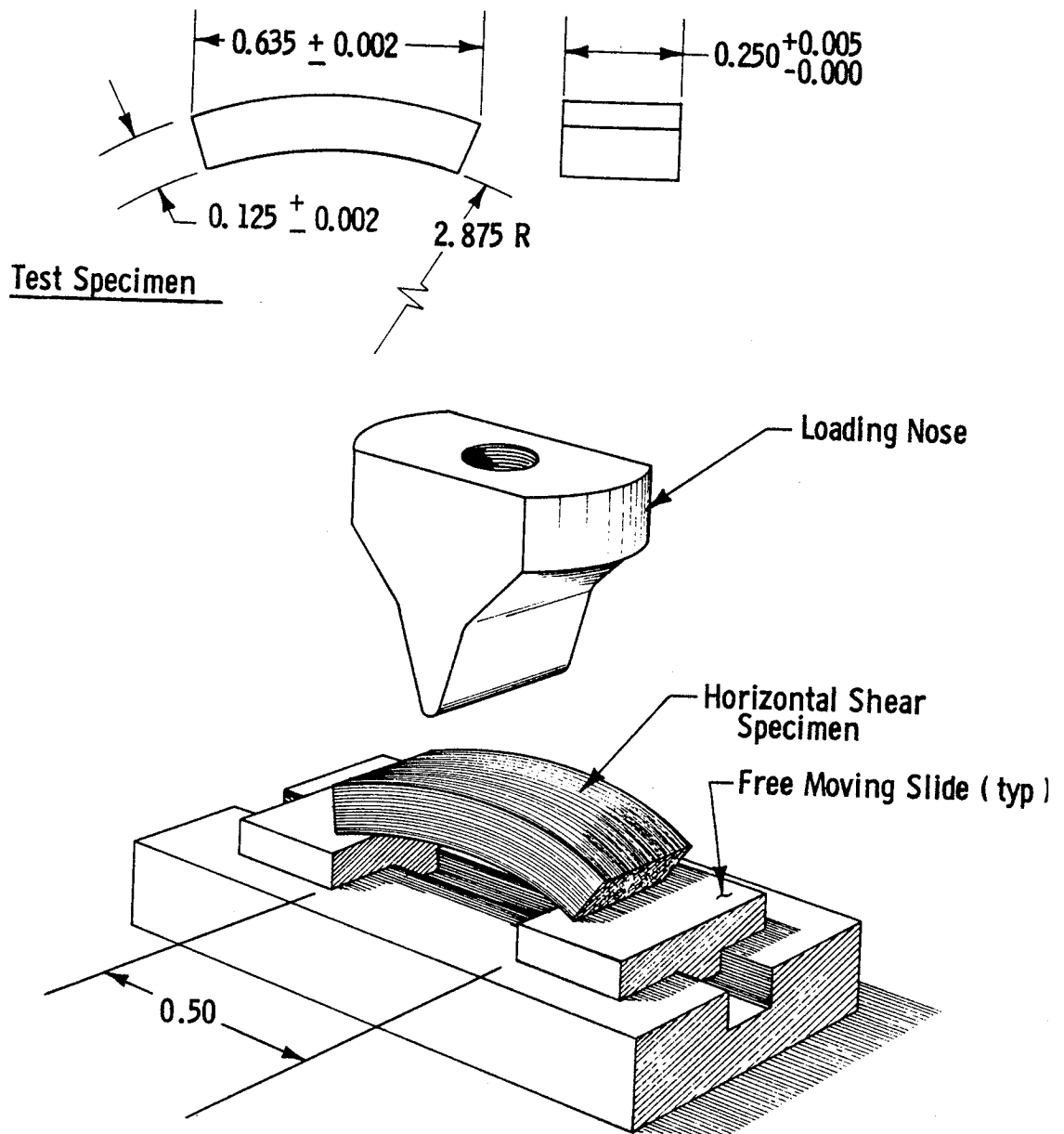


Figure A-14. Horizontal-Shear Test-Fixture Setup

$$S = \frac{3 p}{4 b d}$$

where

S = interlaminar shear strength, psi

p = maximum load at failure, lb

b = specimen width, in.

d = specimen thickness, in.

D. COEFFICIENT OF LINEAR THERMAL CONTRACTION OF CAST RESIN

The linear thermal contraction of cured resin was determined between -400 and +60°F.

1. Apparatus - Fused-quartz-tube dilatometer, micrometer, thermocouple.

2. Specimen Preparation - Thermal-contraction specimens were prepared from the same batch of resin mix used for tensile and notch-toughness specimens. The individual cure schedules given in Table 15 of the main text were followed. After removal from the mold, the castings were cut and sanded into rectangular specimens. The finished specimens (three for each resin system) were 0.35 in. wide by 0.35 in. thick by 2.00 in. long. With a 1/16-in. bit, a hole was drilled halfway through the center of each specimen (normal to the length) for attachment of the thermocouple wire. The copper-constantan thermocouple was potted in the specimen with Shell 911F adhesive.

3. Procedure - The test-specimen length between the two quartz points was measured at room temperature to the nearest 0.001 in. The specimen was placed in a fused-quartz dilatometer tube, the quartz rod was brought into contact with it, and the dial gage was positioned. The assembled specimen and tube were placed in the cryostat. The system was purged with helium gas and was then cooled with LH₂ to cryogenic temperatures. When the temperatures and dial-gage readings were recorded, the specimen was first permitted to stabilize at the cryogenic temperature for 15 min before being warmed to room temperature (by pressurizing the system with helium gas and replacing the LH₂). Dimensional changes were recorded at 10° intervals between -400 and +60°F. Three test runs were made for each system. Before the specimens were tested, a 2-in.-long quartz sample was run in order to provide an instrument correction. A Leeds & Northrup Type K-3 universal potentiometer was used to monitor the temperature.

4. Calculation - The coefficient of linear thermal contraction was calculated from

$$\alpha = \frac{\Delta L}{L \Delta t}$$

where

α = coefficient of linear thermal contraction, in./in./ $^{\circ}\text{F}$

ΔL = change in length due to cooling, in.

L = test length of specimen at room temperature, in.

Δt = difference in temperature over which change in length was measured, $^{\circ}\text{F}$

E. THERMAL-SHOCK RESISTANCE OF CAST RESIN

The resistance of cast-resin specimens to thermal shock was determined by alternate immersions in water and in LH_2 .

1. Apparatus - LH_2 Dewar flask, 2000-ml beaker.
2. Specimen Preparation - The specimens were cut from unused impact specimens and were sanded to form rectangular blocks 0.5 in. wide by 0.5 in. thick by 1.5 in. long.
3. Procedure - After immersion in the LH_2 -filled Dewar flask and equilibration for 15 min, the specimen was removed from the flask and placed in a 2000-ml beaker of water at room temperature. After 15 min, it was removed from the water, dried with compressed air, and inspected for signs of thermal cracking. The test procedure was repeated for a total of five cycles. Three specimens were tested for each resin system.
4. Report - The number of specimens that showed signs of failure, the cycle during which failure occurred, and the temperature range were noted.

F. SPECIFIC GRAVITY OF CAST RESIN

The specific gravity of the resin was determined as the ratio of the weight of a given volume of the material at $73 \pm 4^{\circ}\text{F}$ to that of an equal volume of water at the same temperature.

1. Apparatus - Analytical balance, corrosion-resistant wire, beaker, thermometer.
2. Specimen Preparation - The test specimens were obtained from unused tensile or notch-toughness material. They were of any convenient size or shape, void-free, and not less than 0.2 cu in. in volume.
3. Procedure - A piece of corrosion-resistant wire about 12-in. long was fastened to the hook on a pan support of an analytical balance, and the weight was recorded to the nearest 0.1 mg. The test specimen was attached to the wire so that it was suspended about 1 in. above a beaker support; it was weighed to the nearest 0.1 mg. The suspended specimen was then immersed in a beaker of freshly boiled distilled water at a temperature

of 72°F, and was weighed to the nearest 0.1 mg. The specimen was removed from the wire, and the weight of the wire immersed in water to the same depth was recorded.

4. Calculation - The specific gravity was calculated from

$$\text{Sp gr} = \frac{k - p}{(k - p) - (b - c)}$$

where

k = weight of specimen plus wire in air, g

p = weight of wire in air, g

b = weight of specimen in water plus partly immersed wire, g

c = weight of wire partly immersed in water, g

G. RESIN SHRINKAGE (%) DURING CURE

The shrinkage of a castable resin during cure was determined from (1) volume measurements on the mold and on the cured casting, and (2) specimen weights in air and in water.

1. Apparatus - Semicylindrical mold.

2. Specimen Preparation - The mold (10 in. long and 1 in. in radius) was placed in the curing oven, was carefully leveled, and was preheated to the desired cure temperature. The individual resin mixes were the same degassed batches used in the preparation of tensile, notch-toughness, impact, and other specimens. The molds were filled in the oven and were heated in accordance with the applicable cure schedules.

3. Procedure - The dimensions of the mold cavity were carefully measured before the resin was cured. After removal from the mold, the volume of the cured specimen was determined (a) by direct measurement of the sample dimensions, and (b) by the difference in weight of the sample in air and while immersed in water.

4. Calculation - Specimen shrinkage (%) was calculated from

$$\text{shrinkage} = \frac{V - V_i}{V} (100)$$

where

V = volume of cavity, cu in.

V_i = volume of cured resin, cu in.

H. RESIN AND VOID CONTENTS OF GLASS/RESIN COMPOSITES

The resin and void contents of glass/resin composite specimens were determined by means of a resin-burnout procedure, and from the known specific-gravity values for resin, glass, and glass/resin composite.

1. Apparatus - Analytical balance, desiccator, heat-resistant nonreactive crucible, muffle furnace equipped with temperature control, corrosion-resistant wire, beaker.
2. Specimen Preparation - The test specimens were unused portions of the same NOL rings and short-span-shear panels from which horizontal- and short-span-shear specimens were cut. Each had a minimum weight of 3 g and maximum dimensions of 1 in. by 1 in. by the thickness supplied. The sides were square to the faces, and the edges were not frayed.
3. Procedure - The composite specimen was weighed on an analytical balance in a previously ignited and weighed crucible. It was placed in the furnace at a temperature below 650°F. The furnace temperature was raised to 1150 ± 50°F at a rate that would not cause a loss of glass filaments. The crucible was ignited to constant weight at this maximum temperature (20 min to 2 hours was required, depending on the sample thickness), and was permitted to cool in a desiccator. The weight loss was determined by weighing the residue.

Determination of the void content (vol%) required prior determination of the specific gravity of the resin and of the glass/resin composite by the method described in Section II,F, above. The specific gravity of the S-901 glass filament that was used was 2.45.

4. Calculation - The resin content (wt%) of the glass/resin composite was calculated from

$$\text{Resin content} = \frac{W_a - W_g}{W_a} (100)$$

where

W_a = weight of glass/resin composite specimen in air, g

W_g = weight of glass after resin burnout, g

The void content (vol%) of the glass/resin composite was calculated from

$$\text{Voids} = \left[1 - \frac{SG_a}{W_a} \left(\frac{W_r}{SG_r} + \frac{W_g}{SG_g} \right) \right] (100)$$

where

SG_a = specific gravity of glass/resin composite

SG_g = specific gravity of glass = 2.45

SG_r = specific gravity of resin

W_r = weight of resin in composite specimen, g

III. TASK III - EVALUATION OF CANDIDATE CRYOGENIC RESINS AS FWC SPECIMENS*

A. TENSILE STRENGTH AT FRACTURE, ELONGATION AT FRACTURE, AND MODULUS OF ELASTICITY OF GLASS/RESIN COMPOSITES

The tensile properties of glass-FWC materials prepared with alternate filament orientations were determined by the method described below.

1. Apparatus - Laboratory filament-winding machine, 18-in.-dia winding mandrel, routing fixture (Figure A-1), clamp fixture (Figure A-2), No. 600 sandpaper, tensile-test machine, cryostat facility, extensometer.

2. Specimen Preparation - Various steps in specimen preparation are considered individually below.

a. Mixing of Resin 2 - Empol 1040 (80 g) and DSA (463.6 g) were mixed at ambient temperature and Epon 828 (400 g), preheated to 150°F, was added. The mixture was cooled to room temperature and 4.0 g of BDMA was added, with stirring.

b. Mixing of Resin 4A - Adiprene L-100 (200 g) and Epon 871 (60 g) were heated separately to 150°F and were then mixed. Epon 826 (140 g) was heated to 150°F and was stirred into the L-100/871 mixture. Molten MOCA (110.4 g) was added and the resulting solution was stirred until homogeneous. Because of the short pot life, four successively mixed batches of resin were required for each layer of winding.

c. Winding - A release film (Thalco 225) was applied to the mandrel of the winding machine. The roving was led through a resin bath and was wound directly over the film at a winding tension of 7 lb. With Resin 2, winding was performed at room temperature; with Resin 4A, the mix (temperature >150°F) was poured into a resin pot preheated to 150 to 170°F, and winding was begun promptly. Two heat lamps were trained on the revolving mandrel to keep the winding at 175 to 200°F and thus improve the resin flow and wetting properties.

Four separate layers of glass were prepared (54 by 20 in.) for each resin and filament-orientation pattern.

* Methods for the determination of (1) interlaminar shear strength (NOL horizontal shear), and (2) resin and void content are described in Sections II,C and H, respectively.

d. Filament-Orientation Patterns - Three different patterns of filament orientation were used for each resin system (Figure A-15): (a) unidirectional, 1:0 longitudinal-to-transverse filament ratio, (b) bidirectional, 1:1 longitudinal-to-transverse filament ratio, and (c) bidirectional, 1:2 longitudinal-to-transverse filament ratio.

e. Layup and Cure - Each 5 $\frac{1}{4}$ by 20-in. layer was cut into three equal pieces, approximately 18 in. square. The resulting 12-ply laminates were sandwiched between two layers of burlap (alternating orientation) and three layers of Dacron bleeder cloth on a Teflon-coated steel plate. (For the unidirectional laminate, cross plies of 181-glass cloth were placed between every third layer to reinforce the grip sections of the test specimens and prevent failure in these areas.) The laminate was fitted with a thermocouple in contact with the panel, was placed in a vacuum bag, and was cured on the following day according to the appropriate schedule (Resin 2: 2 hours at 150°F and 4 hours at 300°F, Resin 4A: 5 hours at 285°F). For the Resin 4A panels, the vacuum bag also contained calcium sulfate drying agent.

f. Post-cure Handling - After curing, the panels were cut and routed to a tapered-end specimen configuration (Figure A-5). The specimens were carefully sanded with No. 600 sandpaper to provide a uniform surface and thereby reduce data scatter.

3. Test Procedure and Calculation - See Section I,B,1, above.

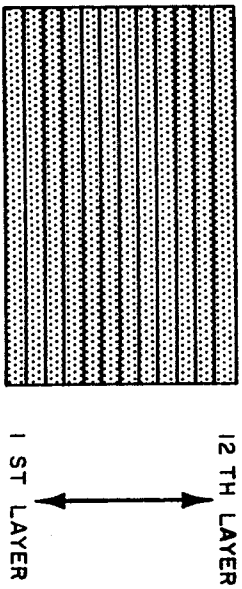
B. THERMAL-SHOCK RESISTANCE OF GLASS/RESIN COMPOSITES

Glass-FWC specimens in the form of arc segments from an NOL ring were tested in interlaminar shear after being cycled between room temperature and -423°F.

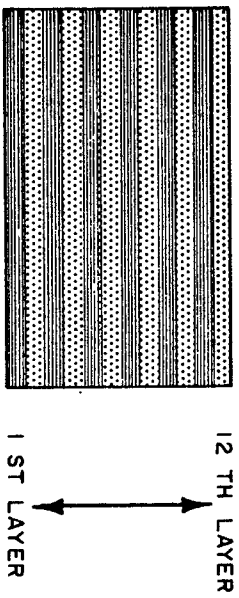
1. Apparatus - LH₂ Dewar flask, 2000-ml beaker, NOL-ring winding machine, tension-measuring device, NOL-ring winding mandrel, curing oven, interlaminar-shear test fixture (Figure A-14), tensile-test machine.

2. Specimen Preparation - The test specimen was a short beam in the form of an arc segment cut from an NOL ring. As finished, it was 0.250 in. wide, 0.635 in. long, and 0.125 in. thick. For Resin 2, Epon 828 (200 g) and Empol 1040 (40 g) were heated separately to 212°F and were then mixed. With stirring, DSA (231.8 g) and BDMA (2.0 g) were added; the mixture was stirred until homogeneous. Resin 4A was mixed in the manner described in paragraph III,A,2,a, foregoing.

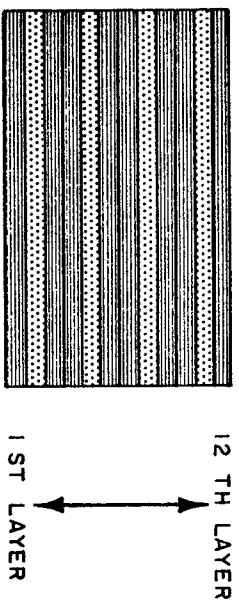
The NOL-ring winding machine was used to pass the roving through a dip tank containing the resin system. The roving was then wound directly (64 turns, 15 \pm 2 lb tension) on the mandrel, which had been pretreated with Thalco 225 mold release. The mandrel was held at approximately 150°F during winding. With a thermocouple as a temperature monitor, the rings were cured according to the individual-resin requirements (see paragraph III,A,2,e, foregoing). They were then removed from the winding fixture and were routed



Unidirectional (1:0)



Bidirectional (1:1)



Bidirectional (1:2)

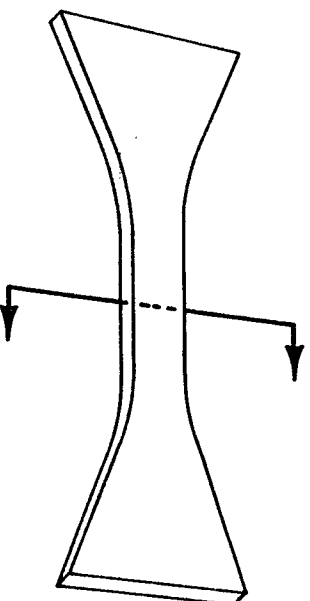


Figure A-15. Filament-Pattern Orientations for Tensile-Strength Specimens

to a thickness of approximately 0.125 in. Excess resin was removed from the rings with No. 280 sandpaper. The required arc segments were cut from each ring, with the width and thickness measured to the nearest 0.001 in.

3. Procedure - The specimens were immersed for 15 min in a Dewar flask filled with LH_2 . They were then removed and placed in a 2000-ml beaker of water at room temperature. After 15 min, they were removed from the water, were dried with compressed air, and were inspected visually for signs of thermal cracking. The test procedure was repeated for a total of five cycles.

Upon completion of temperature cycling, the specimens were mounted in the interlaminar-shear test fixture (Figure A-14) for testing in LH_2 . The specimen was aligned between the loading nose and supports, and was center-loaded on the convex side. The crosshead travel rate was 0.05 in./min, and the specimens were stressed to failure. The interlaminar-shear-strength values obtained as described below were compared with noncycled -423°F data to determine the extent of degradation of the resin-to-glass bond caused by thermal cycling.

4. Calculation - The interlaminar shear strength (horizontal-shear method) was calculated from

$$S = \frac{3 p}{4 b d}$$

where

S = interlaminar shear strength, psi

p = maximum load at failure, psi

b = specimen width, in.

d = specimen thickness, in.

C. COEFFICIENT OF LINEAR THERMAL CONTRACTION OF GLASS/RESIN COMPOSITES

The linear thermal contraction of glass-FWC specimens with unidirectionally oriented filaments was determined from measurements made parallel and transverse to the direction of the filaments.

1. Apparatus - Filament-winding machine, tension-measuring device, flat mandrels, air-circulating oven, fused-quartz dilatometer, micrometer, thermocouple, brush.

2. Specimen Preparation - Various steps in preparation are considered separately below.

a. Mixing of Resins - The two resins were mixed as described in paragraph III,A,2,a, above.

b. Winding - For Resin 2, the winding fixture was used to pass the roving through a dip tank containing the resin and wind it as unidirectional side-by-side filaments on a released 6 by 8-in. flat mandrel (roving tension, 13 lb). Each side of the mandrel had 50 plies (a number later found to be excessive).

A resin tank was not used for Resin 4A; instead, the mix was brush-coated directly on the mandrel. A layer of roving (tension, 12 lb) was wound over the mandrel and additional resin was brushed on. This alternate brushing/winding procedure was continued for 32 plies on each side of the mandrel. A heat gun, trained on the winding, maintained a temperature of approximately 150°F. The resin was held in a 150°F oven during winding, except when it was actually being applied.

It was not possible with either resin to complete the winding in a single day. The partially wound mandrels were removed from the machine and were enclosed in an air-tight cellophane bag that contained calcium sulfate drying agent. On the following day a fresh batch of resin was prepared and the winding was completed. (The resin on the No. 2 panel from the previous day was still workable; that on the No. 4A panel was thick, but blended smoothly into the new batch of resin when the latter was applied.)

c. Layup and Cure - Adjacent to each side of the mandrel-containing panels were placed four layers of Dacron bleeder cloth; each outer layer of Dacron was backed by a 1-in. layer of burlap that had been wrapped in 181-glass cloth. The resulting sandwich was placed on a Teflon-coated steel plate and was fitted with a thermocouple in contact with the panel. The assembly was placed in a vacuum bag and was cured in accordance with the required schedule (see paragraph III,A,2,e, above).

After the cure, the panels were cut and sanded into rectangular beam specimens 2 in. long by 0.35 in. square. Six specimens were prepared for each system, three for testing in the longitudinal direction (parallel to the filament orientation) and three for testing in the transverse direction (normal to the filament orientation). With a 1/16-in. bit, a hole was drilled halfway through the center of each specimen (normal to the length) for attachment of a copper-constantan thermocouple wire. The latter was potted in the specimen with Shell 911F adhesive.

3. Test Procedure and Calculation - See paragraphs II,D,3 and 4, foregoing.

D. INTERLAMINAR SHEAR STRENGTH OF GLASS/RESIN COMPOSITES (HORIZONTAL-SHEAR METHOD)

The interlaminar shear strengths of unidirectional glass-FWC specimens were determined by the horizontal-shear method at +75, -320, and -423°F.

1. Apparatus - NOL-ring winding machine, tension-measuring device, NOL-ring winding mandrel, air-circulating curing oven, test fixture (Figure A-12), tensile-test machine, cryostat facility.

2. Specimen Preparation - Test specimens were prepared as described in Section III,B, foregoing.

3. Test Procedure and Calculation - See paragraphs II,C,3 and 4, above.

APPENDIX B

PREVIOUS AEROJET STUDIES OF GLASS-FILAMENT/RESIN INTERACTION*

The studies summarized in this appendix were made at ambient temperature. They employed 4-in.-dia FWC vessels designed to fail in the heads, because the resin has more influence on the structural integrity of the heads than on the cylindrical section. Vessels were fabricated using three different types of glass filaments and ten different resin formulations. The rovings selected to provide variation in physical properties of the primary structural constituent were Owens-Corning S-994 glass/HTS finish, E-glass/HTS finish, and YM-31A. Four distinct resin systems (epoxy-fatty acid, epoxy-amine, polyester, and epoxy-anhydride) were chosen, and resin ultimate elongation was the basic criterion used in selecting the ten formulations that were developed.

Table B-1 summarizes the characteristics of the resin systems. Formulation variations to produce changes in ultimate elongation had considerable effects on other physical properties; the changes in physical properties did not vary in the same pattern for the four basic systems.

Vessel-hydroburst data were used to calculate longitudinal filament stresses shown in Figure B-1. The values are averages for all specimens of each type of resin, regardless of the change within the resin. The data indicate that the resin significantly influences the stress attained by the filaments. A review of these data also indicates the following influences on pressure-vessel performance:

<u>Kinds of Changes</u>	<u>% of Change in Pressure-Vessel Performance</u>
In glass type	37
In resin type	23
Within a resin type	6 to 17

Linear-regression analyses of 4-in.-dia-specimen data showed that the most important individual physical properties and characteristics of material contributing to the longitudinal filament stress attained in the structure were as follows:

* Derived from the following papers: F. J. Darms, "Glass-Resin Interaction," Fifth Polaris Glass Reinforced Plastic Research and Development Conference, Palo Alto, California, January 1964; Darms, "Glass-Resin Interaction," American Chemical Society Symposium on Chemistry of Matrices Used in Filament Winding, Chicago, September 1964; and O. Weingart, "Development of Improved Process for Filament-Wound Reinforced Plastic Structures," Society of Plastics Industry Conference, Chicago, February 1965.

TABLE B-1

FORMULATIONS AND PHYSICAL PROPERTIES OF RESIN SYSTEMS USED IN 4-IN.-DIA VESSELS*

Resin System (Parts by Weight)	Elon- ga- tion %	UTS ksi	Elastic Modulus ksi	NT	Tough- ness psi	Shear Modulus ksi	Pois- son's Ratio	$\Delta L/L \Delta t^*$	Hardness		
									Shore D Scale	Rockwell	
										M Scale	R Scale
Epoxy-Fatty Acid											
EP 201/Empol 1022/ stannous octoate											
(100/35/1.5)	6.2	6.594	267.0	442	295.1	92.7	0.439	43.5	83	82	122
(100/39/1.5)	15.3	3.366	187.0	401	400.5	48.1	0.467	16.7	81	89	124
(100/41/1.5)	25.2	3.405	163.4	354	664.6	55.5	0.472	44.5	82	92	125
Epoxy-Amine											
DER-322/Epi-Cure 855											
(100/30)	6.6	8.225	334.2	345	420.3	116.6	0.433	51.9	85	93	126
(100/60)	10.5	6.520	260.3	1497	543.7	90.3	0.446	70.1	80	63	118
(100/85)	24.9	4.955	207.6	921	958.0	71.3	0.456	93.2	74	56	106
(100/100)	58.4	2.150	86.9	418	982.9	29.3	0.482	68.8	58	10	38
Polyester											
P43/MEKP											
(100/2)	6.2	5.387	250.4	361	240.4	85.9	0.459	78.2	74	53	84
P43/P13/MEKP											
(50/50/4)	18.6	2.003	57.4	348	276.5	19.3	0.489	47.9	86	92	123
(40/60/4)	30.5	1.757	38.2	355	380.1	12.8	0.493	41.1	79	65	101
Epoxy-Anhydride											
Epon 828/Epon 1031/ MNA/BDMA (Shell 58-68R)											
(50/50/90/0.5)	3.0	11.831	479.7	377	198.3	165.4	0.401	43.9	90	113	128

* UTS = ultimate tensile strength. NT = notch toughness, psi $\sqrt{\text{in.}}$. $\Delta L/L \Delta t$ = coefficient of linear expansion, in./in./°F.

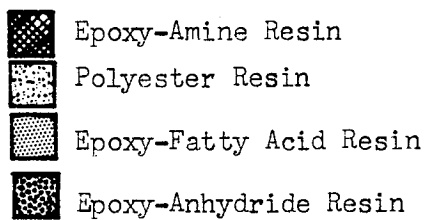
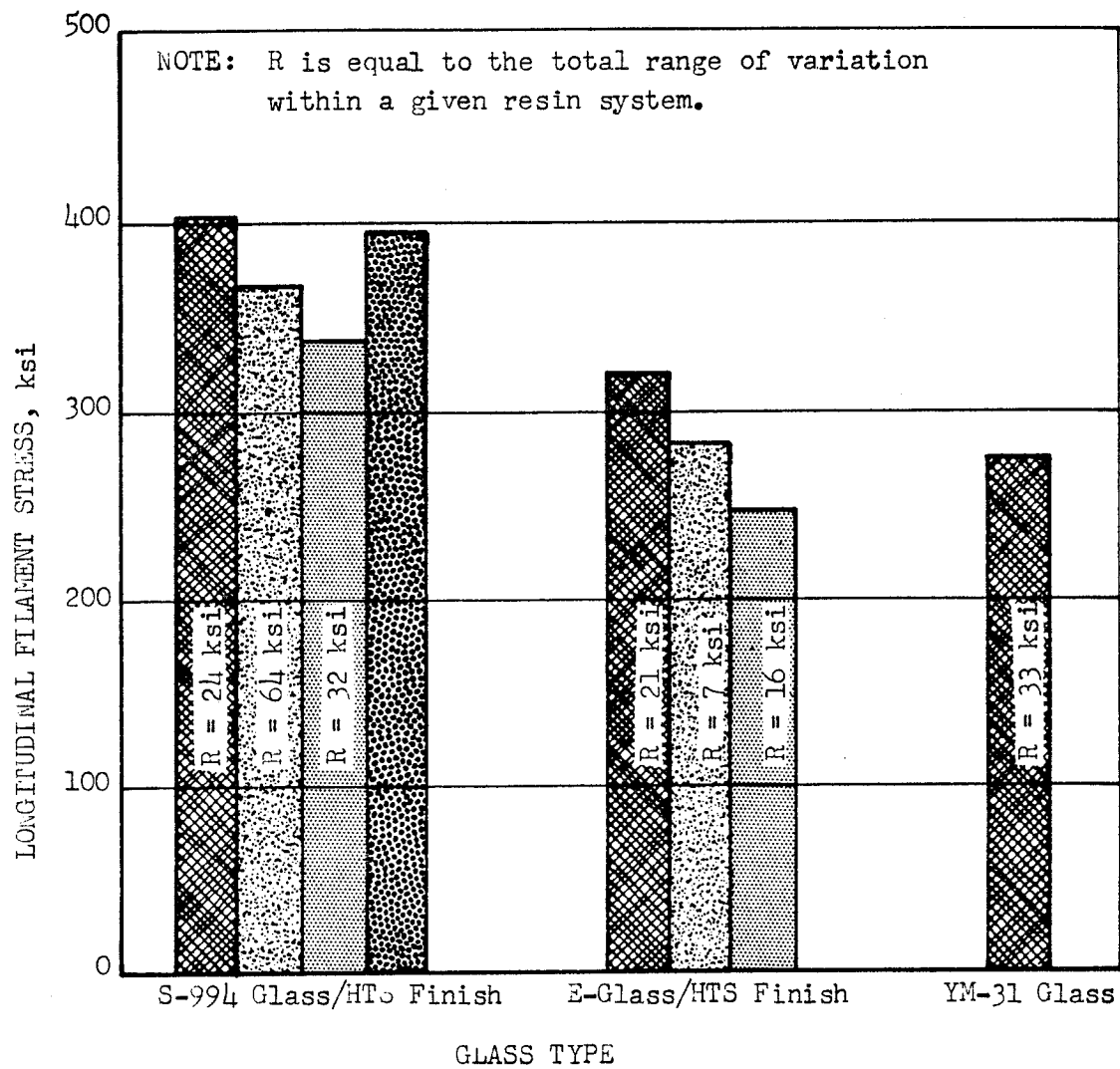


Figure B-1. Filament Stress vs Glass and Resin Types for 4-in.-dia Test Vessels

<u>Component</u>	<u>Property</u>	<u>Contribution, %</u>
Glass fiber	Ultimate tensile strength	62
Resin	Notch toughness	15
Composite	Resin content (volume)	6
Resin	Tensile strength at fracture	2
Resin	Ultimate elongation at fracture	2
Resin	Toughness (area under stress-strain curve)	1

When the cross products of properties from all the resin systems were used in the linear-regression analysis and when the resin content was neglected, the most significant resin properties were ranked as follows:

1. Notch toughness x tensile strength at fracture
2. Tensile strength at fracture
3. Elongation x notch toughness
4. Toughness
5. Tensile strength at fracture x toughness.

An analysis of property data for the epoxy-amine system rated notch toughness times tensile strength at fracture as the primary resin characteristic. Figure B-2 shows the compliance of hydroburst-specimen data to the single factor of tensile strength times notch toughness. The maximum variation of data from predicted values was 2.3%.

Another series of tests were conducted with 4-in.-dia vessels fabricated of S-994 glass/HTS-finish 20-end roving and designed to fail in the hoop filaments. The resin formulations used in the study and their properties are summarized in Table B-2; the values are averages of three to ten tests.

Statistical analysis of the burst-strength data showed that nearly all the measured cast-resin-specimen properties have strong correlations with 4-in.-dia-vessel burst strength. The hoop-filament strength of the vessels correlated positively with resin toughness and elongation, and negatively with the other resin properties. The order of presentation from top to bottom in Table B-2 was based primarily on data from the 4-in.-dia burst tests.

Figure B-3 plots points and lines of regression for 4-in.-dia-vessel burst pressures and resin properties. Figure B-4 shows lines of regression for the relationships between various resin properties. In general tensile strength, modulus, shear strength, and specific gravity decreased as elongation and toughness increased.

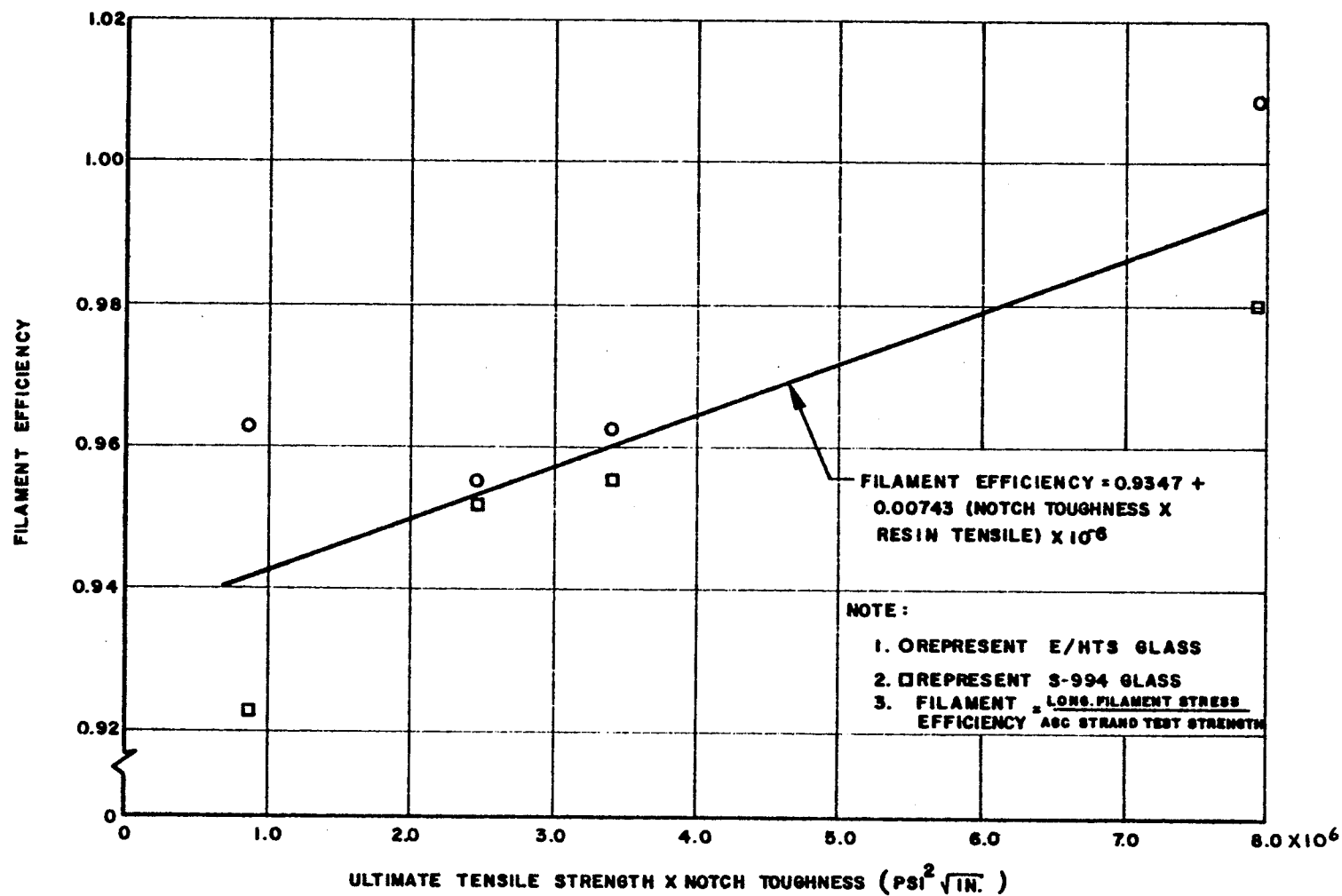


Figure B-2. Filament Efficiency vs Ultimate Tensile Strength Times Notch Toughness, 4-in.-dia Specimens Incorporating Epoxy-Amine Resin Systems

TABLE B-2

SUMMARY OF COMPOSITE AND RESIN PROPERTIES

Resin System	Properties Using S-994 Roving										Resin Properties								
	4-in.-dia Bottles (Av of 5 Tests)										NOL Rings (Av of 5 Rings)								
	Burst Press. psig	Stress, ksi				Resin wt%	Ultimate Stress, ksi				Shear (Av)		Cast-Resin Specific Gravity (Av for 3 Tests)	Mechanical					
		Longitudinal		Hoop			Composite	Fiber	wt%	vol%	No. of Specimens	Stress psi		Tensile Stress psi	Young's** Modulus psi x 10 ³	Elongation, %			
		Fiber	Composite*	Fiber	Composite*											At Ultimate Load	At Fracture	Toughness in.-lb/in. ³	
DER-332/Epi-Cure 855 (20%) (100/90 phr)	4710	403.9	226.2	437.7	163.0	25.19	262.9	344.1	87.2	76.4	10	4,975	1.10	2,841	184.4	4.2	43.0	1008	
DER-332/Epi-Cure 855 (100/34 phr)	4510	394.4	248.0	430.4	179.4	20.74	301.6	394.8	87.2	76.4	5	6,970	1.15	7,903	311.4	4.1	8.0	496	
ERL-2772/ZZL-0803 (100/37.5 phr)	4560	392.0	217.5	428.9	157.7	25.64	312.0	413.8	86.6	75.4	10	8,652	1.18	8,217	441.1	3.1	7.2	446	
DER-332/HHPA/BDMA (100/84/0.5 phr)	4490	383.5	229.9	421.1	167.1	22.16	278.4	366.8	87.9	75.9	6	9,212	1.21	12,350	457.4	6.0	6.0	533	
Epon 1031/Epon 828/MNA/DP-128 (50/50/90/0.5 phr)	4415	379.2	201.2	411.2	145.1	27.61	281.0	388.7	84.5	72.3	10	9,522	1.24	9,897	465.9	2.5	2.5	134	
Shell ERX-36/MPDA (100/14 phr)	4385	378.5	225.4	408.0	156.9	22.46	306.3	409.5	86.2	74.8	10	10,023	1.18	12,230	509.2	4.2	4.2	352	
ERLA-2256/ZZL-0820 (100/25 phr)***	4317	371.0	230.4	403.5	166.6	20.50	308.5	400.6	87.6	77.0	5	9,546	1.23	13,014	666.5	2.5	2.5	187	
Epon 828/Epon 1031/MNA/BDMA (Shell 58-68R) (50/50/90/0.5 phr)****	4425	380.8	211.9	411.8	152.3	25.52	280.1	391.2	84.1	71.6	10	10,157	1.25	9,142	506.7	2.0	2.0	98	
RDGE/DADPS (100/49.5 phr)****	4400	378.2	231.1	413.8	167.6	21.29	284.4	388.5	85.1	73.2	10	12,137	1.34	14,918	528.2	3.8	3.8	378	
DEN-438/MNA/BDMA (100/90/0.5 phr)	4010	344.4	204.5	374.8	147.8	22.60	295.2	406.6	84.8	72.6	10	9,725	1.25	8,322	463.7	2.0	2.0	96	

* Longitudinal based on longitudinal-composite thickness only. Hoop based on cylinder-wall thickness (girth stress).

** Initial tangent modulus. *** Average of three tests. **** Average of four tests.

B-6-1

B-6-2

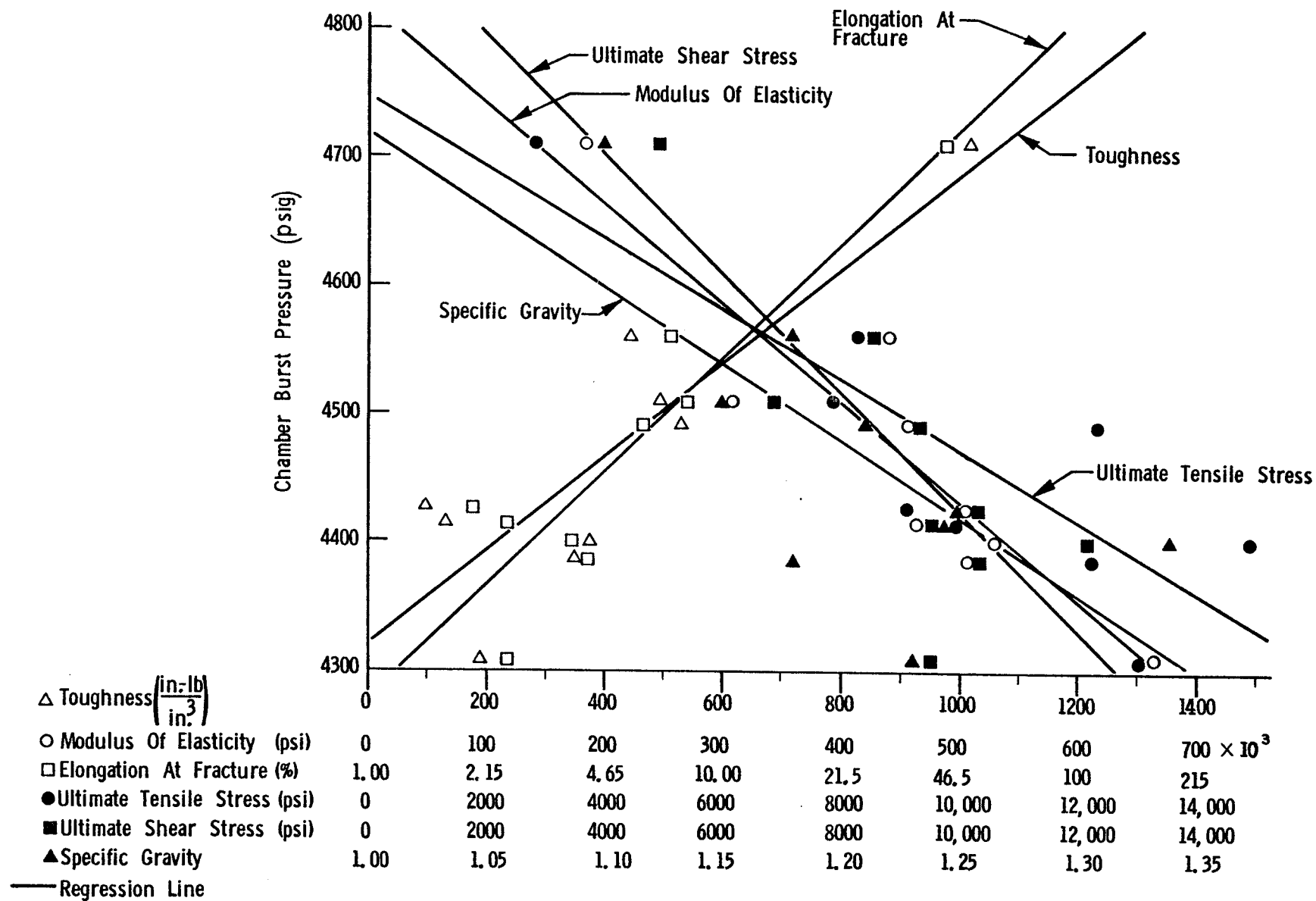


Figure B-3. Vessel Burst Pressure vs Cast-Resin Properties

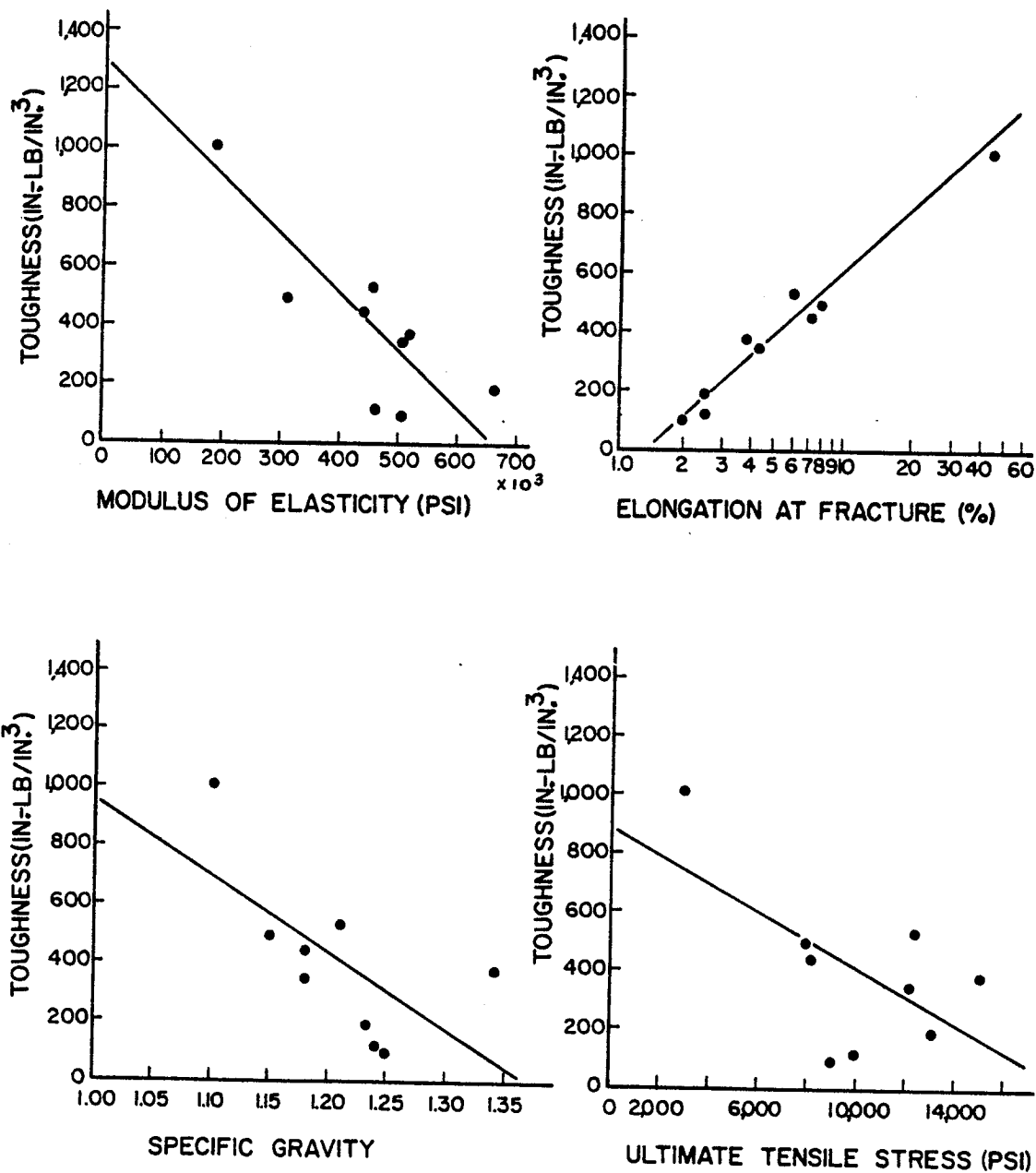


Figure B-4 (1 of 4). Correlations of Cast-Resin Properties

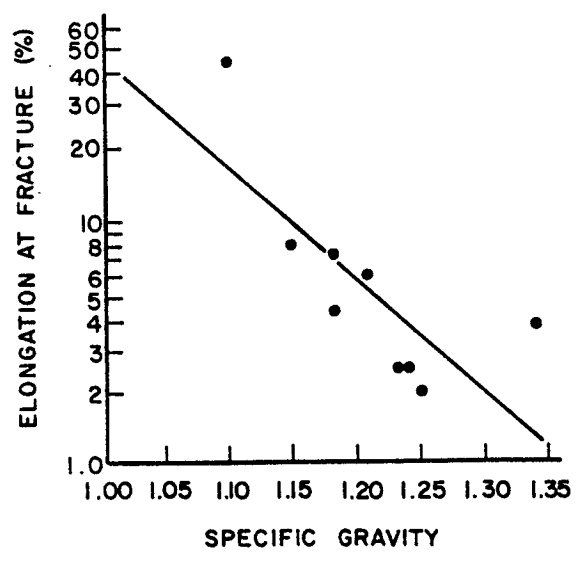
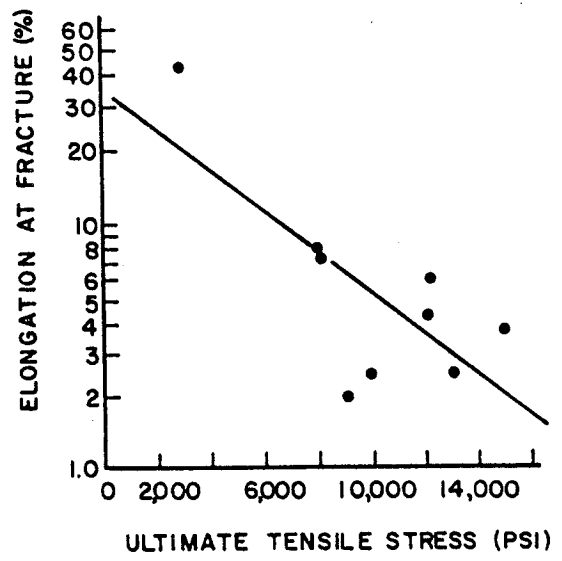
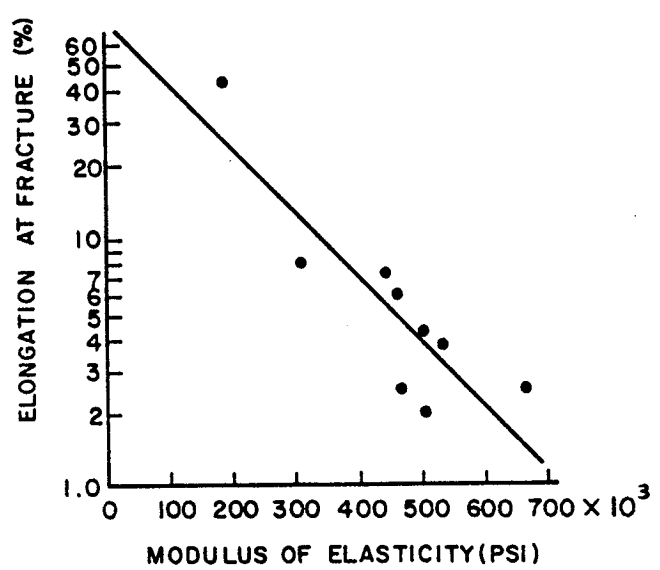
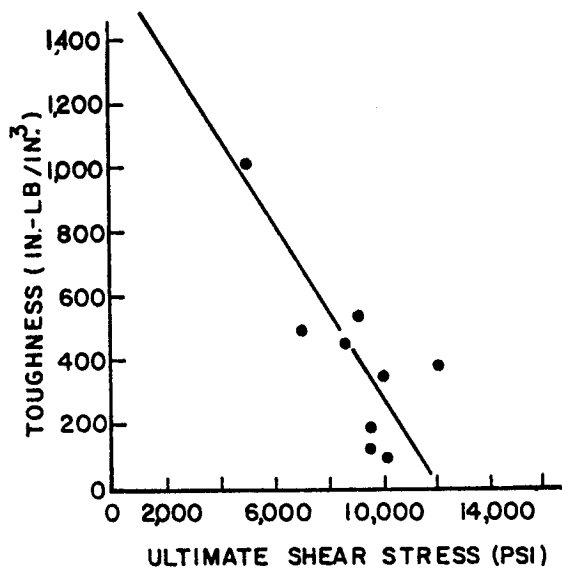


Figure B-4 (2 of 4). Correlations of Cast-Resin Properties

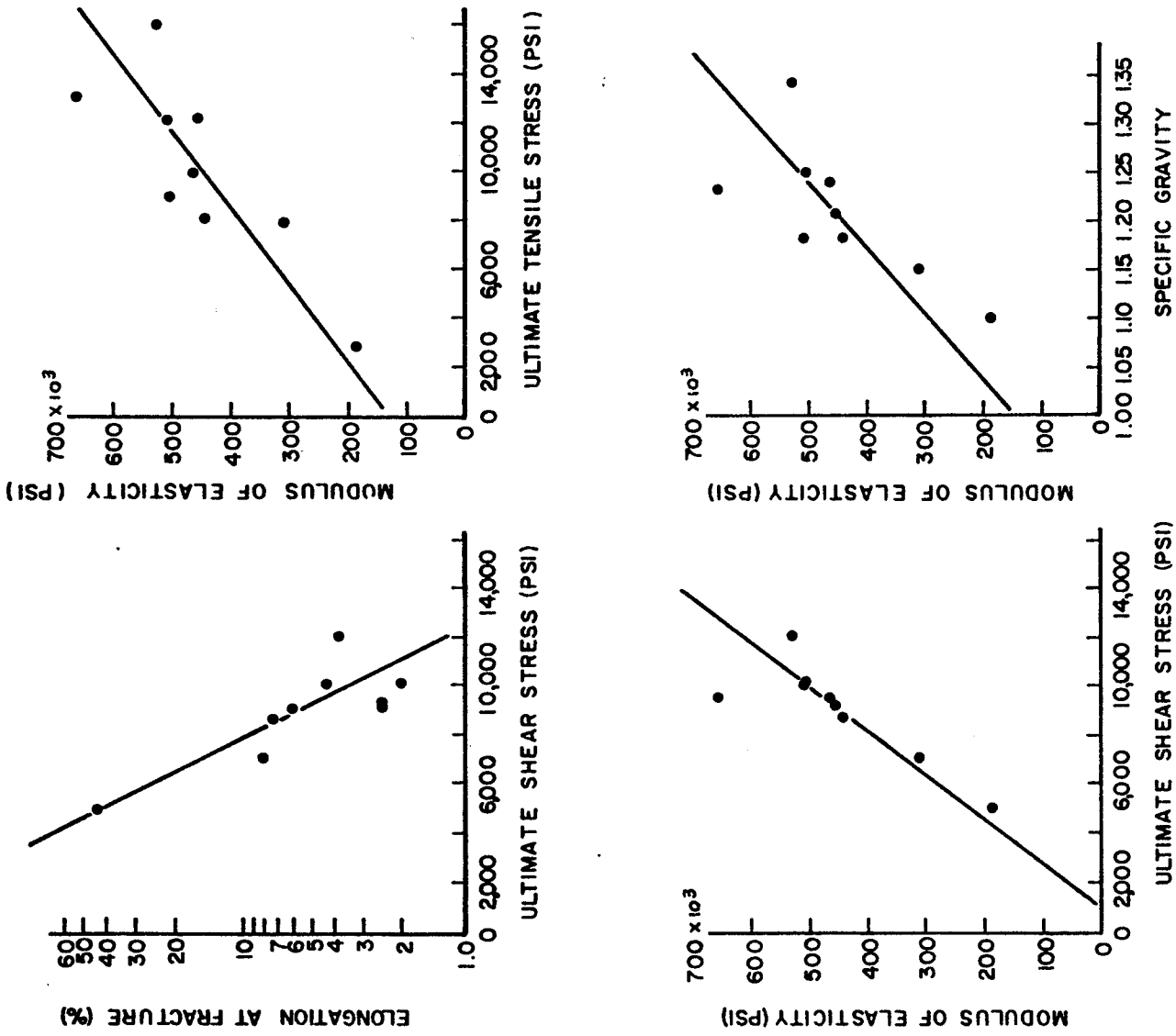


Figure B-4 (3 of 4). Correlations of Cast-Resin Properties

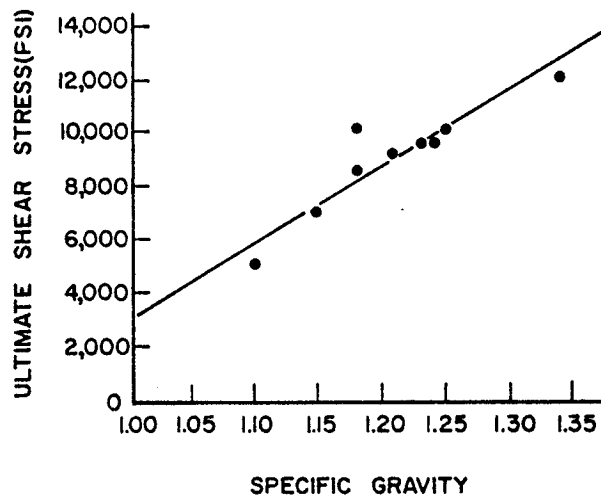
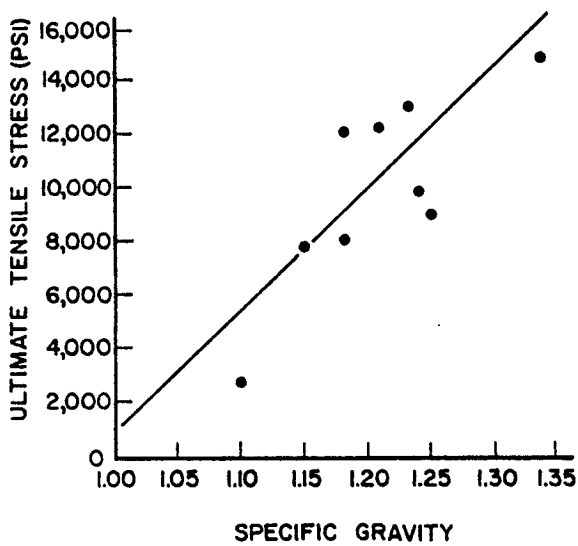
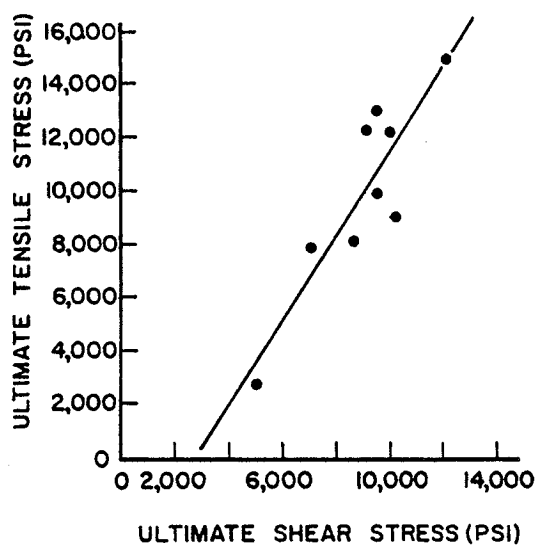


Figure B-4 (4 of 4). Correlations of Cast-Resin Properties

The correlations do not necessarily imply causal relationships - i.e., lower tensile strengths do not necessarily cause high burst strengths; they merely correlate with high burst strengths. It is possible that some other resin property, such as high shear modulus or high toughness, is actually responsible for high burst pressures, and that low tensile strength merely happens to be inherent in a resin that has high burst pressures.

Analysis of the physical properties of the resins used indicates that the various resin properties are not independent - e.g., it may not be possible to formulate a resin that has both high elongation and high Young's modulus.

The correlations between resin properties and glass-filament strength in NOL rings and 4-in.-dia vessels were studied, and Figure B-5 shows correlations of NOL-ring tensile strength and cast-resin properties.

The NOL-ring filament strengths did not correlate as well with the cast-resin properties as did the 4-in.-dia-vessel strengths. When weak NOL-ring correlations were found, they were all opposite in sign to those for 4-in.-dia vessels. It therefore appears that the NOL ring is less sensitive to resin properties than the 4-in.-dia vessels and that NOL-ring response to these properties is different. As the resins became tougher and more flexible, the vessel strength increased. On the other hand, NOL-ring filament stress tended to increase as the resins became stronger and more brittle, although the correlation was poor.

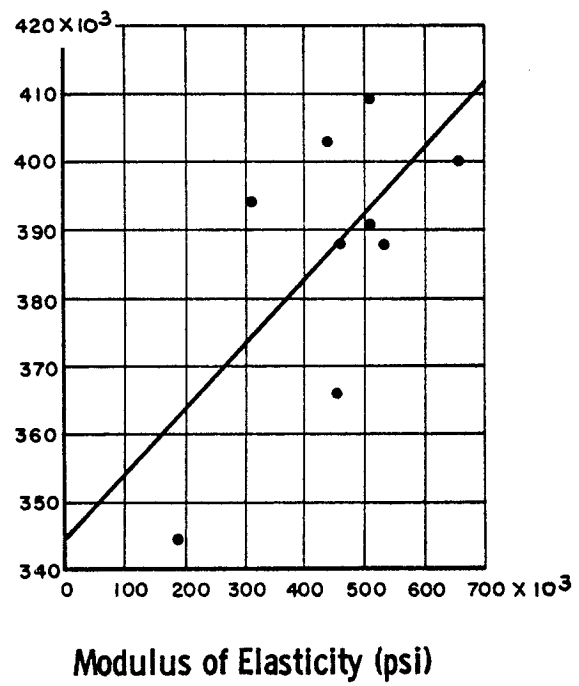
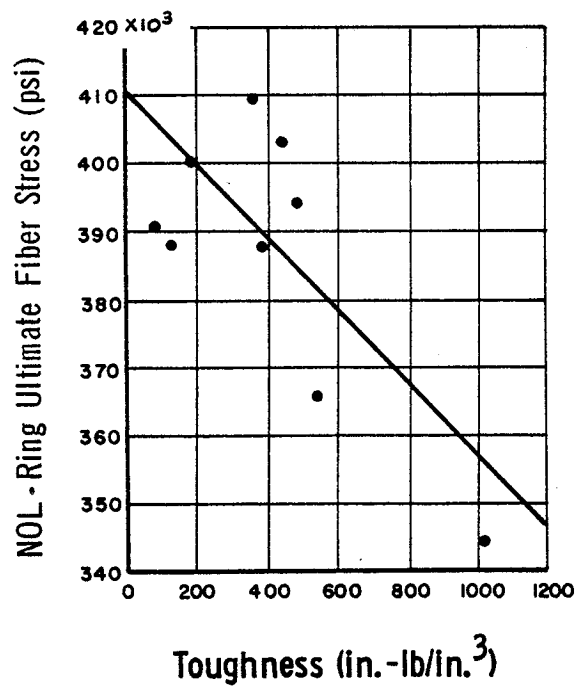
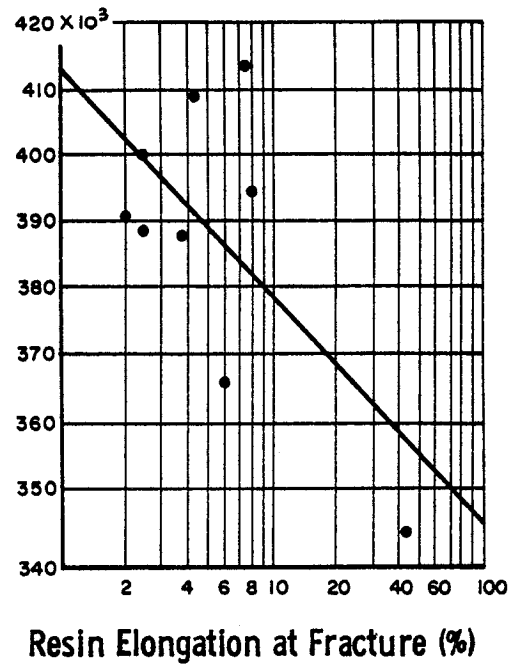
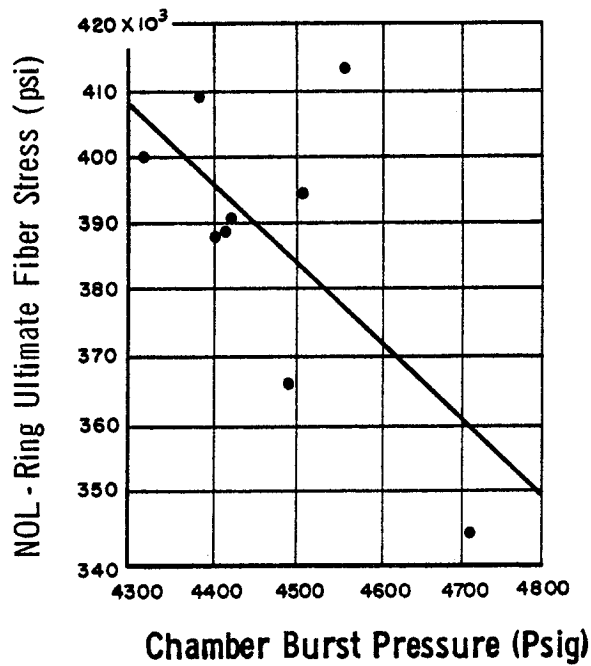
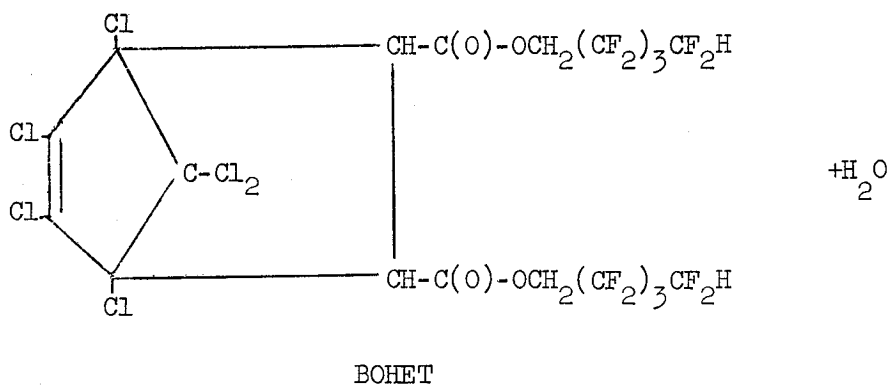
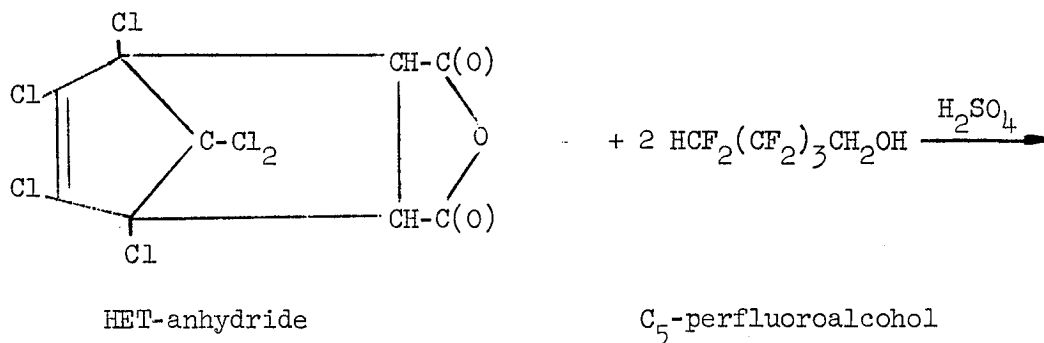


Figure B-5. Correlations of NOL-Ring Ultimate Fiber Stress

APPENDIX C

PREPARATION OF BOHET

BOHET, or HET-acid bis(octafluoropentyl)ester, was prepared on a 1-lb scale as follows:



To a 3-liter, 3-neck flask fitted with a reflux condenser, drying tube, and Stark-Dean trap, and containing 1320 ml of benzene, was added HET-anhydride (288.0 g, 0.78 mole), C₅-perfluoroalcohol (270.4 ml, 1.94 moles) and concentrated sulfuric acid (10.4 ml). The solution was refluxed, with stirring (magnetic stirrer), until a maximum amount of H₂O was collected (17 ml, 11 days). Benzene was removed, first at the water pump and then by hard vacuum. The crude product was taken up in 1200 ml of methylene chloride, and the solution was divided into two parts. Each part was washed successively with two 800-ml portions of 0.5-N Na₂CO₃ solution and two 2000-ml portions of 1% NaCl solution. After drying over Na₂SO₄ for 16 hours, the solutions were filtered and stripped of solvent. Distillation in a short-path apparatus afforded 456 g of BOHET, b.p. 152-154°C (10 microns), yield 72%; saponification equivalent weight 403.9 (theory 408.4).

A second preparation provided 556 g of BOHET, b.p. 148-149°C (5 microns), yield 87.6%; saponification equivalent weight 408.7 (theory 408.4).

APPENDIX D

SOLVENTS FOR EPOXY/POLYURETHANE SYSTEMS

Resin 4 was found to have excellent low-temperature mechanical properties, but a relatively high viscosity and short pot life at room temperature and above. Nevertheless, if a suitable solvent were available, the system might still be considered for use in prepreg. It was found, by the procedure described below, that both acetone and MEK (methyl ethyl ketone) were suitable solvents for the formulation.

Adiprene L-100 (50 g) was added to a beaker containing 150 ml of solvent (either acetone or MEK). Complete solution was obtained after 5 min of rapid stirring. MOCA (21.15 g) was pulverized with a mortar and pestle, and added to the stirred solution over a period of 5 to 10 min. When the MOCA was completely dissolved, Epon 828 (35 g) and Epon 871 (15 g) were added separately, and the mixture was stirred until homogeneous. No separation from the solution occurred on overnight standing.

A similar study was carried out for Resin 4A in order to determine the amount of solvent required to give a workable mix for the fabrication of NOL rings and other glass/resin laminates.

The mixing procedure was as follows: Adiprene L-100 (50 g) was added to 50 ml of MEK, with vigorous stirring. MOCA (27.6 g) was pulverized and added to the stirred solution; after 30 min the MOCA was completely dissolved. Epon 826 (35 g) and Epon 871 (15 g) were stirred into the solution.

Measurements taken with a Zahn No. 5 cup gave a viscosity (at room temperature) of 200 cp when freshly mixed, and 400 cp after standing for 1 hour.

APPENDIX E

CALCULATION OF FILAMENT AND COMPOSITE TENSILE STRESS IN COMPOSITE-TEST SPECIMENS

In analyzing a filament-wound pressure vessel, as well as in analyzing the tapered-end test specimens employed in this program, the assumption was made that the glass filaments are the primary structural material and therefore carry all the load.

A method based on the total glass fibers oriented in the direction of loading was used in determining the filament stress; modification of filament stress by the resin content yields composite stress. To determine these stress levels, an equivalent filament thickness was first calculated from the specific amount of glass roving laid in the test-specimen gage area during winding. This method was used in order to (1) provide a proper basis for comparison of data with regard to filament orientation and resin content, and (2) minimize differences in fabrication-processing effects (resin and void contents, vacuum-bagging techniques, etc.). In this manner, the filament-wound composite test specimens were analyzed on the basis of actual winding data and laboratory tests, thus eliminating the effects of differences in specimen thicknesses caused by nonuniform resin contents or unequal vacuum pressures on the test panels. This calculated equivalent filament thickness is given by

$$t_f = A_e N_1 N_2 N_3 N_4$$

where

A_e = area of single end, sq in.

N_1 = number of ends per strand

N_2 = number of strands per turn

N_3 = number of turns per inch per layer

N_4 = number of layers in test specimen

Therefore,

$$t_f = (21.0 \times 10^{-6})(20)(1)(11.5)(12) = 0.058 \text{ in.}$$

Filament stress was determined by the ratio of load to area, factored by the fraction of filament layers oriented in the direction of loading. The lead of the winding machine and the width of the roving create an angular difference between the filament orientation and the direction of loading, but one so small that it may be ignored in the calculations:

$$\sigma_f = \frac{P}{t_f w} \left(\frac{N_4}{N_5} \right)$$

where

σ_f = ultimate filament stress, psi

P = ultimate load, lb

w = test-specimen width, in.

N_5 = actual layers oriented in direction of load

For composite stress,

$$\sigma_c = \frac{P}{t_c w} = \frac{P}{t_f w} \frac{V_g}{100}$$

where

σ_c = ultimate composite stress, psi

t_c = total equivalent composite thickness = $\frac{t_f}{V_g/100}$

V_g = amount of glass filament in composite, vol% (see Figure E-1)

Examples of the calculations follow. For a filament orientation of 1:2,

$$\sigma_f = \frac{4340}{(0.058)(0.407)} \left(\frac{12}{4} \right) = 551,500 \text{ psi}$$

$$\sigma_c = \frac{4340}{(0.058)(0.407)} (0.65) = 119,500 \text{ psi}$$

For a filament orientation of 1:1,

$$\sigma_f = \frac{5200}{(0.058)(0.402)} \left(\frac{12}{6} \right) = 446,000 \text{ psi}$$

$$\sigma_c = \frac{5200}{(0.058)(0.402)} (0.6875) = 153,300 \text{ psi}$$

For a filament orientation of 1:0,

$$\sigma_f = \frac{5080}{(0.058)(0.233)} \left(\frac{12}{12} \right) = 375,900 \text{ psi}$$

$$\sigma_c = \frac{5080}{(0.058)(0.233)} (0.6237) = 234,400 \text{ psi}$$

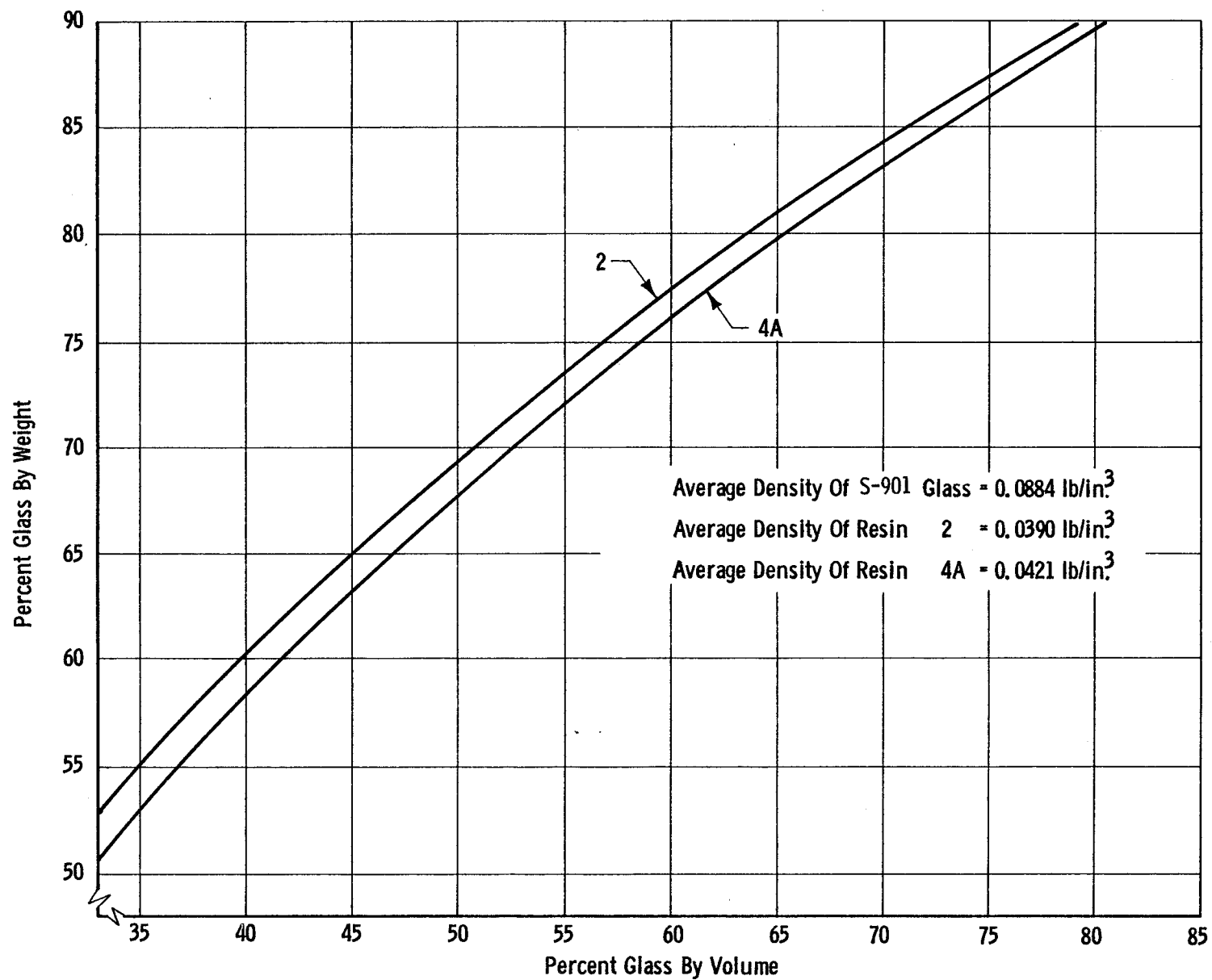


Figure E-1. Typical Physical Properties, Glass/Cryogenic-Resin Composites

APPENDIX F

DESIGN ANALYSIS, 8-IN.-DIA FILAMENT-WOUND PRESSURE VESSELS FOR CRYOGENIC-RESIN EVALUATION

The evaluation of Resin 2 in S-901 glass-FWC pressure vessels subjected to biaxial loading was undertaken in Task IV. This appendix summarizes the design and structural verification of various components of the 8-in.-dia cylindrical vessels employed.

Experience acquired in previous development efforts led to the selection of a closed-end, cylindrical, test vessel fabricated from longitudinally and circumferentially oriented filaments wound over a 0.006-in.-thick metal liner (Type 304 stainless steel). The composite structure was adhesively bonded to the liner to minimize compressive liner buckling. The vessel, approximately 8 in. in diameter by 13 in. long, was designed to achieve a 2.5% strain with a longitudinal-to-circumferential strain ratio of 1.

1. Design-Allowable Strength

Aerojet has developed a systematic approach to the design of filament-wound vessels and is using it in a number of applications. The method involves the use of pressure-vessel design factors, corresponding to a range of dimensional parameters, to determine the allowable design strength for each configuration. The factors are based on data collected over the past 6 years from Aerojet tests on several thousand pressure vessels, which ranged in diameter from 4 to 74 in. and had significant variations in their design parameters. Included as factors used for the selection of design-allowable values are the strength of the glass roving, resin content, envelope dimensions (length and diameter), internal pressure level, axial-port diameters, temperature, sustained-loading requirements, and cyclic-loading requirements. This method of analysis was used in the present program to establish realistic values for the allowable filament tensile strengths in the 8-in.-dia test vessel.

Because earlier investigations of glass/resin interaction in filament-wound pressure vessels had shown that the heads were more sensitive to the resin used than the cylindrical section, the test vessels were designed to fail in the longitudinal filaments of the heads. This allowable longitudinal-filament strength is given by

$$F_{f,1} = K_1 K_2 K_3 K_4 K_5 K_6 (\sec^2 \alpha) F_f^*$$

* From Structural Materials Handbook, Aerojet-General Corporation, Chemical and Structural Products Division, February 1964. These symbols are defined at the end of this appendix.

The following design factors* are based on the specific vessel parameters:

<u>Parameter</u>	<u>Design Factor</u>
$D_c = 7.789 \text{ in.}$	$K_1 = 0.83$
$D_b/D_c = 0.37$	$K_2 = 0.95$
$L/D_c = 1.58$	$K_3 = 1.00$
$t_{f,1}/D_c \approx 0.001$	$K_4 = 0.96$
$T = 75^\circ\text{F}$	$K_5 = 1.00$
$\eta = 3 \text{ min}$	$K_6 = 1.00$
$\alpha = 13^\circ$	

The single-pressure-cycle allowable ultimate filament strength is therefore

$$F_{f,1} = (0.83)(0.95)(1.00)(0.96)(1.00)(1.00)(1.053)(415,000) = 330,000 \text{ psi}$$

2. Determination of Design Burst Pressure

The design burst pressures of the vessel (1338 psi at $+75^\circ\text{F}$, 2087 psi at -320°F , and 1922 psi at -423°F) were established on the basis of (a) a longitudinal-composite thickness of 0.011 in., which is the approximate composite thickness resulting from the use of 12-end, S-901 glass roving, and (b) single-cycle design-allowable strengths for S-901 glass filaments of 330,000 psi at $+75^\circ\text{F}$, 495,000 psi at -320°F , and 445,000 psi at -423°F . These strengths were selected after a review of composite-property data indicating that the strength of glass laminates increases approximately 50% at -320°F and 35% at -423°F over the strengths at $+75^\circ\text{F}$. The dimensional coordinates of the pressure-vessel heads were established by the use of a computer program designed for metal-lined pressure vessels. The computer program, developed by Aerojet under Contract NAS 3-6292, also defined the filament and metal-shell stresses and strains at zero pressure and at the design pressure, the required hoop-wrap thickness for the cylindrical portion of the vessel, the filament-path length, and the weight and volume of the components and complete vessel.

Because of the limited biaxial data available on filament-wound vessels at cryogenic test temperatures, a conservative approach was taken in the design of specific metal components (bolts, bosses, etc.) by utilizing the highest

* Ibid.

Solving for N_4 ,

$$\begin{aligned}
 N_4 &= \frac{\pi D_c t_l P_{vg} \cos \alpha}{A_{end} N_1 N_2 N_3 N_5} \\
 &= \frac{\pi (7.789) (0.011) (0.67) (0.97437)}{(20.0 \times 10^{-6}) (12) (1) (2) (1)} \\
 &= 366 \text{ turns/revolution}
 \end{aligned}$$

b. Hoop

The cross-sectional area of hoop layers (A_h) is given by

$$\begin{aligned}
 A_h &= t_{f,h} L_c \\
 &= A_{end} N_1 N_2 N_6 N_7
 \end{aligned}$$

where

L_c = cylinder length = 7.28 in.

N_6 = number of tapes per layer

N_7 = number of layers = 4

$t_{f,h}$ = hoop-filament thickness, in. = $t_h P_{vg}$

t_h = hoop-composite thickness = 0.022 in.

Solving for N_6 ,

$$\begin{aligned}
 N_6 &= \frac{t_h P_{vg} L_c}{A_{end} N_1 N_2 N_7} \\
 &= \frac{(0.022) (0.67) (7.28)}{(20.0 \times 10^{-6}) (12) (1) (4)} \\
 &= 112 \text{ tapes/layer}
 \end{aligned}$$

4. Bolts

The load per bolt was calculated from

estimated burst pressure (2087 psi at -320°F) in conjunction with the lowest material strength (at +75°F).

3. Winding-Pattern Determination

The filament-wound vessel had two primary winding patterns: (a) a planar or end-for-end pattern designed to provide the total strength in the heads and longitudinal strength in the cylindrical section, and (b) a hoop pattern for circumferential strength in the cylindrical section.

The pattern developed for a pressure vessel requires the application of a specific quantity of glass in a predetermined orientation in order to obtain a desired burst pressure. The pattern is analyzed on the basis of actual winding data and laboratory tests of the glass roving and composite specimens. These data have shown that a cured single layer created by side-by-side orientation of S-901 12-end roving will produce an average composite thickness of approximately 0.0055 in. The minimum thickness for a cylindrical pressure vessel with meridional and circumferential filaments will therefore be 0.011 in. (one revolution of two layers) for the longitudinal composite and 0.022 in. (four layers) for the hoop composite. Assuming these thicknesses and using the value of 20.0×10^{-6} sq in. determined for the area of a single end of S-901 glass roving, the winding pattern for the 8-in.-dia vessel (Figure 31 of the main text) may be calculated as shown below.

a. Longitudinal

The cross-sectional area of longitudinal-filament layers (A_1) is given by

$$A_1 = \pi D_c t_{f,1}$$

$$= A_{\text{end}} N_1 N_2 N_3 N_4 N_5 \frac{1}{\cos \alpha}$$

where

D_c = chamber diameter at longitudinal neutral axis = 7.789 in.

A_{end} = area of single end = 20×10^{-6} sq in.

N_1 = number of ends per strand = 12

N_2 = number of strands per tape = 1

N_3 = number of tapes per turn = 2

N_4 = number of turns per revolution

N_5 = number of revolutions = 1

α = angle between filament and meridional direction = 13°

$t_{f,1}$ = longitudinal-filament thickness, in. = $t_1 P_{vg}$

t_1 = longitudinal-composite thickness = 0.011 in.

P_{vg} = amount of glass filament in composite, volume fraction = 0.67
(based on desired resin content of 19 wt%)

$$P = \frac{p_b \pi d^2}{4N}$$

where

P = load per bolt, lb

p_b = maximum design burst pressure = 2087 psi

d = bolt-circle diameter = 2.52 in.

N = number of bolts = 12

Therefore,

$$P = \frac{(2087) (\pi) (2.52)^2}{(4) (12)}$$

$$= 868 \text{ lb/bolt}$$

For MS 21279 bolts with a tensile strength of 130,000 psi (minimum), the ultimate tensile load per bolt (P_{tu}) is 2600 lb at ambient conditions. The margin of safety (M.S.) is given by

$$M.S. = \frac{P_{tu}}{P} - 1$$

Therefore,

$$M.S. = \frac{2600}{868} - 1 = + \underline{2.0}$$

5. Threads

The shear stress in the threads was determined from

$$\sigma_s = \frac{P}{\pi d_t (0.5 \ell)}$$

where

σ_s = shear stress, psi

d_t = thread diameter = 0.164 in.

ℓ = thread grip length = 0.25 in.

Therefore,

$$\sigma_s = \frac{868}{(\pi) (0.164) (0.5) (0.25)}$$

$$= 13,500 \text{ psi}$$

The ultimate tensile strength (F_{tu}) for Type 304 stainless steel (annealed) is 70,000 psi (minimum). Assuming that

$$F_{su} = \frac{F_{tu}}{2}$$

where

F_{su} = ultimate shear strength, psi

$$F_{su} = \frac{70,000}{2} = 35,000 \text{ psi}$$

Therefore,

$$\text{M.S.} = \frac{F_{su}}{\sigma_s} - 1$$

$$= \frac{35,000}{13,500} - 1 = + \underline{1.6}$$

6. Boss Flange

The most critical section of the boss is located at the base of the flange. Stresses in this area are conservatively determined by assuming the flange to be a flat plate with a concentrated annular load and a fixed inner edge. The end-for-end wrap pattern of the longitudinal filaments produces a rigid band around the boss that supports the flange. Outside this band, the filaments are bridged and therefore offer no additional support. Because a single roll of 12-end roving will be used to wrap the longitudinal pattern, the width of the band is 0.060 in., and the width used in calculating the bending stress is very small. Bending stresses are therefore neglected, with the shear loads at the juncture of the flange and boss predominating. The shear stress there was determined as follows:

$$\sigma_s = \frac{p_b d_f}{4 t_f}$$

where

d_f = diameter at flange-to-boss juncture = 2.75 in.

t_f = thickness of flange = 0.110 in.

Therefore,

$$\begin{aligned}\sigma_s &= \frac{(2087)(2.75)}{4(0.110)} \\ &= 13,050 \text{ psi}\end{aligned}$$

With $F_{tu} = 70,000$ psi (minimum) for Type 304 stainless steel (annealed), assume

$$F_{su} = \frac{70,000}{2} = 35,000 \text{ psi}$$

Therefore,

$$\begin{aligned}\text{M.S.} &= \frac{F_{su}}{\sigma_s} - 1 \\ &= \frac{35,000}{13,050} - 1 = + \underline{1.68}\end{aligned}$$

7. Hydrotest Plug

The stress at the center of the hydrotest plug resulting from the internal pressure is determined by assuming that the plug acts as a solid circular plate, with edges supported, and that a uniform load acts over the entire surface of the plug. The radial stress (σ_r) or tangential stress (σ_t) was calculated as follows:

$$\sigma_r = \sigma_t = \frac{3 W}{8 \pi m t_p^2} (3 m + 1)$$

where

W = total load on plug, lb

$$= \frac{\pi}{4} d^2 p_b$$

p_b = maximum design burst pressure = 2087 psi

m = reciprocal of Poisson's ratio = 3.33

t_p = thickness of hydrotest plug = 0.50 in.

Therefore,

$$\begin{aligned}\sigma_r &= 0.310 \frac{d^2 p_b}{t_p^2} \\ &= \frac{(0.310) (2.52)^2 (2087)}{(0.50)^2} \\ &= 16,400 \text{ psi}\end{aligned}$$

and

$$\begin{aligned}\text{M.S.} &= \frac{F_{tu}}{\sigma_r} - 1 \\ &= \frac{70,000}{16,400} - 1 = + \underline{3.26}\end{aligned}$$

8. Sample Filament-Stress Calculations

As indicated in Section V,A of the body of this report, design burst pressures for the vessel were established at each test temperature by a computer program. This was done on the basis of specific design criteria (see Table 35) and selected single-cycle design-allowable strengths for longitudinal S-901 filaments (330.0 ksi at +75°F, 495.0 ksi at -320°F, and 445.0 ksi at -423°F) at a point on the head contour where the stresses are highest. The following values, taken from the computer-program printout, were used in calculating the actual longitudinal- and hoop-filament stresses at the burst pressure:

Temperature °F	Design Burst Pressure psi	Filament Stress, ksi	
		Longitudinal	Hoop
+75	1338	330.0	304.4
-320	2087	495.0	467.5
-423	1922	445.0	423.9

Because the computer program analysis had already defined the stresses in the metal liner and in the filaments of the vessel, the reported stresses are corrected for that portion of the load supported by the liner. The design-allowable filament stresses from the computer analysis are factored by the direct ratio of actual to design burst pressure and the inverse ratio of actual to design number of winding turns, in order to permit calculation of the actual filament stresses attained at burst pressure. Sample calculations follow.

a. Example for actual stresses at +75°F (Vessel 4):

$$\begin{aligned}\text{Longitudinal-filament stress} &= 330.0 \left(\frac{1490}{1338} \right) \left(\frac{366}{367} \right) = 366.4 \text{ ksi} \\ \text{Hoop-filament stress} &= 304.4 \left(\frac{1490}{1338} \right) \left(\frac{448}{448} \right) = 338.9 \text{ ksi}\end{aligned}$$

b. Example for actual stresses at -320°F (Vessel 10):

$$\text{Longitudinal-filament stress} = 495.0 \left(\frac{1914}{2087} \right) \left(\frac{366}{370} \right) = 449.1 \text{ ksi}$$

$$\text{Hoop-filament stress} = 467.5 \left(\frac{1914}{2087} \right) \left(\frac{448}{446} \right) = 430.6 \text{ ksi}$$

c. Example for actual stresses at -423°F (Vessel 11):

$$\text{Longitudinal-filament stress} = 445.0 \left(\frac{1929}{1922} \right) \left(\frac{366}{368} \right) = 444.2 \text{ ksi}$$

$$\text{Hoop-filament stress} = 423.9 \left(\frac{1929}{1922} \right) \left(\frac{448}{441} \right) = 452.6 \text{ ksi}$$

The allowable hoop-filament stresses are somewhat lower because of the additional hoop filaments used in vessel fabrication to induce failure in the head. In the few instances when the hoop-filament stress was higher than the longitudinal, the number of hoop-filament-winding turns applied was less than the number calculated in paragraph 3,b of this appendix.

9. Calibration of Bow-Tie, Strain-Gage, Displacement Transducers

A single-step, end-to-end calibration was performed on each bow-tie, strain-gage, displacement transducer used in testing. Each test employed three transducers, two for longitudinal displacement and one for hoop. The transducers were calibrated in place on the test vessel, with all instrumentation installed and connected to the data-acquisition equipment (a continuous-strip-chart recorder for each transducer). Laboratory conditions (ambient temperature) were employed, because the strain gages were maintained within the gage-compensation temperature range ($70 \pm 20^{\circ}\text{F}$) during cryogenic testing by manual adjustment of current through bifilar heater windings. During testing, the temperature was monitored by means of a thermocouple very close to the strain gage; although the thermocouple was not located directly on the gage, the beryllium-copper reed of the bow-tie provided an excellent conductive path to the gage. Additional instrumentation details are presented in Section V,C of the body of this report.

For use in calibration, a single washer was spot-welded at the end of each metal-foil band attached to the longitudinal transducers. Two calibration tools were inserted between each attachment tack and the inner surface of the washer, and the signal-conditioning system was adjusted for a zero output reading on the recorder. The distance between the upper and lower attachment posts was accurately measured and recorded. Rotation of the calibration tools produced a displacement of 0.094 in. for each band, with a total displacement of 0.188 in. Strain was then calculated from

$$\text{Strain} = \frac{\Delta L}{L}$$

where

ΔL = total displacement between centers of washers = 0.188 in.
L = distance between centers of attachment tacks

Sample longitudinal-strain calculations for Vessel 10 follow. For Strain Gage No. 2, $L = 6.125$ in. and

$$\text{Strain} = \frac{0.188}{6.125} = 0.0307 \text{ in./in.}$$

For Strain Gage No. 3, $L = 6.188$ in. and

$$\text{Strain} = \frac{0.188}{6.188} = 0.0304 \text{ in./in.}$$

The span control of the signal-conditioning equipment was adjusted so that the instrument would record 30.7% and 30.4% of full scale (based on the foregoing values), to permit strain to be read directly on each strip chart during the pressurization test. This procedure was repeated to ensure reliability.

The procedure used to calibrate the girth (hoop) transducer on each vessel was similar to that described above. The center of the girth band was displaced a predetermined distance on each side of the transducer (total amount, 0.500 in.). The calculations, and the zero and span adjustments, were performed as indicated above, except that values appropriate for girth measurements were used. A sample hoop-strain calculation for Vessel 10 follows.

$$\Delta L = \text{total hoop-band displacement} = 0.500 \text{ in.}$$

$$L = \text{circumference of pressure vessel} = 24.688 \text{ in.}$$

and

$$\text{Strain} = \frac{0.500}{24.688} = 0.0202 \text{ in./in.}$$

Single-point strain-calibration data were obtained for all longitudinal and girth transducers on all vessels before the vessel-burst tests were initiated. Because the data had great uniformity throughout, a single set of calibration curves (Figure F-1) suffices for all the vessels.

Detailed laboratory calibrations were also performed under ambient conditions to determine the degree of transducer linearity and reproducibility. Various displacements were set with the aid of a vernier caliper (reading accuracy of 0.001 in.), and transducer outputs for these displacements were measured with a recording potentiometer. The results are shown in Figure F-2. The curves for displacement vs recorder output as a percentage of chart scale were based on several data points for each configuration. All the data points repeatedly fell within the width of the plot line. Because all the transducers were linear and reproducible to 0.5% within a displacement range from 0.06 to 1.00 in., it was not necessary to perform multiple-point calibration for the individual transducers used in each test setup.

Vessel contraction during cryogenic conditioning before testing did not affect the accuracy of the strain data, because the transducer responses were linear and reproducible. As installed for testing, the transducers were preloaded for a displacement of approximately 1.50 in.

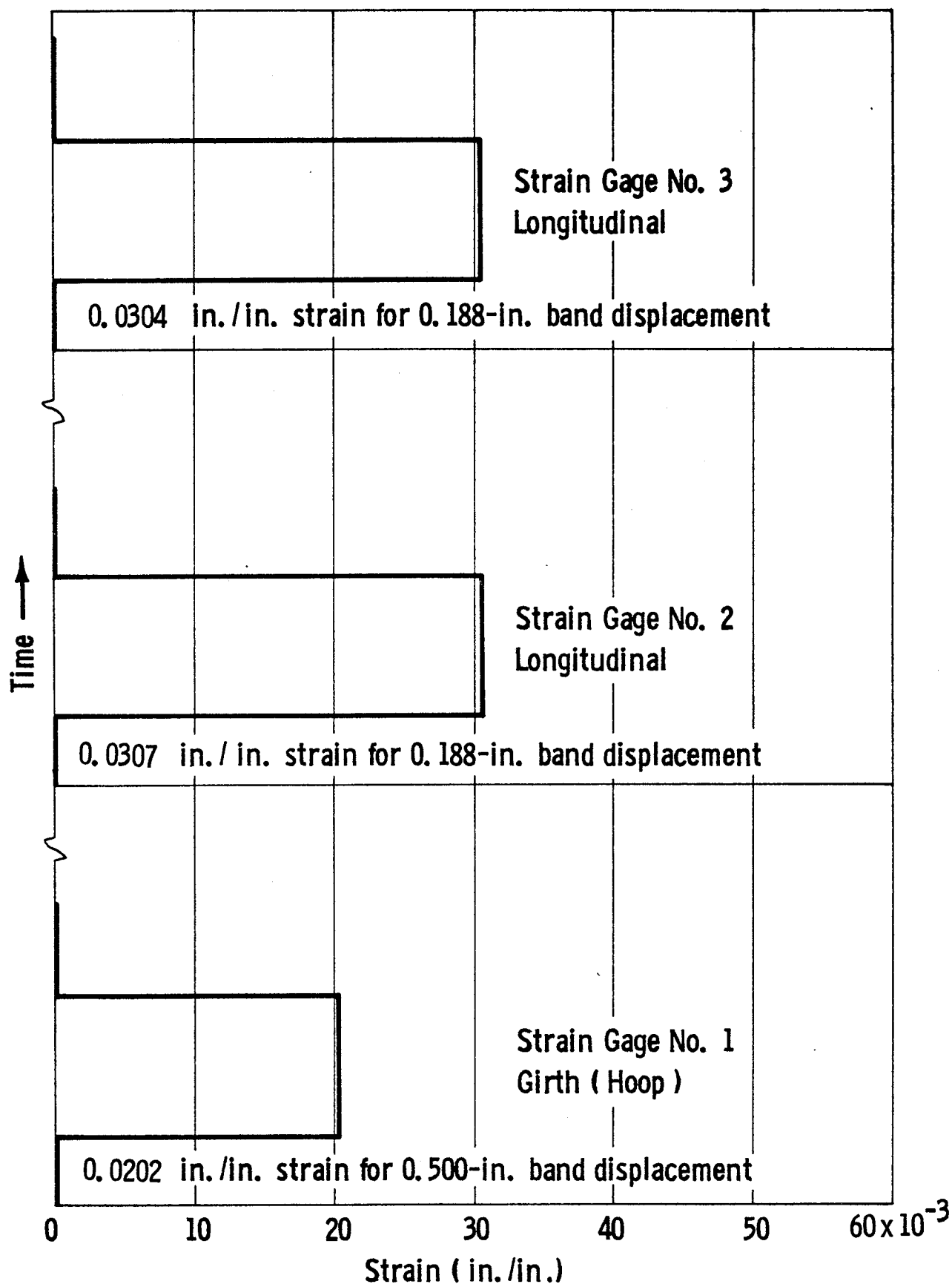


Figure F-1. Calibration Curves for Continuous-Strip-Chart Recorder
Pressure Vessel 10

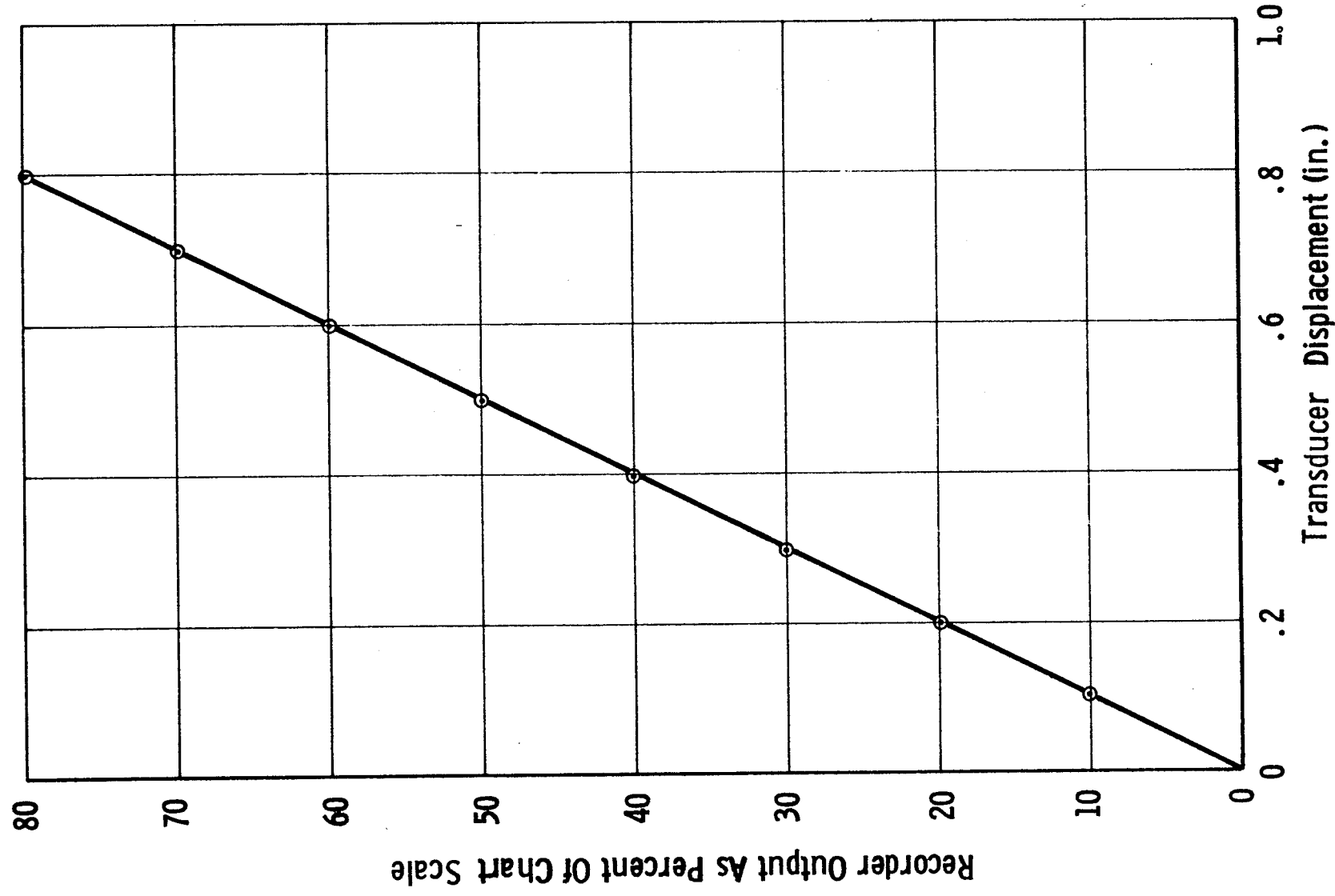


Figure F-2. Calibration Test Data to Demonstrate Linearity of Strain Gage Displacement Transducers

SYMBOLS

D_b	Boss diameter, in.
D_c	Mean diameter of cylinder, in.
F_f	Average ultimate tensile strength for glass roving, psi
$F_{f,1}$	Allowable ultimate strength of longitudinal filaments, psi
K_1	Design factor based on chamber diameter
K_2	Design factor based on boss-diameter to chamber-diameter ratio
K_3	Design factor based on chamber-length to chamber-diameter ratio
K_4	Design factor based on approximation of thickness-to-diameter ratio
K_5	Design factor based on operating temperature
K_6	Design factor based on sustained pressurization loading
L	Chamber length, in.
T	Operating temperature, °F
α	Angle between line in axial direction and filament path, degrees
η	Time under sustained load, min

APPENDIX G

FABRICATION PROCEDURE FOR 8-IN.-DIA CRYOGENIC-RESIN PRESSURE VESSEL

Part Name: Pressure vessel, 8-in.-dia
Part No.: 178156
Test Part Name: Test assembly, 8-in.-dia pressure vessel
Test Part No.: 178169

1. Preliminary Instructions

a. This procedure describes the fabrication of the pressure vessels and provides a permanent record for the data generated. Its purpose is to ensure that optimum results are obtained from the vessels. Deviations in parts, materials, processes, etc. will be recorded. Comments and suggestions should also be noted.

b. A total of 12 pressure vessels (plus one spare if required) will be filament-wound (in-process-impregnated) with S-901 12-end roving.

c. Six vessels will be fabricated with the No. 2 cryogenic-resin system (Epon 828/DSA/Empol 1040/BDMA). These vessels are detailed under Aerojet Part No. 178156-5.

d. Six vessels will be fabricated with the 58-68R standard resin system (Epon 1031/Epon 828/MNA/BDMA). These vessels are detailed under Aerojet Part No. 178156-7.

e. The sequence of fabrication operations is as follows:

- (1) Metal-liner leak test
- (2) Plaster-mandrel fabrication
- (3) Cleaning of metal-liner surfaces
- (4) Application of adhesive coating to metal liner
- (5) Application of longitudinal roving
- (6) Application of circumferential (hoop) roving
- (7) Curing of composite structure
- (8) Plaster-mandrel removal
- (9) Cleaning, dimension-checking, and weighing
- (10) Preparation for testing
- (11) Testing.

f. Extreme care will be exercised in the handling of the metal liner throughout fabrication because of its thin-wall structure (0.006 in.).

g. Clean, white, cotton gloves will be worn when the metal liner is handled after its outer surfaces have been chemically cleaned.

2. Procedure

a. Metal-Liner Leak Test

The metal-foil liner will be leak-tested to verify the impermeability of the metal-shell structure.

(1) Each welded metal liner (Part No. 178155) will be serialized (-1, -2, -3, etc.) in the boss area.

(2) Each will be weighed to the nearest 0.01 g, and the serial number and weight will be recorded (in 5, below).

(3) The liners will be delivered to Test Operations for helium-mass-spectrometer leak testing.

(4) The tested liners will be delivered to the Plaster Shop for the pouring and curing of the plaster mandrel.

(5) Metal-Liner Serial No.: _____. Metal-liner weight: _____ g.

b. Plaster-Mandrel Fabrication

A plaster mandrel will be used inside the metal-liner assembly to provide a firm support for the applied windings of glass filaments.

(1) A slush coat of Kerr DMM plaster will be prepared and poured into the metal liner.

(2) The liner assembly will be pressurized to 10 psig (maximum) and rotated during the hardening of the initial plaster coating.

(3) The plaster coating will be approximately 1.0 to 1.5 in. thick.

(4) The metal-liner/plaster-mandrel assembly will be supported and placed in a circulating oven.

(5) The plaster will be cured for 24 hours at 200°F.

(6) After curing, the metal-liner/plaster-mandrel assembly will be delivered to Test Operations for chemical cleaning.

c. Cleaning of Metal-Liner Surfaces

The exterior of the metal liner will be cleaned chemically to remove contaminants and provide a good bonding surface for adhesive application.

(1) The exterior will be cleaned in accordance with Specification AGC-STD-1221 (Method of Pickling, Hot Nitric Acid).

(2) Each cleaned liner will be placed in a protective plastic bag and delivered to the Filament-Winding Laboratory.

d. Application of Adhesive Coating to Metal Liner

An adhesive will be applied to the exterior of the metal liner in order to obtain a structural bond between the liner and the glass-filament case.

(1) The liner will be handled with clean, white, cotton gloves, and protected with a plastic sheet prior to the application of adhesive.

(2) The adhesive will be a mixture of the following constituents in the quantities shown:

Epon 828	100.0 g
DSA	115.9 g
Empol 1040	20.0 g
BDMA	1.0 g

(3) The Epon 828 and Empol 1040 will be mixed and warmed to 212°F. The mixture will then be cooled to room temperature for the addition of DSA and BDMA (stirring).

(4) A thin coating of the mixture will be applied with a nylon brush to the outer surfaces of the metal liner. (Do not apply adhesive to the face of the boss.) The mixture may be warmed if it appears too viscous for application.

(5) One layer of 0.001-in.-thick, 1-in.-wide, Type 104 glass cloth will be applied over the welded areas of the liner prior to filament winding.

e. Application of Longitudinal Roving

Glass filaments will be wound in the longitudinal direction to support loads induced by internal pressurization.

(1) The winding shaft (T-116962) will be assembled to the metal-liner/plaster-mandrel assembly.

(2) The assembly will be installed in the longitudinal-wrap position of the winding machine. Clean, white, cotton gloves will be worn when the assembly is handled, and the liner will be protected with plastic sheet prior to winding.

(3) All necessary adjustments and machine settings for the winding pattern will be made, and the winding angle, payoff roller, resin-impregnation pot, etc. will be checked. Gear ratio: A = 50, B = 60, C = 73, D = 61.

(4) One roll of the S-901 12-end glass roving will be weighed before winding is initiated. Glass-roll weight before winding: _____ g.

(5) Longitudinal roving will be applied at a tension of 5 \pm 1 lb (one-strand tape).

(6) The longitudinal pattern will be one revolution with 366 turns (plus one turn for tieoff).

(7) Actual number of turns: _____.

(8) The resin for Serial Nos. 4, 5, 6, 10, 11, and 12 will be a mixture of the following constituents in the quantities shown:

Epon 828	200.0 g
DSA	231.8 g
Empol 1040	40.0 g
BDMA	2.0 g

The Epon 828 and Empol 1040 will be mixed and warmed to 212°F, and will then be cooled to room temperature for the addition of DSA and BDMA (stirring). The resin bath may be warmed to and maintained at approximately 95°F if it appears too viscous for filament winding.

(9) The resin for Serial Nos. 1, 2, 3, 7, 8, and 9 will be a mixture of the following constituents in the quantities shown:

Epon 1031	100.0 g
Epon 828	100.0 g
MNA	180.0 g
BDMA	1.0 g

The Epon 1031 will be heated to approximately 200°F or until it melts, and will then be mixed with the Epon 828. The MNA will be added and the mixture stirred until homogeneous. The BDMA will be stirred in prior to winding. The resin bath will be maintained at 150°F during filament winding.

(10) The glass roll will be weighed after winding is completed. Glass-roll weight after winding: _____ g.

f. Application of Circumferential (Hoop) Roving

Glass filaments will be circumferentially wound in the cylindrical section to support loads induced by internal pressurization. The procedures and techniques are essentially the same as those described in Section 2,e, above, except as follows:

(1) Gear ratio: A = 52, B = 100, C = 40, D = 80.

(2) The hoop pattern will be four layers with 112 turns per layer over the 7.28-in. cylindrical distance (see Part No. 178156).

(3) Four instrumentation tacks (two sets of two), used to measure the axial cylindrical strain, will be positioned on the pressure vessel during the winding of the first hoop layer. Each set of two tacks will be placed 180° apart and in the plane of the cylinder axis. One set will be positioned 0.5 in. from the start of the first hoop layer and the other 0.5 in. before the end of the first hoop layer.

(4) Glass-roll weight before hoop winding: _____ g. Glass-roll weight after hoop winding: _____ g.

(5) Actual number of turns after four layers: _____.

g. Curing of Composite Structure

(1) The curing cycle for Resin 2 (Epon 828/DSA/Empol 1040/BDMA) will be as follows: 2 hours at 150°F followed by 4 hours at 300°F.

(2) The curing cycle for the 58-68R resin (Epon 1031/Epon 828/MNA/BDMA) will be as follows: 2 hours at 200°F, followed by 2 hours at 250°F, followed by 4 hours at 300°F.

(3) The pressure vessel will be rotated during the cure.

(4) For both resin systems, the oven heat will be turned off and the chamber will be allowed to cool to room temperature. The oven door will be opened after the temperature drops to approximately 200°F.

h. Plaster-Mandrel Removal

(1) The mandrel will be removed from the oven and the winding-shaft fixture (T-116962) will be disassembled.

(2) The Kerr DMM plaster will be removed with an acetic-acid and hot-water solution (40% acetic acid and 60% water).

(3) The boss faces, including the threaded holes and K-seal area, will be protected during these operations.

i. Cleaning, Dimension-Checking, and Weighing

(1) The inside of the pressure vessel will be cleaned with hot water (150°F maximum). Do not use wire brushes or metal scraping tools on the interior of the vessel. The vessel will be washed with hot water until all foreign matter has been removed, and will be air-dried at room temperature.

(2) The length from boss face to boss face will be measured and recorded: _____ in.

(3) The cylinder diameter (at three places) will be measured with pi tape and recorded: _____ in.
_____ in.
_____ in.

(4) The pressure-vessel weight will be measured and recorded:
_____ g.

(5) The pressure vessel will be sent to Test Operations for cryogenic testing.

j. Preparation for Testing

(1) The test chamber (Part No. 178156), bolts, and plugs (Part No. 177413) will be assembled in accordance with the test-assembly drawing (Part No. 178169).

(2) The test requirements (preparation, instrumentation, etc.) will be in accordance with the Environmental Test Procedure for Cryogenic Pressure Vessels, 8-Inch-Diameter, for Contract NAS 3-6287.

k. Testing

(1) Single-cycle burst-pressurization tests will be conducted on all 12 pressure vessels (Part No. 178156). Four vessels will be tested at +75°F, four at -320°F, and four at -423°F.

(2) The vessels will be tested at the following temperatures:

<u>Serial No.</u>	<u>Temp, °F</u>
1	+75
2	+75
3	-320
4	-320
5	+75
6	+75
7	-320
8	-423
9	-423
10	-320
11	-423
12	-423

(3) The internal volume of the tanks used in the +75°F tests will be determined and recorded before testing:

<u>Serial No.</u>	<u>Volume, cu in.</u>
1	_____
2	_____
5	_____
6	_____

(4) Tests will be conducted in accordance with the Environmental Test Procedure for Cryogenic Pressure Vessels, 8-Inch-Diameter, for Contract NAS 3-6287.